THE UNIVERSITY OF MICHIGAN

INDUSTRY PROGRAM OF THE COLLEGE OF ENGINEERING

LIQUID AND GAS-PHASE MASS TRANSFER ON BUBBLE-CAP TRAYS

(John Wesley)

John W. Begley

A dissertation submitted in partial fulfillment
of the requirements for the degree of
Doctor of Philosophy in the
University of Michigan
1959

October, 1959

IP-395

en m
UM2029

ACKNOWLEDGMENTS

The author wishes to gratefully acknowledge the assistance of the following persons during the course of this study:

Members of the Doctoral Committee

Professor Brymer Williams, Chairman
Associate Professor T. C. Adamson
Professor J. T. Banchero
Assistant Professor K. F. Gordon
Professor R. R. White
Professor J. L. York

A.I.Ch.E. Plate Efficiency Research Assistants

James R. Beissel
Talivaldis Cepuritis
Jon M. Gaston
Kathryn Hilbert
Richard C. Keezer
Charles D. Malloch
Constantinos T. Nikoletopoulos
Robert Norman
Eugene D. Salesin
Robert J. Van Duyne
James Wall
Chi Hua "Ruth" Wu

Shop and Office Personnel in the Department of Chemical and Metallurgical Engineering

Cleatis Bolen
David M. Brown, Mass Spectrometer Lab.
Frank Drogosz
Ludwig Eppler
George Foster
William Hines
Madelaine R. Ingerson

Financial support for the research program was supplied by the A.I.Ch.E. Plate Efficiency Research Committee with funds solicited from approximately 35 industrial organizations. Fellowship grants from Phillips Petroleum Company and the American Institute of Chemical Engineers were a direct assistance to the author during the studies and research work for the doctorate. The chemicals used in the studies were

supplied gratis by the Dow Chemical Company through the arrangements of Messrs. N. Poffenberger and P. C. Dean.

Miss Ruth Wu, one of the research assistants, deserves special mention because of her interest in the research problems and her devotion to the tedious job of transposing the laboratory data to the form used herein. The author would also like to acknowledge the patient work of his wife, Lois Begley, during the preparation of the original draft for the thesis.

TABLE OF CONTENTS

TABLE OF CONTENTS (CONT'D)

LIST OF TABLES

LIST OF TABLES - APPENDIX

LIST OF TABLES - APPENDIX (CONT'D)

LIST OF FIGURES

LIST OF FIGURES (CONT'D)

LIST OF FIGURES (CONT'D)

LIST OF FIGURES (CONT'D)

LIST OF FIGURES (CONT'D)

LIST OF FIGURES (CONT'D)

LIST OF FIGURES - APPENDIX

NOMENCLATURE

a	Constant in correlation equations
a	Interfacial area, ft^2/ft^3 of gas holdup
$\bar{a}$	Interfacial area, ft^2/ft^3 of liquid holdup
a_1	Interfacial area in the bubble formation zone, ft^2/ft^3 of gas holdup
a_2	Interfacial area in the froth and entrainment zones, ft^2/ft^3 of gas holdup
a'	Interfacial area per plate per unit time of gas flow
a''	Interfacial area, ft^2/(sq. in. slot area)(inches of liquid depth)
A	Constant in correlation equations
A_A	The abnormality factor for the solute in Arnold's equation
A_B	The abnormality factor for the solvent in Arnold's equation
A_{sl}	Total slot area per plate, sq. in.
A_T	Active cross-sectional area of the tray, ft^2 (0.615 ft^2 for tray used in present study).
b	Constant in correlation equations
B	Tray width, ft.
B	Constant in correlation equations
B_F	Thickness of liquid film in wetted-wall tower, ft.
c	Constant in correlation equations
C	Concentration in liquid phase, lb moles/ft^3
C	Constant in correlation equations
"C"	Warzel mixing parameter
C^*	Equilibrium liquid concentration, lb moles/ft^3
C''	Constant in correlation equation

C_1, C_2	Constants in the solution to the differential equation which describes the concentration in the liquid as a function of distance along the tray.
C^o_2	Molar density of liquid phase, lb moles/ft^3
C_{2m}	The average concentration of the solvent in the liquid film, lb moles/ft^3
C_i	Concentration in liquid phase at the interface, lb mole/ft^3
C_p	Specific heat of gas, BTU/lb mole-F
C_R	Rotameter calibration factor
C_2, C_3 C_4, C_5	Concentration in liquid phase at four different points on the tray floor, lb moles/ft3
d	Differential operator
d	Constant in correlation equations
d_b	Bubble diameter, ft.
d_o	Orifice diameter, ft.
D	tube diameter, ft.
D_E	Eddy diffusivity, ft^2/hr.
D_G	Gas diffusivity, ft^2/hr.
D_L	Liquid diffusivity, ft^2/hr.
D_{L_o}	Liquid diffusivity at 0°C, ft^2/hr.
D_S	Slot width, ft.
e	Constant in correlation equations
E_{OG}	Overall column efficiency
E_G	Single-phase vapor point efficiency
E_L	Single-phase liquid point efficiency
E_{ML}	Murphree liquid efficiency
E_{MV}	Murphree vapor efficiency

E_{OL}	Over-all liquid point efficiency
f	Constant in correlation equations
f	Friction factor
F	Energy loss due to friction, ft-lb force/lb mass.
F-factor	$U_s\sqrt{\rho_G}$, ft/sec $\sqrt{\text{lb/ft}^3}$
g	Gravitational acceleration, ft/sec^2.
G	Gas or vapor flow rate, lb moles/hr.
G_s	Superficial mass velocity, lb/ft^2-hr.
G_{avg}	Average gas or vapor rates between a point above and below the tray, lb moles/hr.
h	Effective liquid depth, inches
h_G	Gas-phase heat transfer coefficient, BTU/hr-ft^2-°F
h_L	Slot submergence, ft.
H	Henry's Law constant, p/c, atm-ft^3/lb moles or p/x, atm/mol fraction
H	Holdup of gas in froth, ft^3/ft^3
H_L	Height of a liquid-phase mass transfer unit, ft.
H.T.U.	Height of a theoretical mass transfer unit
j_D	j factor for diffusion
k_G	Gas-phase mass transfer coefficient, lb moles/hr-ft^2-atm
k_L	Liquid-phase mass transfer coefficient, lb moles/(hr-ft^2) (lb moles/ft^3)
k'_G	Gas-phase mass transfer coefficient, lb moles/(sec-ft^2) (lb moles/ft^3)
k_q	Gas thermal conductivity, BTU/hr-ft^2-°F/ft
$k_G'a$	Gas-phase mass transfer coefficient, sec^{-1}
$k_L\bar{a}$	liquid-phase mass transfer coefficient, sec^{-1}
$k'_{G_1}a_1$	gas-phase mass transfer coefficient in the bubble formation zone
$k'_{G_2}a_2$	gas-phase mass transfer coef. in froth and entrainment zones

K	Constant
K_{OG}	Over-all gas-phase mass transfer coefficient, lb moles/hr-ft^2-atm.
K_{OL}	Over-all liquid-phase mass transfer coefficient, lb moles/(hr-ft^2)(lb moles/ft^3)
$K_{OG}'a$	Over-all gas-phase mass transfer coefficient, sec^{-1}
ℓ_L	Vertical distance from top of bubble cap slots to top of weir, ft.
ℓ_o	Crest of liquid over top of weir, ft.
ℓ_s	Height of slot, ft.
L	liquid flow rate, lb moles/hr
m	Slope of the vapor-liquid equilibrium curve of y versus x.
m	Constant in a correlation equation
M	Mixing parameter, $LS/D_E Z_c B\rho_{ML}$
M	Constant in a correlation equation
M_A	Solute molecular weight
M_B	Solvent molecular weight
M_G	Molecular weight of gas
n	Number of ideal mixing stages on a tray
n	Constant in a correlation equation
n_b	Bubble frequency
N_A	Rate of mass transfer, lb moles/hr-ft^2
N_G	Number of gas-phase mass transfer units
N_L	Number of liquid-phase mass transfer units
N_S	Number of bubble sources
N_{OG}	Number of over-all gas-phase mass transfer units

N_{OL}	Number of over-all liquid-phase mass transfer units
p^*	Equilibrium partial pressure in gas-phase, atm.
p_i	Partial pressure in gas phase at the interface, atm.
p_G	Partial pressure in gas phase, atm.
p_{BM}	Logrithmic-mean partial pressure of nondiffusing component, atm.
P	Total pressure, atm.
ΔP_T	Total pressure drop across the tray, lb/ft^2
q_i	Rate of circulation, ft^3/hr
Q_G	Volumetric air flow rate per orifice, ft^3/hr.
Q_{GT}	Total volumetric gas flow rate to the tray, ft^3/sec.
Q_{LT}	Total volumetric liquid flow rate to the tray, ft^3/sec.
s	Rate of surface renewal
s'	Distance along the tray, ft.
S	Length of tray, ft.
t	Liquid interfacial contact time, hr.
t_b	Bubble contact time, hr.
t_G	Gas contact time, sec.
t_L	Liquid contact time, sec.
t_{G_1}	Gas contact time in the bubble formation zone, sec.
t_{G_2}	Gas contact time in the froth and entrainment zones
T	Temperature, °F or °K
T_w	Wet bulb temperature, °F
T_{as}	Adiabatic saturation temperature, °F.
u_s	Superficial gas velocity, ft/sec.
u_{avg}	Average superficial gas velocity between a point above and below the tray, ft/sec.

V	Specific volume, ft^3/lb.
V_b	Bubble velocity, ft/hr.
V_f	Froth velocity, ft/sec.
V_A	Molal volume of the solute at normal boiling point, cc/gm-mole
V_B	Molal volume of the solvent at normal boiling point, cc/gm-mole
W	Fraction of distance across the tray
W	Work term in energy balance
x	Liquid concentration, mol fraction
x^*	Equilibrium liquid concentration, mol fraction
x'	Liquid concentration at a point on the tray, mol fraction
x	Liquid concentration at the tray inlet, mol fraction
x_e	Liquid concentration at a point on the tray between the inlet downcomer and the first row of bubble caps, mol fraction
x_i	Liquid concentration at the gas-liquid interface, mol fraction
x_o	Liquid concentration at the tray outlet, mol fraction
x_{avg}	Arithmetic average liquid concentration on the tray, mole fraction
x_L	Liquid film thickness, ft.
X_B	Solvent association parameter
y	Gas concentration, mol fraction
y^*	Equilibrium gas concentration, mol fraction
y'	Gas concentration at a point on the tray, mol fraction
y_i	Gas concentration at the gas-liquid interface, mol fraction
y_{avg}	Average gas concentration above the tray, mol fraction
y_l	Gas concentration below the tray, mol fraction

Z	Potential energy term, ft-lb force/lb mass
Z_c	Average clear liquid height on the tray, in. or ft.
Z_f	Average froth height on the tray, in. or ft.

Greek Symbols

α	Constant in correlation equation
β	Gas holdup, $Z_f - Z_c$, ft.
β_f	Gas holdup in the froth, ft.
β_l	Gas holdup in the bubble formation zone, ft.
β^o	Constant in a correlation equation
β'	Constant in a correlation equation
β''	Constant in a correlation equation
γ	Crozier mixing parameter
Γ	Liquid flow rate, lb/hr/ft.
ϵ	Fractional error
$\}$(	Humidity of the gas, lb vapor/lb dry nitrogen
$\}_{as}$	Humidity of saturated gas at T_{as}, lb vapor/lb dry nitrogen
θ	Residence or contact time of the gas in the plate liquid
λ	mG/L
$\lambda_{T_{as}}$	Latent heat of vaporization at the temperature T_{as}, BTU/lb.
λ_{T_w}	Latent heat of vaporization at the temperature T_w, BTU/lb.
μ_B	Solvent viscosity, cp.
μ_G	Gas viscosity, lb mass/ft-hr.
μ_L	Liquid viscosity, cp or lb mass/ft-hr.
η	Mising parameter
ρ_G	Gas density, lb/ft^3

NOMENCLATURE (CONT'D)

ρ_L	Liquid density, lb/ft^3
ρ_B	Density of solvent, gm/cc.
ρ_{MG}	Molal gas density, lb moles/ft^3
ρ_{ML}	Molal liquid density, lb moles/ft^3
τ	Mean residence time of the total flow
ψ	Mixing flow term in the differential equations describing the transfer of material to a differential element on a tray.
σ^2	Variance of liquid-residence-time distribution
σ_L	Liquid surface tension, $lb\text{-}ft/hr^2\text{-}ft$.
σ_B	Surface tension of solvent, $lb\text{-}ft/hr^2\text{-}ft$.

INTRODUCTION

The separation of materials is a very important operation in any large refinery or chemical plant. The most common type of separation means used in these plants is fractional distillation wherein the difference in volatilities of the components in a liquid or gas mixture are used advantageously to perform a separation. Another basic type of separation means is absorption where a high boiling liquid is used to absorb a particular component or components from a gas mixture. In both operations, liquid and vapor are contacted countercurrently and the separation depends upon mass transfer between these two phases.

In the petroleum industry, the trend for years has been to make sharper separations of basic crude fractions and raw products from cracking operations. For example, the products from thermal cracking of light hydrocarbons and from steam cracking of gas oils and the light ends from catalytic treatment of naphthas and gas oils contain valuable chemical building-blocks such as ethylene, propylene, normal butylenes, isobutylene, butadiene, isoprene and higher boiling liquid. These hydrocarbons are usually required in high purity in the petrochemical or chemical industry. In order to recover these materials efficiently, superfractionation is required. Absorbers are also used in some cases to remove small amounts of impurities from these hydrocarbon streams. The engineer must be in a position to design the equipment required to perform these separations with a considerable degree of accuracy in order to maintain capacity and purity in the new plant and thereby maintain an attractive return on the plant investment. Fractionation and absorption are also basic tools in

the refining of petroleum crudes and in the removing of heavy hydrocarbons from natural gas streams. However, the designs in these cases are usually based on broad experience in these operations. In addition, the designs are not as critical as in the case where a high purity product is of interest.

Using the concepts of the equilibrium stage, the engineer may make a theoretical study of any separation provided vapor-liquid equilibrium data are available. With the use of digital computers, studies of this type are feasible even for multicomponent systems containing twenty to thirty components. However, translating the results from the theoretical study to the separation equipment in the plant requires a basic knowledge of the column performance in relation to theory. The most important information required in this case is the performance of an actual stage (bubble-cap, sieve, or perforated tray) in relation to the theoretical stage This is commonly expressed as plate efficiency, a factor which can be related to the mass transfer on the plate. In order to predict the plate efficiency for a particular plate design, the engineer must also be familiar with the hydraulic characteristics of the tray. In the past, several correlations of plate efficiency have not included factors such as liquid and gas holdup on the tray. But these factors have been shown to be very basic to any prediction of plate efficiency (7,35,36,37,92).

The use of plate efficiency is a convenience which has been accepted by design engineers. Basically, the design of a fractionator can be made by use of rate-process concepts. Stage-wise calculations could be performed on a non-equilibrium-stage basis as opposed to the equilibrium stage calculations commonly used today. In this case, the

rate of transfer between the gas and liquid phases would have to be known for each component in the system. Similarly, when using the equilibrium-stage design method and plate efficiency which is related to mass transfer on the tray, the efficiency for each component in the mixture must be known. Therefore, it is necessary to know the effect of physical properties on the rate of mass transfer in a system of this kind.

Plates are used in industry in order to obtain efficient contacting in most cases when large diameter columns are required. Where the column diameter is below two to three feet, packed columns are used. The factor commonly used to describe the performance of packed columns in relation to the theoretical stage is the height of a theoretical plate, HETP. This factor can also be related to the rate of mass transfer occurring in the column. On this basis, it is not difficult to see the similarity between the two types of equipment. The principal difference is the method of contacting. In addition, it is conceivable that some of the information from the studies of mass transfer in a plate column can be applied in the studies of packed columns or vice versa. In the following sections, the discussion will be limited to plate efficiency.

Several basically different plate efficiencies have been studied, correlated, and used by the engineer in the past. These are:

1. Point efficiency,

$$E_{OG} = \frac{y'_n - y'_{n-1}}{y^{*'}_n - y'_{n-1}} \qquad (1)$$

where the primes indicate vapor concentrations at discrete points lying on a vertical line through the tray, and

where y'_n = vapor concentration above the tray, mol fraction.

y'_{n-1} = vapor concentration below the tray, mol fraction.

$y_n^{*'}$ = concentration of vapor in equilibrium with the liquid on the tray, mol fraction.

2. Murphree plate efficiencies.

(a) In terms of vapor composition,

$$E_{MV} = \frac{y_n - y_{n-1}}{y_n^* - y_{n-1}} \qquad (2)$$

where y_n = average concentration of the vapor leaving the tray, mol fraction.

y_{n-1} = average concentration of the vapor entering the tray, mol fraction.

y_n^* = concentration of the vapor in equilibrium with the liquid leaving the tray, mol fraction.

(b) In terms of liquid composition,

$$E_{ML} = \frac{x_n - x_{n+1}}{x_n^* - x_{n+1}} \qquad (3)$$

where x_n = concentration of the liquid leaving the tray at the outlet downcomer, mol fraction.

x_{n+1} = concentration of the liquid entering the tray at the inlet downcomer, mol fraction.

x_n^* = concentration of the liquid in equilibrium with the gas or vapor leaving the tray, mol fraction.

For the case of straight, but not parallel, operating and equilibrium lines, E_{MV} and E_{ML} may be related by the following material balance relationships,

$$E_{MV} = \frac{E_{ML}}{E_{ML} + \frac{mG}{L}(1 - E_{ML})} \tag{4}$$

or

$$E_{MV} = \frac{E_{ML}}{E_{ML} + \frac{HG}{PL}(1 - E_{ML})} \tag{5}$$

where m = the slope of the vapor-liquid equilibrium curve of y versus x.

H = Henry's Law constant, $H = p/c$.

3. Overall Column Efficiency,

$$E_o = \frac{\text{number of ideal plates}}{\text{number of actual plates}}, \tag{6}$$

where E_o = overall column efficiency.

The amount of academic research work on plate efficiencies in the past is probably greater than the work on any other piece of equipment used by the chemical and petroleum industries. This work includes studies of the following types:

1. Investigations of plate efficiency wherein small columns or single trays were used to study the effect of one or two variables on the efficiency of a particular system.
2. Investigations of the hydraulic characteristics of single trays including studies of entrainment, flooding, and gas and liquid holdup on the trays.
3. Investigations directed toward a better understanding of of the mechanisms involved in contacting a gas and liquid on a bubble tray. These investigations include studies of the mechanism of bubble or interfacial-area formation and the mechanism of mass transfer in each phase of the two-phase system.

The petroleum and chemical industries have relied heavily on past experiences and specific tests in the pilot plant to design fractionation equipment. This work plus the academic research on plate efficiencies add-up to a very large effort and cost for one type of equipment. In spite of this tremendous amount of effort, a general relationship between plate efficiency and the many independent variables is still lacking. However, the results of the previous research has shown the following variables to be important in the prediction of plate efficiency:

1. Properties of the vapor and liquid.
   (a) Vapor-liquid equilibrium.
   (b) Viscosity, surface tension, molecular weight, and density.
   (c) Mass diffusion rates.
   (d) Thermal properties, heat capacity and conductivity.

2. Equipment variables.

   (a) Tower diameter and plate spacing.

   (b) Bubble-cap design: type, size, slot dimensions, number of slots per cap, etc.

   (c) Plate layout: bubble-cap arrangement, number of bubble-caps, skirt clearance.

   (d) Type and height of weirs.

3. Operating variables.

   (a) Vapor and liquid flow rates.

   (b) Temperature and pressure.

In view of the number of variables involved and the number of different possible designs, it is understandable why a general correlation of plate efficiencies does not exist today. One of the problems which has limited the engineer in his efforts to relate plate efficiency with the fundamental variables involved has been his inability to completely describe the geometric, kinematic, and dynamic characteristics of a gas emerging from a slot and flowing through a gas-liquid mixture. Ideally, one would like to be able to describe the geometry and fluid dynamics of the system well enough in order to use the results from small scale experiments such as mass transfer to or from a gas flowing from a single slot or orifice submerged in a liquid to generalize the prediction of mass transfer on a bubble tray. Attempts have been made to do this but the relationships developed are not believed to be generally applicable. However, these studies have aided in the interpretation and correlation of the data from test trays.

In 1952, the American Institute of Chemical Engineers inaugurated a research program for the study of plate efficiency. The primary purpose of this effort has been to study efficiencies for both small and large trays and to develop a method of predicting the efficiencies for trays of any size by use of a generalized correlation of the data from the research program. The small trays were used to study the effects of gas and liquid properties on plate efficiencies while the larger trays were used to study the effects of tray design variables on plate efficiencies. An effort was made to interpret the data by use of the concepts of mass transfer in a two-phase system such as, the two-film theory or theory of additive resistances. The present investigation was sponsored by the American Institute of Chemical Engineers with the primary purpose of increasing the knowledge of the relationship between plate efficiencies and liquid properties.

TRANSFER OF MATERIAL BETWEEN PHASES

Whitman(96) proposed the "two-film" theory which has been used as a model to describe the process of interphase transfer. This model implies that there is a fluid "film" in each fluid adjoining the interface, and the principal resistance to interphase transfer is this double film. The relative resistances for the general case in a gas-liquid system depend upon two distinct sets of factors:

(a) Physical factors: solubility of the gas in the liquid, diffusivity of the gas in the liquid and vapor phases, and concentration in each phase.

(b) Hydrodynamic factors: geometry and scale of equipment, viscosity and density of the two phases, and flow-rates of the two phases.

If it is assumed that the mass transfer through the adjacent vapor and liquid films takes place at steady-state and that equilibrium exists at the interface, it is possible to equate the rates of diffusion through each film to the rate through the interface.

$$N_A = k_G (p_G - p_i) = k_L (C_i - C) = K_{OG} (p_G - p^*) \qquad (7)$$

where K_{OG} = over-all mass transfer coefficient, lb. moles/(hr.)(sq.ft.)(atm).

k_G = gas phase mass transfer coefficient, lb. moles/(hr.)(sq.ft.)(atm).

k_L = liquid phase mass transfer coefficient, lb. moles/(hr.)(sq.ft.)(lb. moles/cu.ft.).

p_G = partial pressure in gas phase, atm.

p_i = partial pressure in gas phase at the interface, atm.

C = concentration in liquid phase, lb. mole/cu.ft.

C_i = concentration in liquid phase at the interface, lb. mole/cu.ft.

If Henry's Law applies

$$p_i = HC_i \tag{8}$$

and

$$p^* = HC \tag{9}$$

Then the relationship between the over-all and the individual film coefficients may be obtained by eliminating C_i and p_i in Equations (7) and (8).

$$\frac{1}{K_{OG}} = \frac{1}{k_G} + \frac{H}{k_L} \tag{10}$$

$$\frac{1}{K_{OL}} = \frac{1}{k_L} + \frac{1}{Hk_G} \tag{11}$$

In the case where the equilibrium data are in terms y-x diagrams, Equations (10) and (11) become

$$\frac{1}{K_{OG}P} = \frac{1}{k_G P} + \frac{m}{k_L \rho_{ML}} \tag{12}$$

and

$$\frac{1}{K_L \rho_{ML}} = \frac{1}{k_L \rho_{ML}} + \frac{1}{mk_G P} \tag{13}$$

where m = the slope of the equilibrium curve.

ρ_{ML} = molal density of the liquid, lb. moles/cu.ft.

Three different models for describing the mechanism of mass transfer in the liquid phase have been proposed. These are:

1. Whitman[96]: laminar film.
2. Higbie[42] : systematic surface renewal.
3. Danckwerts[22]: random surface renewal.

In the Whitman model the liquid at the surface is assumed to be in laminar flow parallel to the surface while the liquid below the surface is in turbulent motion. The rate of absorption is determined by molecular diffusion in the surface layers. Although the relative importance of transport by diffusion and by turbulence will vary with the depth below the surface, the model implies a completely stagnant layer of effective thickness, X_L. The thickness of the film is assumed to be small enough for the absorption process to be treated as one of steady-state diffusion through the stagnant layer.

In Higbie's[42] model of systematic surface renewal, each element of liquid surface is assumed to be exposed to the gas for the same length of time and to absorb gas during this time at a changing rate as though it were a stagnant layer of infinite depth. The model proposed by Danckwerts[22] is identical to Higbie's model except for the time of exposure for each liquid element. In the Danckwerts model, it is assumed that there is no correlation between the time of exposure and the chance of an element being remixed.

The physical significance given to k_L is different in each of the three models as can be seen from the following expressions for the rate of absorption:

Whitman: $$N_A = (C^* - C)\frac{D_L}{X_L} \qquad (14)$$

Higbie: $$N_A = (C^* - C)\, 2\sqrt{\frac{D}{\pi t}} \qquad (15)$$

Danckwerts: $$N_A = (C^* - C)\, 2\sqrt{Ds} \qquad (16)$$

where s = the rate of surface renewal.

t = contact time of a liquid element with the gas.

BASIC RELATIONSHIPS BETWEEN POINT EFFICIENCY AND MASS TRANSFER COEFFICIENTS

The point efficiency is the most basic factor to consider since it does not depend on mixing or concentration gradients on the tray but only upon the hydrodynamic and physical factors which affect the mass transfer. Murphree(59) was probably the first to use the "two-film" theory proposed by Whitman(96) to derive the fundamental relation between point efficiency and the interphase mass transfer on a bubble plate. For his derivations, Murphree assumed:

1. A negligible change in total vapor volume during its passage through the liquid on a given plate.
2. Complete mixing of the liquid on the plate, i.e., no liquid concentration gradient on the tray.
3. The composition of the gas entering the plate is uniform along the length of the plate.
4. A gradual and continuous change in composition of the vapor during its upward passage through the liquid, with no back-mixing of the gas, i.e., plug flow of the gas through the liquid.

Murphree's derivation is as follows:

$$-G\, dy = K_{OG}\, a' (p_G - p^*)\, d\Theta \qquad (17)$$

where $K_{OG}\,a'$ = overall vapor mass transfer coefficient, mols/(unit contact time)(unit of pressure driving force).

a' = interfacial area per plate per unit time of gas flow.

θ = residence or contact time of gas in the plate liquid.

G = gas or vapor rate, mols per unit time.

Since $p_G = Py$ and $p^* = Py^*$

$$-G\,dy = K_{OG}a'\,P\,(y - y^*)\,d\theta \tag{18}$$

or

$$-\int\frac{dy}{(y - y^*)} = \int\frac{K_{OG}a'P}{G} \tag{19}$$

If it is assumed that $K_{OG}a'$ P, G, and y^* are independent of time of contact or in other words, independent of the position in the liquid on the tray, Equation (19) may be integrated between the limits, $y = y_1$ at $\theta = 0$ and $y = y$ at $\theta = 0$, to obtain the following relationship between point efficiency and the mass transfer coefficient and time of gas contact.

$$E_{OG} = \frac{y - y_1}{y^* - y_1} = 1 - e^{-m} \tag{20}$$

where E_{OG} = over-all vapor point efficiency

y_1 = concentration in gas entering the tray, mol fraction of component being exchanged or transferred from gas to liquid phase or vice versa.

y = concentration in gas leaving the tray, mol fraction of component being exchanged or transferred from gas to liquid phase or vice versa.

$$m = \frac{K_{OG}\, a'\, P\, \Theta}{G} = N_{OG}$$

The point efficiency is therefore defined as the ratio of the actual amount of material transferred and the amount which would be transferred if the vapor leaving the tray were in equilibrium with the liquid on the tray.

Walter[89] expressed the time of contact, Θ, as directly proportional to the effective slot submergence below the liquid level, h. This relation implies vertical movement and constant velocity of the gas bubble in the liquid and does not account for the gas hold-up in the liquid on the tray which increases the length of the path traveled by the gas bubble. Walter also observed that the term, m, was essentially independent of the gas rate, G. In terms of Walter's definition,

$$m = \frac{P\, K_{OG}\, a'\, \Theta}{G} = \frac{P\, K_{OG}\, a''\, A_{sl}\, h}{G} = N_{OG} \qquad (21)$$

where $K_{OG}\, a''$ = over-all gas film mass transfer coefficient, lb.moles/(hr.)(atm)(sq.in. slot area)(in. liquid depth)

A_{sl} = total slot area per plate, sq. in.

h = effective liquid depth, in. (taken to be the distance from the middle of the slots to the top of the weir).

Geddes[34] attempted to study separately the factors which determine the bubble size, the time of contact, and the value of K_{OG}. The time of contact was calculated from the liquid seal on a foam-free basis and an empirical equation for the velocity of rise of individual gas bubbles through liquids. Chu[17], Narsimhan[60], West[93], and Colburn[20], have made similar studies where attempts have been made to separate the effects on point efficiency. In all of these studies, it has been recognized that the contact time of the gas with the liquid on the tray is one of the variables involved in N_{OG} but there has been considerable variation in the individual definition for the contact time (see Table I).

Recently, Gerster[1] proposed the following definition for gas contact time,

$$t_G = \frac{Z_f - Z_c}{u_s} = \frac{\beta}{u_s} \tag{22}$$

$$m = N_{OG} = K'_{OG}\ a\ t_G \tag{23}$$

where Z_f = observed froth height on the tray, ft.

Z_c = observed average clear liquid depth on the tray, ft.

$Z_f - Z_c$ = effective gas holdup on the tray, ft^3/ft^2 of bubbling area on the tray

u_s = superficial gas velocity through the tray, ft/sec.

t_G = gas contact time, sec.

$K'_{OG}a$ = over-all coefficient, sec^{-1}.

Using this definition, Gerster was able to correlate Ashby's vaporization data for several systems including water and organic liquids and gases like Freon 12, helium, air, and nitrogen. The correlation is as follows,

$$k'_G a = C\, u_s^{0.23} \qquad (23a)$$

where $C = 18.19\, D_G^{0.33}$

D_G = gas diffusivity coefficient, sq.ft./hr.

k'_G = mass transfer coefficient for gas phase, cu. ft./(sq.ft.)(sec).

a = interfacial area, sq.ft./cu.ft. of gas holdup.

u_s = superficial gas velocity, ft./sec., based on tray bubbling area.

Ashby's data were obtained at one weir height, 1-1/2 inch, by e of the equipment used in the present investigation. Therefore, it is of interest to investigate the applicability of Gerster's definition as the liquid submergence on the tray and physical properties of the liquid are varied.

In the derivation of Equation (20) the assumption was made that the molal rate of gas does not change as the gas flows across the tray. In the absorption of components from a dilute gas mixture, the desorption of components from a dilute liquid mixture, the vaporization of a pure liquid at low vapor pressure, or in a distillation system where the assumption of constant molal overflow applies, Equation (20) is applicable. However, in cases where the foregoing conditions do not exist, the differential equation for mass transfer at a point in the froth on a plate is

$$- G\,dy - y\,dG = K_{OG}\,a\,P\,(y - y^*)\,d\beta A_T \tag{24}$$

or

$$- \frac{dy}{y - y^*} - \frac{y}{y - y^*}\frac{dG}{G} = \frac{K_{OG}\,a\,P\,d\beta A_T}{G} \tag{25}$$

If the change in G is caused by absorption of a single component from the gas, desorption of a single component from the liquid, or evaporation of a liquid by the gas, the change in G is a function of the change in the gas composition. A material balance for the inert gas (gas not transferred from gas to liquid phase) is,

$$G - Gy = G_1 - G_1 y_1 \tag{26}$$

$$G = G_1\,(1 - y_1)/(1 - y) \tag{27}$$

If G is a function of gas composition on the tray,

$$dG = \frac{dG}{dy}\,dy \tag{28}$$

and

$$dG = \frac{G_1\,(1 - y_1)}{(1 - y)^2}\,dy \tag{29}$$

Substituting Equations (27) and (29) into Equation (25)

$$\frac{-dy}{(y - y^*)(1 - y)} = \frac{K_{OG}\,a\,P\,A_T\,d\beta}{G} \tag{30}$$

If K_{OG} a P is constant throughout the froth and if G equals G_{avg}, Equation (30) can be integrated between the limits $y = y_1$ at $\beta = 0$ and $y = y$ at $\beta = \beta$ to give the following relationship,

$$N_{OG} = \frac{K_{OG}\,a\,P\,\beta A_T}{G_{avg}} = \frac{1}{1 - y^*}\,\ln\left[\left(\frac{y^* - y}{y^* - y_1}\right)\left(\frac{1 - y_1}{1 - y}\right)\right] \tag{31}$$

By introducing the molal gas density, ρ_{MG},

$$\frac{K_{OG}\ a\ P\ \beta A_T}{G_{avg}} = \frac{K_{OG}\ a\ P\ \beta}{u_s\ avg\ \rho_{MG}} = K'_{OG}\ a\ t_G \qquad (32)$$

where

$K'_{OG}\ a$ = over-all mass transfer coefficient, sec^{-1}.

t_G = gas contact time, sec.

MURPHREE LIQUID POINT EFFICIENCY

$$E_{OL} = \frac{x - x_1}{x^* - x_1} \tag{33}$$

Murphree introduced the liquid efficiency concept chiefly for application to the case where the mechanism of vapor-liquid interphase mass transfer makes this efficiency the more fundamental one to use, such as, a rain of liquid droplets falling through a well-mixed vapor. In this example, the composition of the vapor in a given stage would be constant while the liquid composition would undergo a gradual, continuous, change. It is also applicable in the case of cross-flow of liquid on a bubble tray where the gas composition does not change enough to significantly affect the equilibrium concentration, x^* In cases where there is an appreciable change in the gas composition across the tray in the direction of gas flow, an average value of the gas composition should be used in evaluating the liquid point efficiency. To be mathematically correct, this average should be determined by a double integration, i.e., an integration in the direction of gas flow and then an integration in the direction of liquid flow.

The relationship between liquid point efficiency and the number of mass transfer units may be derived in an analogous manner to that used for vapor point efficiency. If it is assumed that the change in total liquid flow rate is negligible, a material balance on a differential element of liquid in the froth is,

$$L\,x - K_{OL}\,a\,\rho_{ML}(x - x^*)\,Z\,A_T dW = L(x + dx) \tag{34}$$

$$- K_{OL}\,a\,\rho_{ML}(x - x^*)\,Z\,A_T dW = L\,dx \tag{35}$$

Now if it is assumed that plug flow of the liquid exists and that x^* and $K_{OL}\,a\,Z$ are constant along the length of the tray, Equation (35) may be integrated between the limits $x = x_1$ at $W = 0$ and $x = x$ at $W = 1$.

$$- \frac{K_{OL}\,a\,\rho_{ML}\,Z\,A_T}{L} \int_0^1 dW = \int_{x_1}^{x} \frac{dx}{(x - x^*)} \tag{36}$$

$$- \frac{K_{OL}\,a\,\rho_{ML}\,Z\,A_T}{L} = \ell n \left(\frac{x - x^*}{x_1 - x^*}\right) \tag{37}$$

$$N_{OL} = \frac{K_{OL}\,a\,\rho_{ML}\,Z\,A_T}{L} = -\ell n\,(1 - E_{OL}) \tag{38}$$

Much like the case of N_{OG}, the specific interfacial area in N_{OL} has been defined in several different ways depending upon the investigator. In Table I, the definitions of N_{OG} and N_{OL} used by several investigators are presented. Gerster[2] has defined the specific interfacial area as square feet per cubic feet of liquid holdup on the tray. In this case, N_{OL} is defined as follows,

$$N_{OL} = \frac{K_{OL}\,a\,\rho_{ML}\,Z\,A_T}{L} = \frac{K_{OL}\,\bar{a}\,\rho_{ML}\,Z_c\,A_T}{L} = K_{OL}\,\bar{a}\,t_L \tag{39}$$

where $\bar{a}$ = interfacial area, ft^2/ft^3 liquid holdup on the tray.

Z_c = clear liquid height on the tray, ft.

The relationship between the point efficiency and the resistance in each phase may be derived as follows:

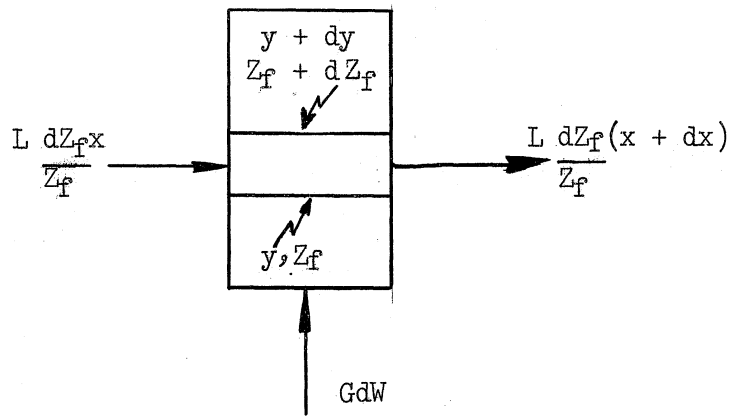

Material Balance on a Differential Element in the Froth

$$- k_G a P(y - y_i) dZ_f \left(\frac{Z_f - Z_c}{Z_f}\right) A_T dW = G dy dW \tag{40}$$

$$k_L \bar{a} \rho_{ML}(x_i - x) dZ_f dW A_T \frac{Z_c}{Z_f} = L \frac{dZ_f}{Z_f} dx \tag{41}$$

$$- K_{OG} a P(y - y^*) dZ_f \left(\frac{Z_f - Z_c}{Z_f}\right) dW A_T = G dW dy \tag{42}$$

If $y = mx$, Equations (40), (41), and (42) may be combined to obtain the following relationships,

$$\frac{1}{\frac{K_{OG} a d(Z_f - Z_c) A_T}{G}} = \frac{1}{\frac{k_G a d(Z_f - Z_c) A_T}{G}} + \frac{\frac{mG}{L}}{\frac{k_L \bar{a} \rho_{ML} d Z_c A_T}{L}} \tag{43}$$

$$\frac{1}{K'_{OG} a dt_G} = \frac{1}{k'_G a dt_G} + \frac{mG/L}{k_L \bar{a} dt_L} \tag{44}$$

$$\left(\frac{1}{K'_{OG} a} - \frac{1}{k'_G a}\right) \int_0^{t_L} dt_L = \frac{mG/L}{k_L \bar{a}} \int_0^{t_G} dt_G \tag{45}$$

$$\left(\frac{1}{K'_{OG} a} - \frac{1}{k'_G a}\right) t_L = \frac{mG/L}{k_L \bar{a}} t_G \tag{46}$$

$$\frac{1}{K'_{OG}\, a\, t_G} = \frac{1}{k'_G a\, t_G} + \frac{mG/L}{k_L a\, t_L} \tag{47}$$

$$\frac{1}{N_{OG}} = \frac{1}{N_G} + \frac{mG/L}{N_L} \tag{48}$$

TABLE I

DEFINITIONS OF N_{OG} AND N_{OL}

Investigator	N_{OG}	a	t_G, Θ	A_{sl}	Z_v, h, Z_c	K_{OG}	β
Murphree(59)	$P K_{OG} a \Theta/G$	area per unit time of gas contact	gas residence time on plate			lb. moles/(hr)(ft^2)(atm)	
Walter, et al.(89)	$\frac{P K_{OG} a A_{sl} h}{G}$	area per unit liquid depth per unit slot area		slot area	effective liquid depth	lb. moles/(hr)(atm)(ft^2)	
West, et al.(93)	$K_{OG} a Z_V/G$	area per foot of foam			form height above plate	lb. moles/(hr)(ft^2)(atm)	
Sherwood and Pigford(78)	$K_{OG} a Z_V/G$	area per foot of liquid hold-up			effective depth of liquid	lb. moles/(hr)(ft^2)(atm)	
Gerster(1)	$\frac{K'_{OG} a \beta}{u_s} = K'_{OG} a t_G$	area per unit volume of gas hold-up	$\frac{\beta}{u_s}$ = gas contact time			lb. moles per (hr)(ft^2) (lb. moles/ft^3)	gas hold-up ft^3 per ft^2 tray area

	N_{OL}	a	t_L	A_{sl}	Z_v, h, Z_c	K_{OL}
Walter, et al.(89)	$\frac{K_{OL} a A_{sl} h}{L}$	area per unit liquid depth per unit slot area		slot area	effective liquid depth	lb. moles/(hr)(ft^2) (mol fraction)
Sherwood and Pigford(78)	$\frac{K_{OL} a \rho_{ML} Z_V}{L}$	area per foot of liquid hold-up			effective depth of liquid	lb. moles/(hr)(ft^2) (lb. mole/ft^3)
Gerster(1)	$\frac{K_{OL} a \rho_{ML} Z_c A_T}{L}$	area per cubic foot of liquid hold-up	liquid contact time		average clear liquid height on tray	lb. moles per (hr)(ft^2) (lb. moles/ft^3)

BASIC RELATIONSHIPS BETWEEN POINT EFFICIENCY AND PLATE EFFICIENCY

The relationships between point efficiency and plate efficiency have been derived by use of the basic rate-process concepts. The liquid flows in the horizontal direction across the tray and contacts gas flowing in the vertical direction. Therefore, the concentration in the liquid changes continuously across the tray and if the gas entering the tray is uniform in concentration, the driving force for mass transfer varies along the length of the tray. Kirschbaum[50,51], Stone[85], and Peavy and Baker[66], removed liquid samples from various points on a bubble plate in relatively large columns and found appreciable differences in concentration. Gerster[2] and Warzel[92] found significant concentration gradients on trays of medium size. Gadwa[31] took liquid samples from a five-inch tower and found small horizontal liquid concentration gradients but concluded that their effect was negligible. In order to predict plate efficiency starting from a general correlation of point efficiency, it is necessary to be able to predict the variation of the liquid concentration with distance along the tray. This problem has been studied by several investigators[4,21,30,32,50,51,72,85] and the solution to the problem has varied considerably, depending upon the method or model used to characterize the liquid mixing on the tray. The differential equations or difference equations and the solutions to these equations which have been used by various investigators to describe the system of mass transfer and liquid mixing on bubble trays are presented in Table II.

The necessity for knowing the amount of liquid mixing can be best explained by presenting the derivations for some of the relationships between point efficiency and plate efficiency.

TABLE II

RELATIONSHIPS BETWEEN POINT AND PLATE EFFICIENCY

Investigator	Terms in Differential Equation: Flow	Mixing ($\psi - \psi'$)	Interphase Transfer	Boundary Conditions	Relationship Between Point and Plate Efficiency
Lewis(53)	$L\frac{dx}{dW}$	Plug flow = 0	$E_{OG}(mx - y_1)$	$x = x_o$ at $W = 1$	$E_{MV}/E_{OG} = (e^{\lambda E_{OG}} - 1)/\lambda E_{OG}$
Warzel(92)	$L\frac{dx}{dW}$	$(C - 1)L\, dx/dW$	$E_{OG}(mx - y_1)$	$x = x_o$ at $W = 1$	$E_{MV}/E_{OG} = (e^{\frac{\lambda E_{OG}}{C}} - 1)/\frac{\lambda E_{OG}}{C}$
Crozier(21)	$\frac{L\, d[x_n(W)]}{dW}$	$Kd[x\,(W+\Delta W)]$	$E_{OG}(mx - y_1)$	$x = x_o$ at $W = 1$	$E_{MV}/E_{OG} = (e^{\frac{\lambda E_{OG}}{1+\gamma}} - 1)/\frac{\lambda E_{OG}}{1+\gamma}$
Robinson(72)	$L\, dx/dW$	$\frac{-D_E Z_c B \rho_{ML}}{S}\frac{d^2x}{dW^2}$	$E_{OG}(mx - y_1)$	$x = x_o$ at $W = 1$; $dx/dW = 0$ at $W = \infty$	$E_{MV}/E_{OG} = \frac{e^{\eta} - 1}{\eta}$
Robinson(72)	$L\, dx/dW$	$\frac{-D_E Z_c B \rho_{ML}}{S}\frac{d^2x}{dW^2}$	$E_{OG}(mx - y_1)$	$x = x_o$ at $W = 1$; $\frac{dx}{dW} = 0$ at $W = 1$	$E_{MV}/E_{OG} = \frac{1 - e^{-(\eta+M)}}{(\eta+M)(\frac{2\eta+M}{\eta})} + \frac{e^{\eta} - 1}{\eta(\frac{2\eta+M}{\eta+M})}$
Anderson(4)	$L\, dx/dW$	$\frac{-D_E Z_c B \rho_{ML}}{S}\frac{d^2x}{dW^2}$	$E_{OG}(mx - y_1)$	$x = x_o$ at $W = 1$; $\frac{dx}{dW} = 0$ at $W = 1$; $x_1 = x_e - \frac{D_E Z_c B \rho_{ML}}{ZL}\frac{dx}{dW}$ at $W = 0$	$\frac{E_{ML}}{1 - E_{ML}} = \frac{[1 - \eta(\frac{\eta+M}{M})]}{(2\eta+M)e^{\eta+M}} + (1 - \frac{\eta}{2\eta+M})(1 + \frac{\eta}{M})e^{\eta}$

A material balance for a differential element in the froth on a bubble tray is shown in Figure (1) for the material being transferred from the gas to the liquid phase or vice versa.

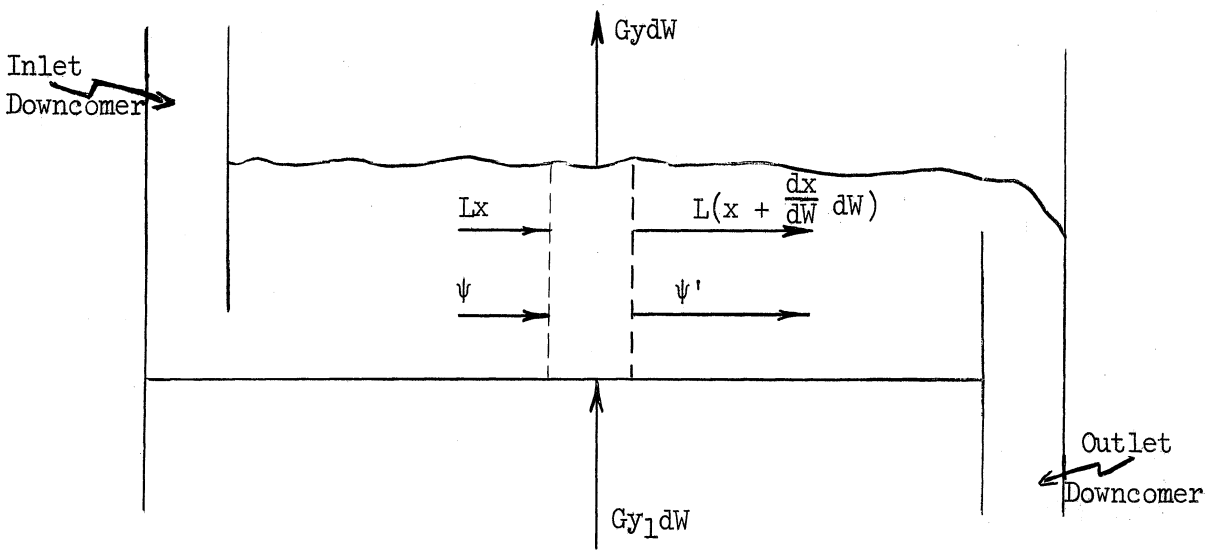

Figure 1. Mixing Model Used to Derive Relationships Between Point and Plate Efficiency.

The material transferred to and from the elements by liquid mixing on the tray is represented by the terms, ψ and ψ'. For the case of plug flow of the liquid, material balance on the element is,

$$Lx + Gy_1 dW = L(x + \frac{dx}{dW} dW) + GydW \tag{49}$$

or

$$L \frac{dx}{dW} = - G(y - y_1) \tag{50}$$

By use of the definition for point efficiency, $E_{OG} = (y - y_1)/(mx - y_1)$, the term, $(y - y_1)$, may be replaced by $E_{OG}\ (mx - y_1)$ to give the following result:

$$\frac{dx}{dW} + \frac{mG}{L} E_{OG}\, x = \frac{G\, E_{OG}}{L} y_1 \tag{51}$$

The general solution to the above first-order differential equation is,

$$x - y_1/m = C_1 e^{-\lambda E_{OG} W} \tag{52}$$

if it is assumed that E_{OG} is independent of the position on the tray. Other assumptions which are implied in the derivation of this equation are: (1) the gas entering the tray is homogenous in concentration, (2) the number of moles of gas remains constant as it rises through the liquid, and (3) gas distribution is uniform over the plate.

If the boundary condition of $x = x_o$ at $W = 1$ is applied, the relationship which may be used to predict the concentration at any point on the tray is,

$$\frac{x - y_1/m}{x_o - y_1/m} = e^{\lambda E_{OG}(1 - W)} \tag{53}$$

where

$$\lambda = mG/L$$

In order to arrive at the relationship between point and plate efficiency, Equation (53) must be combined with the definitions for E_{OG}, Murphree point efficiency, and E_{mv}, Murphree plate efficiency.

$$E_{OG} = \frac{y - y_1}{mx - y_1} \tag{54}$$

or $$y = E_{OG}\, mx - E_{OG}\, y_1 + y_1 \tag{55}$$

$$E_{MV} = \frac{y_{avg} - y_1}{mx_o - y_1}$$

where

y_{avg} = the average concentration of the gas leaving the tray.

mx_o = y^*, the gas in equilibrium with the liquid leaving the tray.

If the following definition for y_{avg} is used,

$$y_{avg} = \frac{\int_o^1 y\,dW}{\int_o^1 dW} = \int_o^1 y\,dW \tag{57}$$

$$y_{avg} = \int_o^1 E_{OG}\, mx\,dW - \int_o^1 E_{OG}\, y_1 dW + \int_o^1 y_1 dW \tag{58}$$

Substituting in Equation (58) the relationship for x as a function of W,

$$y_{avg} = \int_o^1 E_{OG}\, m(x_o - y_1/m)\, e^{\lambda E_{OG}(1 - W)}\, dW + \int_o^1 y_1 dW \tag{59}$$

or

$$y_{avg} = E_{OG}\, m(x_o - y_1/m)\left(\frac{e^{\lambda E_{OG}} - 1}{\lambda E_{OG}}\right) + y_1 \tag{60}$$

$$\frac{y_{avg} - y_1}{mx_o - y_1} = E_{OG}\left(\frac{e^{\lambda E_{OG}} - 1}{\lambda E_{OG}}\right) \tag{61}$$

$$E_{MV}/E_{OG} = \frac{e^{\lambda E_{OG}} - 1}{\lambda E_{OG}} \tag{62}$$

Equation (62) is the relationship derived by Lewis[53] for the case where liquid flows across the tray without mixing and the vapor entering the tray is uniform in concentration. Lewis developed equations for two other types of vapor-liquid contacting but these are not thought to be applicable in most bubble plate columns.

In the cases where the mixing terms, ψ and ψ', in Figure 1, are not zero (i.e., when the assumption of plug flow does not apply), these terms must appear in the material balance on the differential element used to derive the differential equation which describes the system. Warzel[92] defined a mixing parameter "C" in terms of the terminal concentrations on a bubble-cap tray identical in design to the one used in the present investigation. Warzel's definition of "C" is,

$$C = \frac{x_1 - x_o}{x_e - x_o} \tag{63}$$

where x_o = concentration in liquid leaving the tray, mol fraction.

x_1 = concentration in liquid entering the tray, mol fraction.

x_e = concentration in liquid at a point on the tray between the inlet down comer and the first row of bubble caps.

According to Warzel's definition, "C" approaches one as plug flow is approached and approaches infinity as complete mixing is approached. The material balance on the differential element for the case where the mixing parameter "C" is used is as follows:

$$CLx + Gy_1 dW = CL(x + \frac{dx}{dW} dW) + GydW \tag{64}$$

The differential equation for this case is,

$$CL \frac{dx}{dW} = - G(y - y_1) \tag{65}$$

Thus, according to Warzel's definition, the mixing on the tray is characterized by an effective flow rate, (C-1)L. The solution to Equation (65) is similar to the equation for the case of plug flow.

$$\frac{x - y_1/m}{x_o - y_1/m} = e^{\frac{\lambda E_{OG}}{C}(1 - W)} \tag{66}$$

The relationship between point efficiency, E_{OG}, and plate efficiency, E_{mv}, is obtained by using Equation (66) and the procedure used for the case of plug flow.

$$\frac{E_{MV}}{E_{OG}} = \frac{e^{\frac{\lambda E_{OG}}{C}} - 1}{\lambda E_{OG}/C} \tag{67}$$

Crozier[21] used a differential difference equation to derive a relationship between point efficiency and plate efficiency using a mixing parameter very similar to that used by Warzel. Crozier defined the mixing parameter in terms of the terminal concentrations on the bubble tray as follows,

$$\gamma = \frac{x_1 - x_o}{x_e - x_o} - \frac{x_1}{x_e} \tag{68}$$

where the nomenclature is identical to that used in the definition of the parameter, "C".

Using the above definition, Crozier derived the following relationship,

$$\frac{E_{MV}}{E_{OG}} = \frac{(e^{\frac{\lambda E_{OG}}{1 + \gamma}} - 1)}{\lambda E_{OG}/(1+\gamma)} \tag{69}$$

Another approach to the problem of mixing has been through the use of the concept of ideal mixing stages. Kirschbaum[50,51] was probably the first to report the use of ideal mixing stages in relating plate and point efficiency. Others who have studied the problem of using ideal mixing stages are Nord[61], Gautreaux and O'Connell[32], and Foss[30].

Gautreaux and O'Connell[32] were able to derive the following analytical expression to relate point and plate efficiency which is much simpler than the suggested solution by Kirschbaum.[51]

$$\frac{E_{MV}}{E_{OG}} = \frac{1}{\lambda E_{OG}} \left[\left(1 + \frac{E_{OG}\lambda}{n}\right)^n - 1 \right] \tag{70}$$

They postulated that "n", the number of ideal mixing stages, is a function of the length of liquid flow path and liquid and gas rates. According to Kirschbaum[51] and Gantreaux and O'Connell[32], a tray with an infinite number of ideal mixing stages corresponds to the case of plug flow, and a tray with one mixing stage corresponds to a perfectly mixed tray. A tray with the number of ideal mixing stages between one and infinity represents the case of partial or incomplete mixing.

A third method of characterizing the mixing on bubble trays has been the use of eddy diffusivity where the mixing terms, ψ and ψ' in Figure 1 are determined by the concentration gradient in the froth. The material balance on the differential element in Figure 1 for this case is as follows,

$$\begin{aligned} Lx + Gy_1 dW - \frac{D_E Z_c B \rho_{ML}}{S} \frac{dx}{dW} &= L\left(x + \frac{dx}{dW} dW\right) + G y dW \\ &- \frac{D_E Z_c B \rho_{ML}}{S} \left(\frac{dx}{dW} + \frac{d\left(\frac{dx}{dW}\right)}{dW} dW\right) \end{aligned} \tag{71}$$

$$\frac{D_E Z_c B \rho_{ML}}{S} \frac{d^2x}{dW^2} - L \frac{dx}{dW} - G(y - y_1) = 0 \tag{72}$$

Replacing $y - y_1$ by $E_{OG}(mx - y)$,

$$\frac{D_E Z_c B \rho_{ML}}{S}\frac{d^2x}{dW^2} - \frac{Ldx}{dW} - G E_{OG} mx = - E_{OG} G y_1 \qquad (73)$$

$$\frac{d^2x}{dW^2} - \frac{LS}{D_E Z_c B \rho_{ML}}\frac{dx}{dW} - \frac{G S E_{OG} mx}{D_E Z_c B \rho_{ML}} = - \frac{G S E_{OG}}{D_E Z_c B \rho_{ML}} y_1 \qquad (74)$$

The general solution to this second-order differential equation is,

$$x - y_1/m = C_1 e^{(\eta+M)W} + C_2 e^{-\eta W} \qquad (75)$$

where

$$\eta = - \frac{M}{2} + \sqrt{\frac{M^2}{4} + \lambda E_{OG} M}$$

$$\eta + M = \frac{M}{2} + \sqrt{\frac{M^2}{4} + \lambda E_{OG} M}$$

$$M = \frac{L_S}{D_E Z_c B \rho_{ML}} = \frac{S^2}{D_E t_L}$$

The constants, C_1 and C_2, in Equation (75) are determined by the boundary conditions at the terminal points of the tray. Gerster and Robinson[35] applied the boundary conditions,

$$x = x_o \text{ at } W = 1$$

$$\frac{dx}{dW} = 0 \text{ at } W = 1$$

and obtained the following relationship between liquid concentration and the fraction of distance along the tray.

$$\frac{x - y_1/m}{x_o - y_1/m} = \frac{\eta}{2\eta + M} e^{(\eta+M)(W-1)} + \left(1 - \frac{\eta}{2\eta + M}\right) e^{\eta(1-W)} \qquad (76)$$

When this equation and the equation which defines E_{OG} are combined and the integration along the length of the tray is performed, the following

relationship between E_{OG} and E_{MV} is obtained:

$$\frac{E_{MV}}{E_{OG}} = \frac{1 - e^{-(\eta+M)}}{(\eta+M)\left(\frac{2\ \eta+M}{\eta}\right)} \quad \frac{e^{\eta} - 1}{\left(\frac{2\ \eta+M}{\eta+M}\right)} \tag{77}$$

Anderson[4] applied the same set of boundary conditions to obtain a solution very similar to Equation (77) by Robinson.[72] However, Anderson used the boundary condition at the inlet to the tray, i.e.,

$$x_1 = x_e - \frac{D_E\ Z_c\ B\ \rho_{ML}}{SL} \frac{dx}{dW} \tag{78}$$

to obtain the following relationship:

$$\frac{x_1 - y_1/m}{x_o - y_1/m} = \frac{\left[1 - \eta\left(\frac{\eta+M}{M}\right)\right]}{(2\ \eta+M)} e^{-(\eta+M)}$$

$$+ \left(1 - \frac{\eta}{2\ \eta+M}\right)\left(1 + \frac{\eta}{M}\right) e^{\eta} \tag{79}$$

Now if $y_1/m = x^*$,

$$\frac{x_1 - y_1/m}{x_o - y_1/m} = \frac{x_1 - x^*}{x_o - x^*} = \frac{E_{ML}}{1 - E_{ML}} \tag{80}$$

Equation (80) is valid only in the case where the change in concentration of the gas does not change significantly as it flows across the tray, i.e., when $y_1 = y_{avg}$ above the tray.

Foss[30] has shown the plate efficiency to be a function of the residence-time distribution of the liquid on the tray. The rate of mixing was characterized by Foss[30] by the rate-of-increase-of-variance of the ages of fluid elements as they flowed across the tray. The expressions derived by Foss included a distribution function, f(t), of the liquid residue time on the tray.

$$\frac{E_{MV}}{E_{OG}} = \frac{1 - \int_o^\infty e^{-\lambda E_{OG} t/\tau} f(t)dt}{\lambda E_{OG} \int_o^\infty e^{-\lambda E_{OG} t/\tau} f(t)dt} \tag{81}$$

where τ = mean residence time of the total flow.

t = residence time of a differential fluid stream.

The result for the Murphree liquid efficiency is,

$$E_{ML} = \frac{1 - \int_o^\infty e^{-\lambda E_{OG} t/\tau} f(t)dt}{1 - \lambda^{-1}[1 - \int_o^\infty e^{-\lambda E_{OG} t/\tau} f(t)dt]} \tag{82}$$

The integrals in Equations (81) and (82) are the La Place transformation of $f(t)$ and it is possible to use a table of transforms to compute E_{MV}/E_{OG} and E_{ML} quickly when a functional form of $f(t)$ is given.

Foss showed that the rate-of-change-of-variance determined during his investigation could be correlated with the froth momentum as follows,

$$\frac{d\sigma^2}{dW\ Z_c} = A\ (\frac{Z_c}{Z_f}\ V_f)^{-2.8} \tag{83}$$

where Z_c/Z_f = froth density.

By use of the relationships between eddy diffusion coefficient and the residence-time distribution developed by Danckwerts[23], Foss also showed that the rate-of-change-of-variance for the liquid-residence-time distribution could be related to the diffusion coefficient by the following equation,

$$\frac{d\sigma^2}{dW} = \frac{2\ D_E}{V_f^3} \tag{84}$$

where σ^2 = variance of liquid-residence-time distribution.

V_f = mean linear froth velocity, ft/sec.

In addition, Foss[30] used Wharton's[95] eddy diffusion data for a seive tray, 1-foot wide and 5-feet long, and Equation (84) to calculate the rate-of-change-of-variance for the seive tray and showed that the resulting data were correlated very well by use of Equation (83). Thus, Equation (84) seems to be the link between the eddy diffusion coefficient and the residence-time distribution.

The eddy diffusion coefficients reported by Wharton[95] were determined by injecting a salt solution into the froth and then measuring the concentration in the froth at several points upstream from the injection. The gradient on the tray was used to determine the eddy diffusion coefficient by use of the following equation,

$$\log C = - \frac{V_f s}{D_E} + K \qquad (85)$$

which is the solution to the differential equation for unidirectional flow. Stone[85], Robinson[72], and Brown[9] have obtained similar data for bubble-cap trays.

PREVIOUS INVESTIGATIONS OF THE EFFECT OF LIQUID PROPERTIES-VISCOSITY AND DENSITY

In Table III, some of the systems studied in the academic field of research are tabulated. In addition, the type of equipment used, range of efficiencies obtained, and the estimated range of liquid density and viscosity covered by the systems are included in Table III. One possible explanation for the limited data on the effect of liquid viscosity on plate efficiency is the fact that the greatest interest has been in the field of fractionation. The liquids are in many cases at their boiling point in fractionation and therefore only small changes in liquid viscosity are encountered. This follows to a certain extent from the rule-of-thumb that liquids at their normal boiling points exhibit about the same viscosity. The highest liquid viscosity used to-date in a study of plate efficiency is about 22 centipoise. This work was done by Walter.(89) The equipment consisted of a 2-inch diameter column with a segment of a 2-inch diameter cap. Propylene and isobutylene were absorbed in a virgin heavy naphtha, viscosity 1.04 centipoises at 77°F; a virgin gas oil, viscosity 6.2 centipoises at 77°F; and a mixture of a virgin gas oil and an S.A.E. 30 "Zerice" lubricating oil, viscosity 23 centipoises at 77°F. The data from this study plus the data of Horton(44) and Fairbrother(28) for the desorption of carbon dioxide from water and from glycerol-water solutions were used to calculate mass transfer coefficients by use of the relationship suggested by Murphree.(59)

$$E_{MV} = 1 - \exp\left(\frac{-K_G a'' A_{s\ell} h}{G}\right) \qquad (86)$$

where $K_G a$ = over-all gas film coefficient, lb. moles/(hr.)(sq.in. slot area)(in liquid depth)(mole fraction driving force).

$A_{s\ell}$ = total slot area per plate, sq. in.

h = effective liquid depth, in (taken to be the distance from the middle of the slots to the top of the weir or in some cases, the differences between the dydrostatic head and the height of the middle of the slots above the plate.

G = gas rate, lb. moles/hr.

Values of the single film coefficients were then obtained by use of the following relationship:

$$1/K_G a = 1/k_G a + \frac{1}{Hk_L a} \tag{87}$$

The results for $k_L a$ at a constant slot velocity were correlated by the following equation:

$$k_L a = 3.4/\mu_L^{0.58} \tag{88}$$

In order to develop a relationship between all of the variables involved in their study and the over-all mass transfer coefficient, Walter and Sherwood[89] used the data of Carey et. al.[11] for the rectification of ethanol-water to estimate the effect of slot velocity. The over-all coefficient was shown to be proportional to the cube root of the slot width. The effect of liquid viscosity on the gas-phase mass transfer coefficient was assumed to be identical to that found for the liquid coefficient (see Equation 88). Experimental data were used to show that the

TABLE III

SUMMARY OF PREVIOUS EFFICIENCY STUDIES

Investigator	Distillation Systems	Column-Size	Liquid Properties* Density	Liquid Properties* Viscosity	Pressure, ATM	Range of Efficiency, %
Gadwa(31)	Alcohols-water, benzene-carbon tetrachloride	5-inch square				E_{MV}, 70 to 99
Langdon and Keyes(52)	Isopropanol-water					E_{MV}, 70 to 92
Lewis and Smoley(53) and Nord(61)	Benzene-toluene-xylene					E_{MV}, 30 to 75
Carey, Griswold, Lewis and McAdams(11)	Benzene-toluene	8-inch and 6-inch diameter				E_{MV}, 70
	Ethanol-water	6-inch diameter (single plate)				E_{MV}, 50 to 100
	Aniline-water	8-inch diameter (ten plates)				E_{MV}, 58
Uchida and Matsumoto(87)	Ethanol-water, methanol-water	25-cm diameter (41 plates)				E_{MV}, 85 E_{MV}, 70
Rhodes and Slachman(71)	Ethanol-water, benzene-toluene					E_{MV}, 80 E_{MV}, 65
Peavy and Baker(66)	Ethanol-water	18-inch diameter (10, 3-inch caps 3 plates)				
Grohse, et al.(31)	Extractive distillation of C_4 hydrocarbons	13-inch diameter (ten plates, 13 caps per plate)				E_{MV}, 47 to 61
Schilling, Beyer, and Watson(75)	Ethanol-water	18-inch diameter (5 plates, 10, 3-inch caps per tray)				E_{MV}, 100 E_{OG}, 83
Oliver and Watson(64)	Acetone-water, ethanol-water, ethylene dichloride - toluene	18-inch diameter (5 plates, 10, 3-inch caps per tray)				E_{MV}, 40 to 100 E_{MV}, 95
Mayfield, et al.(56)	Propanol-sec-butanol					E_{MV}, 63
Rush and Stirba(73)	Acetic acid-water, methyl isobutyl ketone-water	18-inch diameter (sieve tray)				
	Humidification Systems					
Walter(89)	Humidification of air	2-inch diameter (segment of a 2-inch cap)			1	$E_{MV} = E_{OG}$, 85 to 90
Farrell and Vyverberg(29)	Humidification of air	2-inch diameter (segment of a 2-inch cap)			1 - 4	$E_{MV} = E_{OG}$
Polich(68)	Humidification of air	10-inch diameter (4, 2.4-inch caps)			1	$E_{MV} = E_{OG}$, 68 to 92
Gerster, et al.(35)	Humidification of air	13-inch diameter (13, 1.5-inch caps)				$E_{MV} = E_{OG}$, 87 to 98
West, et al.(93)	Humidification of air	3-1/4 x 2 inches (sieve tray 83, 1/8-inch diameter holes)				$E_{MV} = E_{OG}$, 76 to 95
Ashby(7)	Adiabatic vaporization of water and several organic liquids	7-1/2 x 11-13/16 inches (9, 1-1/2-inch caps)		0.6 - 2.86		$E_{MV} = E_{OG}$, 78 to 96
	Absorption Systems					
Walter(89)	Propylene and isobutylene petroleum fractions	2-inch diameter (segment of a 2-inch cap)		1 - 20 cp	3.15 - 4.5	E_{ML}, 12.5 to 65
Horton(44)	Carbon dioxide in water	18-inch diameter (7, 4-inch caps)		1.1 - 1.3 cp	1	E_{ML}, 60 to 90
Fairbrother(28)	Desorption of carbon dioxide from glycerol-water solutions and water	5-inch square (one 3-1/2 inch cap)		0.5 - 3.7 cp		E_{ML}, 35 to 81
Etherington(27)	Absorption of propane in heavy naphtha containing vistanex	2-inch diameter (segment of a 2-inch cap)		0.4 - 5.0 cp	5.4	
Stone(85)						
Gerster, et al.(35)	Desorption of oxygen from water	9.5 x 45 inches			1	E_{ML}, 25 to 80
Polich(68)	Desorption of oxygen from water	10-inch diameter (4, 2.4-inch caps)			1	E_{ML}, 45 to 92
West, et al.(94)	Desorption of carbon dioxide from water	4 x 3-1/4 inches (sieve plate 83, 1/8-inch holes)			1	E_{ML}, 67 to 85
Warzel(92)	Absorption and desorption, carbon dioxide-water	7-1/2 x 11-13/16 inches (9, 1-1/2-inch caps)			1	E_{ML}, 40 to 90

* Where not otherwise indicated, density and viscosity of the systems are estimated to be in the ranges of 0.5 - 1.0 gm/cc and 0.5 - 1.5 cp.

single phase coefficients were proportional to $V/A_s\ell$. These results and assumptions were then used with Equation (87) to develop the following correlation:

$$E_{MV} = (1 - e^{-m}) \tag{89}$$

where

$$m = \frac{h}{(2.50 + 0.370/HP)\mu_L^{0.58} D_s^{0.33}} \tag{90}$$

Etherington[27] studied the effect of viscosity upon the mass transfer on a bubble cap tray by absorbing propane in a single oil and varying the viscosity of the oil by adding small amounts of "Vistanex", a high molecular weight polymer of isobutylene. The small 2-inch diameter column used by Walter was also used by Etherington. Runs were made at oil viscosities of 0.9, 7.9, and 16 centipoises. Pure propane was used as the gas in order to eliminate the effect of the gas phase resistance. Values of the liquid-film coefficient were calculated by use of the equations used by Walter and Sherwood.[90] (See Equations 86 and 87).

Etherington used the following relationship to correlate his data plus the data by Walter[90], Horton[44], and Fairbrother[28]:

$$\frac{(PK_L a'')(C_{2m}/C_2^{\circ})[\sigma_L(\ell_s + D_s)]^{0.52}}{T^{1.67}(D_L')^{0.67}(\rho_L)^{0.78}} = \frac{B}{\mu_L^A} \tag{91}$$

where B and A are functions of liquid viscosity and where

C_{2m} = the average concentration of the solvent in the liquid film, lb. mols/cu.ft.

C_2° = molal density of the liquid phase, lb. moles/cu.ft.

This relationship was derived by use of the following basis:

1. The equivalent of the Chilton-Colburn[15] evaluation of the total effective liquid-film thickness
2. Geddes'[34] method of evaluating gas bubble diameter, velocity, and flow path in the bubble plate liquid.
3. Arnold's[5] empirical equation for liquid diffusivity.
4. Sherwood's[76] definition of liquid diffusivity and the liquid-film mass transfer coefficient.

In effect, Etherington's results indicate that the dependence of the liquid phase coefficient on liquid viscosity varies with the liquid viscosity. Etherington attributed this effect to a transition from film resistance to eddy resistance controlling liquid-phase mass transfer, or, in other words, a transition from laminar to turbulent film resistance in the liquid. In the range of viscosity between 0.4 and 3.0 centipoises, Etherington reported the value of A in Equation (91) to be 0.17 and between 4.0 and 20.0 centipoises the value was 0.73. Between 3.0 and 4.0 centipoises a transition region was indicated.

During the course of Ashby's studies[7] on the effect of gas physical properties upon mass transfer in the gas phase, the liquid viscosity was varied between 0.5 and 2.5 centipoise. The data from this study have been correlated satisfactorily without including liquid viscosity in the correlation.[1] Quigley, Johnson and Harris[70] studied the effect of liquid properties, viscosity and density, upon the gas holdup due to air flowing through square-edged orifices submerged in various liquids. The liquid density was varied from 62.4 to 98.0 lb./cu. ft. and viscosity from 1.0 to 400 centipoises. Holdup was found to be a

function of the air flow rate only.

$$H = 2.44 \times 10^{-4} Q_G \, 0.84 \qquad (92)$$

where H = holdup of gas in froth, cu.ft./cu.ft. of froth.

Q_G = volumetric air flow rate per orifice, cu. ft./hr.

Average bubble sizes were determined by a stroboscopic light technique. The effect of liquid viscosity on the bubble diameter was found to be small as indicated by the following equation,

$$d_b = 0.222 \, d_o^{\,0.33} \, Q_G^{\,0.125} \, \mu_L/\rho_L^{\,0.02} \qquad (93)$$

where d_b = diameter of equivalent spherical bubble, ft.

d_o = orifice diameter, ft.

μ_L/ρ_L = kinematic liquid viscosity, sq.ft./hr.

Smolin[81] studied the hydraulics for air water on a tray very similar to the one used in the present investigation. The tray was 10 by 12 inches and contained 1-1/2 inch diameter caps. The arrangement of the caps and the skirt clearance were varied. The viscosity of the water was varied over a narrow (up to 5 cp) by the addition of glycerol. Although the cap arrangement on the tray and the cap skirt clearance affected the gas and liquid hold-up on the tray, no effect due to change in liquid viscosity was noted.

Studies directed toward determining the effect of liquid density on plate efficiency are noticeably lacking. Efficiency data are available for systems which cover a narrow range of densities, water and hydrocarbons, but no attempt has been made to correlate these data directly.

Geddes[34] arbitrarily assumed that the bubble formation could be described by equating the buoyant force to the surface tension force at incipient break away of the bubble from the slots. The diameter of the bubble in this case is inversely proportional to the liquid density to the one-third power and the interfacial area is inversely proportional to liquid density to the two-thirds power. Experimental studies of bubble formation at orifices and slots have shown that the assumption made by Geddes is valid only at very low gas rate. Silberman[74] reports that there are actually three regimes of bubble formation depending on the gas rate through the orifice or slot. These are:

(1) The single bubble regime, bubble size dependent on surface tension, liquid density, and orifice diameter and independent of gas rate.

(2) An intermediate regime, bubble size and production rate increase with increase in gas-flow rate.

(3) Jet regime, gas emerges in a more or less continuous jet which breaks up outside the orifice to form bubbles. The rate of bubble formation is nearly constant and the size increases with gas-flow rate.

Correlations of over-all tower efficiency for numerous commercial-size fractionators with liquid viscosity have been presented by Drickamer and Bradford[26] and O'Connell.[62] Drickamer and Bradford's correlation is as follows:

$$E_o = 0.18 - 0.60 \log_{10}\mu_L \qquad (94)$$

where μ_L = molal average viscosity of the feed at the average column temperature, centipoises.

E_o = over-all column efficiency.

This correlation was improved by O'Connell by including relative volatility. Chu[18] has recently proposed the addition of two more factors, liquid to vapor mass ratio and submergence, to improve the correlation.

PURPOSE OF PRESENT INVESTIGATION

The primary purpose of the present investigation is to decrease the uncertainties in accounting for the effects of the liquid properties, viscosity and density, on the mass transfer in the two-phase system on a bubble plate. Although the effect of liquid viscosity has been studied over a significant range in previous investigations, several factors have not been investigated thoroughly during these studies. The most important of these are:

1. When the viscosity or density of the liquid on a bubble plate is varied it is very likely that the hydraulic characteristics of the tray, or more directly, the gas and liquid holdup on the tray, vary accordingly. Now if the results of the mass transfer studies are interpreted without accounting for these variations in gas and liquid holdup as liquid viscosity is varied, nothing has been gained toward determining how viscosity affects plate efficiency. It is of value to determine whether a change in viscosity affects the interfacial area for mass transfer, the mechanism by which mass is transported in the individual phases, or both of these.
2. The effect of diffusivity on mass transfer in the liquid phase has been taken into account in previous studies by use of the dimensionless number, $\frac{\mu_L}{D_L \rho_L}$, the Schmidt Number. In most cases, the liquid properties, viscosity and density, were not varied over a significant range to

justify the use of the Schmidt number. In fact, the liquid diffusivity could have been used to give an equally good correlation. The penetration theory proposed by Higbie[42] and Danckwerts[22] predicts that the mass transfer coefficient is proportional to the liquid diffusivity to the one-half power. In the present investigation an attempt was made to determine whether the Schmidt number or liquid diffusivity is needed in the correlation of mass transfer coefficients for bubble-cap trays.

3. Data on the effect of liquid viscosity on mass transfer in the gas phase have not been reported. This is especially true for the case where the viscosity has been varied over a significant range. A liquid with a high viscosity and adequate vapor pressure was used in the present study to determine this effect by adiabatic vaporization of the liquid.

Efficiency data have been obtained using various liquids of different densities. However, the range of densities covered is approximately 0.5 to 1.0 gm/cc and no significant effect of liquid density has been reported. If the Schmidt number is used to correlate the data for mass transfer in the liquid phase, liquid density is automatically included in the correlation with same power on liquid density and diffusivity. Of course, this combination does not necessarily have to correlate the data. Some investigators[18,34] in attempts to correct for liquid density have assumed that bubbles are produced at the slots, one at a time, with the size of each determined primarily by the orifice diameter, surface tension,

and buoyancy in order to develop a relationship describing the interfacial surface area on a bubble tray. In this case the interfacial area is inversely proportional to the liquid density to the two-third power and independent of the gas rate. However, studies of the bubble size formed as gas flows through slots and orifices submerged in liquid indicate that the above mechanism does not apply since bubble size has been found to be a function of the gas rate.

Although the variation in liquid density will not be as great as the variation in liquid viscosities in most fractionators or absorbers, it is conceivable that a range of 0.2 to 3.0 gm/cc would not be out of the question. Ethylene dibromide with a density of about 2.2 gm/cc was used to extend the range of liquid density used in the investigation of mass transfer in the gas phase.

SUMMARY OF EXPERIMENTAL INVESTIGATIONS

The experimental studies in this investigation are divided into the following three categories:

(1) The mass transfer resistance in the gas phase on a bubble tray where liquid viscosity and density are varied.

(2) Mass transfer resistance in the liquid phase where the liquid viscosity is varied.

(3) Studies of the hydraulics, gas and liquid holdup, on a bubble tray where the liquid viscosity and density are varied.

These studies were performed by use of the following techniques:

(1) Gas phase resistance,

   (a) Adiabatic vaporization of cyclohexanol; gas phase, nitrogen; liquid viscosity varied by varying liquid temperature.

   (b) Adiabatic vaporization of ethylene dibromide; gas phase, nitrogen; liquid density about 2.2 gm/cc.

(2) Liquid phase resistance,

   (a) Absorption of carbon dioxide in cyclohexanol; liquid viscosity varied by varying liquid temperature.

   (b) Liquid concentrations at four points on the bubble-cap tray were used to correct plate efficiency to point efficiency.

(3) Hydraulic characteristics, gas and liquid holdup,

(a) Average liquid holdup was determined by measuring the hydrostatic head of liquid at four different points on the tray.

(b) Gas holdup was determined by subtracting the average liquid holdup from the average froth height. The average froth height was determined visually by use of a graduated scale on the glass window which covered one side of the tray.

MATERIALS

Nitrogen and Carbon Dioxide

Nitrogen and carbon dioxide in cylinders were obtained from the Liquid Carbonics Corporation by the General Stores at the University of Michigan and was supplied for use in the present investigation.

Cyclohexanol ($C_6H_{11}OH$)

The cyclohexanol was supplied gratis by the Dow Chemical Company, Midland, Michigan. Some of the properties of the cyclohexanol were given by Dow.[25] These are presented in Table IV.

TABLE IV

PHYSICAL PROPERTIES OF DOW CYCLOHEXANOL[25]

Freezing Point*, °C	-9**
Boiling Range, 5-95% at 760 mm Hg, °C	156-163
Specific Gravity, 25/25°C	0.948
lb/gal at 25°C	7.89
Refractive Index at 25°C	1.469
Flash Point, °F	145

* Sets to a glasslike solid, no freezing point.

** Literature value for pure cyclohexanol, 23.9°C.[67]

The impurities reported by Dean[24] are phenol, maximum, 0.5 weight percent; cyclohexanone, maximum, 0.1 weight percent; and water, maximum, 0.5 weight percent.

Ethylene Dibromide (CH_2BrCH_2Br)

The ethylene dibromide was also supplied gratis by the Dow Chemical Company. The properties of ethylene dibromide reported by Dow[25] are presented in Table V.

TABLE V

PHYSICAL PROPERTIES OF DOW ETHYLENE DIBROMIDE[25]

Freezing Point, °C	9.3
Boiling Point, °C at 760 mm Hg	131.4
Specific Gravity, 25/25°C	2.172
lb/gal at 25°C	18.07
Refractive Index at 25°C	1.536

The data in Table V are approximately the same values reported in the literature[67] indicating that the ethylene dibromide supplied by Dow does not contain significant amounts of impurities.

EQUIPMENT AND LABORATORY PROCEDURES

A detailed description of the equipment and laboratory procedures is presented in Appendix A, B, and C. In this section, a brief description of the equipment and a summary of the laboratory procedures are presented.

Equipment

The equipment used in this study was also used by Warzel(92) and Ashby.(7) Certain modifications of the equipment were made in order to perform the studies in the present investigation. The modifications are listed in Appendix A. Figure 2 is a general view of the test column plus the auxiliary equipment. The bottom tray in the column was used for a test tray and the second tray from the bottom served as an entrainment separator for the first tray. The dimensions of the tray and the tray layout are presented in Table VI. Briefly, the tray was 7-1/2 inches wide and 11-13/16 inches long and contained 9, 1-1/2 inch diameter, caps. A close-up view of the test tray equipped with caps and the adjustable splash baffle is shown in Figure 3. The outlet weir on the tray was adjustable and studies were made at weir heights of 1-1/2, 2, and 3-1/2 inches. In order to eliminate a large hydraulic gradient on the tray, a splash baffle near the outlet weir was used. This baffle was positioned one-half inch above the top of the weir and one inch in front of the weir in all studies performed. A glass panel in the front of the test tray was used to permit observation of the hydraulic characteristics of the tray.

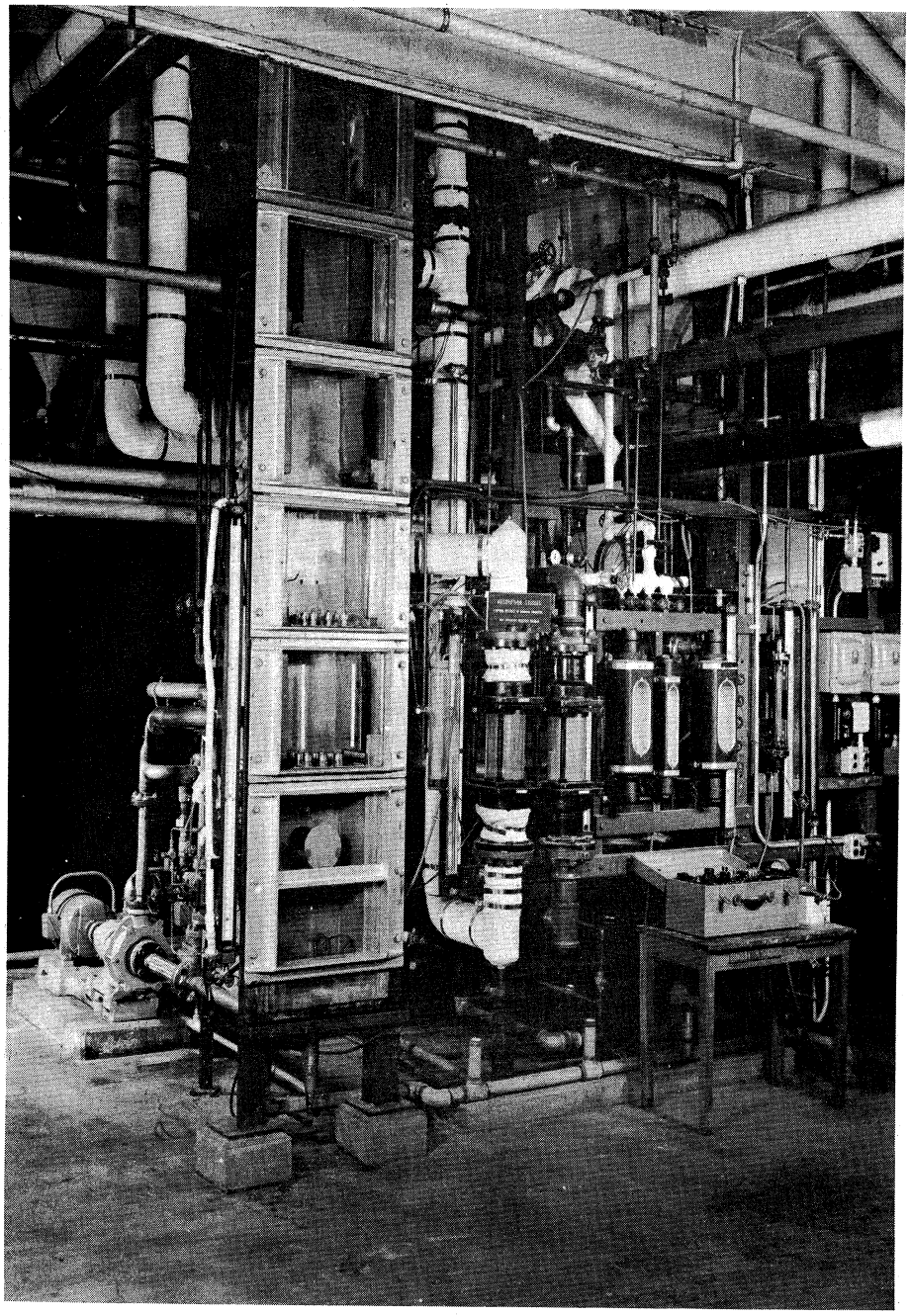

Figure 2. Front View of Test Column and Auxiliary Equipment.

TABLE VI

CHARACTERISTICS OF THE TRAY LAYOUT

Cap		
	Diameter (O.D.)	1-1/2 inch
	Height	1-1/2 inch
	Metal Thickness	1/16 inch
Slot		
	Height	3/4 inch
	Width	1/8 inch
	Number, per cap	18
	Area, per cap	0.0117 sq. ft
	Area, per plate	0.105 sq. ft.
	Area, fraction of bubbling area	0.171
Risers		
	Diameter (O.D.)	1 inch
	Diameter (I.D.)	7/8 inch
	Area, per cap	0.00417 sq. ft.
	Area, per plate	0.0375 sq. ft.
	Area, fraction of bubbling area	0.061
Weir (variable)		
	Length	7-3/8 inches
	Height	1-1/2, 2, and 3-1/2 inches
Splash Baffle (variable)		
	Length	7-3/8 inches
	Clearance above tray floor	2,2-1/2 and 4 inches
Downcomer		
	Size	7-3/8 x 2-1/8 inches
	Area, cross sectional	0.137 sq. ft.
Bubbling Area (taken as space between downcomer and splash baffle)		
	Width	7-1/2 inches
	Length	11-13/16 inches
	Area	0.615 sq. ft.
Tray Spacing		18 inches

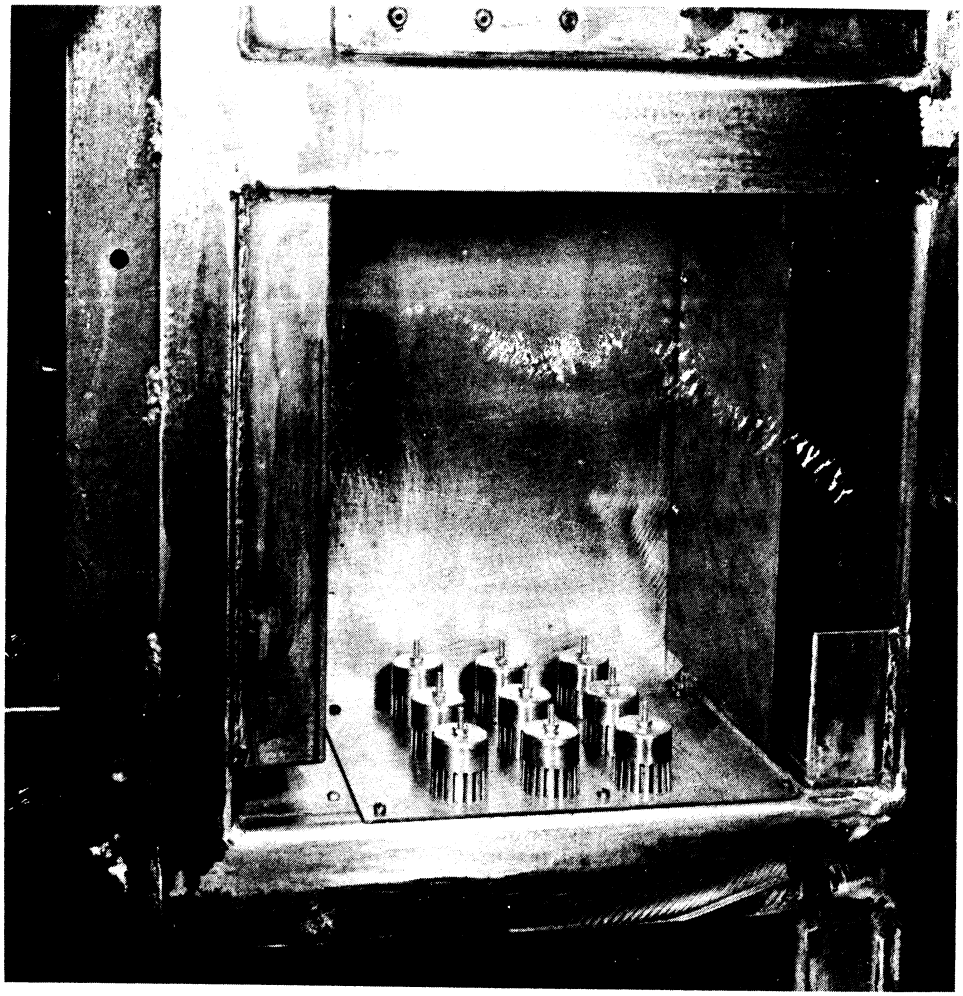

Figure 3. Single Tray in Absorber, Showing Removable Deck and Adjustable Splash Baffle.

A rotary blower (two rotary blowers in the absorption studies) was used to recirculate the gas to the test tray. A Durco pump equipped with a mechanical seal was used to recirculate liquid to the test tray. In the vaporization studies, a second Durco pump was used to recirculate the same liquid as used in the tests to a 12-inch diameter, 4-plate sieve column where the gas from the test tray was dehumidified by countercurrent contact at a lower temperature than the temperature on the tray. In the absorption studies, one of the pumps was used to feed liquid from the sieve column to the test tray and the other one was used to take liquid from the test tray and return it to the sieve-tray column. The sieve-tray column in this case was used to desorb carbon dioxide from the liquid with air from the laboratory. The air to the sieve-tray column was supplied by a third rotary blower.

The liquid and gas to the test tray were metered by use of calibrated Fischer-Porter rotameters. Calibration data for these rotameters are presented in Appendix D. The temperatures of the gas and liquid at the test tray were controlled by use of heat exchangers in the gas and liquid lines. Calibrated mercury-in-glass thermometers were used to measure the temperatures at the test tray. The pressure in the system was controlled by addition of nitrogen in the vaporization studies and by addition of carbon dioxide in the case of the absorption studies. The rate of addition was controlled by a "Pancake" pressure regulator. The pressure above the test tray was measured by a mercury manometer.

Laboratory Procedures - Vaporization Studies

In the vaporization studies, the mass transfer on the tray was determined by measuring the concentration of the gas entering and leaving the tray. These concentrations were determined experimentally by sampling the inlet and outlet gas after adiabatic conditions were established on the tray. The humidity charts in Appendix B were used to calculate the inlet gas temperature when the humidity of the inlet gas and the liquid temperature or adiabatic saturation temperature of the gas were known. The vapor in the gas was determined by passing gas samples from the test column through a series of three U-tubes filled with glass beads and immersed in ice baths. The amount of organic vapors condensed in the U-tubes was determined by weighing the tubes before and after sampling. The volume of each sample was determined by metering the gas in a wet-test meter after leaving the series of U-tubes. The inlet and outlet samples were taken simultaneously while the temperatures on the tray were maintained at adiabatic conditions. The data recorded for each run are shown in the sample data sheet in Appendix F.

Laboratory Procedures - Absorption Studies

The change in the concentration of carbon dioxide in the gas across the test tray was not great enough to be determined accurately. Therefore, liquid samples at the inlet and outlet of the tray were taken and analyzed to determine the amount of mass transfer on the tray. In addition, samples of the liquid at four different points on the floor of the tray were taken and analyzed in order to correct the over-all plate efficiency to a point efficiency. The concentrations of the liquid in the froth were determined at three different horizontal positions for

one series of runs. The locations of the liquid sampling points on the test tray are shown in Figure 4. The position of the sample points on the tray floor in relation to the position of the caps is shown in Figures 5 and 6. The liquid samples were obtained by use of either a hypodermic syringe or a valve connected to the sample point by a 1/4 inch stainless steel tube. When the hypodermic syringe was being used to take samples the desired volume of liquid was withdrawn and injected into the sample bottle which contained 50 ml of 0.1 $Ba(OH)_2$ and was sealed with a syringe stopper. However, when the samples were being taken through the 1/4 inch line and valve, the liquid flowed directly into the sample bottle and a magnetic stirrer was used to mix the cyclohexanol and barium hydroxide. The two methods of sampling were compared by taking consecutive samples from the same point and analyzing for carbon dioxide. At the higher concentrations (at tray outlet) the results agreed within one percent while at the lower concentrations the disagreement was as much as five percent. The amount of carbon dioxide in the samples was determined by titration of the excess barium hydroxide in the sample bottles by use of 0.1 N HCl. Phenolphthalien was used for an end-point indicator.

A sample of the gas leaving the tray was obtained during each run and analyzed for carbon dioxide in order to determine the equilibrium concentration on the tray. The analyses of the gas samples were made by use of a CEC mass spectrometer, Type 21-103C.

Laboratory Procedures - Hydraulic Data

The hydraulic data obtained during this study consist of the average froth height, the clear height or hydrostatic liquid head at four different points on the tray, and the pressure drop in the gas flowing

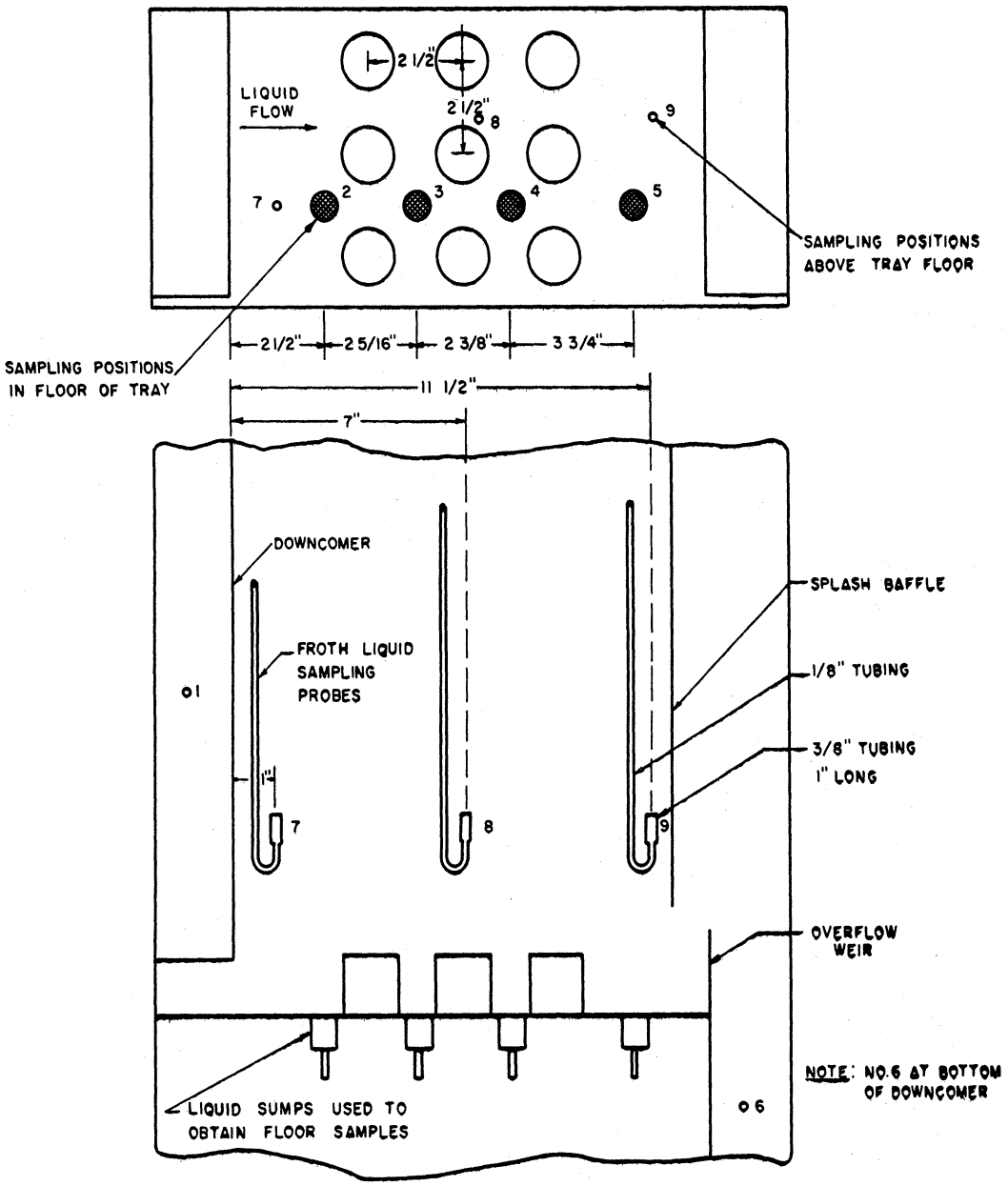

Figure 4. Location of Sampling Points on Test Tray - Points 2,3,4 and 5 Used Also to Measure Hydrostatic Head at Respective Points

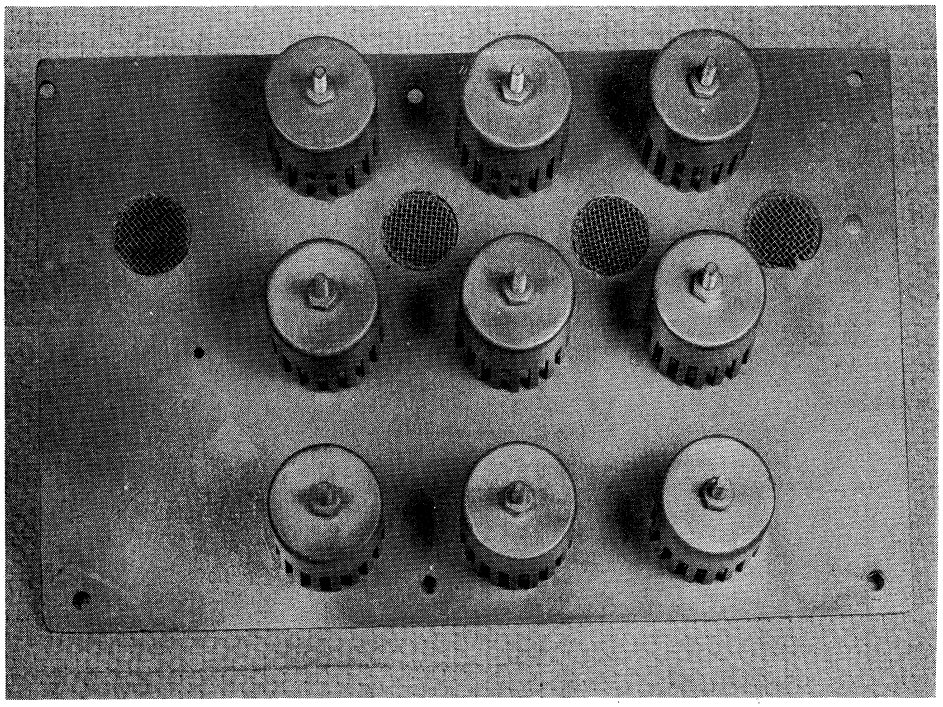

Figure 5. Top View of Removable Tray, Showing Bubble Caps and Location of Liquid Sampling Points.

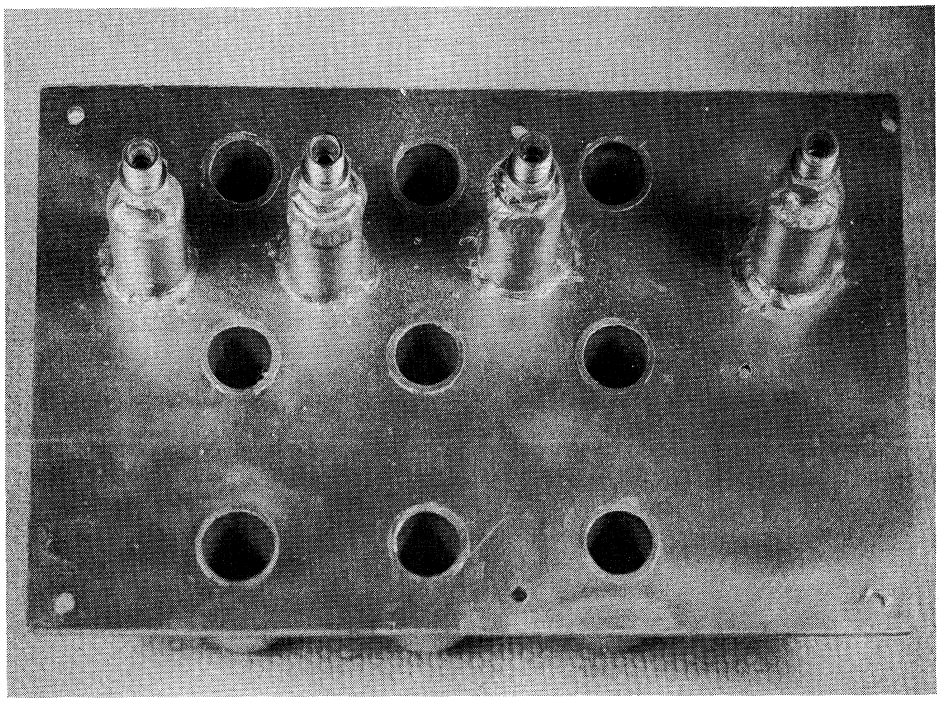

Figure 6. Bottom View of Removable Tray, Showing Inlet to Risers and Liquid Sumps Below Sampling Point.

across the tray. These data were recorded during the course of the studies of vaporization and absorption. The measurement of the froth height was done by visually observing the average height of the froth above the tray floor. Two scales with 0.1 inch graduations placed near the edges of the bubbling area but on the glass panel covering the front of the tray were used to determine the average height. The variations in froth height across the tray plus the fluctuations due to instability of the system were taken into account when determining the froth height. The clear liquid heights were measured at the four points indicated in Figure 4. The pressure drop across the tray was measured by use of a water manometer attached to pressure probes above and below the tray.

PRESENTATION OF DATA

Hydraulic Data - General Observations

The general observations of the hydraulic characteristics which were made during the mass transfer studies and which are worth consideration in the interpretation of these data pertain to the effect of the following variables:

1. Gas rate.
2. Liquid rate.
3. Weir height.
4. Liquid viscosity and density.

Some of the effects of varying liquid and gas rate at a constant weir height and constant liquid viscosity and density can be seen by examining the photographs in Figures 7 and 8. These photographs were made by enlarging single frames from movies made at a film speed of 64 frames per second. In Figure 7, the general appearance of the froth holdup on the tray for the carbon dioxide-cyclohexanol system is shown for the cases of F-factor, 0.62; liquid viscosity, 55 centipoises; and weir height, 3-1/2 inches, at liquid rates of 26.4, 16.2, and 6.6 gpm. The detail in the photographs is not great enough to show the bubbles, or maybe better described as globules, in the froth. However, the photographs do show clearly the effect of the entering liquid on the froth holdup. At the liquid rate of 6.6 gpm, the three rows of caps on the tray were active and the froth was fairly uniform along the length of the tray. But as liquid rate was increased to 13.2 gpm the slots on the side of the first row of caps nearest the inlet downcomer became inactive and a large eddy began to develop in the volume of froth between the first row of caps and the inlet downcomer. At a liquid rate of 26.4

liquid rate, 26.4 gpm

F-factor, 0.62

liquid rate, 13.2 gpm

F-factor, 0.62

liquid rate, 6.6 gpm

F-factor, 0.62

Figure 7. Froth Holdup on Test Tray, Carbon-Dioxide-Cyclohexanol System; Weir Height, 3-1/2 Inches; Splash Baffle Height, 4 Inches; F-Factor, 0.62; Liquid Viscosity, Approximately 55 cp.

gpm, the liquid eddy extended almost to the center of the tray and the gas ensuing from the caps passed through the froth at an angle to the vertical. At a higher gas rate, the entrance effects of the liquid were not as pronounced. In Figure 8, the froth holdup on this tray is shown for the cases of F-factor, 1.1, and liquid viscosity, 55 centipoises, at liquid rates of 26.4, 16.2 and 6.6 gpm. In these cases the slots on the side of the first row of caps nearest the inlet downcomer were completely active or intermittently active. Also the gas seemed to rise almost vertically through froth at a liquid rate of 26.2 gpm and not so much at an angle to the vertical as in the case of a lower gas rate of F-factor, 0.62. It therefore appears that the liquid entrance effects disappear at gas rates above F-factor equals one. However, these effects are significant at high liquid rates and at gas rates below F-factor equals one.

Another observation which can be made by examining the photographs in Figures 7 and 8 concerns the amount of froth holdup in the outlet downcomer as the liquid and gas rates are varied. As might be expected, the holdup in the outlet downcomer increased as the liquid or gas rate increased.

Photographs or movies of the froth holdup on the tray at lower weir heights were not obtained. However, the liquid entrance effects were observed to be similar to those shown in Figures 7 and 8. The principal difference between the characteristics of the froth at 1-1/2 and 2 inch weir heights and those at 3-1/2 inch weir was the form in which the gas flowed through the liquid. At 1-1/2 inch and 2 inch weir heights, there were two distinct types of bubbling. At low gas rates, the gas

flowed through the froth in form of globules or bubbles. At high gas rates, the globules seem to disappear and the gas flowed through the froth in channels or sheets. The value of the gas rate at which the globules disappeared and the gas began to flow through the froth in channels was a function of weir height. With the weir height at 1-1/2 inches the gas globules were broken-up at gas rates above 0.8 F-factor while with the weir height at 3-1/2 inches this did not occur at all up-to an F-factor of 1.2.

The effects of the liquid properties, viscosity and density, on the visual appearance of the froth holdup were very noticeable when the froth holdup for the carbon dioxide-cyclohexanol and nitrogen-ethylene dibromide systems were compared. In the case of the cyclohexanol, at all viscosities, 10-100 centipoises, the gas flowed through the froth in the form of large globules or channels depending on the velocity and weir height with very few smaller bubbles or globules formed due to break-up of the larger gas volumes. The froth holdup for the ethylene dibromide system contained many small gas bubbles giving it a very uniform appearance. However, the small bubbles masked the action of the gas flowing from the caps and it was impossible to see the size of gas particles in that area.

Hydraulic Data - Gas and Liquid Holdup

The clear liquid height or hydrostatic head of liquid was measured at four different points on the tray floor (see Figure 4). The arithmetic average of these four measurements was used as the average clear liquid height or the liquid holdup on the tray. The froth height was determined by visually averaging the variations in froth height along

the length of the tray and the time fluctuations due to the instability of the system. These data were obtained during the course of the mass transfer studies. The gas holdup was determined by subtracting the average clear liquid height from the froth height.

In Figure 9, the clear liquid height on the tray is presented for the nitrogen-cyclohexanol system as a function of the superficial velocity in the column for variable conditions of weir height, liquid viscosity, and liquid rate. Similar data for the nitrogen-ethylene dibromide system are presented in Figure 10. The effect of increasing the weir height is about what would be predicted, i.e., one-half inch or two inch increase in weir height increases clear liquid height about the same amount. This is not exactly true as can be seen in Figure 9 for the nitrogen-cyclohexanol where an increase of one-half inch and two inches in the weir height increased the liquid holdup by 0.4 - 0.5 inch and 1.0 - 1.4 inches, respectively. It should be noted that in no case does the clear liquid height equal the weir height in Figure 9 except in the case of data for the 3-1/2 inch weir where the clear liquid height decreased to a value below the weir height as the gas velocity was increased. For the nitrogen-ethylene dibromide system, the liquid holdup for 3-1/2 inch weir and 7.9 gpm was equal to the weir height and independent of gas velocity. In all cases in Figures 9 and 10, the liquid holdup is not highly dependent on gas velocity.

The effect of increasing the liquid rate is shown by data for the 2 inch weir in Figure 9 and for the 3-1/2 inch weir in Figure 10. In each case the liquid holdup increased as the liquid rate was increased indicating an increased liquid head required to overcome the resistance

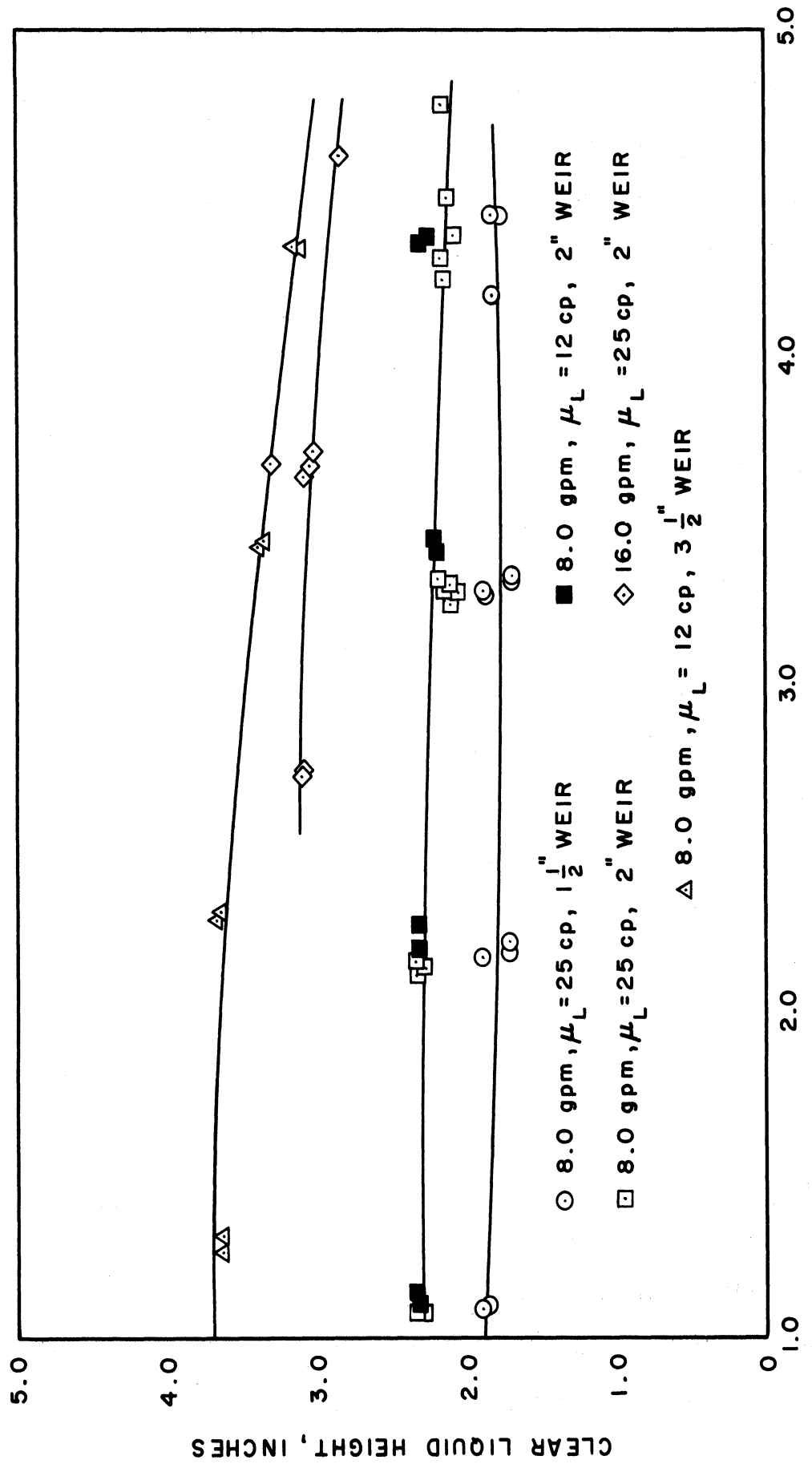

Figure 9. Clear-Liquid-Height Data for Nitrogen-Cyclohexanol System

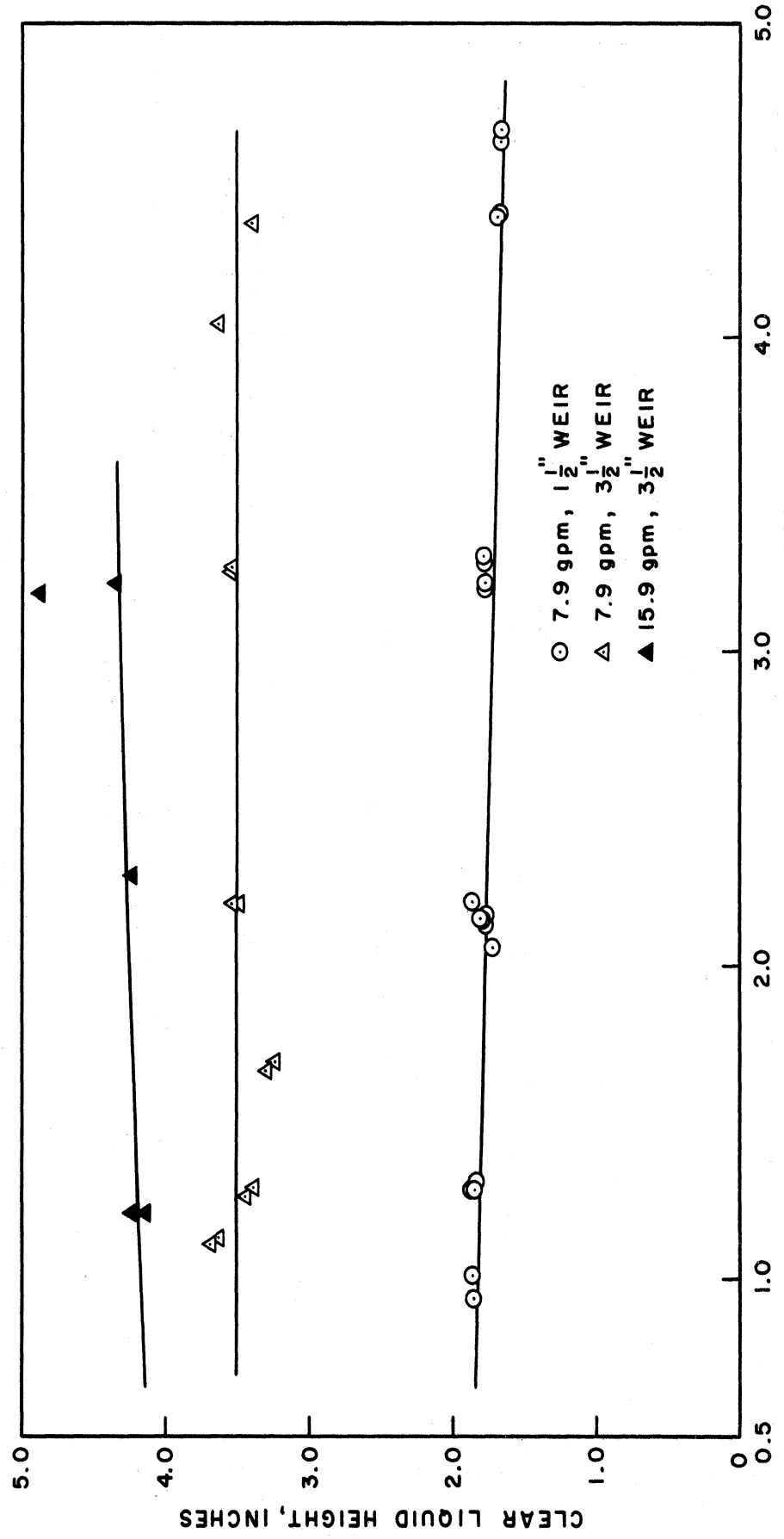

Figure 10. Clear-Liquid-Height Data for Nitrogen-Ethylene Dibromide System

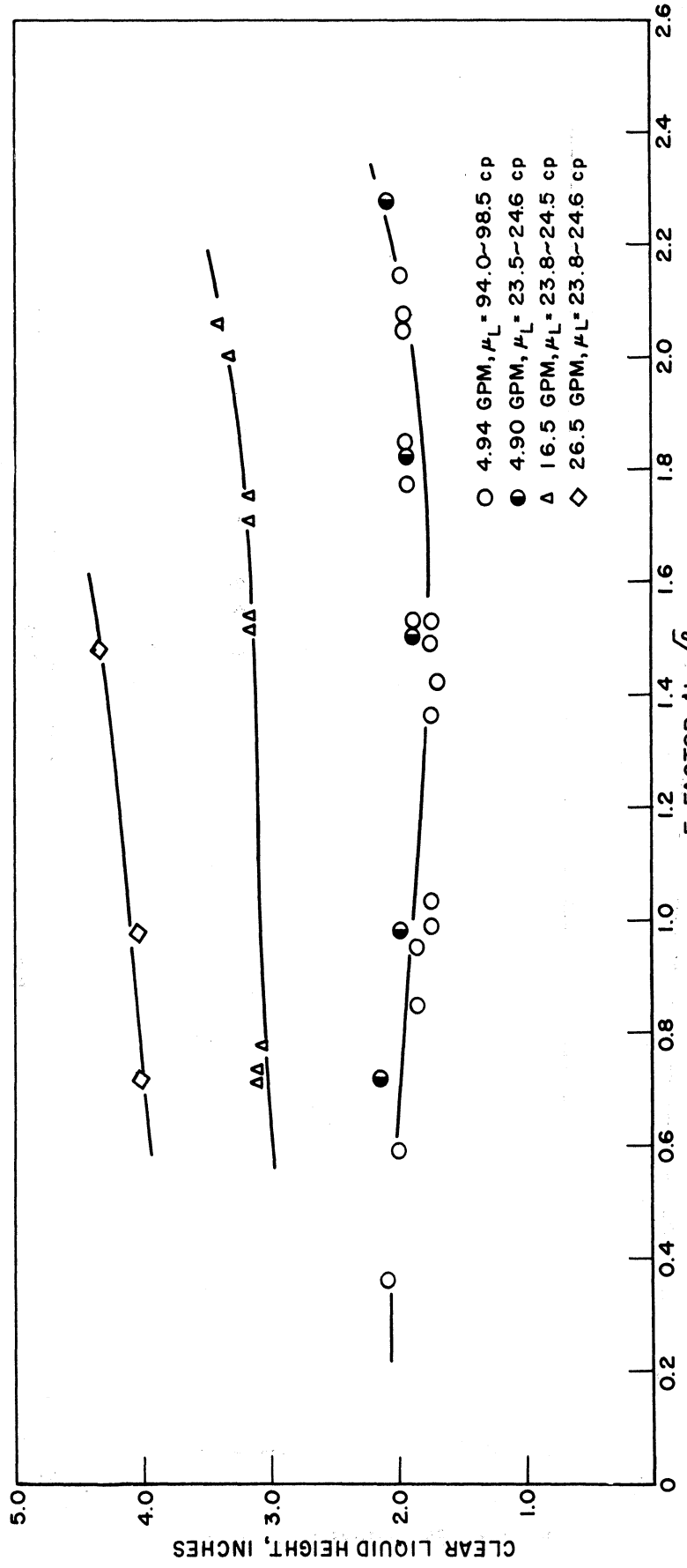

Figure 11. Clear-Liquid-Height Data for Carbon dioxide-Cyclohexanol System at High Gas Rates and Two-Inch Weir Height.

to flow at the splash baffle and weir. Liquid viscosity effects are not considered significant since the data for the two systems in Figure 9 and 10 are about the same at comparable weir heights and liquid rates. The only effect of viscosity is the possible difference in the dependence of liquid holdup on gas velocity. In the case of the cyclohexanol system, the liquid holdup at 3-1/2 inch weir height decreased as the gas rate was increased but the data for the ethylene dibromide system was practically independent of gas velocity at the same conditions.

In Figure 11, the clear liquid height for the carbon dioxide-cyclohexanol system is presented as a function of gas velocity with variable conditions of liquid rate and viscosity. The range of gas velocity in this case is almost twice that for the data in Figures 9 and 10.

Froth height data for the three systems, nitrogen-cyclohexanol, nitrogen-ethylene dibromide, and carbon dioxide-cyclohexanol are presented in Figures 12, 13, and 14 as a function of gas velocity with parameters of liquid rate, weir height, and liquid viscosity. The effect of weir height and liquid rate on froth height is very similar to the effect on clear liquid height. That is, as weir height or liquid rate are increased froth height increases proportionately. However, froth height is definitely dependent on gas velocity in contrast to the almost complete independence of clear liquid height and gas velocity. Liquid viscosity or density does not appear to affect froth height significantly even though the viscosity is varied over the range of 1.5 to 25 centipoises and density over the range of 0.94 to 2.15 gm/cc.

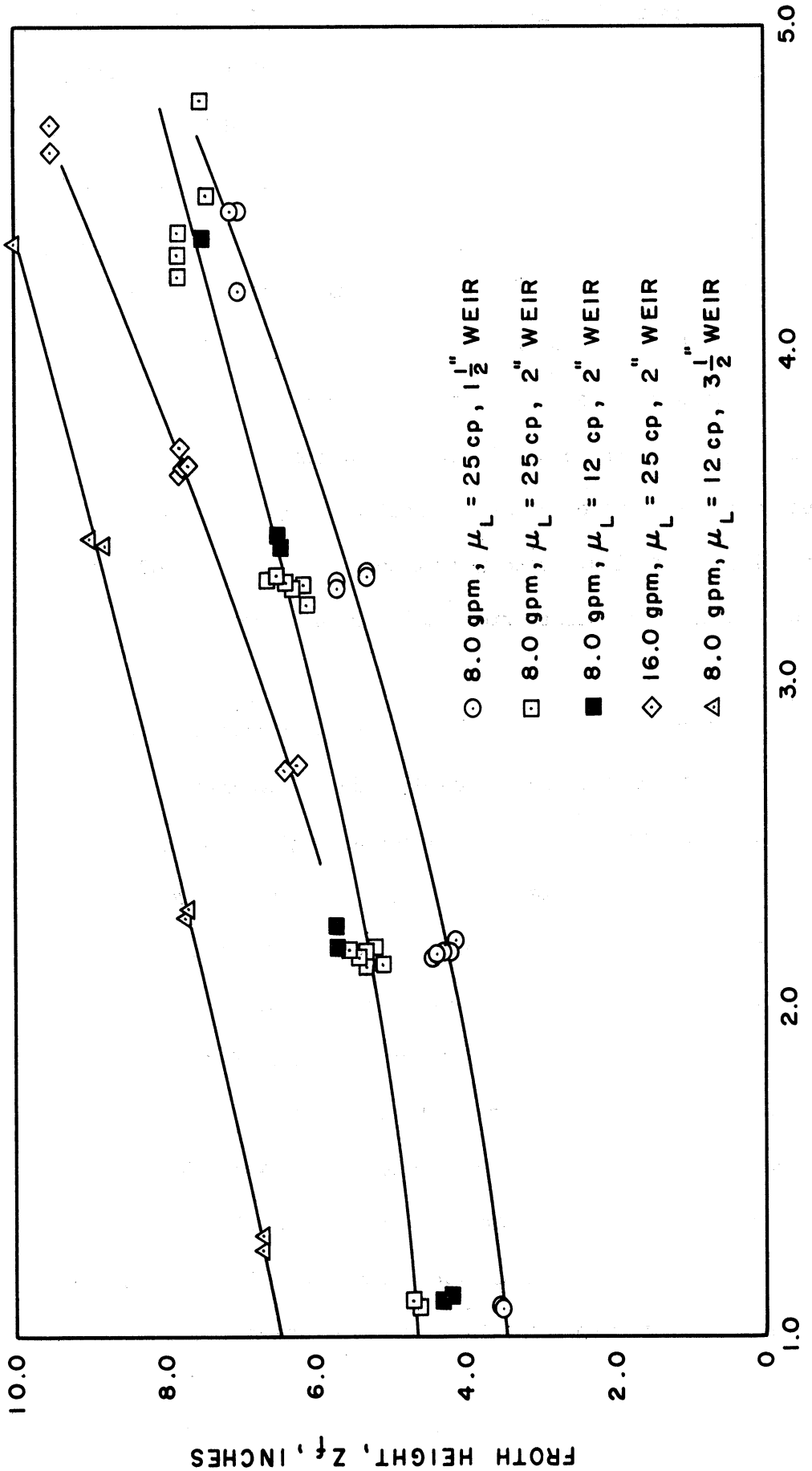

Figure 12. Froth-Height Data for Nitrogen-Cyclohexanol System. Data Are Presented as a Function of Superficial Gas Velocity With Parameters of Weir Height, Liquid Viscosity and Liquid Rate.

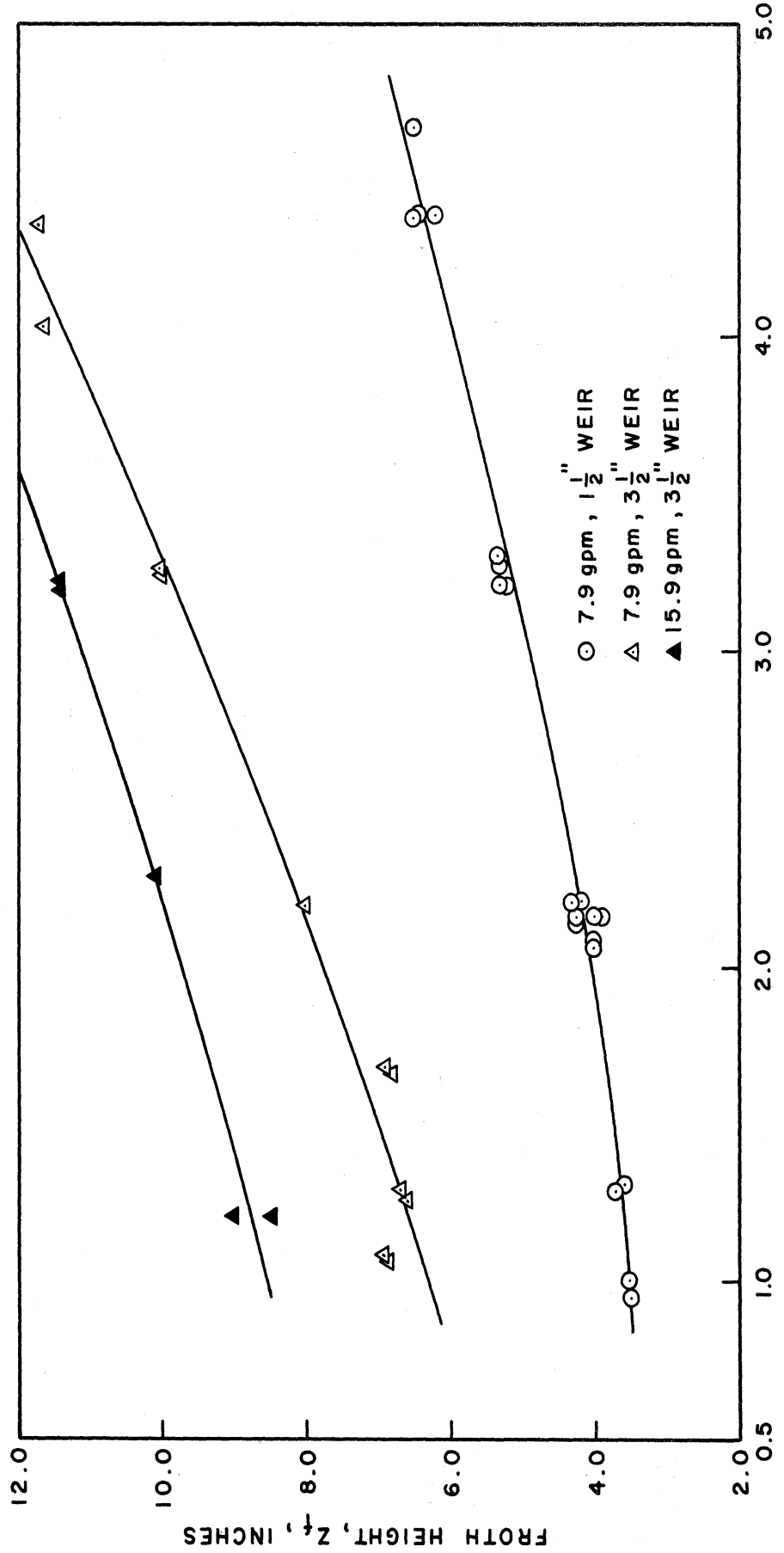

Figure 13. Froth-Height Data for Nitrogen-Ethylene Dibromide System. Data are Presented as a Function Superficial Gas Velocity With Parameters of Weir Height and Liquid Rate

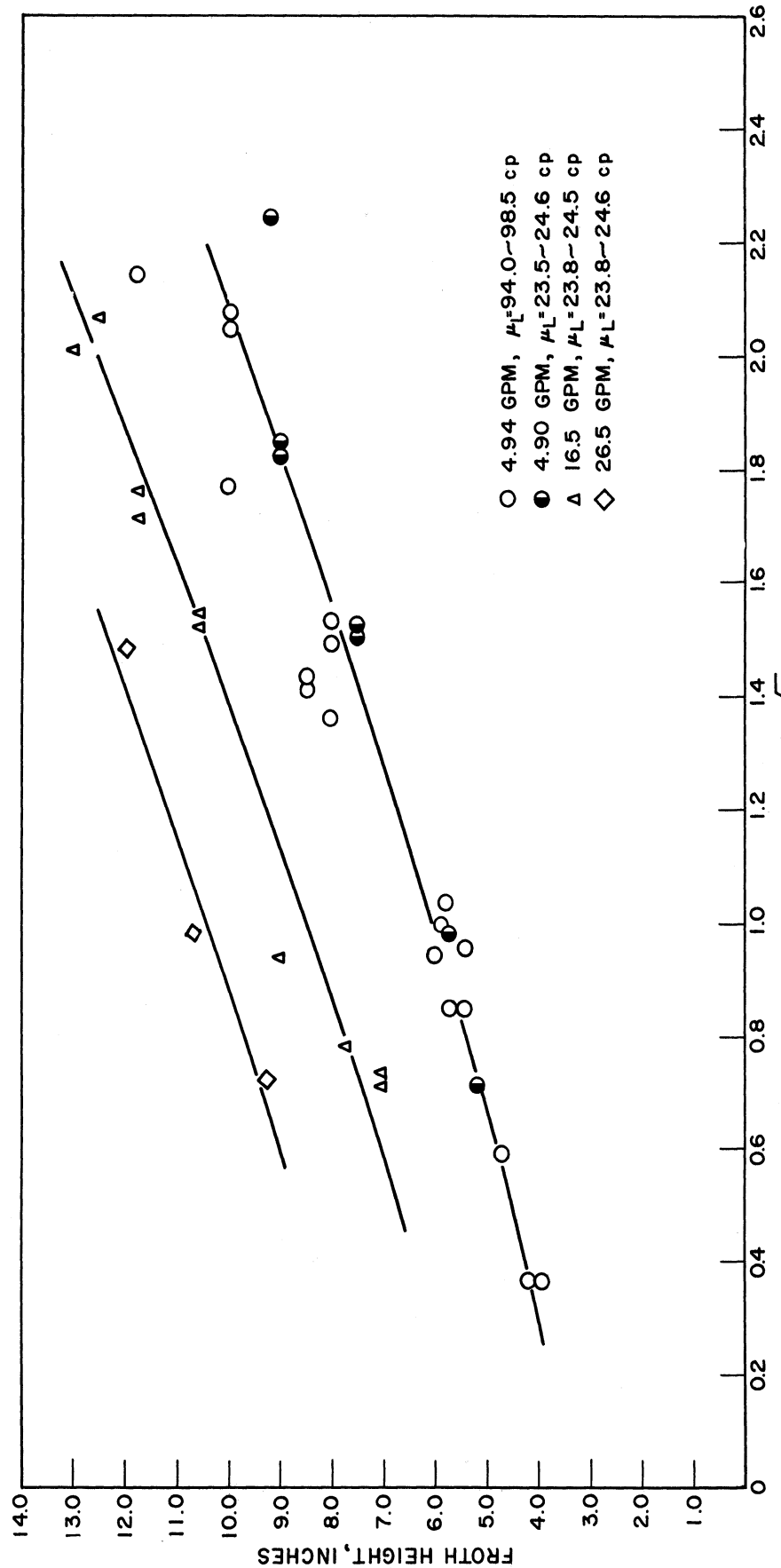

Figure 14. Froth Height Versus F-Factor-Carbon Dioxide-Cyclohexanol System Variable Liquid Viscosity 2-Inch Weir; 2½-Inch Splash Baffle.

In Figures 15 and 16 the froth height data obtained by Ashby[7] plus the data for the nitrogen-cyclohexanol and nitrogen-ethylene dibromide systems are plotted versus gas velocity and F-factor. In Figure 15, where the data are plotted versus gas velocity the best curves through the individual sets of data do not coincide. However, when the same data are plotted versus F-factor, the data may be represented by one curve. Therefore, it appears that the major variables at constant liquid rate and weir height are gas velocity and gas density and not liquid viscosity and density. It should be noted that the ranges of liquid density and viscosity represented by the systems in Figures 15 and 16 are 0.78 to 2.15 gm/cc and 0.5 to 24 centipoises, respectively.

Gas holdup was determined by subtracting the average clear liquid height from the froth height. These data for the nitrogen-cyclohexanol and nitrogen-ethylene dibromide systems are plotted in Figures 17 and 18. Of course, the effects of weir height and liquid rate are similar to the effects of these variables on clear liquid height and froth height. In addition, comparison of the data in the two figures reveals no great effect of liquid viscosity and density except at 3-1/2 inch weir height and high gas velocity. This is shown more effectively in Figure 19 where the data are plotted versus F-factor. Ashby's data are also included in Figure 19. The data for 1-1/2 inch weir height are represented by one curve with no significant deviations due to liquid properties. However, the data for 3-1/2 inch weir height at comparable liquid rates can not be represented by one curve. The gas holdup for the nitrogen-ethylene dibromide system is greater than that for the cyclohexanol and water systems with the lowest values for

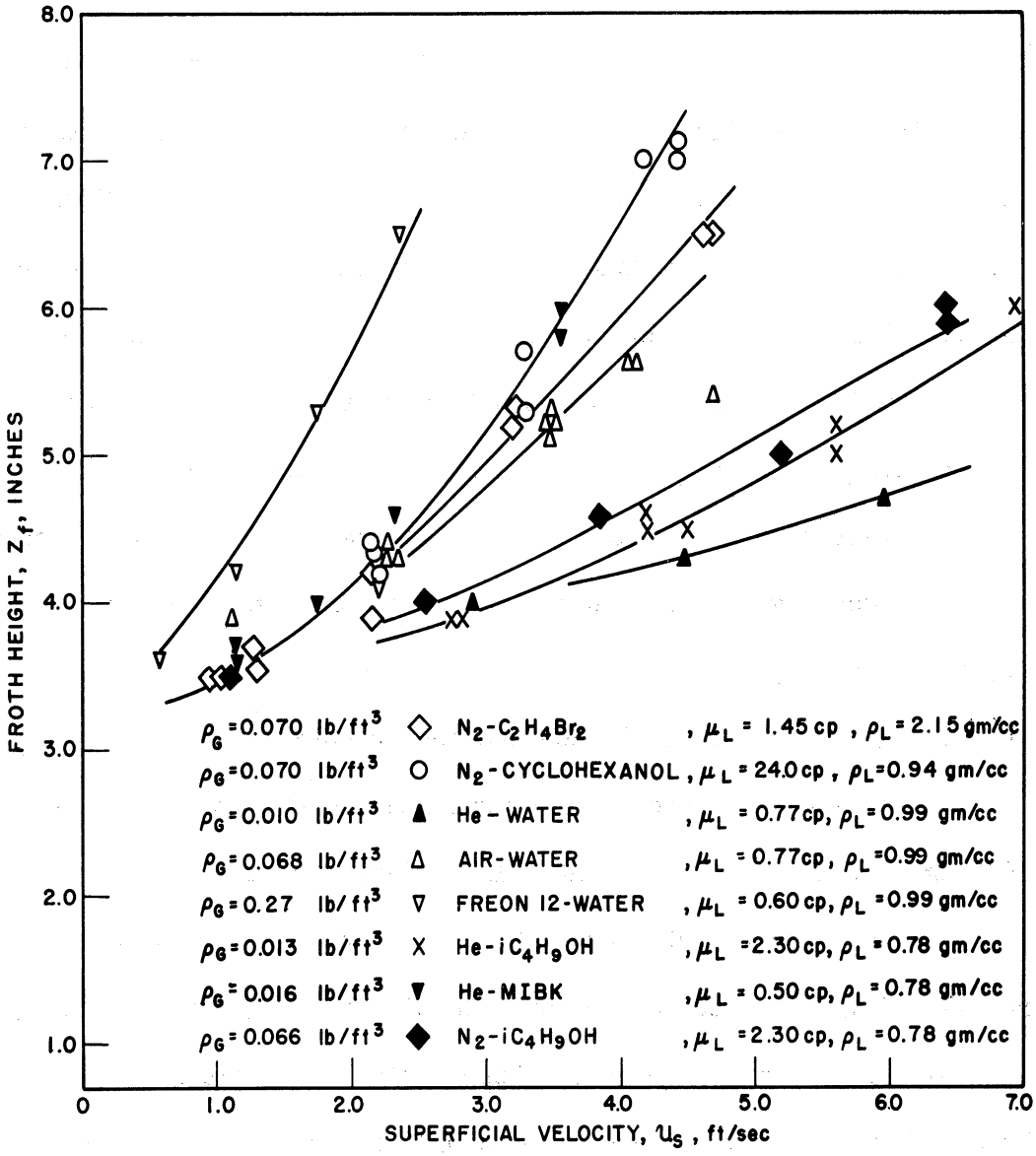

Figure 15. Froth-Height Data for Several Systems Used in Vaporization Studies. Data are Presented as a Function of Superficial Gas Velocity With Parameters of Liquid Viscosity and Density and Gas Density; 1-1/2 inch Weir Height; 8.0 GPM

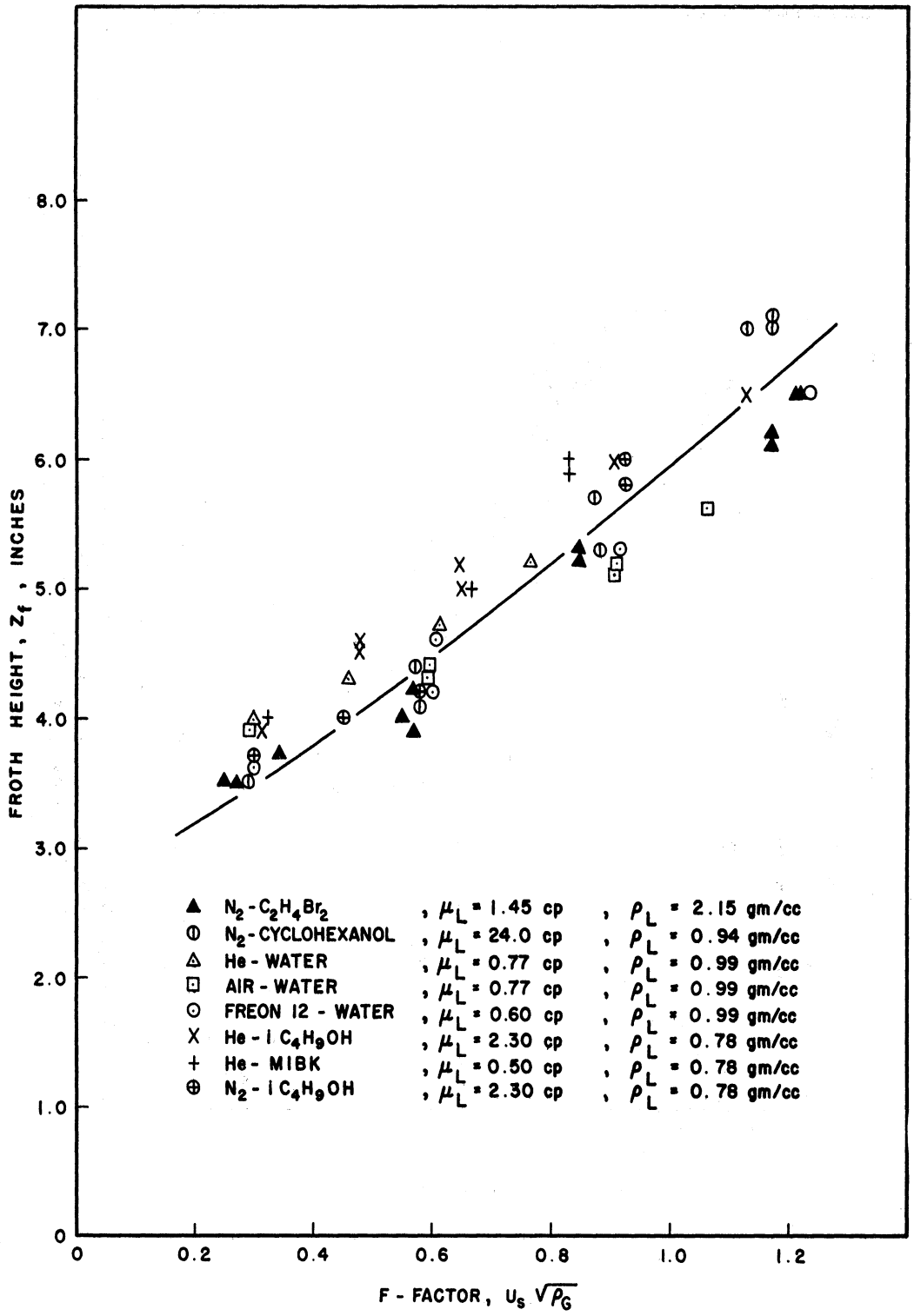

Figure 16. Froth-Height Data for Several Systems Used in Vaporization Studies. Data are Presented as a Function of F-Factor with Parameters of Liquid Viscosity and Density; 1-1/2 inch Weir Height; 8.0 GPM.

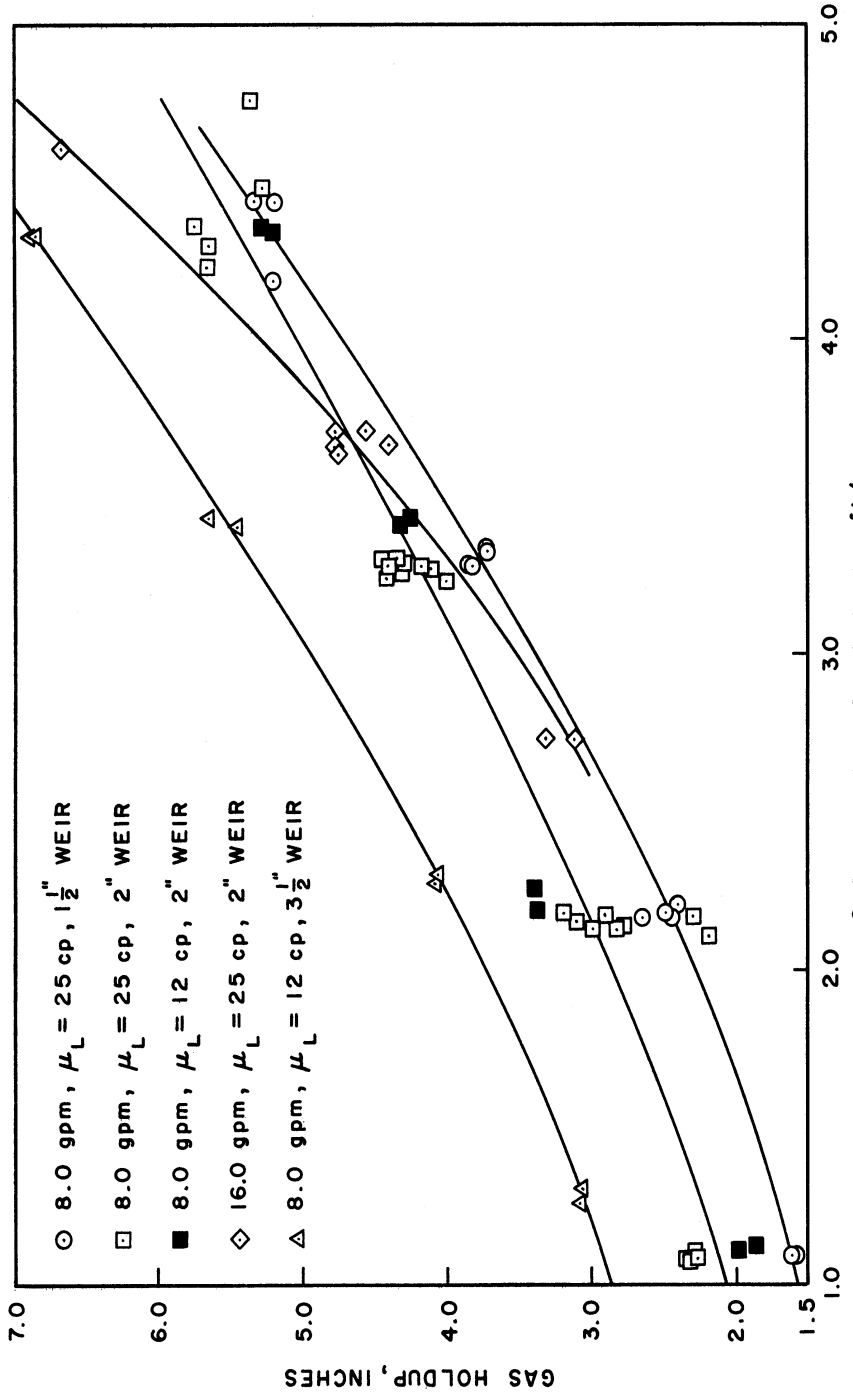

Figure 17. Gas Hold-Up Data for Nitrogen Cyclohexanol System. Data Are Presented as a Function of Superficial Gas Velocity With Parameters of Weir Height, Liquid Viscosity, and Liquid Rate.

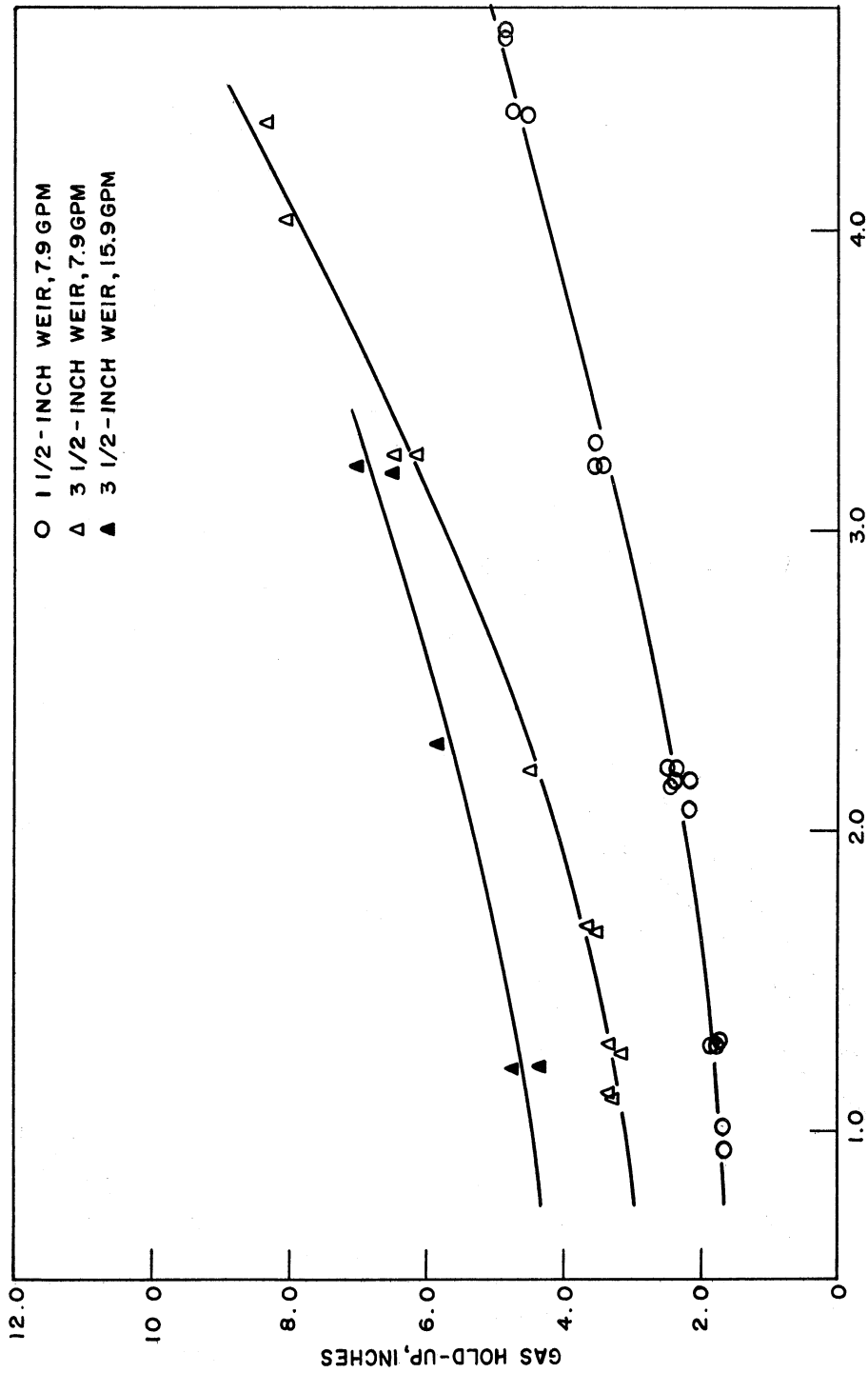

Figure 18. Gas Hold-Up Data for Nitrogen-Ethylene Dibromide System, Data Presented as a Function of Superficial Gas Velocity With Parameters of Weir Height and Liquid Rate.

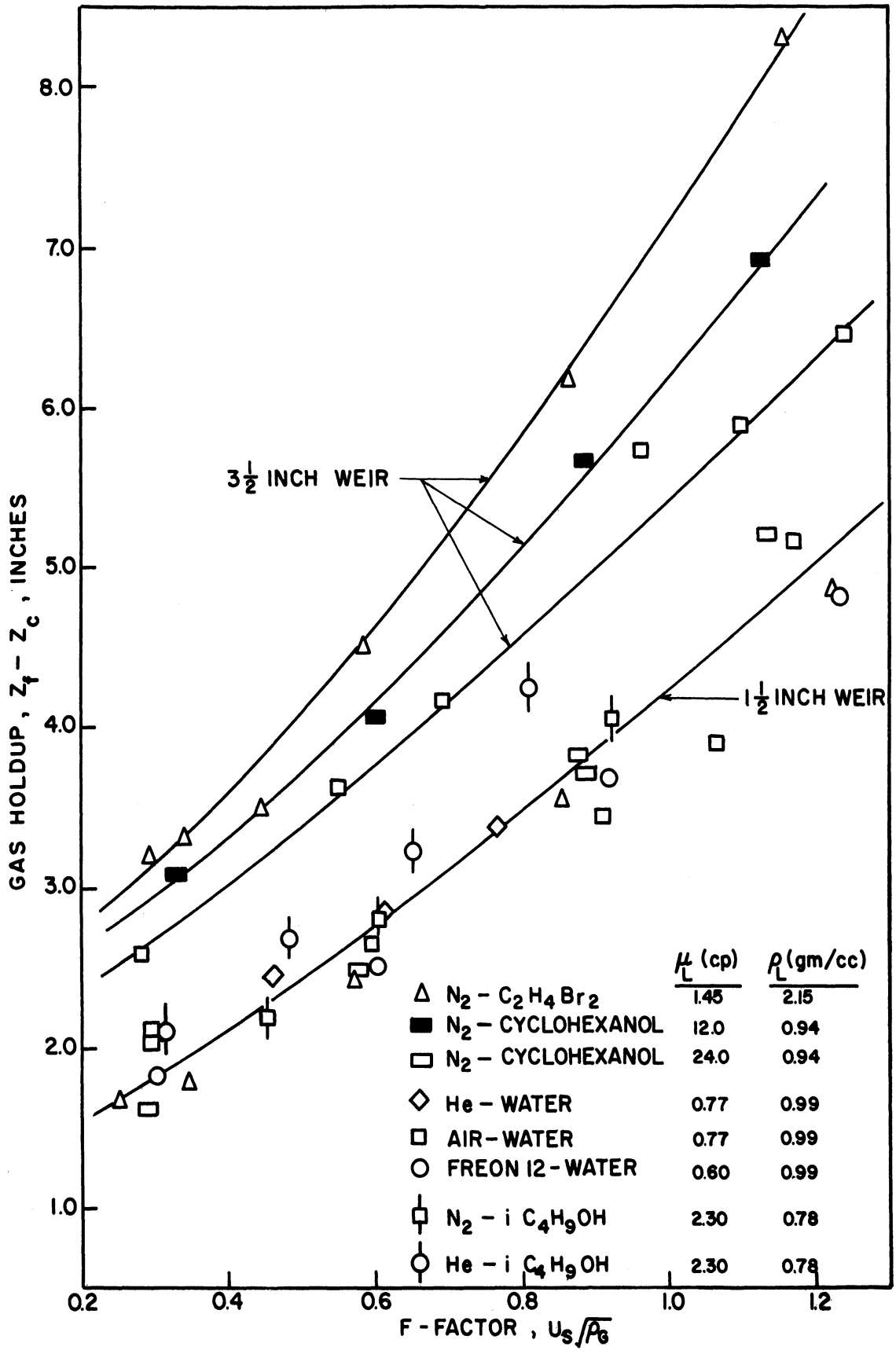

Figure 19. Gas Holdup Data for Several Systems. Data are Presented as a Function of F-Factor with Parameters of Liquid Viscosity and Density and Weir Height; 8.0 GPM.

the air-water system. Therefore, it appears that gas holdup at weir heights above 1-1/2 inch increases as either liquid viscosity or density is increased. Additional evidences of a liquid viscosity effect is indicated in Figures 20, 21, 22, and 23 where the gas holdup data for the carbon dioxide-cyclohexanol system and Warzel's data[92] for the air-water system are compared at equivalent weir heights and liquid rates. In all cases except in Figure 23 the gas holdup for the cyclohexanol system is higher or equal to the gas holdup for the air-water system. The data for the air-water system in Figure 23 were obtained at a slightly higher liquid rate than used in obtaining the data for the carbon dioxide-cyclohexanol system. This might account for the reverse relationship between gas holdup and viscosity.

The difference between the gas holdup for the air-water systems and the cyclohexanol systems is, in most cases, no greater than one inch. In fact, the average deviation is probably nearer one-half inch. The significance of these deviations is questionable since the data are from two independent investigators and the greatest deviations were found at the higher gas velocities where the visual measurement of froth height is more difficult because of the rapid time fluctuations in the froth.

Hydraulic Data - Relative Froth Density

Relative froth densities were calculated by dividing the clear liquid height in the middle of the tray by the froth height. If there were no significant stratification of the froth, this ratio would be a good estimation of the relative froth density. Crozier[21] used a light transmission technique to determine the froth stratification on a tray identical to the one used in the present investigation. Considerable

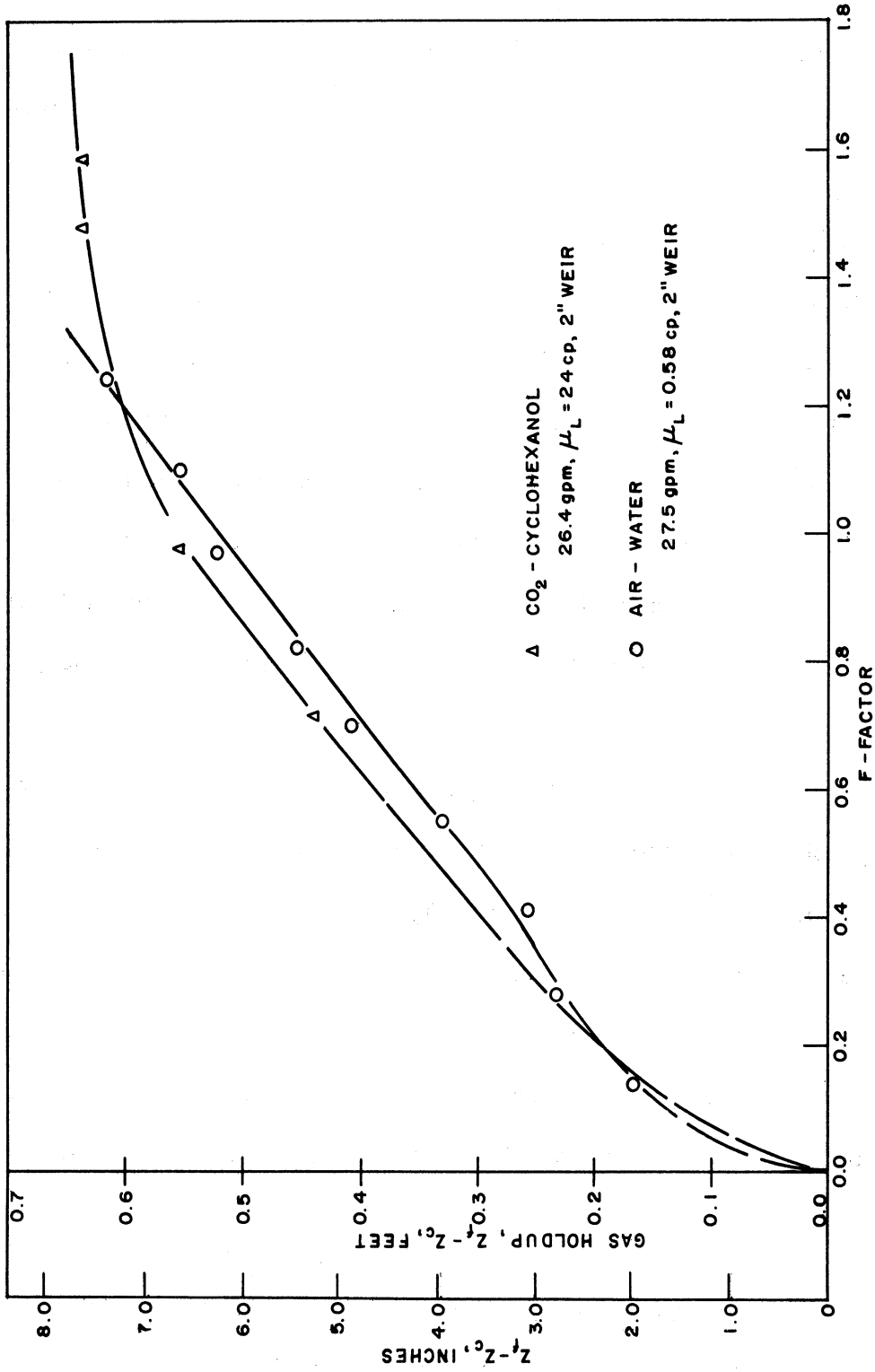

Figure 20. Gas Holdup Data for Carbon Dioxide-Cyclohexanol and Air-Water Systems as a Function of F-Factor.

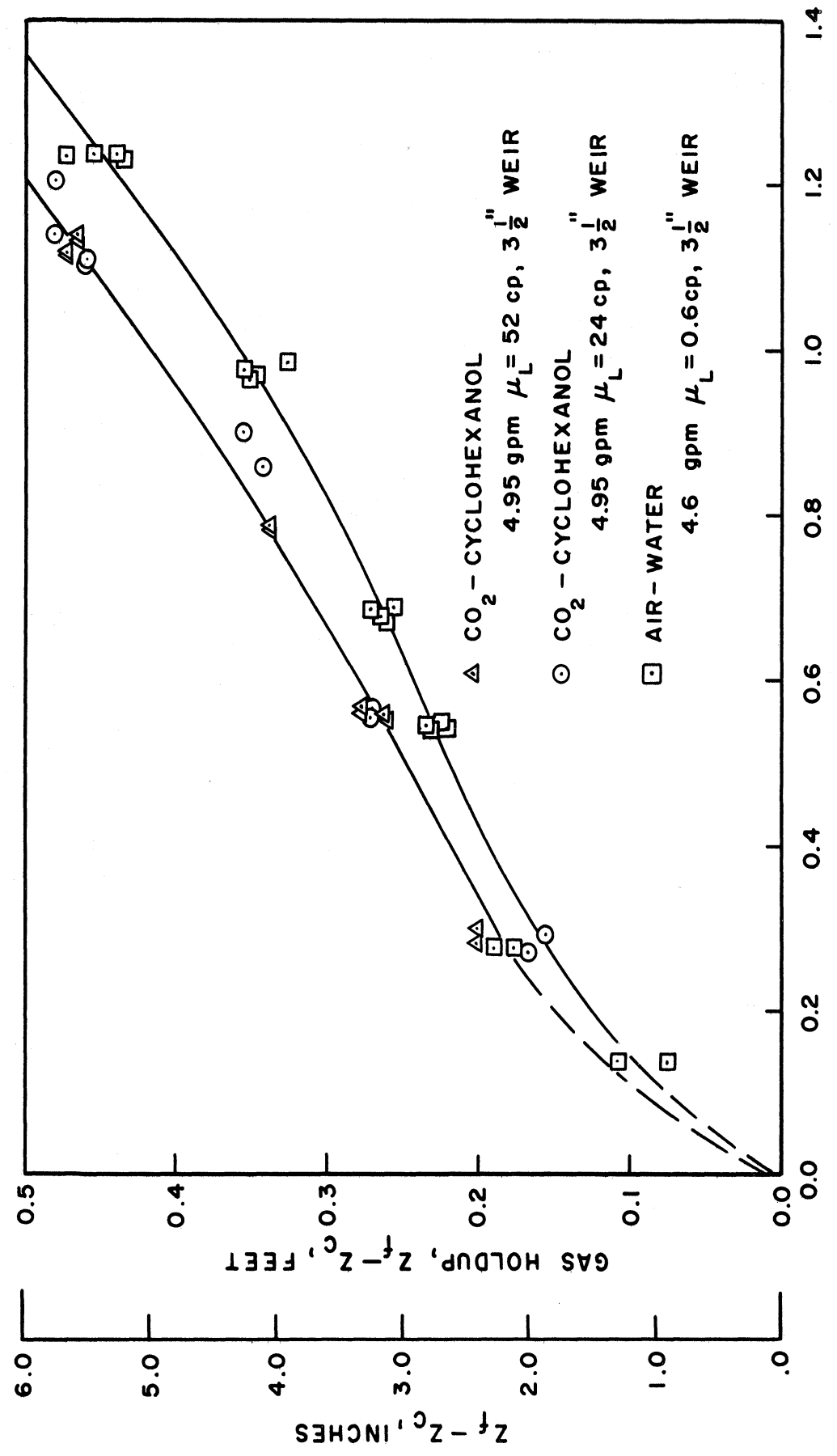

Figure 21. Gas Holdup Data for Carbon Dioxide-Cyclohexanol and Air-Water Systems as a Function of F-Factor.

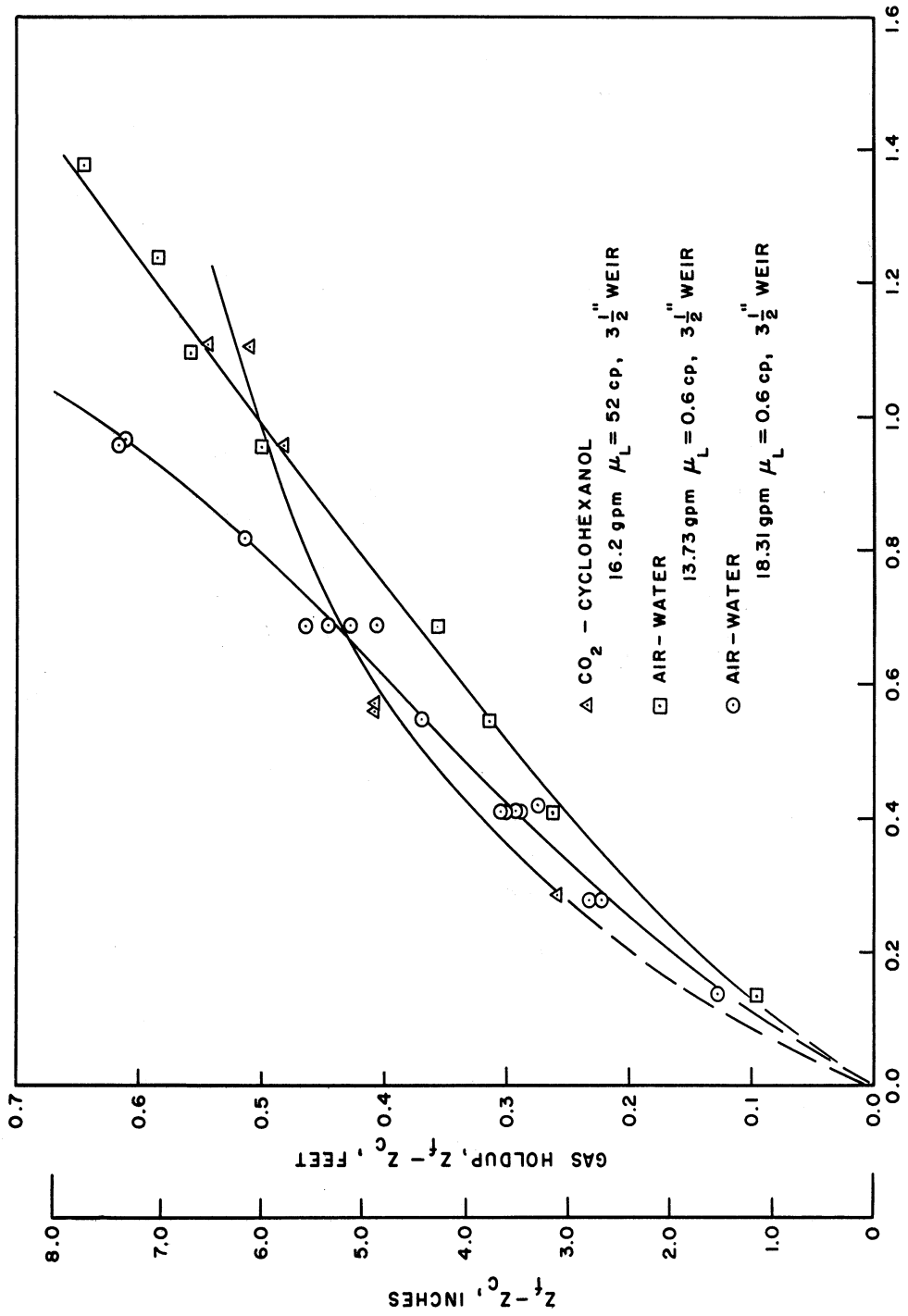

Figure 22. Gas Holdup Data for Carbon Dioxide-Cyclohexanol and Air-Water Systems as a Function of F-Factor.

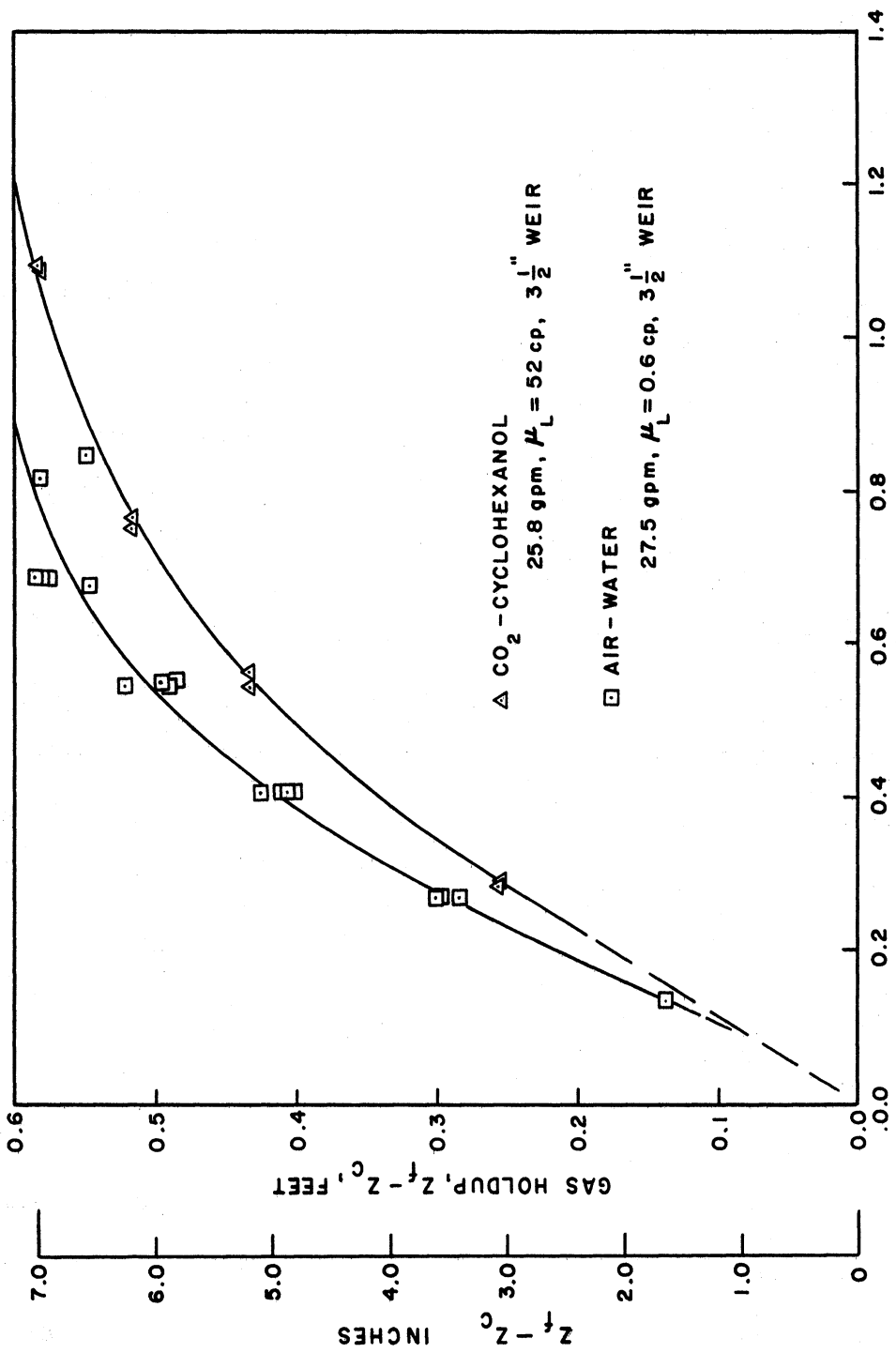

Figure 23. Gas Holdup Data for Carbon Dioxide-Cyclohexanol and Air-Water Systems as a Function of F-Factor.

variation of the froth density in the vertical direction was found for the air-water system at gas rates up-to a F-factor of 1.2 and liquid rates from 5 to 32 gpm. At low gas rates, this stratification can be seen by simply observing the froth holdup on the tray. The appearance of the froth for the organic systems and the air-water system were compared by this technique. The froth stratification for the cyclohexanol systems was believed to be greater than that for air-water system. One possible explanation for this difference is the higher liquid viscosity which caused the gas to flow through the froth in large globules without breaking-up to form a more uniform froth density. The froth for the nitrogen-ethylene dibromide system contained many small bubbles and was more uniform in appearance than that for either the cyclohexanol or water systems. With considerable stratification in the froth, the ratio of the clear liquid height and froth height has less meaning as froth density. However, this ratio might be very useful in describing the hydraulic characteristics of the tray.

In Figure 24, the relative froth density for the systems studied in this investigation plus the data of Ashby(7) and Warzel(92) are plotted versus F-factor. These data are for weir heights of 1-1/2, 2, and 3-1/2 inches and represent a considerable range for liquid rate and liquid properties. Although the maximum deviation from a single curve through the data would be about 0.1, no definite trend with liquid properties is noted. This is shown more effectively in Figures 25, 26, and 27 where the density data for each weir height are plotted versus F-factor. The average deviation from a single curve through the data is smaller than the average deviation in Figure 24. However, the

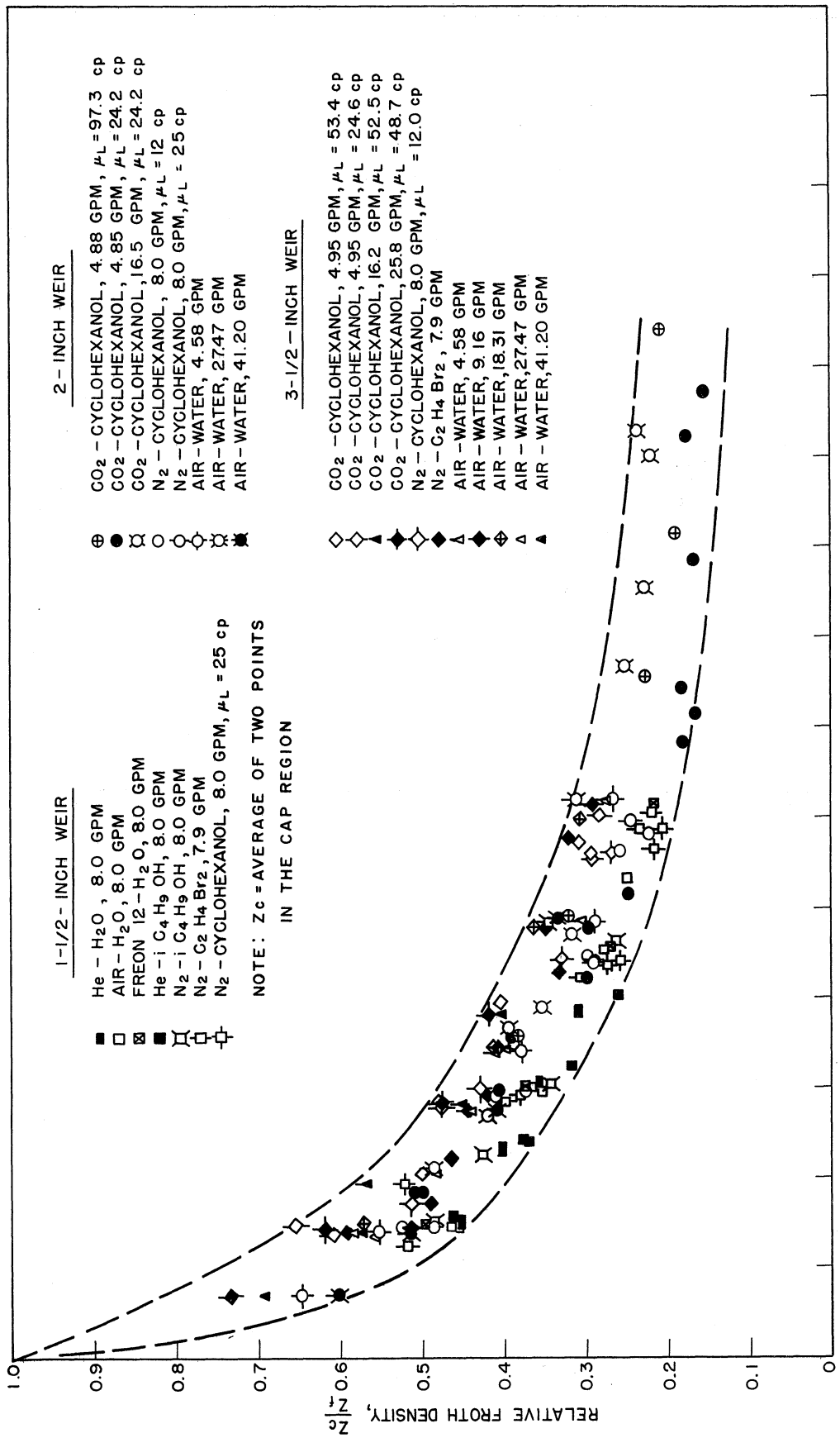

Figure 24. Relative Froth Density For Several Systems. Data Presented as a Function of F-Factor with Parameters of Weir Height, Liquid Rate, and Liquid Properties.

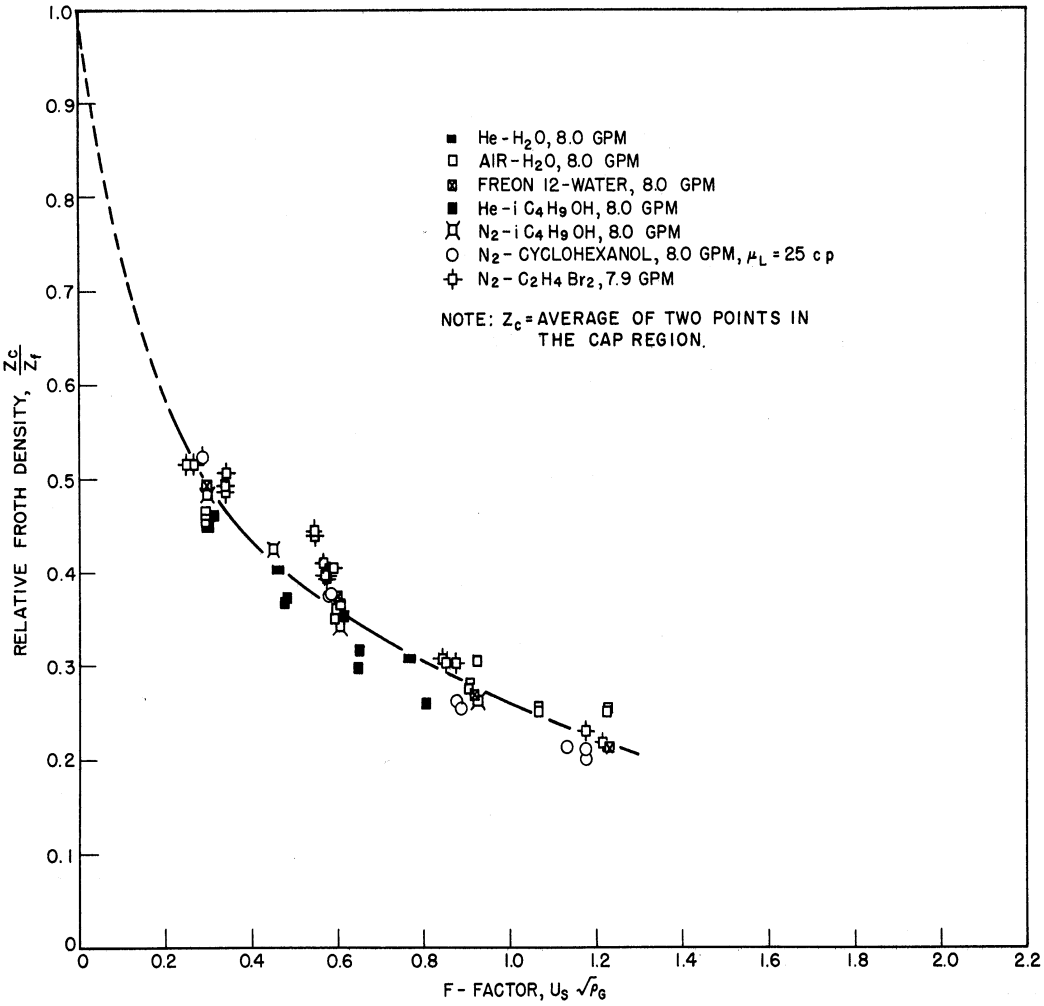

Figure 25. Relative Froth Density for Several Systems. Data are For 1½-Inch Weir and Constant Liquid Rate of About 8.0 GPM.

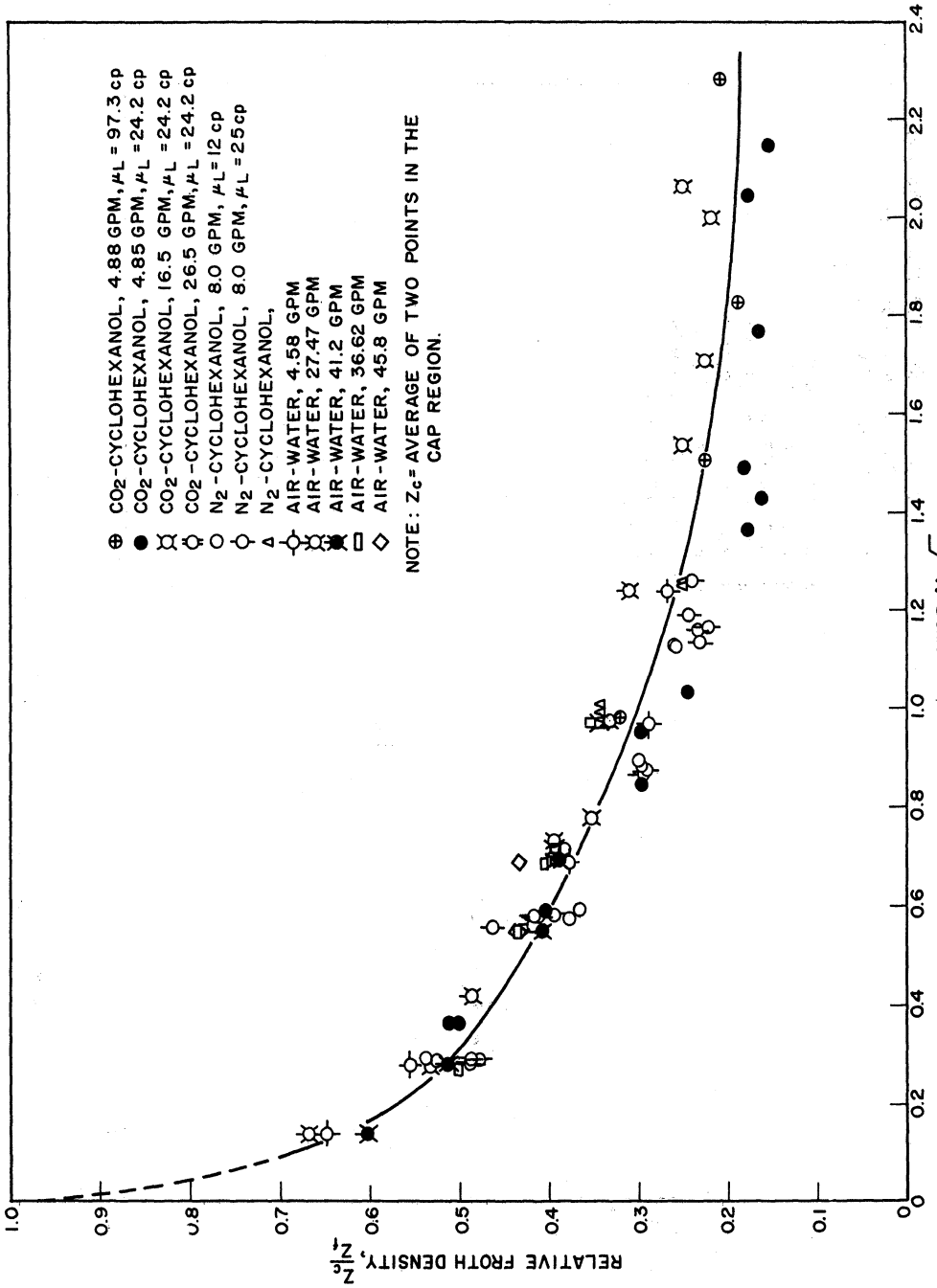

Figure 26. Relative Froth Density for Several Systems. Data are For 2-Inch Weir, Variable Liquid Rate and Liquid Properties.

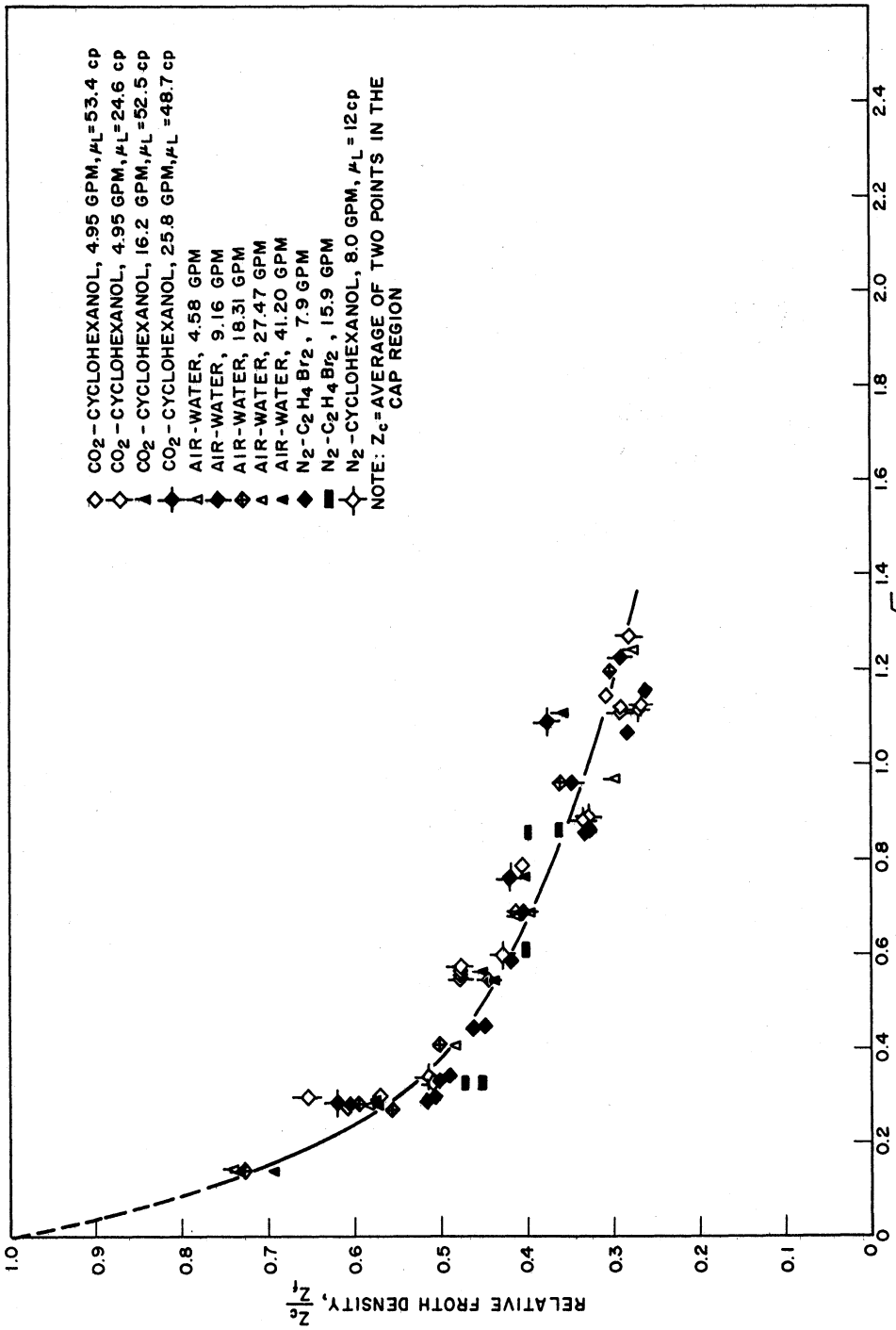

Figure 27. Relative Froth Density for Several Systems. Data are For 3½-Inch Weir, Variable Liquid Rate and Liquid Properties.

deviations are considerable and are a function of liquid rate and not liquid properties. In each of the Figures 25, 26, and 27, the data for the low liquid rates fall below the curves while the data for the high liquid rates fall above the curves. Therefore, a complete correlation of these data could be accomplished by including liquid rate and weir height. However, as illustrated in Figure 28, this correlation could not be used to predict the relative froth density for a large tray where a splash baffle is not used. In Figure 28, the data for the carbon dioxide-cyclohexanol and air-water systems at 3-1/2 inch weir height and variable liquid rate are compared with data obtained by Gerster (2) for a larger tray without a splash baffle but with a tray layout similar to the one used in the present investigation. The effect of the splash baffle is analogous to the effect of increased liquid rate since the splash baffle presents an added resistance to liquid flow and a greater liquid head on the tray is required to overcome this resistance and maintain the rate of liquid flow.* A similar effect would be expected if the outlet downcomer were not designed to handle the flow from the tray. There was some evidence that this might be the case for the tray used in this investigation. At the higher liquid and gas rates the outlet downcomer became filled with froth which sometimes extended above the top of the weir. For these reasons, the hydraulic data should not be used to predict hydraulic characteristics of a larger tray. However, the observations regarding liquid properties should be applicable to the larger trays.

---

* The clear liquid height is therefore equal to or greater than the liquid height for the tray with a weir and no splash baffle.

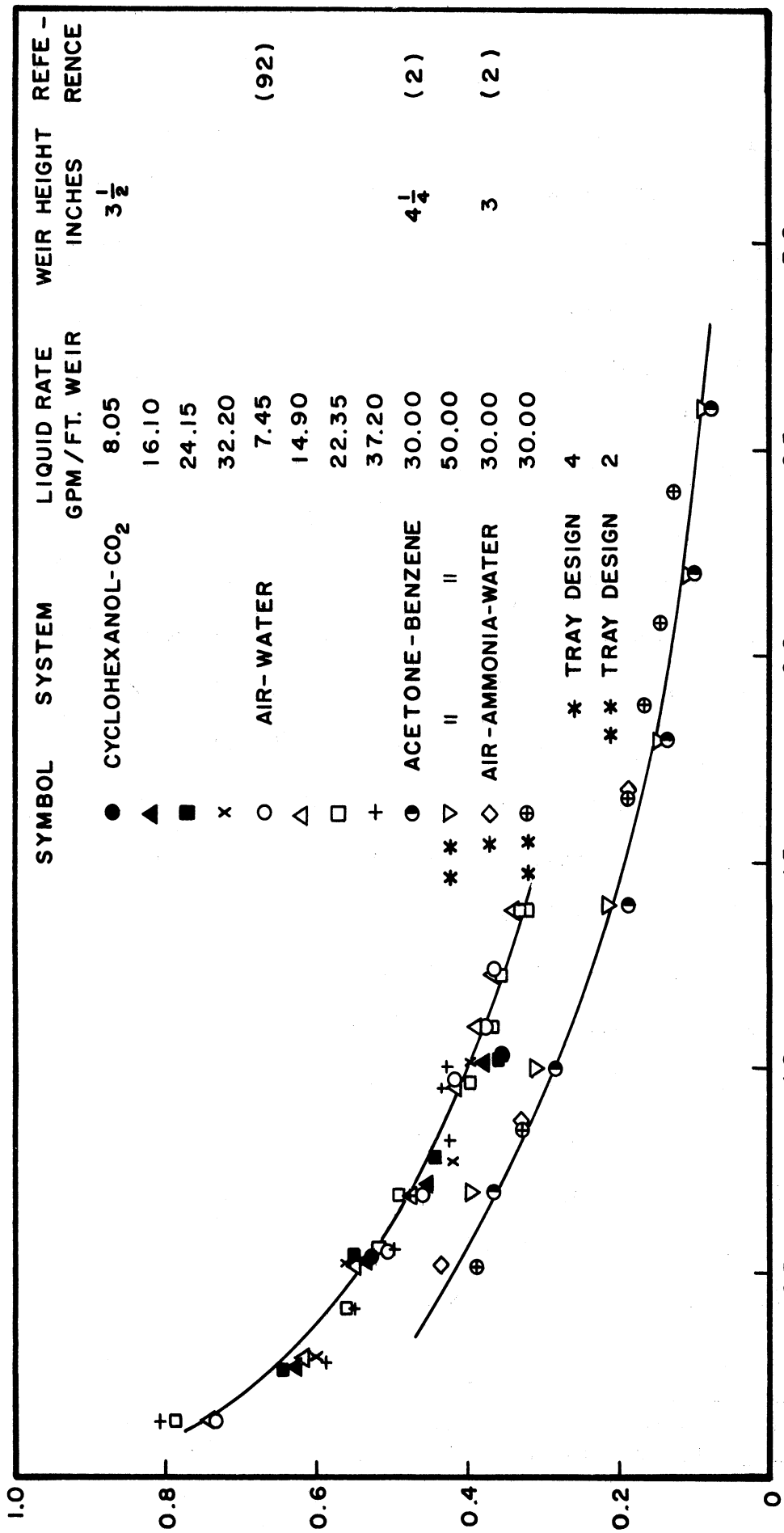

Figure 28. Comparison of Relative Froth Density on the Tray Used in the Present Investigation and the Density Reported by Gerster[2] for a Similar Tray with No Splash Baffle

Mass Transfer Data - Vaporization Studies

The two systems used in the vaporization studies were nitrogen-cyclohexanol and nitrogen-ethylene dibromide. The conditions used in these studies are summarized as follows:

I. Nitrogen-cyclohexanol

(a) 1-1/2 inch weir height; μ_L, 25 cp; liquid rate, 8.0 gpm.

(b) 2 inch weir height; μ_L, 25 and 12 cp; liquid rate, 8.0 and 16.0 gpm.

(c) 3-1/2 inch weir height; μ_L, 12 cp; liquid rate, 8.0 gpm.

II. Nitrogen-ethylene dibromide

(a) 1-1/2 inch weir height; liquid rate, 7.9 gpm.

(b) 3-1/2 inch weir height; liquid rate, 7.9 gpm and 15.9 gpm.

The range of superficial gas velocity in each of these studies was 1.0 to 4.5 ft/sec.

A sample data sheet and calculation procedure for the vaporization data are presented in Appendix F. The detailed data are presented in Table I-G. The efficiency data for the nitrogen-cyclohexanol system are plotted versus superficial velocity in Figure 29. There are three important points in regards to these data which are worth discussion. These are: (1) decrease in plate efficiency when weir height was increased; (2) increase in efficiency when liquid viscosity was increased; and (3) increase in efficiency with increased gas velocity.

The decrease in plate efficiency with increased weir height was not expected since the froth holdup or gas holdup on the tray increased

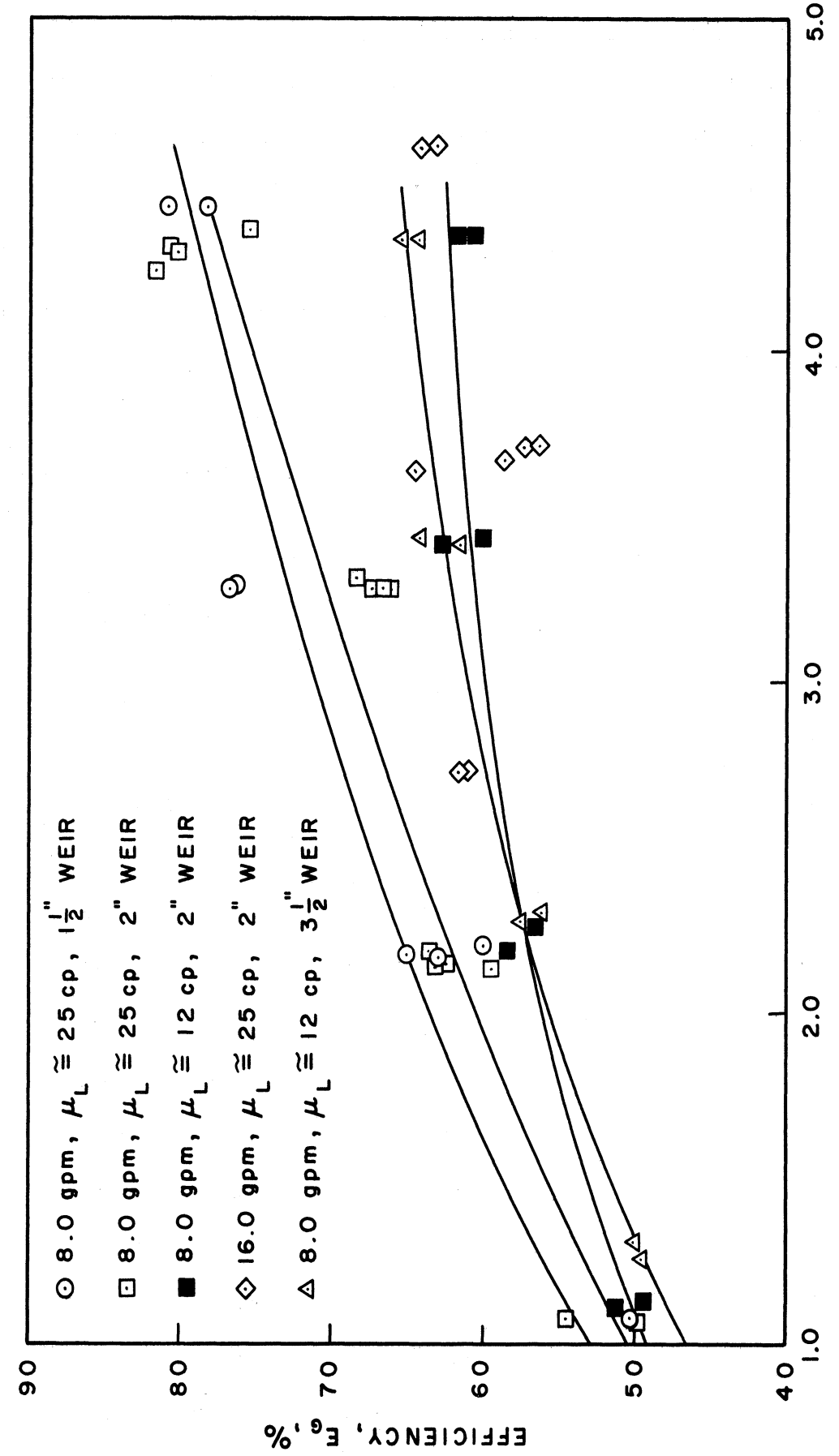

Figure 29. Gas-Phase Efficiencies for Nitrogen-Cyclohexanol System. Data are Presented as a Function of Superficial Gas Velocity with Parameters of Weir Height, Liquid Rate, and Liquid Viscosity

and the gas contact time increased accordingly. Assuming that the mass transfer coefficient, $k_G a$, is independent of the froth height, the efficiency should have increased. Therefore, the results in Figure 29 indicate that the mass transfer coefficient is not independent of the weir height or the liquid holdup on the tray but decreases as liquid holdup increases. In fact, the decrease in the mass transfer coefficient is so great that the effect is not counterbalanced by the increase in gas contact time with increased weir height.

The effect of liquid viscosity is shown in Figure 29 by the efficiency data for a 2 inch weir height and viscosities of 12 and 25 centipoises. The efficiency data at 12 centipoises are lower than the data at 25 centipoises at all gas velocities with the possible exception of the data at the gas velocity of 1 ft/sec. Thus these data suggest that the dependence of efficiency on gas velocity is a function of liquid viscosity. This variation of the relationship between efficiency and gas velocity with liquid properties is more apparent when the efficiency data in Figure 30 for the nitrogen-ethylene dibromide system are compared with the data for the nitrogen-cyclohexanol system. The viscosity for the ethylene dibromide was 1.45 centipoises and the density was 2.15. The efficiency for the ethylene dibromide system is almost independent of gas velocity. The change in efficiency over the complete velocity range is not greater than 4 efficiency percent in contrast to the change of 15 - 30 efficiency percent for the cyclohexanol system over the same velocity range. Ashby's data[7] for several systems having low liquid viscosities were also practically independent of velocity.

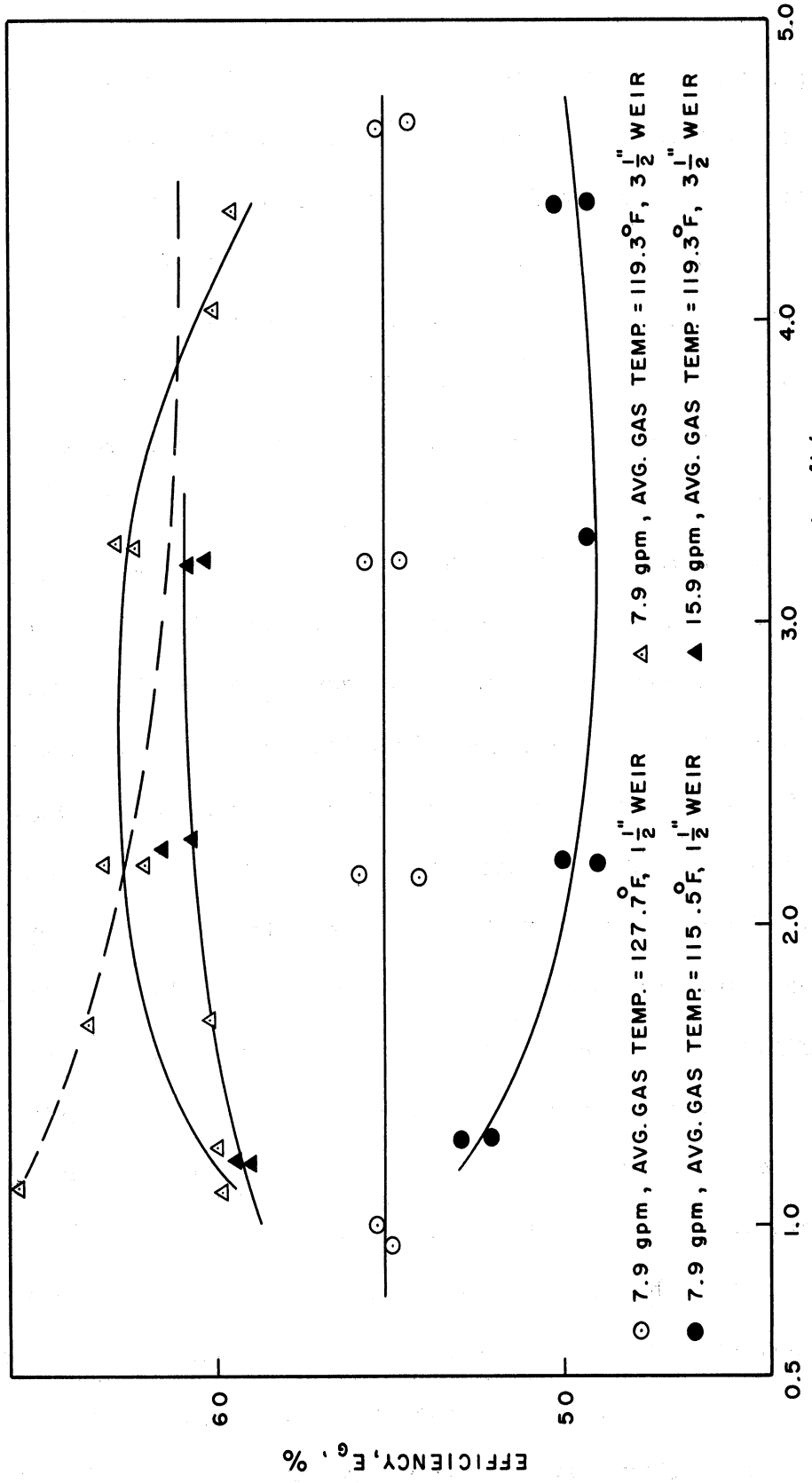

Figure 30. Gas-Phase Efficiencies for Nitrogen-Ethylene Dibromide System. Data are Presented as a Function of Superficial Gas Velocity with Parameters of Weir Height and Liquid Rate

Another comparison which can be made between the data from the present study and Ashby's data concerns the level of the efficiency values. The lowest efficiency value reported by Ashby was 78 percent for the helium-isobutyl alcohol system. The data for the other systems were above this value with highest value of 97 percent for the Freon 12-water system. In contrast, the efficiency values for the nitrogen-cyclohexanol and nitrogen-ethylene dibromide systems were as low as 50 percent.

In the studies with the nitrogen-ethylene dibromide system several runs were made before it was realized that an error had been made inadvertently in the humidity chart for this system. These data are indicated in Figure 30 by the open circles and are included herein to give some idea of the errors in the data due to the possibility of non-adiabatic conditions in some cases. A decrease of about 12°F in the average gas temperature decreased the resulting efficiency by 7 efficiency percent in some cases. The possibility of the adiabatic conditions being in error by the amount indicated above is very unlikely since in every run the gas temperature was adjusted until the inlet and outlet liquid temperatures were within 0.1 to 0.2°C.

The efficiency data for the nitrogen-ethylene dibromide system at 3-1/2 inch weir height and low gas velocity were not as reproducible as were the data at higher gas velocities or 1-1/2 inch weir. Of the five data points obtained in the low velocity range and at the 3-1/2 inch weir, three data points were low and two were high. This is the reason for two separate curves through the data in Figure 30. The reason for this non-reproducibility was not known. However, it was observed that the tray was operating in an unstable region at the low

velocities as indicated by the gas flowing through part of the caps at one time and through another part a few seconds later. There is a good possibility that the caps were leaking liquid during the time gas was not flowing through them. This could not be determined however. This cycling was very apparent and it might be the cause for the scatter in the data since liquid leaking through the caps could have caused the inlet-gas sample concentrations to be in error.

The efficiency data from the vaporization studies were converted to the number of mass transfer units by use of Equation (95)

$$N_{OG} = -\ell n(1 - E_{OG}) \tag{95}$$

This equation applies in this case since there were no concentration differences along the length of the tray (pure liquid) and $E_{MV} = E_{OG}$, i.e., plate efficiency equals point efficiency. In addition, the conditions on the tray were controlled so that the resistance to mass transfer was believed to be gas phase in which case $E_{OG} = E_G$ so that Equation (95) may be written as follows:

$$N_G = -\ell n(1 - E_G) \tag{96}$$

The data for the two systems are plotted in Figures 31 and 32. One point which should be remembered in regards to Equation (96) is that any error in E_G is magnified in the resulting N_G. This can be shown by the following relationship,

$$dN_G = \frac{dE_G}{(1 - E_G)} \tag{97}$$

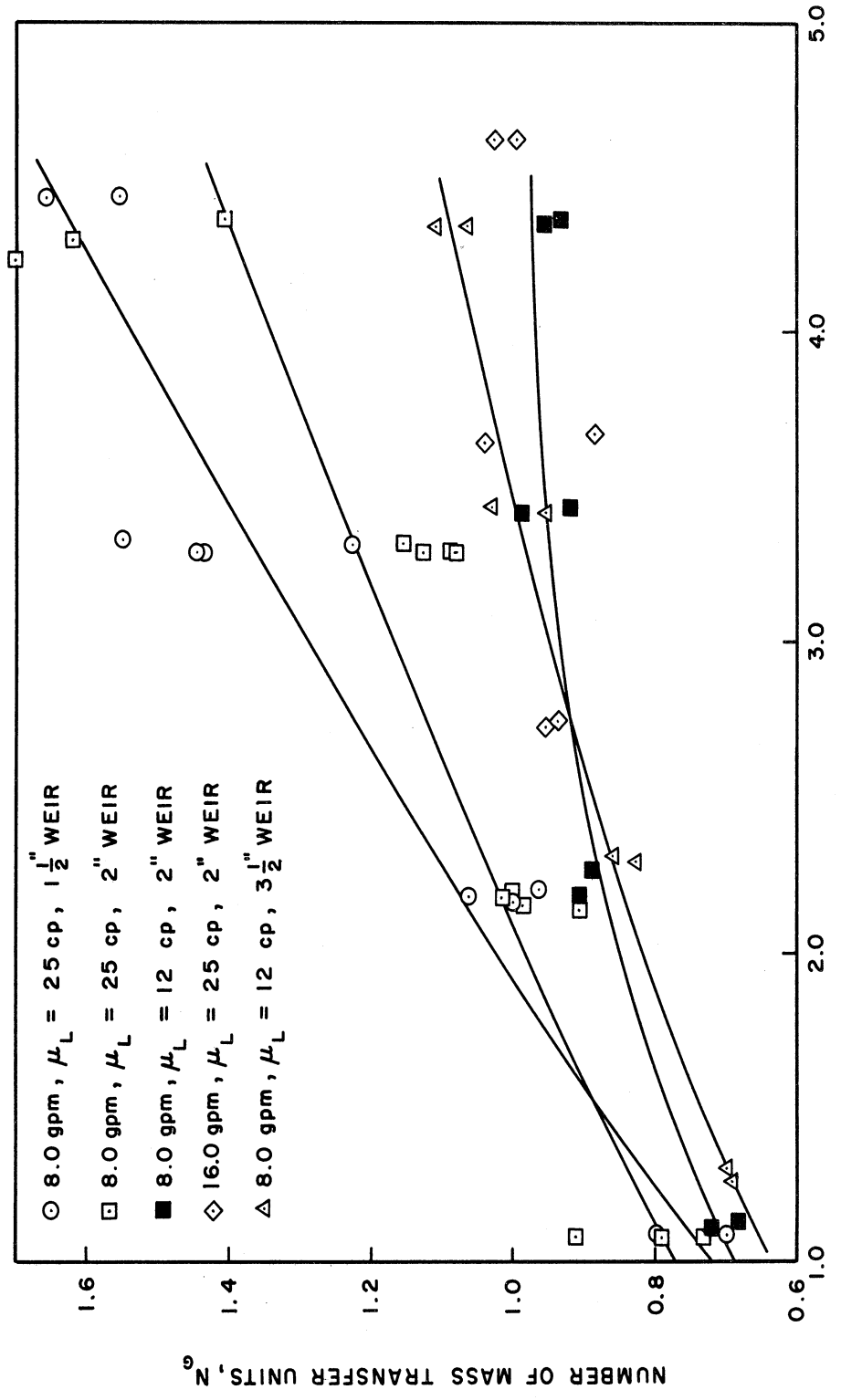

Figure 31. Number of Mass Transfer Units for Nitrogen - Cyclohexanol System. Data are Presented as a Function of Superficial Gas Velocity with Parameters of Weir Height, Liquid Rate, and Liquid Viscosity.

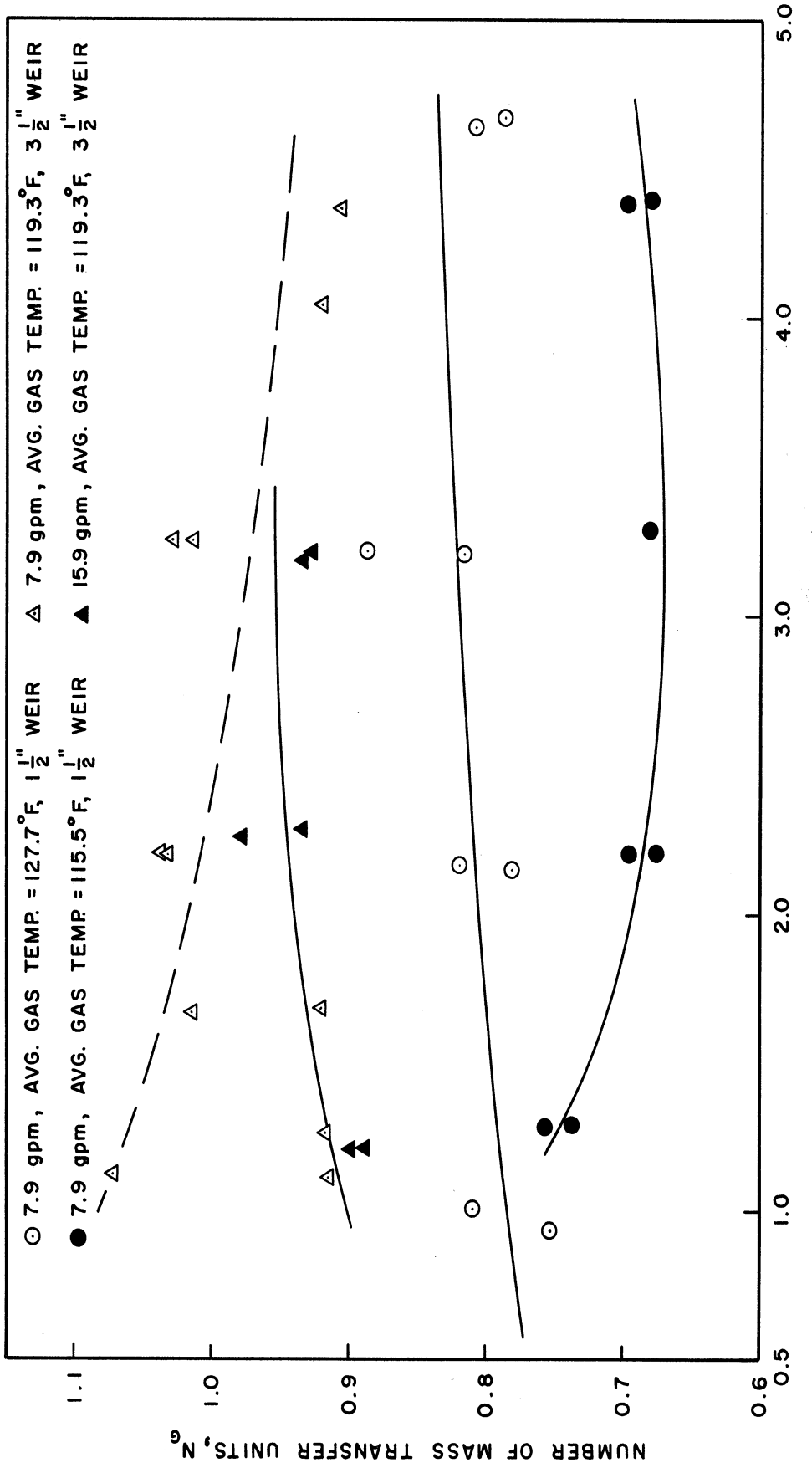

Figure 32. Number of Mass Transfer Units for Nitrogen - Ethylene Dibromide System. Data are Presented as a Function of Superficial Gas Velocity with Parameters of Weir Height and Liquid Rate

As the point efficiency approaches 100 percent, any errors in the efficiency data are magnified many times in the N_G data. An error analysis for the vaporization studies is presented in Appendix C.

Mass Transfer Data - Absorption Studies

The absorption studies consisted of absorbing carbon dioxide in cyclohexanol at various gas rates, liquid rates, weir heights, and liquid viscosities. The experimental conditions are summarized as follows:

I. 3-1/2 inch weir height.

(a) Liquid rate, 4.95 gpm; gas velocity, 0.9-3.5 ft/sec.; liquid viscosity, 24.6 cp.

(b) Liquid rate, 4.92 gpm; gas velocity, 0.9-3.5 ft/sec.; liquid viscosity, 53.5 cp.

(c) Liquid rate, 16.5 gpm; gas velocity, 0.9-3.5 ft/sec.; liquid viscosity, 52.5 cp.

(d) Liquid rate, 26.4 gpm; gas velocity, 0.9-3.5 ft/sec.; liquid viscosity, 48.7 cp.

II. 2 inch weir height.

(a) Liquid rate, 4.94 gpm; gas velocity, 1.0-7.0 ft/sec.; liquid viscosity, 24.2 cp.

(b) Liquid rate, 4.90 gpm; gas velocity, 2-7.2 ft/sec.; liquid viscosity, 97.2 cp.

(c) Liquid rate, 16.5 gpm; gas velocity, 2.2-6.8 ft/sec.; liquid viscosity, 24.1 cp.

(d) Liquid rate, 26.5 gpm; gas velocity, 2.2-4.9 ft/sec.; liquid viscosity, 24.1 cp.

The liquid viscosity of the cyclohexanol was varied by changing the temperature of the liquid.

The Murphree liquid efficiencies for the 3-1/2 inch weir height are plotted versus F-factor in Figure 33 and the data for the 2 inch weir height in Figure 34. These efficiencies are based on the liquid concentrations at point 5 on the tray shown in Figure 4 . A sample data sheet and calculation procedure are presented in Appendix F. The detailed data are presented in Table III-G.

The data for both weir heights are dependent on gas velocity or F-factor, liquid rate, and liquid viscosity. The increase in Murphree liquid efficiency with increasing gas velocity reflects the increase in gas holdup on the tray which provides more interfacial area for mass transfer and possibly an increase in the mass transfer coefficient. At a constant liquid viscosity an increase in liquid rate causes the efficiency to decrease and probably is due to the greater flow rate and not so much to any change in the specific interfacial area, ft^2/ft^3, or in the mass transfer coefficient. Any rationalization at this point concerning the effect of liquid rate is complicated by the fact that the total interfacial area increased as the liquid rate was increased and the driving force also increased because of the lower level of concentrations in the liquid phase. The decrease in efficiency with increased liquid viscosity is no doubt caused by decreased diffusivity in the liquid phase and possibly by an effect of liquid viscosity on total interfacial area or specific interfacial area and the mass transfer coefficient.

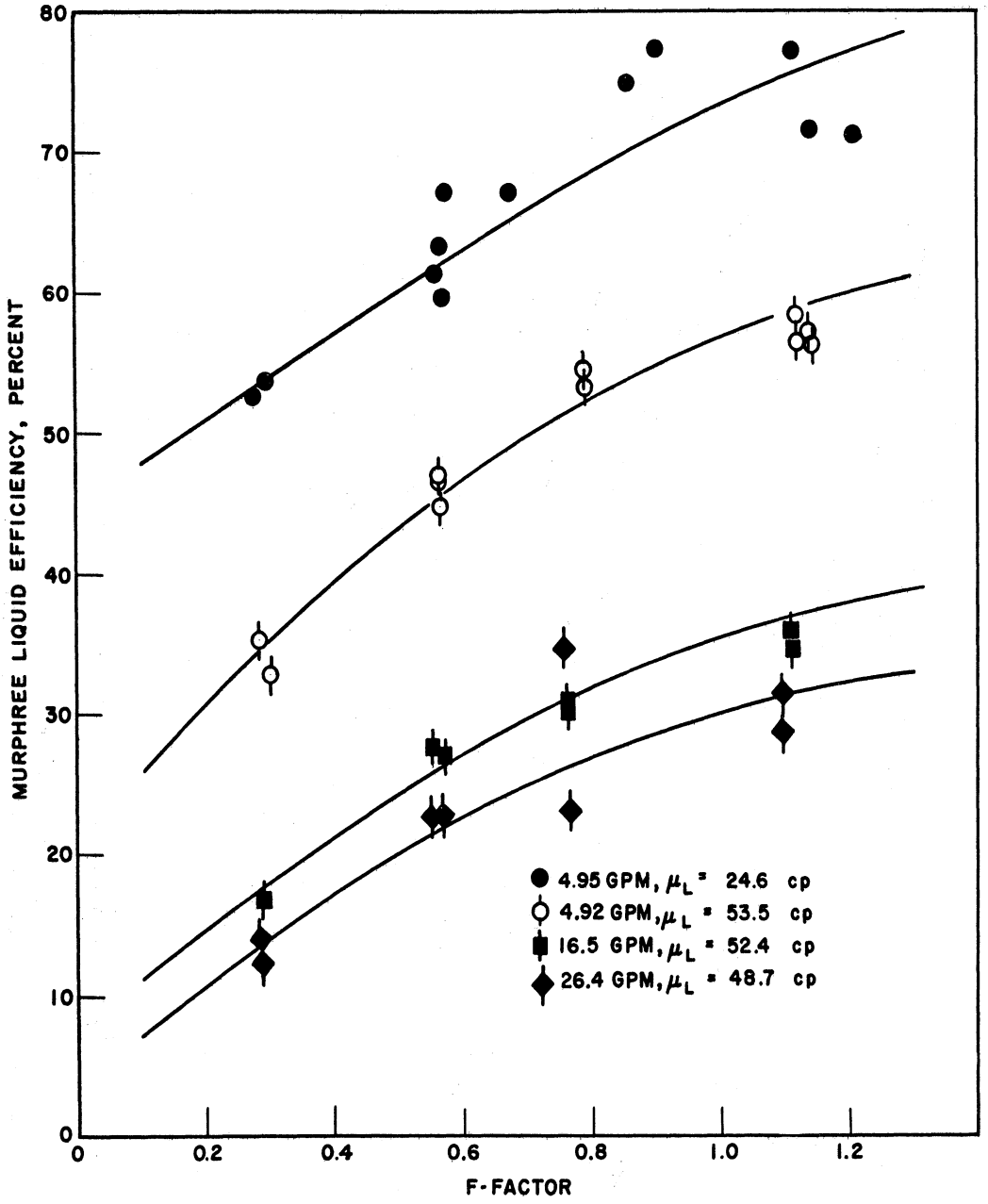

Figure 33. Murphree Liquid Efficiencies for Carbon Dioxide - Cyclohexanol System - Variable Liquid Rate and Liquid Viscosity - 3-1/2 inch Weir, 4-inch Splash Baffle

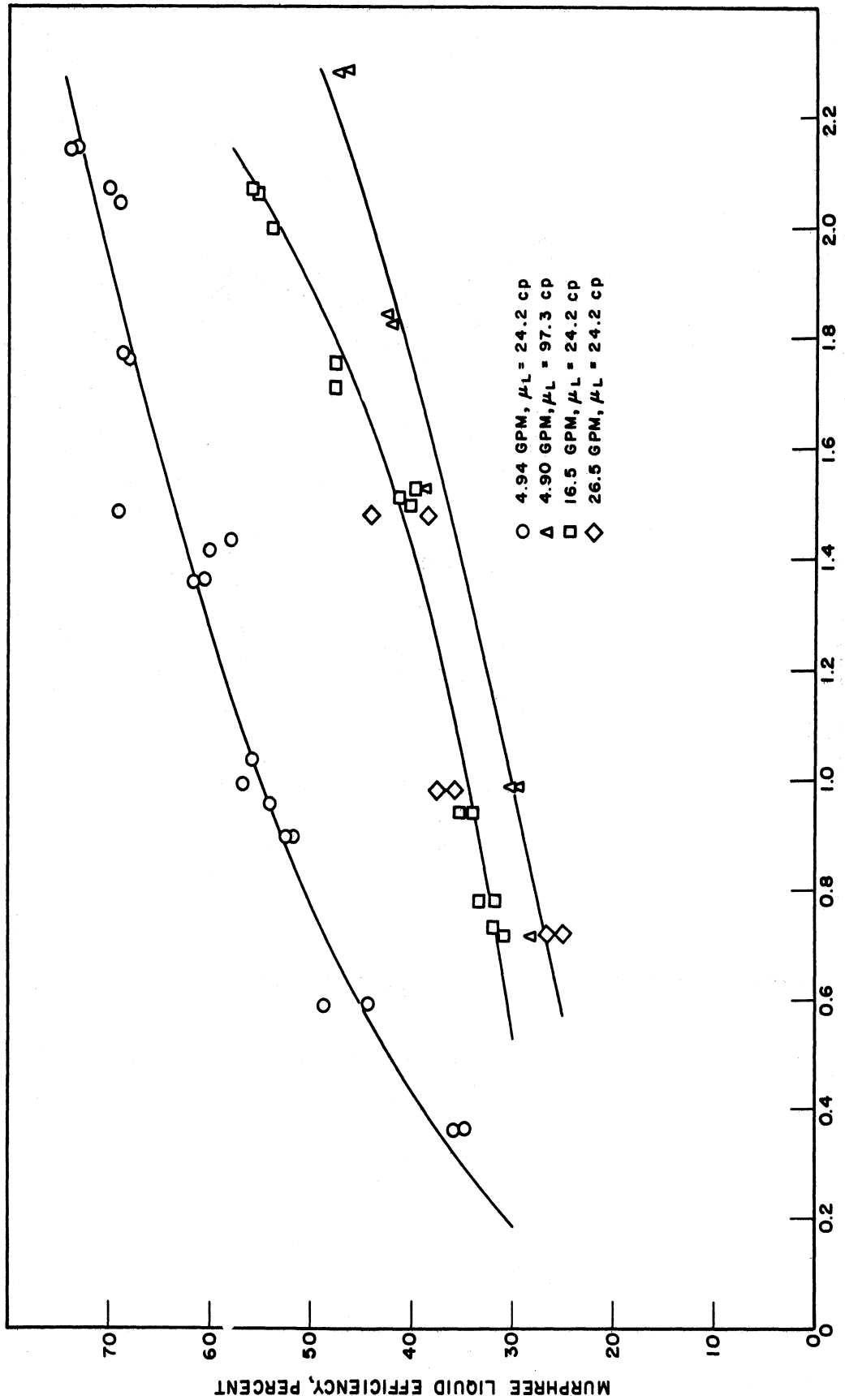

Figure 34. Murphree Liquid Efficiencies for Carbon Dioxide-Cyclohexanol System - Variable Liquid Rate and Liquid Viscosity-2-Inch Weir, 2¾-Inch Splash Baffle.

The conversion of the plate efficiency to point efficiency was not as simple in the absorption studies as in the vaporization studies. The expressions which have been used to relate plate efficiency and point efficiency were discussed in a previous section. The main thing to keep in mind is that these relationships are merely ways of accounting for the variable driving force due to the continuously increasing or decreasing concentration in the liquid as it flows across the tray. In the present study, concentrations at four different points on the tray were determined concurrently with each efficiency and these were used to determine an average liquid concentration on the tray. The average liquid concentration was used in the following relationship to calculate the point efficiency.

$$\frac{E_{MV}}{E_{OG}} = \frac{x_{avg} - y_1/m}{x_o - y_1/m} = \frac{x_{avg} - x^*}{x_o - x^*} \tag{98}$$

The value for E_{MV} was calculated by use of the material balance relationship, Equation (62). Equation (98) was derived as follows:

$$E_{MV} = \frac{y_{avg} - y_1}{mx_o - y_1} \tag{99}$$

where y_{avg} = the average concentration of the gas leaving the tray.

y_1 = the concentration of the gas entering the tray.

mx_o = the concentration of the gas in equilibrium with the liquid leaving the tray.

$$E_{OG} = \frac{y' - y_1}{mx' - y_1} \tag{100}$$

where y' = the concentration of the gas leaving at a point on the tray.

mx' = the concentration of the gas in equilibrium with the liquid at the same point on the tray.

If y_{avg} is defined as follows,

$$y_{avg} = \int_o^1 y' dW \tag{101}$$

where w = fraction of distance across the tray,

then

$$y_{avg} = \int_o^1 [E_{OG}\, mx' - E_{OG}\, y_1 + y_1] dW \tag{102}$$

and

$$y_{avg} = E_{OG}\, m \int_o^1 x' dW - E_{OG}\, y_1 + y_1 \tag{103}$$

if E_{OG}, m, and y_1 are assumed to be independent of the position on the tray. Representative concentration profiles for the studies at 3-1/2 inch weir height are presented in Figure 35. The concentration was found to be essentially linearly dependent upon the distance along the tray for all conditions studied. Since the distances between the four points on the tray were about the same, it was thought that the integral in Equation (103) could be approximated by the arithmetic average of the four concentrations. That is,

$$E_{OG}\, m \int_o^1 x'\, dW = E_{OG}\, m \left[\frac{C_2 + C_3 + C_4 + C_5}{4\rho_{ML}}\right] \tag{104}$$

$$= E_{OG}\, m\, x_{avg} \tag{105}$$

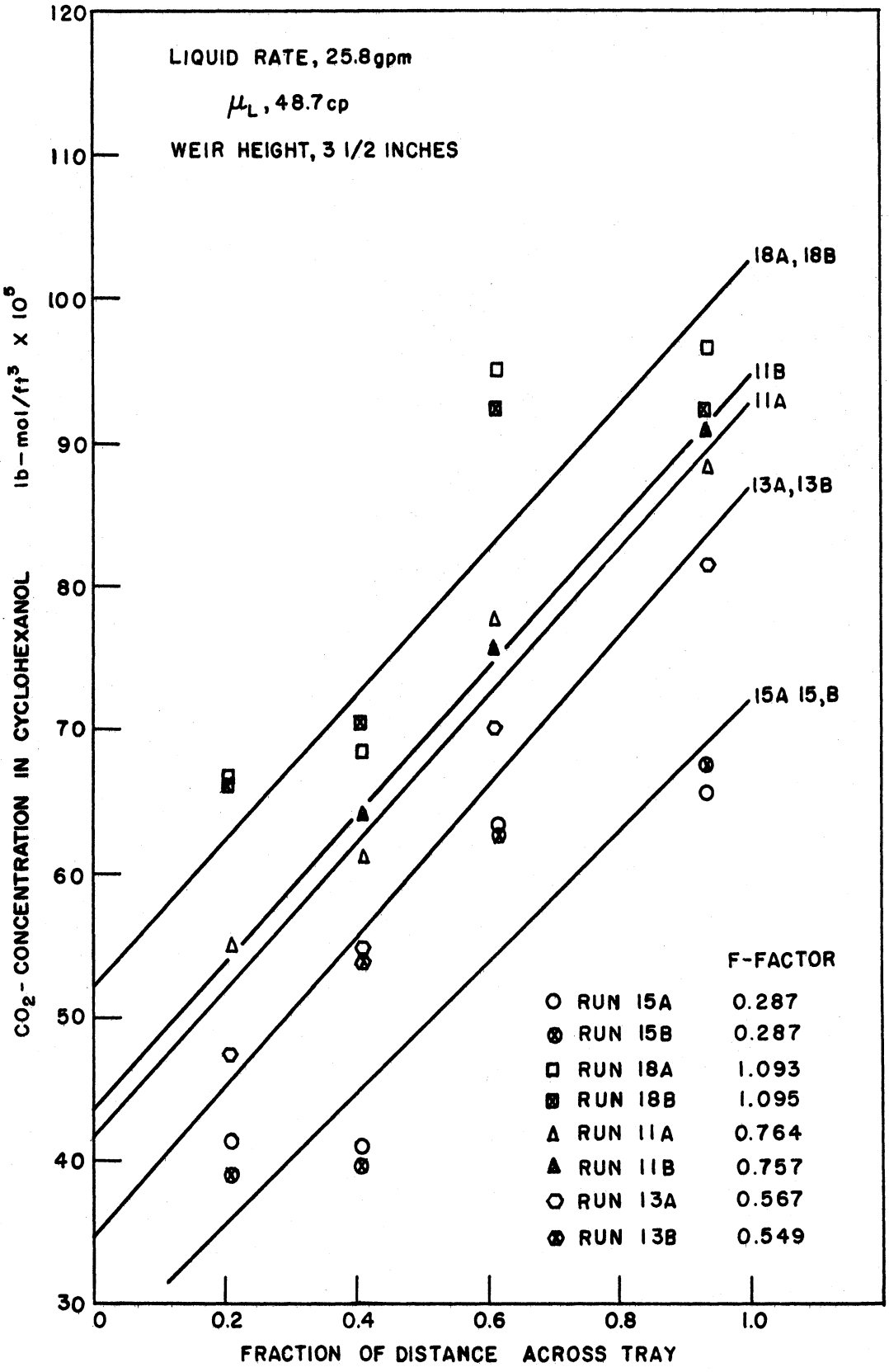

Figure 35. Liquid Concentrations on Tray Floor - Carbon Dioxide - Cyclohexanol System

where C_2, C_3, C_4 and C_5 are the concentrations at the four sample points shown in Figure 4 .

Equation (103) then becomes,

$$y_{avg} - y_1 = E_{OG} (m x_{avg} - y_1) \qquad (106)$$

If Equation (103) is substituted in Equation (99), the relationship between point efficiency and plate efficiency (Equation 98) is obtained.

The point efficiencies were used to calculate the number of liquid transfer units by use of Equation (48) which is an equation combining the resistances in the gas and liquid phases and the over-all resistance to mass transfer. Since the concentration of carbon dioxide in the gas phase was always above 50 percent and in most cases in range of 70-90 percent, the gas phase resistance in Equation (48) was neglected. The values of N_L calculated in this manner are presented in Table IV-G and plotted versus F-factor in Figures 36 and 37.

In the derivation of Equation (95) which relates the point efficiency and the mass transfer coefficient, and in the derivation of the relationship between point and plate efficiency, the assumption was made that the concentration of the liquid is independent of the vertical position in the froth at a fixed position along the tray. In order to establish the validity of this assumption, liquid samples were obtained by use of the sampling probes shown in Figure 4. These data plus the concentrations on the tray floor are presented in Table VII and plotted versus F-factor in Figure 38. The best lines through the concentrations on the tray floor are straight and parallel, an indication that the rate of approach to complete mixing with increasing gas velocity is practically

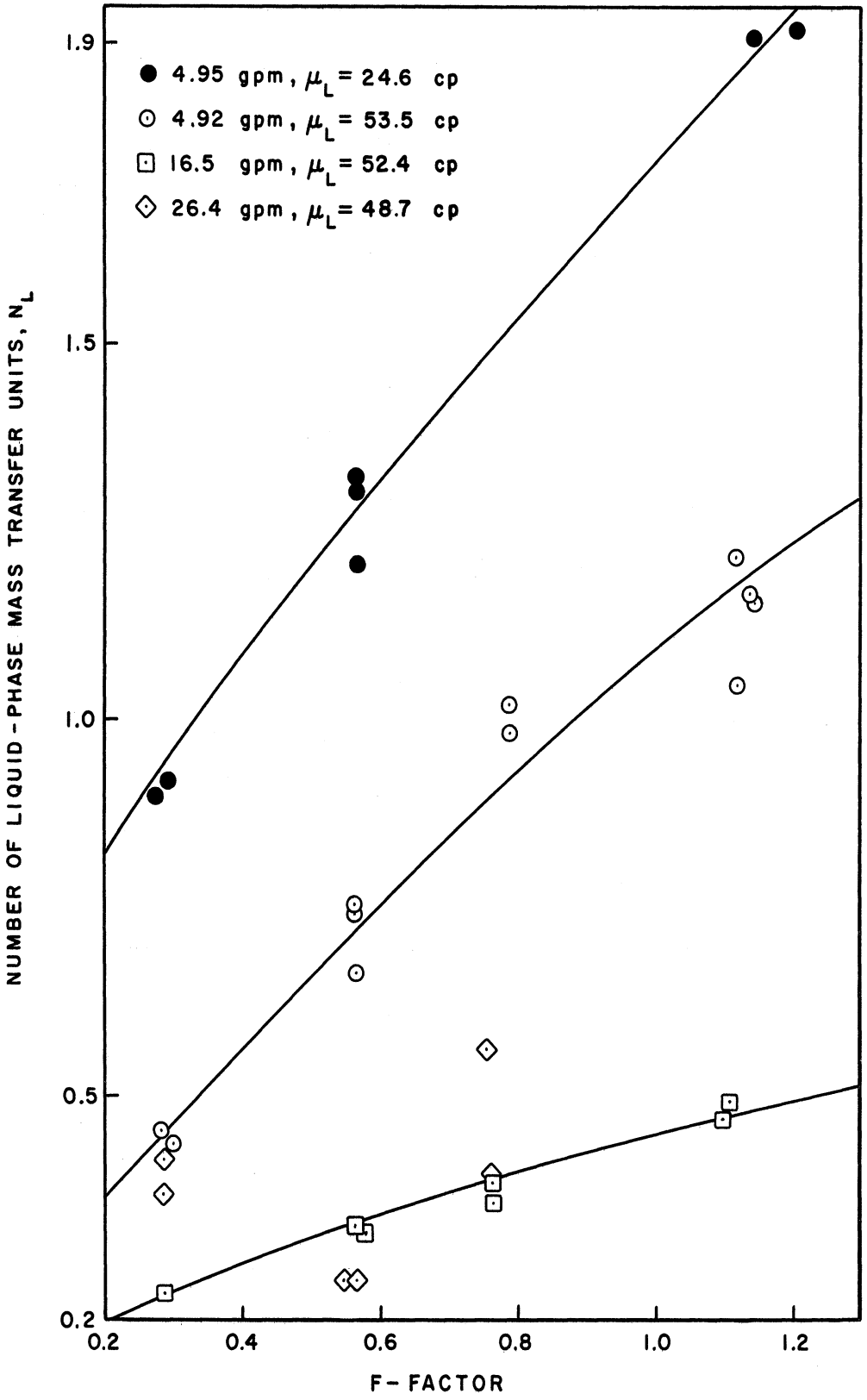

Figure 36. Number of Liquid-Phase Mass Transfer Units for Carbon Dioxide - Cyclohexanol System - Variable Liquid Rate and Liquid Viscosity - $3\frac{1}{2}$-inch Weir, 4-inch Splash Baffle

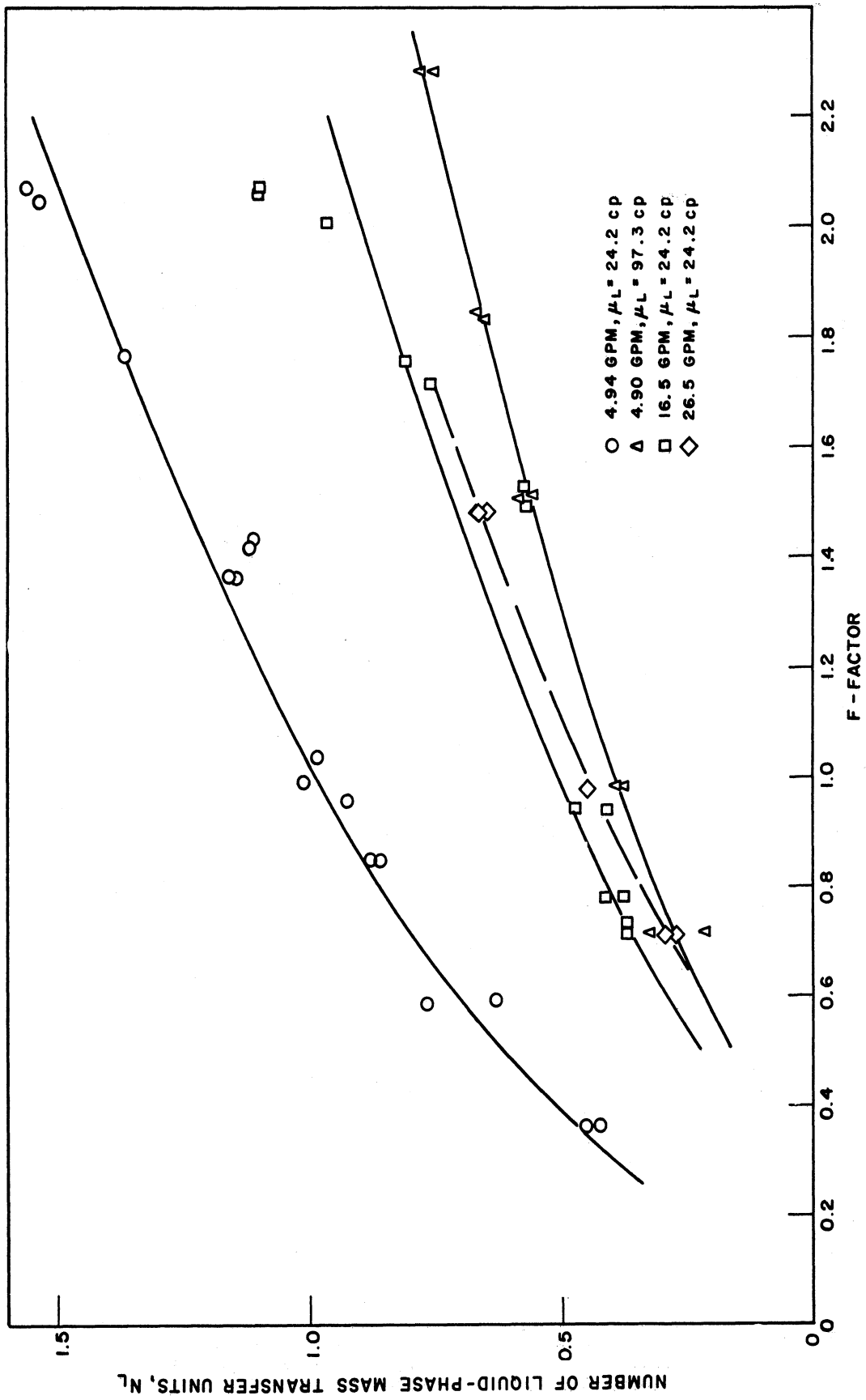

Figure 37. Number of Liquid-Phase Mass Transfer Units for Carbon Dioxide - Cyclohexanol System - Variable Liquid Rate and Liquid Viscosity - 2-inch Weir, 2½-inch Splash Baffle

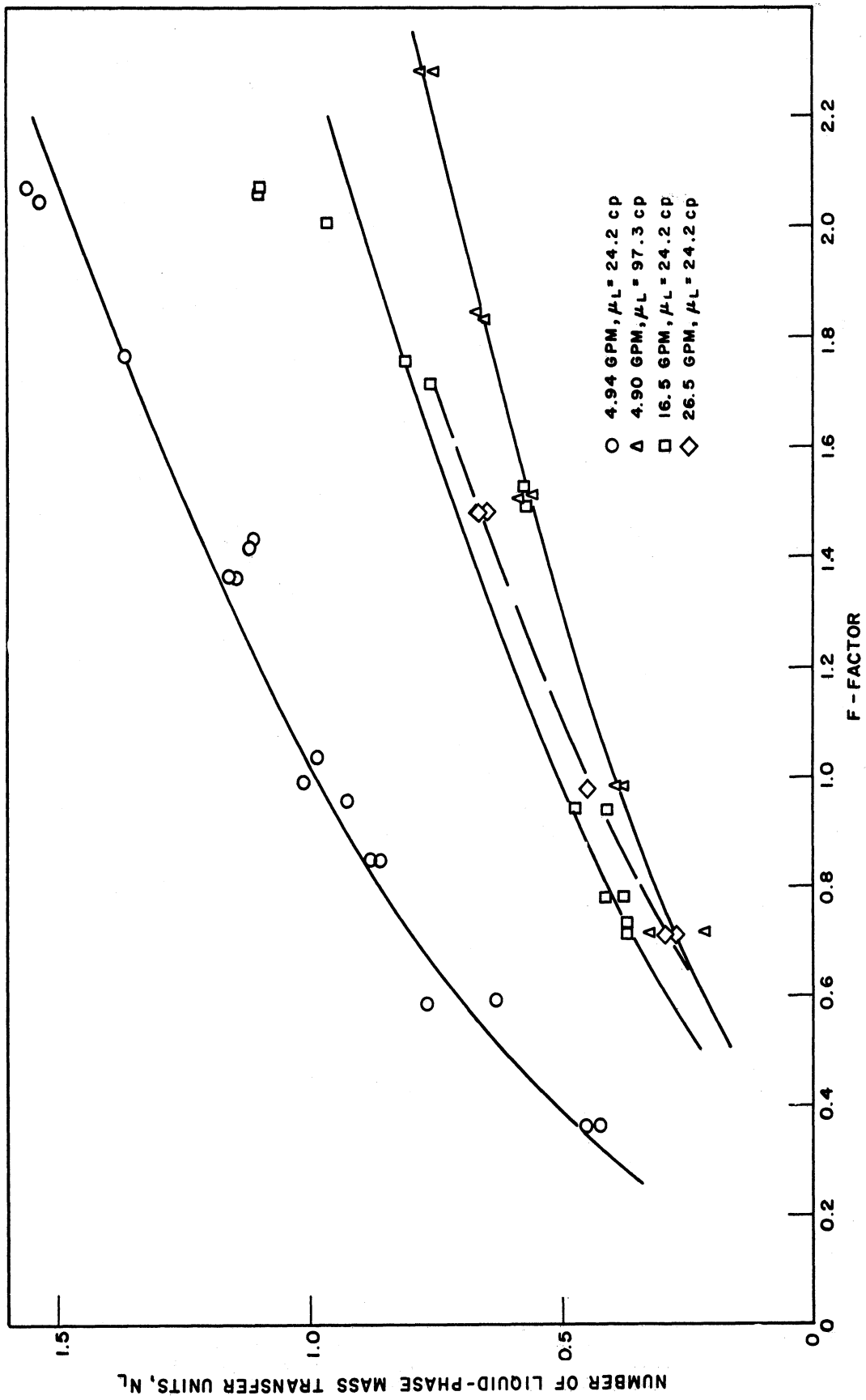

Figure 37. Number of Liquid-Phase Mass Transfer Units for Carbon Dioxide - Cyclohexanol System - Variable Liquid Rate and Liquid Viscosity - 2-inch Weir, 2½-inch Splash Baffle

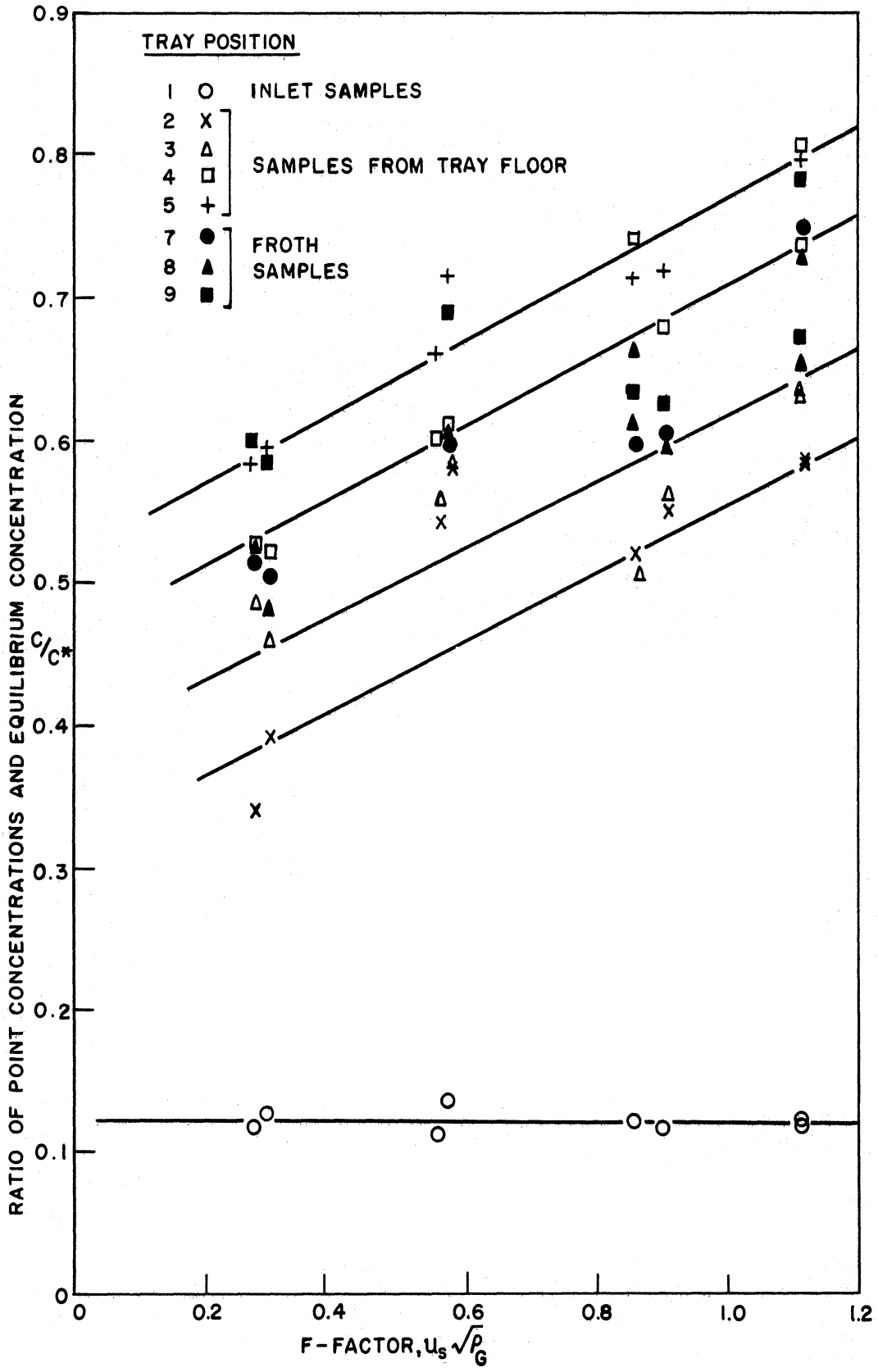

Figure 38. Ratio of Point Concentrations and Equilibrium Concentration on Test Tray; 3-1/2 inch Weir Height; Liquid Rate, 4.95 gpm

nil. The concentrations in the froth are shown by the solid points in Figure 38. The sampling probes in the froth were positioned such that the concentration at position 7 should agree with the concentration at position 2, the concentration at position 8 should fall between the concentrations at positions 3 and 4, and the concentration at position 9 should agree with the concentration at position 5 if there were no concentration gradients in the vertical direction of the froth. If the three data points for position 9 at the high F-factor's are discounted as being in error, the concentrations at that position in the froth agree with the concentrations on the tray floor directly below. The data for position 8 are between the data for positions 3 and 4. Thus it is concluded that no significant vertical concentration gradients were present in the froth in the area between the middle and the outlet of the tray. The concentrations at position 7 in the froth are higher than the data for the corresponding point on the tray floor. In fact, the concentrations are about the same as the data for position 8. The reason for these concentrations being about the same is believed to be caused by the recirculation of the liquid from the center of the tray to the inlet downcomer. This is partially due to the presence of the inactive area between the inlet downcomer and the first row of caps. The presence of a concentration gradient in the froth near the inlet downcomer does not discount the validity of the assumption of no gradient since the gas did not flow this area. In this regard, it would have been of interest to investigate the concentration in the froth above the first row of caps and not near the inlet downcomer. However, the results at points 8 and 9 in the froth verify the validity of the assumption for the major part of the tray and would seem to justify the use of this assumption in the general case.

CORRELATION OF DATA

Vaporization Studies

Two different methods for correlating the vaporization data were considered. These were: (1) correlation by use of an equation of dimensionless groups and least-square fit to the data and (2) correlation by graphical analysis of the data using Equation (23a) as a mathematical model.

$$N_G = k'_{Ga} (Z_f - Z_c)/u_s \qquad (23a)$$

The latter method proved to be the more reliable method for this particular case. The dependent variable in both correlations was the number of mass transfer units. However, in the graphical method, the final form of the correlation can easily be converted to a correlation of the mass transfer coefficient. Both correlations are discussed in the following sections.

In choosing the independent variables to include in the dimensional analysis, there was no question about including the following variables: gas velocity, u_s; gas density, ρ_G; gas viscosity, μ_G; gas diffusivity, D_G; liquid density, ρ_L; liquid viscosity, μ_L; surface tension, σ_L; and a characteristic length, D_S. However, there was some question whether the additional variables which are required to completely define the system should be the variables, liquid rate and weir height, or gas and liquid holdup. It was finally decided that one additional variable, gas holdup, should be sufficient to complete the system of variables. The main reason for choosing gas holdup was because the hydraulic characteristics of this tray were believed to be affected by

the splash baffle and the liquid entering the tray. Had the variables liquid rate and weir height, been used, the exponents on these variables would not necessarily apply to larger columns and would therefore be misleading to anyone not completely familiar with the characteristics of the tray used in the present study. Of course, the use of gas holdup alone discounted the possibility of additional effects of liquid rate and liquid holdup. However, this omission is believed to be justified on the basis of the final fit of the data.

In functional notation, the dependent variable, N_G, may be expressed as a function of the independent variables as follows:

$$N_G = f[(Z_f - Z_c),\ u_s,\ \rho_G,\ \mu_G,\ D_G,\ \rho_L,\ \mu_L,\ \sigma_L,\ D_S] \qquad (107)$$

By use of dimensional analysis, these variables were combined to form the dimensionless groups in Equation (108).

$$N = A \left(\frac{Z_f - Z_c}{D_s}\right)^a \left(\frac{\mu_G}{\rho_G D_G}\right)^b \left(\frac{D_s u_s \rho_G}{\mu_G}\right)^c \left(\frac{\rho_L}{\rho_G}\right)^d \left(\frac{\mu_L}{\mu_G}\right)^e \left(\frac{D_s \sigma_L \rho_L^f}{(\mu_L)^2}\right) \qquad (108)$$

The values of the gas viscosity and diffusivity used in calculating the dimensionless groups in Equation (108) were predicted by use of the correlations of Bromley and Wilke[8] and Wilke and Lee[97], respectively. The liquid density and viscosity of cyclohexanol were determined experimentally and are reported in Tables I-E and II-E and Figures 1E and 2E in Appendix E. Since the ethylene dibromide was relatively pure, the liquid density and viscosity for this liquid were obtained from the literature.[47]

Ashby[7] and Warzel[92] also studied the effect of gas phase resistance to mass transfer on the same tray as used in the present study. These data were included in the present correlations to broaden

the ranges of the several variables involved. In Table VIII the gas and liquid properties are presented for the systems used in the author's studies plus those for the systems used by Ashby and Warzel. Ashby reported the physical properties of the systems used in his study and these are included in Table VIII. The properties for the air-water system used by Warzel were obtained from the literature.(67) The gas viscosity and diffusivity for all systems in Table VIII were calculated by the Bromley and Wilke(8) and Lee and Wilke(97) methods, respectively.

In the actual process of correlating the vaporization data it was decided to start with Ashby's data and determine the constants in Equation (108). Then Warzel's data were added to Ashby's data and another set of constants were determined. Finally, the author's data were added to Ashby's and Warzel's data and the correlation was performed for a third time. A summary of these correlations is presented in Table IX. It should be mentioned that these correlations were performed by use of an IBM 650 electronic computer and the regression analysis program prepared by J. G. Wendel was used in the computer to solve for the coefficients in Equation (108) by the method of least squares.

The reason for grouping the data and performing the correlation for each group was to determine whether the complete set of data could be correlated by Equation (108) and if not, to determine where it failed to correlate the data satisfactorily. The absolute average deviation between the experimental values and the calculated values of N_G was not determined for each correlation. However, the standard deviation of the natural logarithm of N_G was determined and is presented for each correlation in the last column of Table IX. The smallest standard deviation is

TABLE VIII

SUMMARY OF GRAPHICAL ANALYSIS OF VAPORIZATION DATA

System	ρ_G lb/ft^3	μ_G lb/ft-hr	N_{sc} $\mu_G/\rho_G D_G$	μ_L cp	D_G ft^2/hr	ρ_L lb/ft^3	a	1 + a = n	$C^{(1)}$	$\rho_G^{n/2}$	$\rho_G^{1/2}$	$C''^{(2)}$
1. N_2 - Cyclohexanol	0.0676	0.0464	2.98	11.84	0.231	57.8	-0.23	0.77	2.276	0.3544	0.260	1.670
2. N_2 - Cyclohexanol	0.0708	0.045	3.02	24.14	0.210	57.9	-0.042	0.958	2.855	0.2834	0.268	2.70
3. N_2 - Et Br_2	0.0706	0.0456	1.90	1.45	0.341	134.0	-0.558	0.442	2.920	0.5568	0.266	1.395
4. Air - H_2O	0.06893	0.0472	0.56	0.764	1.21	61.7	-0.620	0.380	11.58	0.6015	0.262	5.044
5. He - iC_4H_9OH	0.01303	0.0504	2.20	2.38	1.74	49.1	-0.491	0.509	9.26	0.3311	0.114	3.188
6. N_2 - iC_4H_9OH	0.06693	0.0451	1.54	2.310	0.438	49.1	-0.544	0.456	7.67	0.5398	0.272	3.865
7. Freon 12 - H_2O	0.2737	0.0351	0.24	0.598	0.522	61.9	-0.642	0.358	9.22	0.7930	0.523	6.081
8. He - H_2O	0.01048	0.0485	1.09	0.779	4.22	62.0	-0.666	0.334	17.09	0.4672	0.102	3.731
9. Air - NH_3 - H_2O	0.07305	0.0434	0.613	0.851	1.04	61.7	-0.496	0.504	7.68	0.5171	0.270	4.010
0. He - MIBK	0.01636	0.0427	1.76	2.856	1.48	49.0	-0.595	0.405	10.93	0.4350	0.128	3.216

(1) $N_G = C\ u_s^{n-1}\ (Z_f - Z_c)^{0.72}$

(2) $N_G = C''\ (\text{F-Factor})^{n-1}\ (Z_f - Z_c)^{0.72}$

TABLE IX

SUMMARY OF VAPORIZATION DATA CORRELATION
BY USE OF EQUATION (108) AND REGRESSION ANALYSIS

Correlation Equation (Equation 108) $N = A\left(\frac{Z_f - Z}{D_s}\right)^a \left(\frac{\mu_G}{\rho_G D_G}\right)^b \left(\frac{D_s u_s \rho_G}{\mu_G}\right)^c \left(\frac{\rho_I}{\rho_G}\right)^d \left(\frac{\mu_L}{\mu_G}\right)^e \left(\frac{D_s \sigma_L \rho_L}{(\mu_L)^2}\right)^f$

Constants in Equation	A	a	b	c	d	e	f	Average Absolute Deviation	Average Absolute % Deviation	Maximum % Deviation	Standard Deviation of Logarithm N_G
Ashby's data	5.502	0.713 (0.070)	0	-0.584 (0.046)	-0.422 (0.028)	0.600 (0.024)	0.304 (0.013)				0.0580
Ashby's data	0.938	0.683 (0.073)	-0.146 (0.100)	-0.571 (0.046)	-0.372 (0.044)	0.401 (0.139)	0.202 (0.071)				0.0580
Ashby's plus Warzel's data	3070	0.588 (0.050)	-0.834 (0.120)	-0.480 (0.034)	-0.125 (0.038)	-0.600 (0.156)	-0.321 (0.076)				0.1005
Ashby's, Warzel's, and author's data	4528	0.532 (0.040)	-0.892 (0.020)	-0.408 (0.029)	-0.070 (0.023)	-0.694 (0.042)	-0.370 (0.020)	0.221	11.59	31.78	0.1170
Ashby's data	24.14	0.607 (0.072)	-0.427 (0.020)	-0.532 (0.047)	-0.271 (0.028)	0.004 (0.008)	0	0.144			0.0612
Ashby's plus Warzel's data	10.86	0.556 (0.053)	-0.341 (0.030)	-0.441 (0.035)	-0.236 (0.029)	0.056 (0.010)	0				0.1080
Ashby's, Warzel's, and author's data	6.279	0.548 (0.069)	-0.696 (0.029)	-0.514 (0.050)	-0.129 (0.040)	0.056 (0.016)	0	0.304	19.64	77.80	0.2039

Numbers in parentheses are standard errors for the coefficients.

for the correlation of Ashby's data. The standard deviation for logarithm of N_G is 0.0580 in this case. The standard deviation increased to 0.1005 when Ashby's data plus Warzel's data were correlated and to 0.1170 when the author's data were added to Ashby's and Warzel's data. The absolute average percent deviation for the latter case was 11.59 with a maximum deviation of 31.78 percent indicating a fairly reasonable fit of the data. However, judging from the difference between the standard deviation of the logarithm of N_G for this correlation and the correlation of Ashby's data alone, the correlation of Ashby's data is much better.

The regression analysis program was planned so that the standard error for the constants in Equation (108) were determined. In addition, in cases where the value of any one of the constants was less than two times the standard error for that constant, the particular group involved was not included in the correlation. In the case of Ashby's data, the exponent on the Schmidt group was less than two times the standard error and the correlation was performed without this group. The correlation was also performed with the Schmidt number included by rejecting the test procedure in the analysis program where the machine made the decision to drop this group. The standard deviation for the logarithm of N_G in each of these cases was 0.0580. Thus it is concluded that the variable; gas diffusivity, D_G; is not necessary to correlate Ashby's data satisfactorily. It should be noted, however, that the exponents on the remaining groups changed significantly when the Schmidt number was not included in Equation (108). Ashby varied the diffusivity in the gas phase by changing the liquid being vaporized and the gas used to vaporize the liquid. The physical properties of the gas phase for each of the systems used by Ashby are

included in Table VIII. By close examination of these data, a high order of correlation between gas diffusivity and gas density can be seen. Therefore, in the correlation without the Schmidt number in Equation (108), the effects of the variations in gas physical properties are adequately correlated by gas density and viscosity and possibly the properties of the liquid. This does not mean that gas diffusivity per se is not an important variable. It does mean that with the type of equation used to correlate the data, gas diffusivity is not required to correlate the data satisfactorily.

The variations of the constants in Equation (108) depending on the data used in the correlation are considerable. The largest variations are in the exponents on the Schmidt number (-0.146 to -0.892), the density ratio (-0.372 to -0.070), the viscosity ratio (0.401 to -0.694) and the surface tension group, (0.202 to -0.370). The largest change in the constants in comparison with those for Ashby's data alone was found when Warzel's data were added to Ashby's data. The differences between the constants for correlation where the author's data were included and those for the correlation of Ashby's plus Warzel's data are not believed to be significant (see the standard errors in Table IX). Possible explanations for the variations of the constants in Equation (108) depending on the data used in the correlation are: (1) The data from the studies by Warzel and the author are in error considerable in relationship to Ashby's data. Of course, the reverse of this could be true. The statistician would make this statement by saying that one of the sets of data is biased. (2) The form of the equation used to correlate the data will not satisfactorily fit the data. (3) The variables

are not completely linear independent, or in other words, an orthogonal set of variables, therefore, the results presented in Table IX would be expected even for a slight bias in one or two sets of data.

The partial correlation coefficients for the dimensionless groups in Equation (108) are presented in Table X. All three sets of data (Warzel's, Ashby's, and author's data) were used in determining these coefficients by the method outlined by Hildebrandt.[43] This method was a part of the regression analysis program used in the computer and the coefficients were a part of the data printed-out for each correlation. The square of any one of the numbers in Table X represents the approximate percentage of the variation in the dimensionless group at top of the particular column which can be accounted for by the group in the left hand column but in the same row. The reverse is also true. The highest order of correlation is between the surface tension group, $D_s\sigma_L\rho_L/(\mu_L)^2$ and the viscosity ratio, μ_L/μ_G. The partial correlation coefficient for these two groups is 0.933 indicating that about 86 percent of the variation in either group can be accounted for by the other one. Because of this, the three groups of data were correlated by Equation (109) which does not include the surface tension group. The constants for the new correlations are also presented in Table IX. The

$$N_G = A\left(\frac{Z_f - Z_c}{D_s}\right)^a \left(\frac{\mu_G}{\rho_G D_G}\right)^b \left(\frac{D_s u_s \rho_G}{\mu_G}\right)^c \left(\frac{\rho_L}{\rho_G}\right)^d \left(\frac{\mu_L}{\mu_G}\right)^e \qquad (109)$$

variations in the constants are not as great as in the cases where the surface tension group was included in the correlation equation. Also, the standard deviations for the logarithm of N_G indicate that Ashby's and Warzel's data are correlated as well as in the cases where this group was

TABLE X

PARTIAL CORRELATION COEFFICIENTS FOR THE DIMENSIONLESS GROUPS IN EQUATION 108

Dimensionless Group	Z_f-Z_c/D_S	$\mu_G/\rho_G D_G$	$D_S u_s \rho_G/\mu_G$	ρ_L/ρ_G	μ_L/μ_G	$D_S \sigma_L \rho_L/(\mu_L)^2$
Z_f-Z_c/D_S	1.000	-0.187	0.627	-0.117	0.029	0.027
$\mu_G/\rho_G D_G$	-0.187	1.000	-0.742	0.783	-0.247	-0.095
$D_S u_s \rho_G/\mu_G$	0.627	-0.742	1.000	-0.816	0.048	0.161
ρ_L/ρ_G	-0.117	0.783	-0.816	1.000	-0.115	-0.081
μ_L/μ_G	0.029	-0.247	0.048	-0.115	1.000	-0.933
$D_S \sigma_L \rho_L/(\mu_L)^2$	0.027	-0.095	0.161	-0.081	-0.933	1.000

used. For the correlation where the author's data were included, the standard deviation for the logarithm of N_G and the average absolute percent deviation for N_G are both greater than in the case where the surface tension group was used in the correlation equation. The latter result indicates that the surface tension group does improve the correlation when the liquid properties, viscosity and density, are varied significantly.

The greatest variation in the constants for the cases where the surface tension group was not included in the correlation equation is in the exponent on the Schmidt number. The range of variation is -0.341 to -0.696 and compares with the range of 0 to -0.892 in the case where the surface tension group was used in the correlation. These ranges of values for the exponent on the Schmidt number bracket the value of 0.5 which has been used by several investigators.(78,1,94) The value of two thirds has also been used however.(64,10)

The results in Table IX indicate that Warzel's and Ashby's data are satisfactorily correlated by using the variable, gas holdup, in the correlation equation. Ashby's studies were conducted at 1-1/2 inch weir height while Warzel's studies were for 2 and 3-1/2 inch weir. Ashby(7) correlated his data by using in place of gas holdup, the height of liquid above the bottom of the slot opening which was determined by use of the height of liquid over the weir as defined by the Francis weir formula and an equation for slot opening as a function of gas rate and liquid density. The other groups in Ashby's correlation equation were similar to those used in Equation (108). Ashby used his correlation in an attempt to predict Warzel's data for the absorption of ammonia in

water and found that the predicted values of N_G were about 40 percent higher than the experimental values reported by Warzel. Ashby attributed this difference to the correction for the liquid-phase resistance which Warzel made for the ammonia absorption data. The liquid-phase resistance was estimated by use of Warzel's data for the carbon dioxide-water system. Ashby reasoned that the small bubbles in the froth which tend to be recirculated contribute more to the mass transfer in the case of a low efficiency system (absorption of carbon dioxide in water) than in a high efficiency system (absorption of ammonia) where the gas is nearly saturated. He believed that this difference would cause the liquid-phase resistance for the carbon dioxide-water system when corrected for differences in liquid properties to be high in relation to the resistance which actually existed for the ammonia-water system. The results of the present analysis do not support this reasoning since Ashby's and Warzel's data are satisfactorily correlated by either Equation (108) or Equation (109). It is believed that the choice of the variable, $\frac{h_L}{D_S}$, by Ashby was improper. The more direct variable seems to be gas holdup. However, Ashby's correlation probably could have been improv
cluding data over a wider range of the variable, $\frac{h_L}{D_S}$.

Correlations of the vaporization data by use of Equation (108) or Equation (109) are not satisfactory from the standpoint of being assured that the results can be extrapolated beyond the range in the variables studied. Although the constants in the equation were more reproducible when the surface tension group was not included, the correlation was not satisfactory for the author's data obtained for a system of high liquid density and systems of high liquid viscosities. For these reasons, it was decided that a graphical analysis of the data should be performed.

The graphical analysis of the data was approached by use of the relationship developed previously and used by Gerster[35] to correlate Ashby's data. This relationship was presented previously as Equation (23a).

$$N_G = k_G' a \frac{Z_f - Z_c}{u_s} \tag{23a}$$

Using the foregoing definition for $k_G' a$, Gerster correlated Ashby's data as follows:

$$k_G' a = C\, u_s^{0.23} \tag{23b}$$

where $C = 18.19\, D_G^{0.33}$

The data from the present study were used to calculate values of $k_G' a$ by use of Equation (23a) and the gas holdup and the superficial linear velocity for each run. The resulting data for the mass transfer coefficients are plotted in Figures 39 and 40. The value of the mass transfer coefficients for the nitrogen-cyclohexanol system are dependent on both the weir height and superficial gas velocity. The coefficients for 1-1/2 inch weir height are more than one and one-half times the values for the 2 inch weir and about two times the values for the 3 inch weir. The effect of weir height is not as great for the nitrogen-ethylene dibromide system in Figure 40. In this case, the values for the coefficients at the 3-1/2 inch weir height are about two-thirds of the values at 1-1/2 inch weir. The results in Figures 39 and 40 clearly indicate that the equation used by Gerster to correlate Ashby's data needs to be modified in order to correlate the data at the higher weir heights from the present study. Apparently, the successful correlation of Ashby's

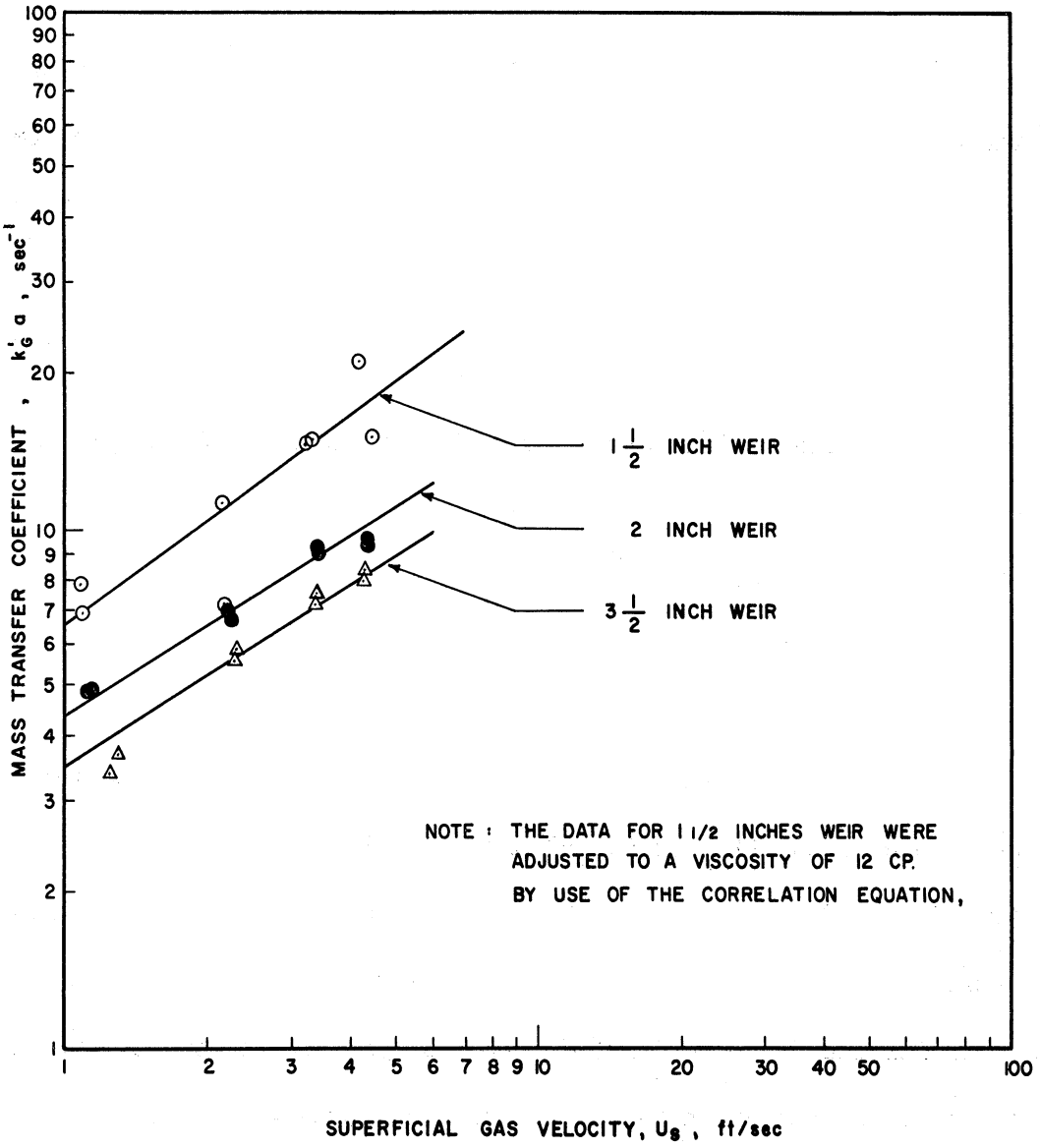

Figure 39. Mass Transfer Coefficients for Nitrogen-Cyclohexanol System at Three Different Weir Heights - Liquid Viscosity = 12cp.

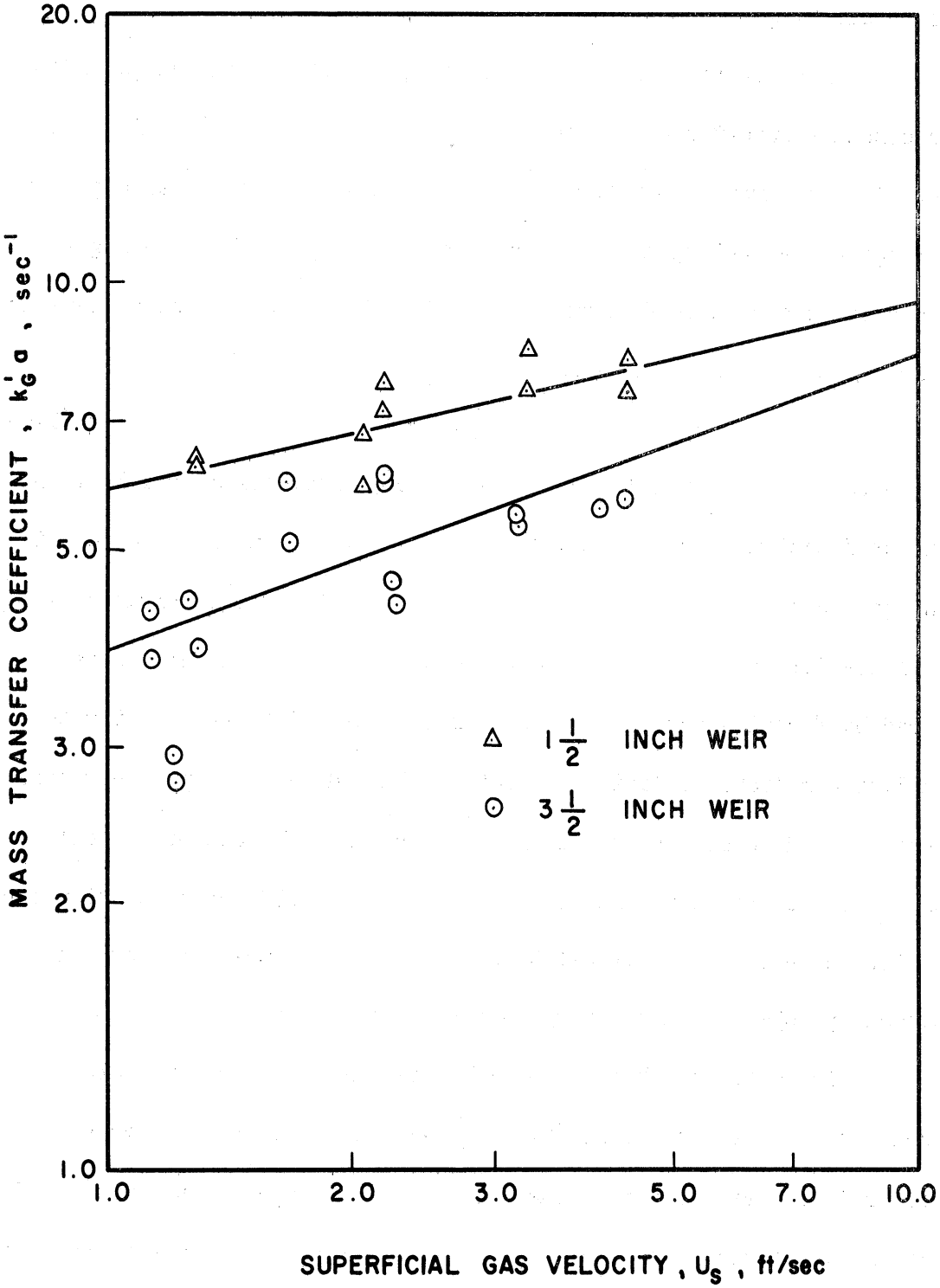

Figure 40. Mass Transfer Coefficients for Nitrogen-Ethylene Dibromide System at 1-1/2 and 3-1/2 inch Weir Height.

data by Equation (23b) is due to the fact that these data were obtained at one weir height, 1-1/2 inch.

In order to examine the relationship between N_G and gas holdup at a constant superficial gas velocity the data of Warzel[92] for the absorption of ammonia in water were used. These data cover an appreciable range of gas holdup at a constant gas velocity as shown in Figure 41. These data were used to determine the constants in the following equation by the method of least squares.

$$N_G = C\, u_s^{a}(Z_f - Z_c)^{b} \qquad (110)$$

The constant, b, was found to be equal to 0.72 indicating that N_G is not a linear function of gas holdup for these data. A similar relationship is suggested by the data from the present investigation in Figures 39 and 40. These data cover approximately the same range of gas holdup as covered by Warzel's data but the number of data points are too few to establish a reliable relationship between N_G and gas holdup. Therefore, it was decided to use the relationship established by use of Warzel's data and to determine whether this relationship would satisfactorily correct for the effect of weir height or gas holdup on the data for the nitrogen-cyclohexanol and nitrogen-ethylene dibromide systems.

The data of Ashby and Warzel plus the author's data were used to calculate the values of $N_G/(Z_f - Z_c)^{0.72}$ which are plotted versus F-factor in Figure 42. Since the gas density for each system presented in Figure 42 is essentially constant over the range of F-factor, the data of $N_G/(Z_f - Z_c)^{0.72}$ could have been plotted versus gas velocity with the

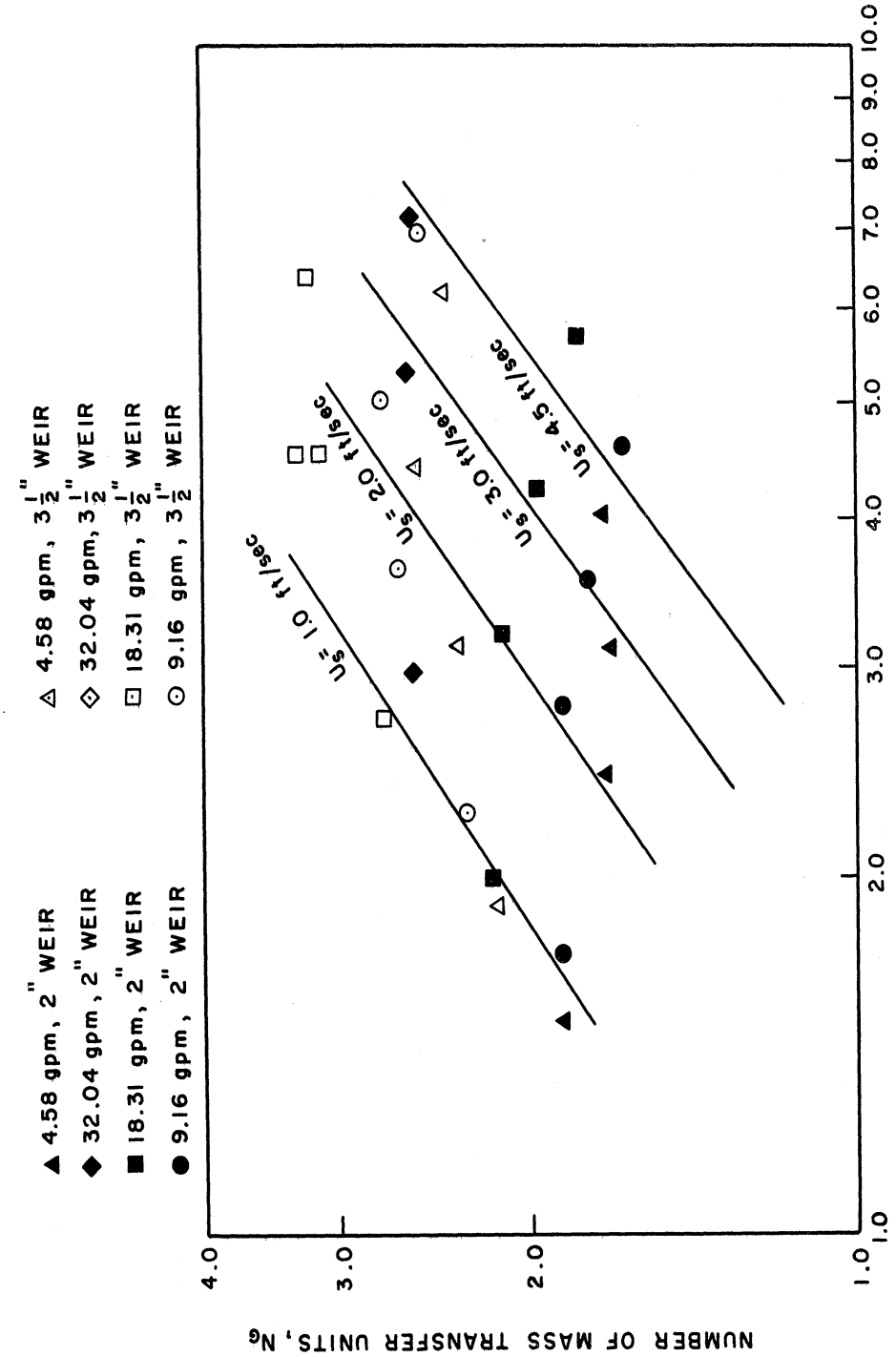

Figure 41. Number of Mass Transfer Units for Ammonia-Water System Data of Warzel(92)

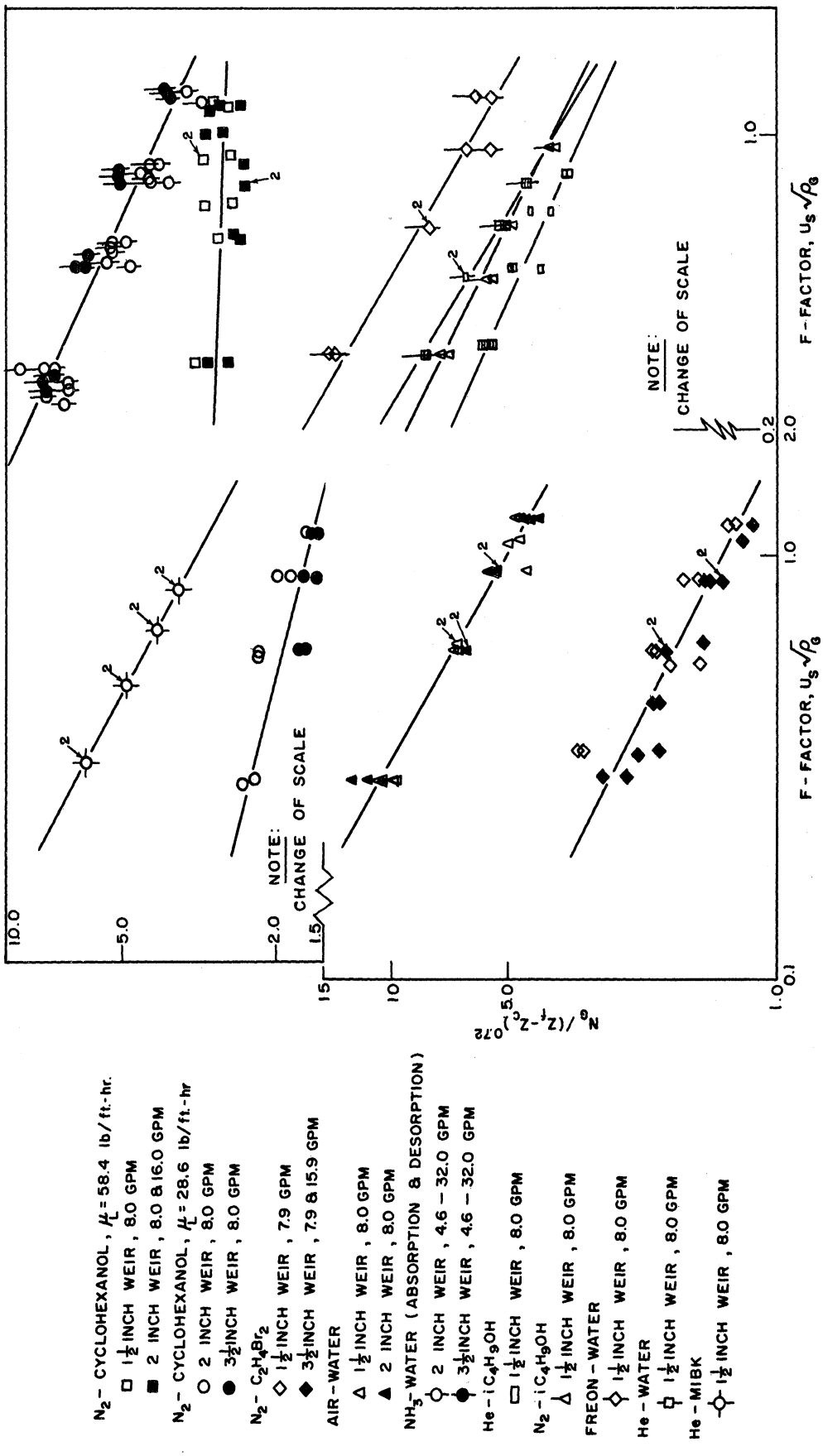

Figure 42. The Effect of Liquid Properties Upon the Relationship Between $N_G/(Z_f - Z_c)^{0.72}$ and F-Factor

result being the same. The results in Figure 42 indicate that the use of the function $N_G/(Z_f - Z_c)^{0.72}$ does correct for the effect of gas holdup or weir height on the data from the present investigation. The deviations from the straight line through each set of data are appreciable in some cases but there is no definite trend with weir height. Another important observation concerning Figure 42 is the variation of the slopes of the best straight lines through the data. In fact, if the slopes of these lines are plotted versus kinematic liquid viscosity, the correlation in Figure 43 is obtained. The slope of the straight line through each set of data was determined by a least-squares fit of the data to the following equation,

$$\frac{N_G}{(Z_f - Z_c)^{0.72}} = C'' \text{ (F-factor)}^a \qquad (111)$$

The values of the constants, "a" and C", for each system are presented in Table VIII.

The data in Figure 43 could be fitted to an equation of proper form but the form required would not be the most convenient to use in the final correlation equation. When the values of 1 + a for the different systems are plotted versus kinematic viscosity, the data can be represented by a straight line as shown in Figure 44. The plot of 1 + a versus liquid viscosity is also presented in Figure 44. The use of kinematic liquid viscosity appears to be the correlating variable since the data point for the high liquid-density system, nitrogen-ethylene dibromide, is better correlated by use of this variable with no obvious change in the correlation of the other data points. The best straight line through the data of 1 + a versus kinematic viscosity was determined by the method of

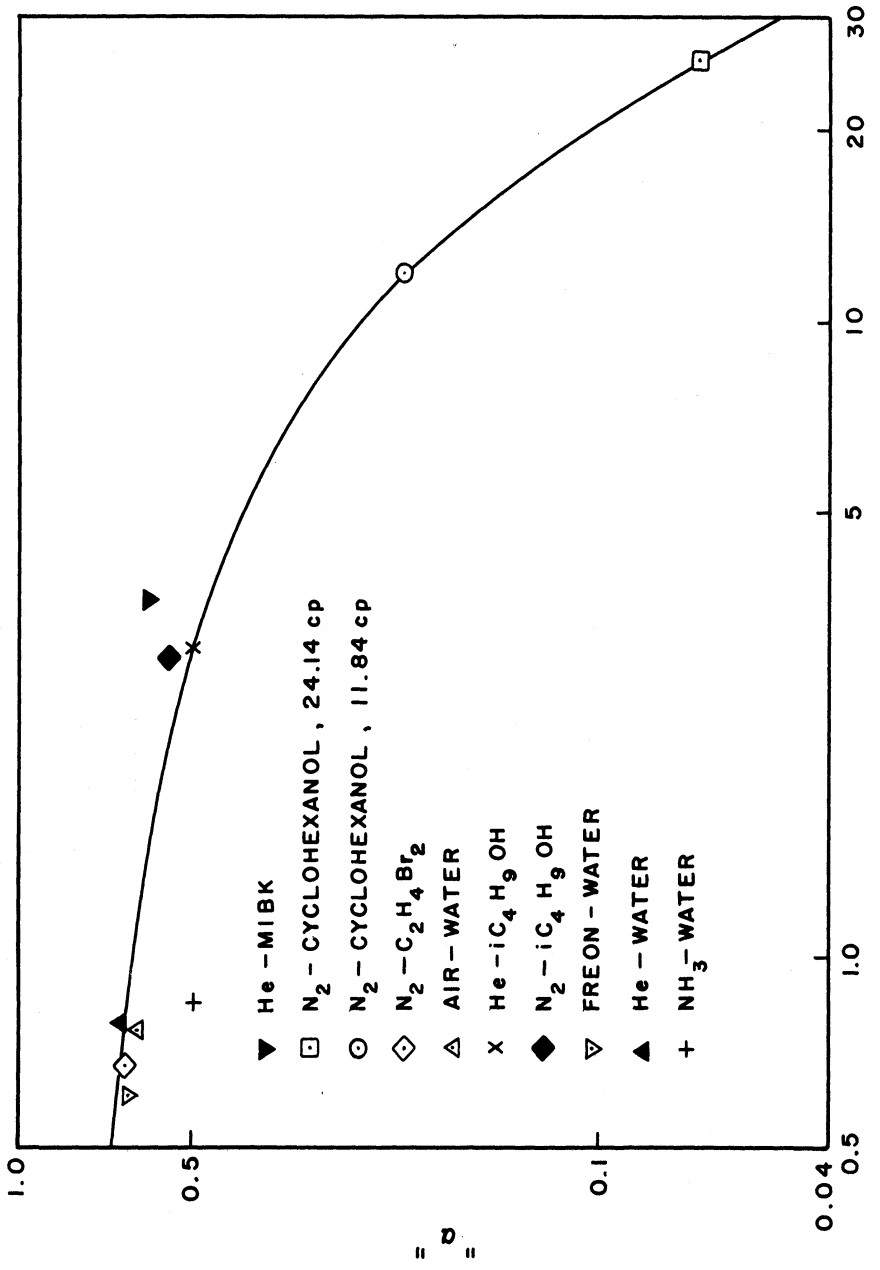

Figure 43. Correlation of the Constant "a" in the Equation $N_G/(Z_f - Z_c)^{0.72} = C'' \rho_G^{a/2} u_s^a$ with Kinematic Liquid Viscosity

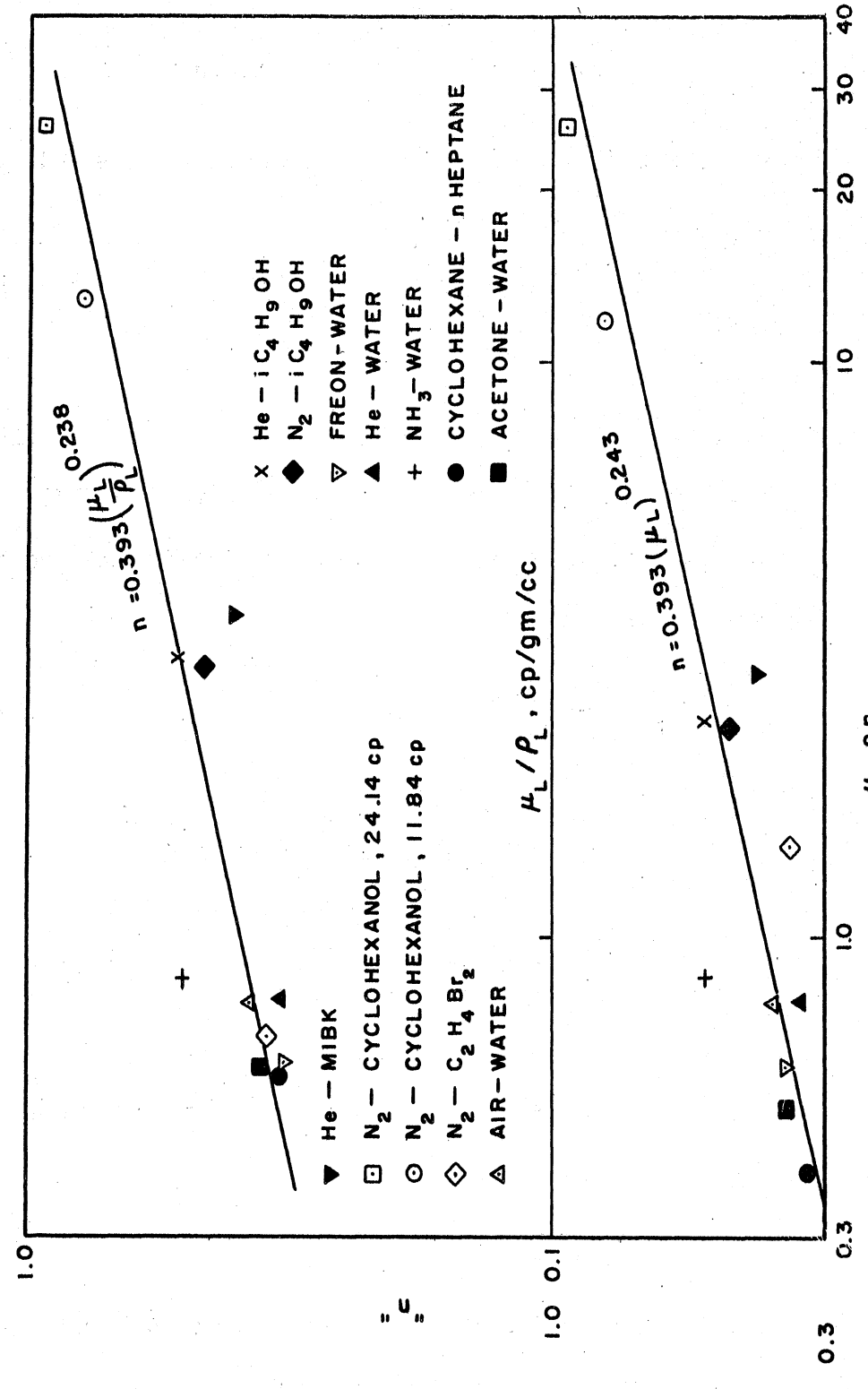

Figure 44. Correlation of "n" in the Equation $K_Ga' = C''\rho_G^{n/2}u_s^{n=1+a}/(Z_f-Z_c)^{0.28}\ \rho_G^{1/2}$ with Liquid Absolute Viscosity and Liquid Kinematic Viscosity

least squares. The correlation equation is,

$$n = 1 + a = 0.393 \left(\frac{\mu_L}{\rho_L}\right)^{0.238} \tag{112}$$

where $\frac{\mu_L}{\rho_L}$ = kinematic viscosity, centistokes.

Up-to this point the correlation of N_G may be represented as follows,

$$N_G = C'' \, u_s^{n-1} \, \rho_G^{n-1/2} (Z_f - Z_c)^{0.72} \tag{113}$$

An equally valid correlation might be

$$N_G = C \, u_s^{n-1} \, (Z_f - Z_c)^{0.72} \tag{114}$$

The constants, C and C", for each system are presented in Table VIII. Equation (113) or Equation (114) may be converted as follows to a correlation of $k'_G a$ by use of the definition,

$$N_G = k'_G a \, \frac{Z_f - Z_c}{u_s} \tag{23a}$$

Therefore,

$$k'_G a \, \frac{(Z_f - Z_c)}{u_s} = C'' \, u_s^{n-1} \, \rho_G^{n-1/2} \, (Z_f - Z_c)^{0.72} \tag{115}$$

and

$$k'a = C'' \, \frac{u_s^{n} \, \rho_G^{n/2}}{\rho_G^{1/2} \, (Z_f - Z_c)^{0.28}} \tag{116}$$

By use of Equation (114), the relationship for the mass transfer coefficient is

$$k'a = \frac{C \, u_s^{n}}{(Z_f - Z_c)^{0.28}} \tag{117}$$

Equation (116) and (117) are identities and the constants may be related by the following equation if $(\text{F-factor})^{n-1}$ is considered to

be the correct way for combining gas velocity and density.

$$\frac{C}{\rho_G^{n/2}} = \frac{C''}{\rho_G^{1/2}} \tag{118}$$

However, if superficial gas velocity is considered as the correlating variable with the exponent, n-1, instead of F-factor, then the relationship between C and C" is not Equation (118) but some other relationship which can be determined only after C has been properly correlated. In the final analysis of the data, the use of F-factor and superficial gas velocity were examined.

In order to complete the correlations, the variables required to correlate the constants C and C", were determined by trial and error. The variables which were believed to be necessary in these correlations were: (1) gas diffusivity, D_G; (2) gas viscosity, μ_G; (3) gas density, ρ_G; (4) liquid density, ρ_L; and (5) liquid viscosity, μ_L. The range in the gas viscosity covered by the different systems is 0.0351 to 0.0504 lb/ft.hr. with the majority of the systems having a viscosity in the range of 0.0427 to 0.0485 lb/ft.hr. Therefore, in the first attempts to correlate the constants in Equations (116) and (117) gas viscosity was not included. The variable, $C''/\rho_G^{1/2}$, was first correlated as a function of the variables, D_G, ρ_L, and μ_L. The correlation is,

$$\frac{C''}{\rho_G^{1/2}} = 16.43 \frac{D_G^{0.526}\ \mu_L^{0.032}}{\rho_L^{0.83}} \tag{119}$$

where

D_G = gas diffusivity, $ft^2/hr.$
ρ_G = gas density, $lb/ft^3.$
ρ_L = liquid density, gm/cc.
μ_L = liquid viscosity, cp.

The exponent on liquid viscosity in Equation (119) is not great and is probably not significant. For this reason, the correlation was repeated by using only gas diffusivity and liquid density. The equation for this correlation is as follows:

$$\frac{C''}{\rho_G^{1/2}} = 16.67 \frac{D_G^{0.526}}{\rho_L^{0.834}} \qquad (120)$$

The group, $C'' \rho_L^{0.834}/\rho_G^{1/2}$, is plotted versus gas diffusivity in Figure 45. The absolute average percent deviation between the values of $C''/\rho_G^{1/2}$ used in the correlation and the values predicted by Equation (120) is 8.28. The maximum deviations from the correlation line are for the two systems at high liquid viscosities (nitrogen-cyclohexanol).

Equations (113) and (120) were used to predict the values of N_G for the runs indicated in Table II-G. The absolute average percent deviation between the experimental values of N_G and the predicted values using this correlation is 14.59 with a maximum deviation of 65.36. The corresponding values for the correlation of the data by Equation (108) are 11.59 and 31.78, respectively.

An attempt was made to improve the correlation of the data by including gas viscosity in the correlation of C". This was done by arbitrarily including the gas viscosity and gas diffusivity in the correlating equation as follows,

$$\frac{C'' \mu_G^{1/2}}{\rho_G^{1/2} D_G^{1/2}} = f(\mu_L, \rho_L) \qquad (121)$$

The correlation obtained is presented as Equation (122),

$$\frac{C'' \mu_G^{1/2}}{\rho_G^{1/2} D_G^{1/2}} = 3.14 \frac{\mu_L^{0.023}}{\rho_L^{0.653}} \qquad (122)$$

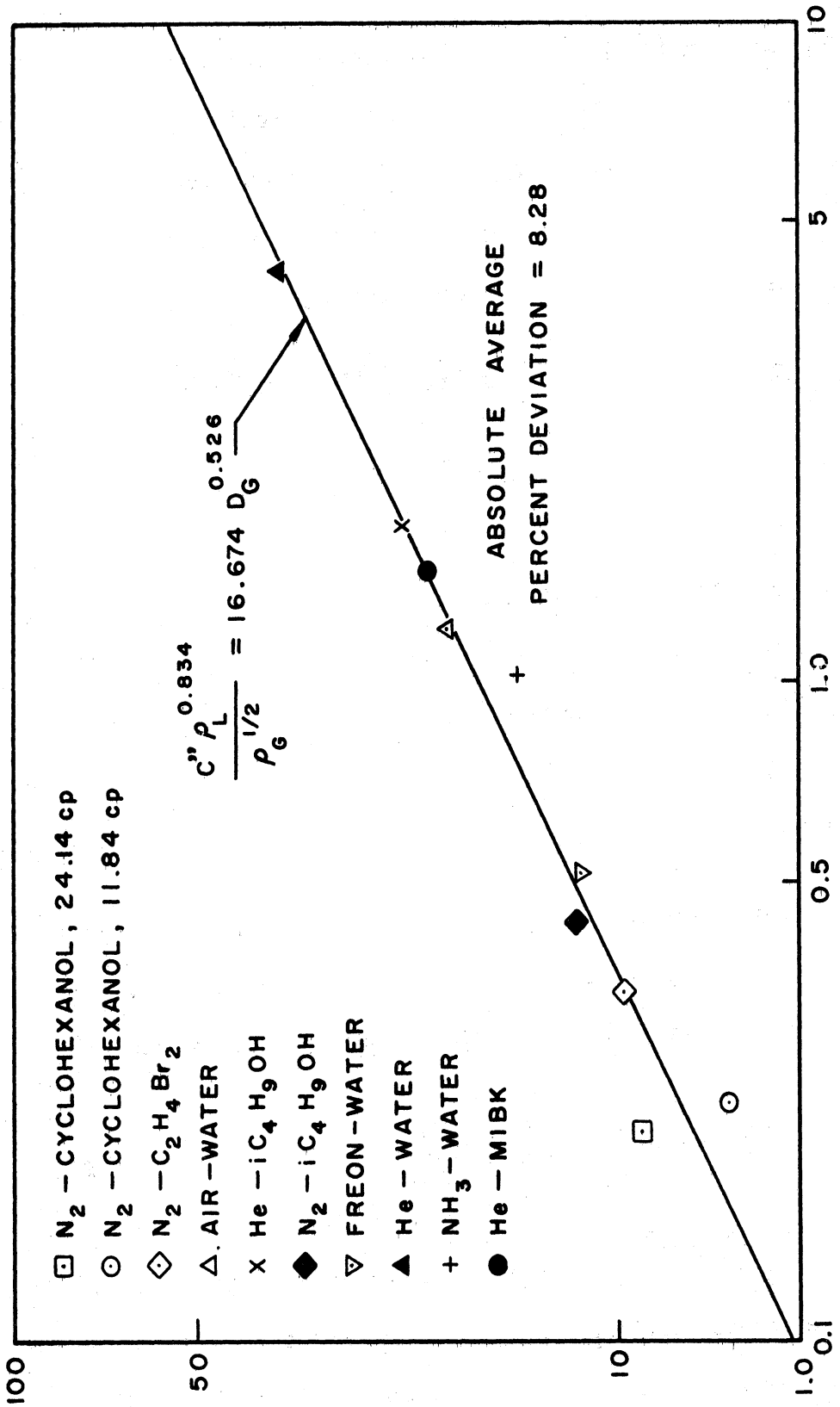

Figure 45. Correlation of "C" in the Equation $k'_G a = C'' \rho_G^{n/2} u_s^{1+a=n} / (Z_f - Z_c)^{0.28} \rho_G^{1/2}$ with Physical Properties of Gas and Liquid

The deviations between the values of C" used in this correlation and the predicted values are greater than the deviations for the correlation by Equation (120). The absolute average percent deviation is 15.9 with a maximum deviation of 33.0. The corresponding values for Equation (120) were 8.28 and 27.3. On this basis, the correlation of C" by Equation (120) was chosen as the best fit of the data. Therefore, the recommended correlation of N_G using Equation (23a) is,

$$N_G = 523.9 \frac{D_G^{0.526} \rho_G^{1/2}}{\rho_L^{0.834}} (\text{F-factor})^{n-1} (Z_f - Z_c)^{0.72} \qquad (123)$$

where

$$n = 0.852 \left(\frac{\mu_L}{\rho_L}\right)^{0.238}$$

D_G = gas diffusivity, $ft^2/hr.$

ρ_G = gas density, $lb/ft^3.$

ρ_L = liquid density, $lb/ft^3.$

μ_L = liquid viscosity, lb/ft.hr.

$(Z_f - Z_c)$ = gas holdup, ft.

To determine whether the correlation of N_G should be in terms of $(\text{F-factor})^{n-1}$ or u_s^{n-1}, the constants, C, for Equation (117) were correlated by use of the variables ρ_G, D_G, ρ_L, and μ_L. The result is as follows,

$$C = 10.582 \frac{D_G^{0.405} \rho_G^{0.048}}{\rho_L^{0.816} \mu_L^{0.248}} \qquad (124)$$

The function, $\frac{C\rho_L^{0.816} \mu_L^{0.248}}{\rho_G^{0.048}}$, is plotted versus D_G in Figure 46. The absolute average percent deviation between the values of C used in the correlation and the values predicted by Equation (124) is 13.74. The

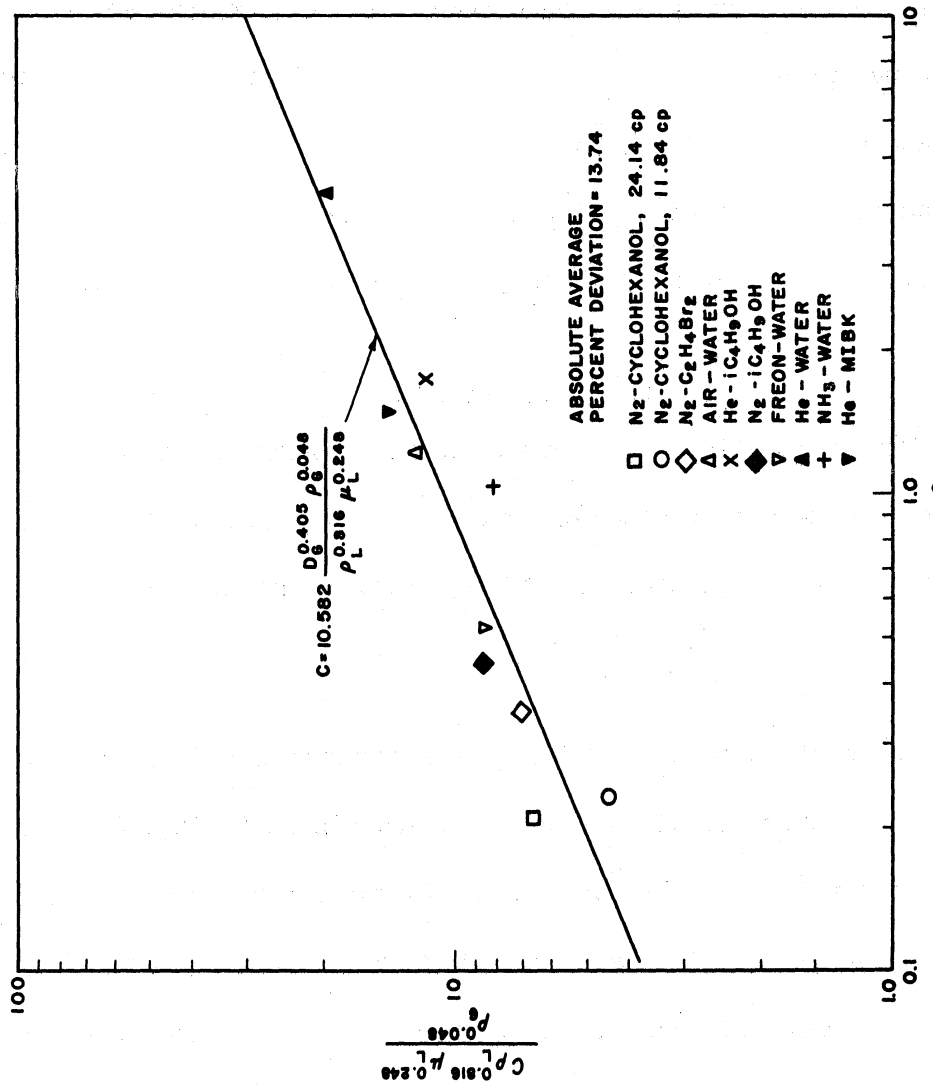

Figure 46. Correlation of the Constant "C" in the Equation $k_G a' = C\, u_g^{1+a-n}/(Z_f - Z_d)^{0.28}$ with Physical Properties of Gas and Liquid

absolute average percent deviation between the experimental values of N_G and the values predicted by use of Equations (114) and (124) is 21.08 with maximum deviation of 115 percent. Therefore, the correlating variable, $(\text{F-factor})^{n-1}$, and not w_s^{n-1}, appears to be the one to use for the best fit of the data by the model represented by Equation (23a).

Absorption Studies

The correlation of the data for the absorption of carbon dioxide in cyclohexanol was accomplished with some degree of success by use of the following equation to define a mass transfer coefficient,

$$N_L = k_L \bar{a}\, t_L \tag{39a}$$

The final correlation consists of the mass transfer coefficient as a function of F-factor, liquid diffusivity, and kinematic liquid viscosity. The major uncertainty in the correlation is correct value of the liquid diffusivity for carbon dioxide in cyclohexanol. The experimental values of diffusivity reported recently by Schoenborn(3) and values predicted by the semi-empirical equations of Chang and Wilke(13) and Arnold(5) were used to indicate the different interpretations of the data which may be made depending on the diffusivities used in the correlation.

Mass transfer coefficients were calculated by use of Equation (39a). The liquid contact time was determined by use of the following equation,

$$t_L = \frac{(Z_f A_T - \text{volume of caps})\, Z_c/Z_f}{Q_L} \tag{125}$$

where Q_L = volumetric rate of liquid to the tray, $ft^3/sec.$

A_T = area of the tray.

The calculated data are presented in Table IV-G in Appendix G and the mass transfer coefficients are plotted versus F-factor in Figure 47. The use of Equations (39a) and (125) to determine a mass transfer coefficient appears to correct for the effects of liquid rate and weir height and certainly simplifies the correlation involved in accounting for these variables. The data for the liquid viscosity of 24.1 - 24.8 centipoises and variable liquid rate at 2 and 3-1/2 inch weir heights are satisfactorily correlated by a straight line with possible exceptions of five or six data points. The effect of liquid viscosity is very apparent by the three-fold decrease in the mass transfer coefficient with a four-fold increase in viscosity. The straight line through the sets of data at different liquid viscosities are parallel, however. Apparently, liquid viscosity does not affect the relationship between the coefficient and F-factor as was found for the gas-phase coefficients.

Liquid diffusivities for the carbon-dioxide cyclohexanol system were first calculated by use of the correlation by Wilke and Chang[13] and used to correlate the mass transfer coefficients. The resulting correlation is presented in Figure 48. The exponent on diffusivity was taken to be 0.5, the value which was predicted by Higbie[42] and Danckwerts[22] for mass transfer through an interface which is continuously renewed. With the possible exception of the data at the high viscosity, 97.3 centipoises, the use of liquid diffusivity to the one-half power corrects for the effect of viscosity. It was pointed out previously in the section entitled, "Experimental Procedure", that the viscosity of the liquid was varied by varying the liquid temperature. Therefore, these results indicate that the change in liquid viscosity

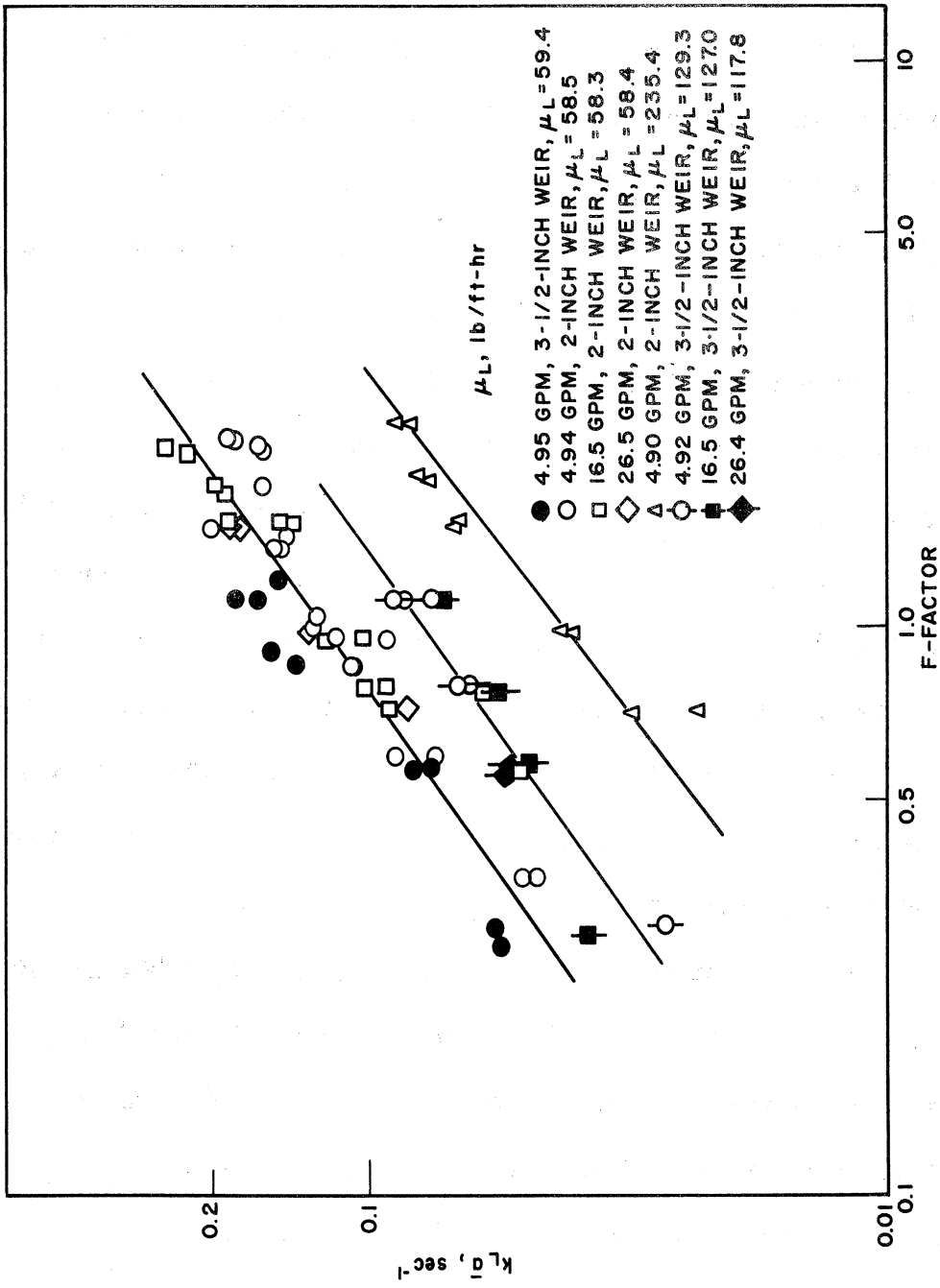

Figure 47. Mass Transfer Coefficients for Carbon Dioxide-Cyclohexanol System. Variables: Gas Rate, Liquid Rate, Weir Height, and Liquid Viscosity.

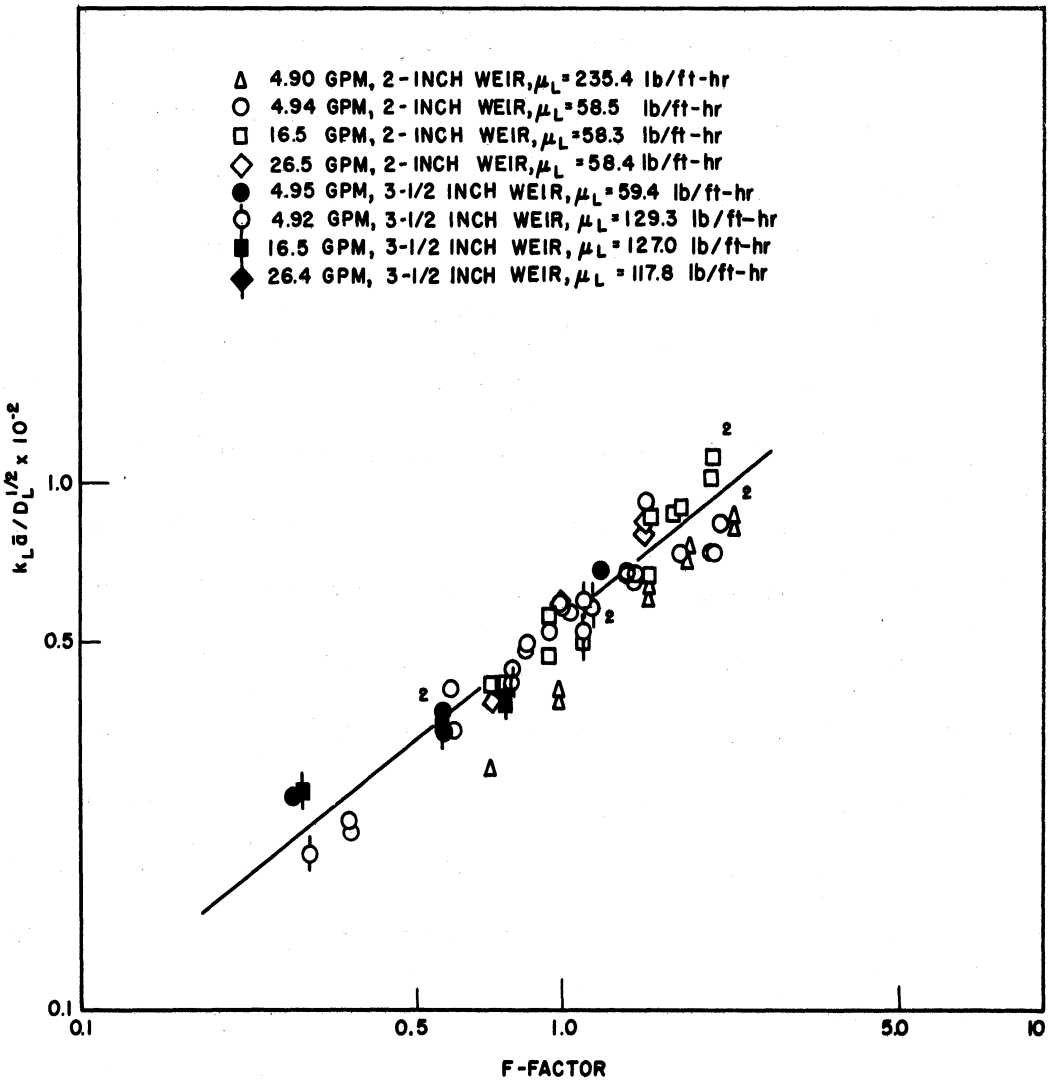

Figure 48. Correlation of Mass Transfer Coefficients for Carbon-Dioxide-Cyclohexanol System

can be accounted for by a diffusivity correction. Also according to these results the effect of viscosity on the specific interfacial area or mechanism of transfer is not great.

In order to compare the data for the carbon dioxide-cyclohexanol system with the data for a system of low liquid viscosity, the data obtained by Warzel[92] were used. These data are presented in Table V-G. The Wilke and Chang correlation was also used to calculate the liquid diffusivity for carbon dioxide in water. The data are plotted as mass transfer coefficient divided by diffusivity to the 0.5 power versus F-factor in Figure 49. Warzel's studies were conducted at a constant temperature at 77°F. Therefore, there should be no variations due to improper correction of liquid diffusivity for the data in Figure 49. The deviations in these data are considerable, however, and by examination it can be seen that the deviations are a function of weir height. In fact, at low values of F-factor, the values of $k_L\bar{a}/D_L^{1/2}$ range from 0.21 to 0.36×10^2. The lower value is for the data at 3-1/2 inch weir height. This effect of weir height is similar to that found in the case of the gas-phase coefficients and could be caused by the same phenomenon. It is also possible that the data were obtained in such a way to cause these variations with weir height. Maybe, the outlet liquid samples were not taken at the proper position on the tray.

If the correlation in Figure 49 is compared with the one for the carbon dioxide-cyclohexanol data in Figure 48, it can be seen that the slope of the straight line through the data for the water system is smaller than that for cyclohexanol system. The difference is not great, however. Both sets of data (Warzel's and the author's data) were used to determine the constants in the following equation by the method of

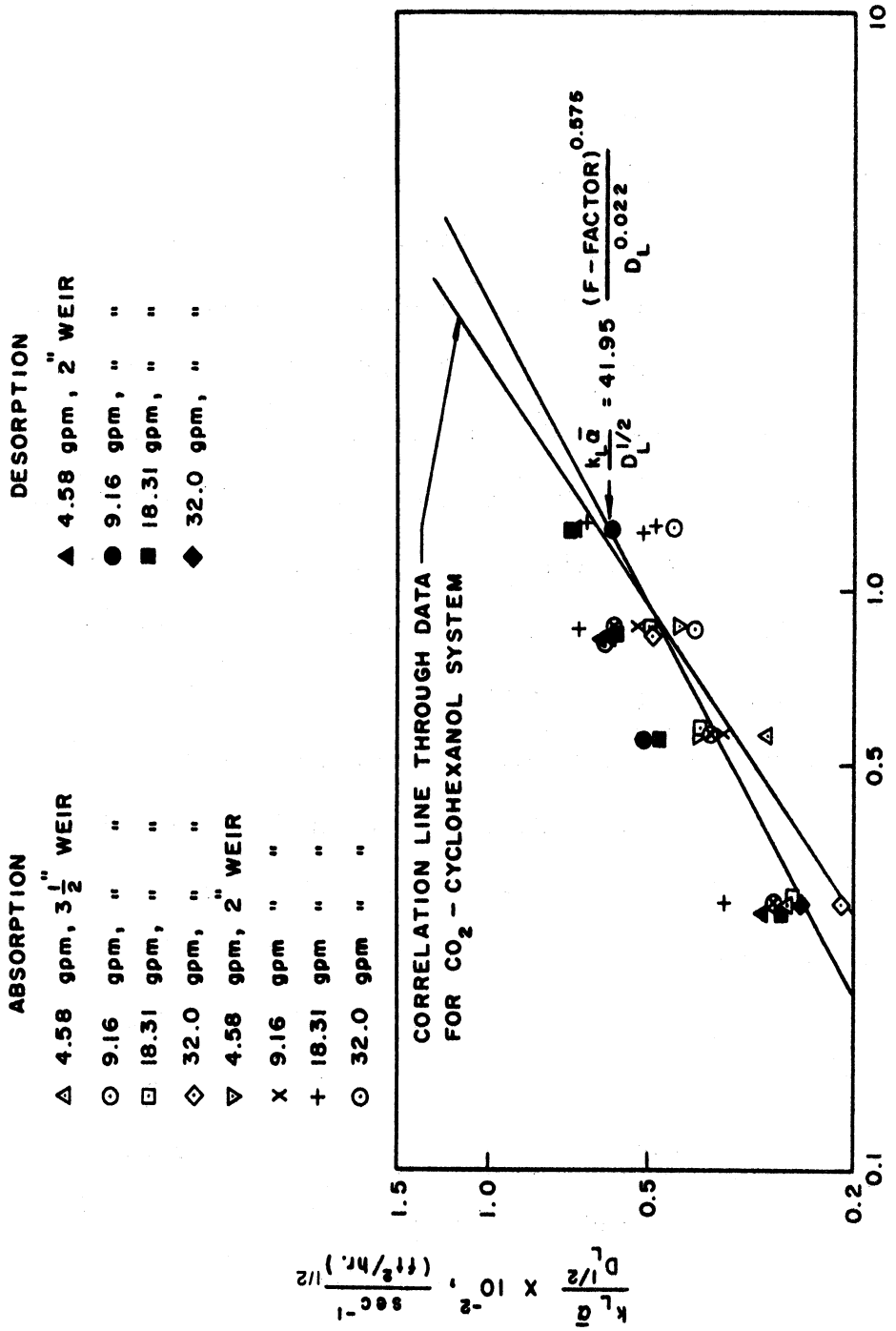

Figure 49. Correlation of Mass Transfer Coefficients for Carbon Dioxide-Water System.

least squares.

$$\frac{N_L}{t_L} = k_L\bar{a} = 41.95\ D_L^{0.478}\ (\text{F-factor})^{0.575} \qquad (126)$$

where

D_L = liquid diffusivity, $ft^2/hr.$

This equation is plotted in Figure 49 in order to compare the correlation line with the data for the carbon dioxide-water system. The absolute average percent deviation between the predicted values for both sets of data is 14.51 with a maximum deviation of 38.62. The absolute average percent deviation for the carbon dioxide-cyclohexanol system is 14.08 with a maximum deviation of 38.62. For the carbon dioxide-water system the corresponding values are 15.41 and 35.35, respectively. Therefore, the correlations for the individual sets of data are about the same.

Although the foregoing correlation of the data is satisfactory, there is some question about its validity because of the uncertainty in the values of the liquid diffusivities as determined by the Wilke-Chang correlation. This is especially true for the diffusivities of carbon dioxide in cyclohexanol, a high viscosity liquid. The data used by Wilke and Chang in the correlation were for diffusion in dilute solutions where the viscosity of the solvent was not varied over a very large range. Gerster[38] used the data of Jordan, et. al.[49] and other data for systems of high liquid viscosities to demonstrate that the Wilke-Chang correlation is not accurate for systems of high viscosities. The Wilke-Chang equation is as follows,

$$D_L = \frac{28.68\ (x_B M_B)^{1/2} T}{\mu_B\ (V_A)^{0.6}} \qquad (127)$$

where

V_A = molal volume of the solute at normal boiling point, cc/gm-mole.

M_B = molecular weight of solvent.

T = absolute temperature, °K.

μ_B = solvent viscosity, cp.

x_B = an association parameter to define the effective molecular weight of the solvent with respect to the diffusion process.

D_L = diffusion coefficient, ft^2/hr.

Equation (127) was used by Gerster[38] to predict the values of the diffusivity for oxygen in water-sucrose solutions and the results were compared with the data obtained by Jordan et al.[49] for the same system. These data are presented in Table XI.

TABLE XI

COMPARISON OF DIFFUSIVITIES FOR OXYGEN IN WATER-SUCROSE SOLUTIONS PREDICTED BY WILKE-CHANG CORRELATION AND EXPERIMENTAL DATA BY JORDAN ET AL.[49]*

% Sucrose	Viscosity of Solution, cp	D_L, $cm^2/sec \times 10^5$ Experimental	D_L, $cm^2/sec \times 10^5$ Predicted
0	0.89	2.12	2.41
30	3.00	1.54	0.848
54.5	25.0	0.67	0.124
62.5	67.0	0.43	0.0504
65.0	125.0	0.25	0.0278

* Table prepared by Gerster.[38]

The values of the diffusivities predicted by use of the Wilke-Chang correlation are about one-tenth of the experimental values at the liquid viscosities of 67.0 and 125.0 centipoises. Incidently, the Jordan data were obtained by use of a polarigraphic technique. Gerster made a similar comparison for hydrocarbon systems with the results similar to those presented in Table XI.

Several years ago, Arnold[5] presented a correlation for liquid diffusivities. Due to the more recent correlation by Wilke-Chang and also due to the fact that the equation contains some factors which are not readily available, the correlation by Arnold has not been used widely. The correlation equation was developed by extending a modified kinetic theory of gases to liquids and is similar to the Gilliland equation for gases.

$$D_L = 0.0387 \frac{\left[\frac{M_A + M_B}{M_A M_B}\right]^{1/2}}{A_A A_B \mu_B^{1/2} (V_A^{1/3} + V_B^{1/3})^2} \qquad (128)$$

where

M_A = molecular weight of the solute.

M_B = molecular weight of the solvent.

μ_B = viscosity of the solvent, cp.

V_A = molal liquid volume of the solutes at the normal boiling point, cc/gm-mole.

V_B = molal liquid volume of the solvent at the normal boiling point, cc/gm-mole.

A_A = the abnormality factor for the solute.

A_B = the abnormality factor for the solvent.

Equation (128) is limited to a temperature of 20°C. For a temperature coefficient Arnold recommended the following equation.

$$D_L = D_{LO}(1 + bt) \qquad (129)$$

where

$$b = 0.020[\mu_B/\rho_L^{2/3}]^{1/2}$$

μ_B = viscosity at 20°C, cp

ρ_L = density at 20°C, gm/cc

The Wilke-Chang and Arnold correlations were used to predict the diffusivity of carbon dioxide in water at several temperatures. These data are compared with experimental data from several literature sources[46,12,6,65] in Figure 50. The values predicted by the Wilke-Chang correlation agree satisfactorily with the experimental data in the temperature range of 10 - 20°C but at a temperature of 40°C the predicted value is about 16 percent higher than the experimental values. The predicted values by Arnold are also in good agreement with the experimental values near 20°C. At higher temperatures the departure from the experimental values is significant however. In fact, the temperature coefficient suggested by Arnold is not satisfactory outside of the range of 15 - 25°C.

Wilke and Chang reported association factors for four different solvents. These were: Water, x = 2.6; methyl alcohol, x = 1.9; ethyl alcohol, x = 1.5, and benzene, x = 1.0. Arnold reported values of A_A and A_B for several solvents and solutes. However, in both these correlations the principal problem is the determination of the association factors for systems besides those reported. In order to estimate the abnormality factor for cyclohexanol, an attempt was made to correlate

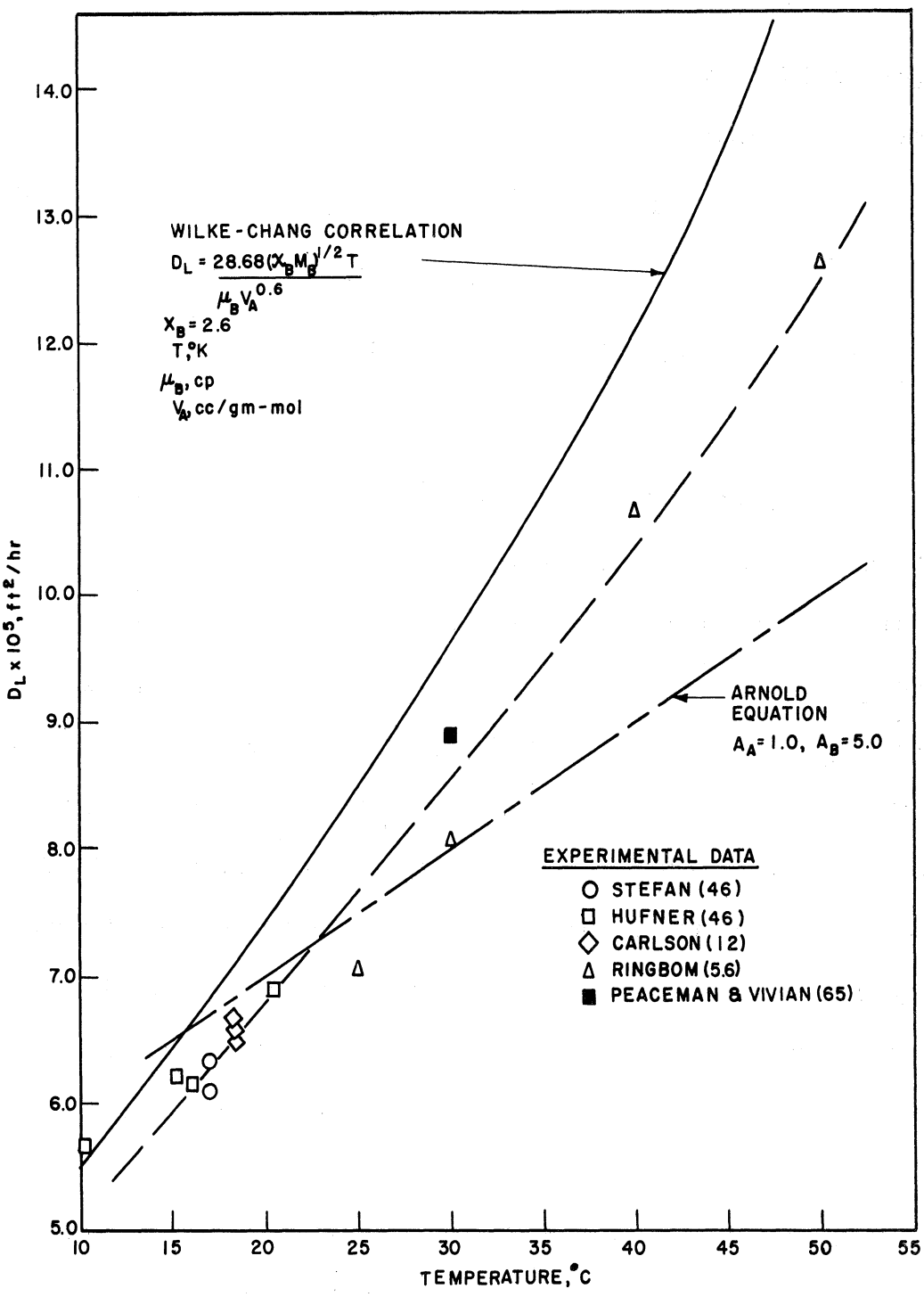

Figure 50. Comparison of Experimental Diffusivities and Diffusivities Predicted by Wilke-Chang Correlation and Arnold Equation

the values reported by Arnold plus values determined by use of diffusivity data from the literature. The correlating parameter which was finally chosen was the parachor which is defined by Equation (130).

$$[P] = \frac{M \sigma^{1/4}}{\rho_L} \tag{130}$$

The correlation is presented in Figure 51. The values of the parachors were obtained from the extensive list prepared by Quayle(69) and are presented in Table XII. Two important observations in regards to Figure 51 are worth consideration: (1) For certain solvents the abnormality factor is equal to 1.0 at the solvent parachor equal to 200 and greater but increases with decreasing values for the parachor and (2) the abnormality factor for the hydrocarbon systems are less than 1.0 indicating a higher diffusivity than would be predicted by generalizing the data from substituted hydrocarbon or non-hydrocarbon systems. Gerster explained the latter phenomenon by the existence of immobility in the hydrocarbon systems at low temperatures which creates holes for the diffusing molecules to flow through at a greater rate than would be possible in the case where solvent molecules are in random motion.

The value of the parachor for cyclohexanol is 248. The predicted value of the abnormality factor from Figure 51 is 1.0 but could be as high as 1.15. The latter value was used in Equation (128) to calculate the values of liquid diffusivities for carbon dioxide in cyclohexanol. It was assumed that the carbon dioxide does not associate with cyclohexanol which means that A_A in Equation (128) is 1.0. The calculated diffusivities are compared with the data reported by Schoenborn(3) in Figure 52. The variation of the calculated diffusivities with

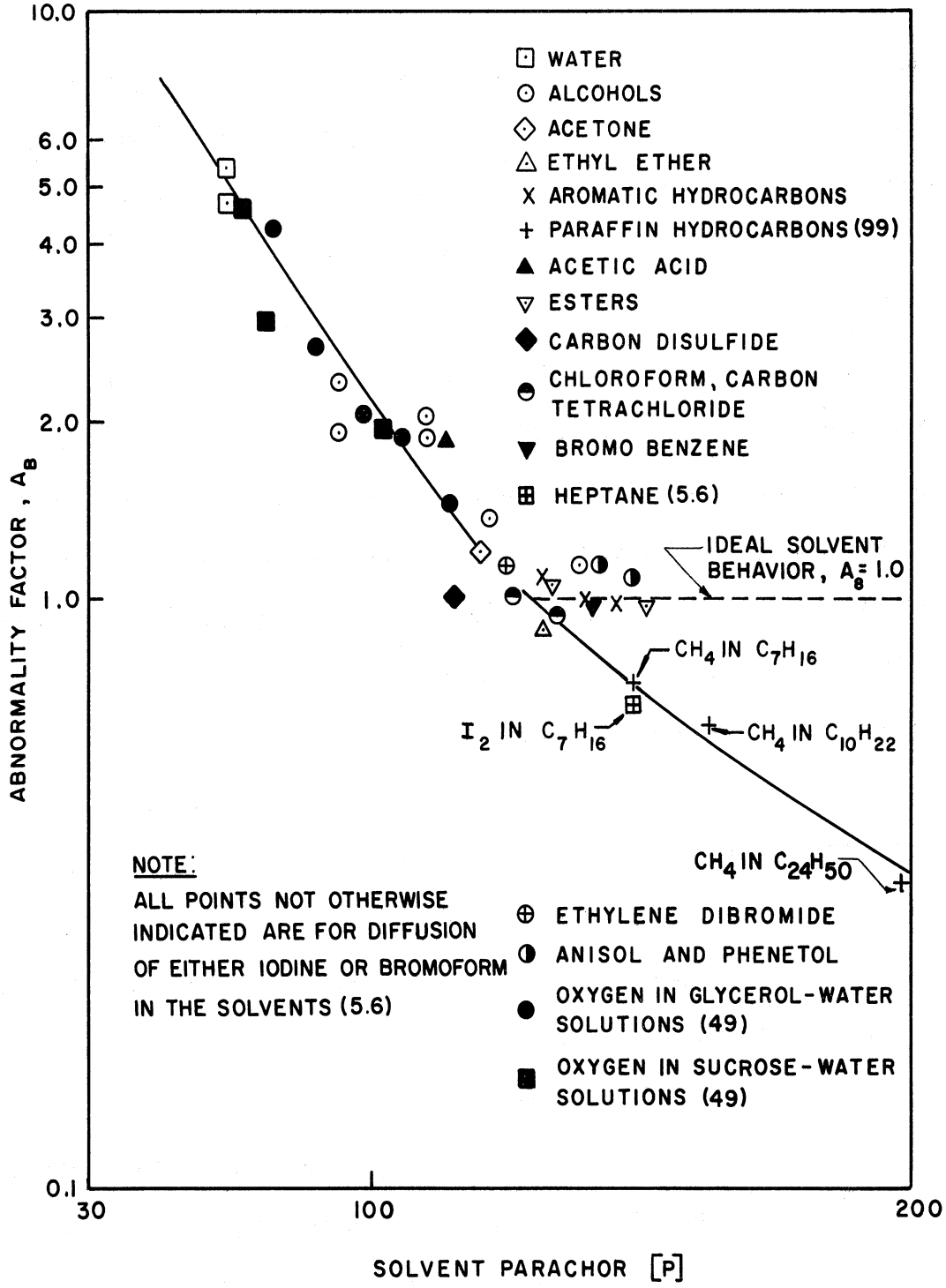

Figure 51. Correlation of the Solvent Abnormality Factor in Arnold's Equation with the Parachor for Several Organic Compounds, Water, and Aqueous Solutions

* Arnold, J. H., J. Am. Chem. Soc. 52, 3937 (1930).

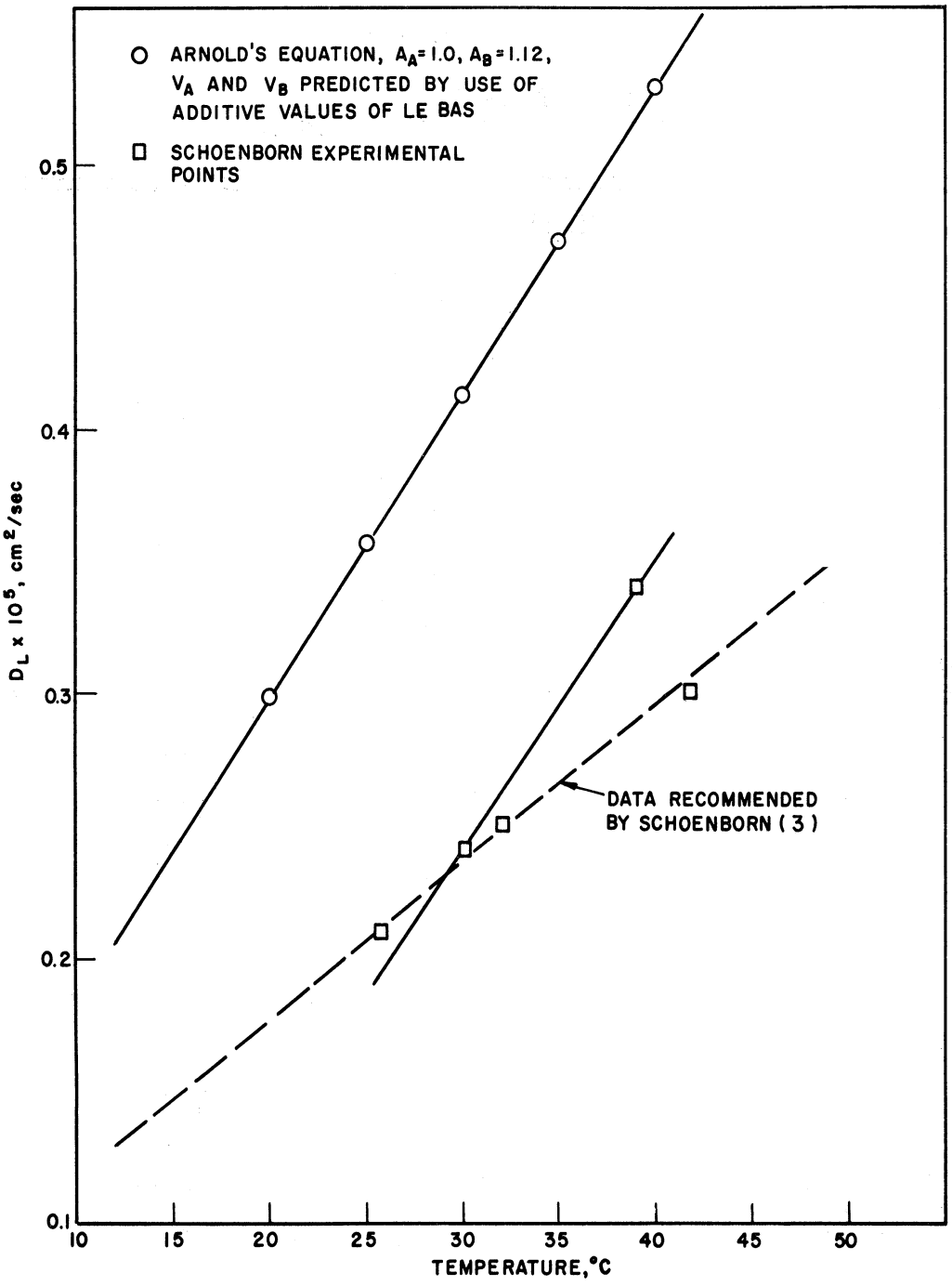

Figure 52. Liquid Diffusivities for Carbon Dioxide-Cyclohexanol System-Comparison of Values Predicted by use of Arnold's Equation with Experimental Values of Schoenborn

TABLE XII

SOLVENT ABNORMALITY FACTORS
AND PARACHORS USED IN FIGURE 51

Solvent	A_B	[P]
Diffusion of Iodine(58)		
Benzene	1.08	205.7
Toluene	0.99	246 avg.
M-Xylene	0.97	284.5
Bromabenzene	0.97	257.8
Chloroform	1.00	183.4
Carbon tetrachloride	0.94	219.9
Carbon disulfide	1.00	143.6
Heptane	0.66	311.3
Ethyl Acetate	1.06	216
Amyl Acetate	0.97	335.1
Anisole	1.14	265.6
Phenetole	1.08	303.7
Ethylene dibromide	1.13	215.7
Acetylene tetrabromide	1.62	310.0
Acetic Acid	1.86	131.2
Ethyl Alcohol	1.88	126.6
Methanol	2.325	88.2
Water	5.38	54.2
Diffusion of Bromoform(63)		
Ethyl Ether	0.89	211.9
Benzene	1.08	205.7
Acetone	1.19	161.7
Water	4.70	54.2
Methanol	1.91	93.2
Ethyl Alcohol	2.04	126.6
Propyl Alcohol	1.36	165.0
Amyl Alcohol	1.14	243.3

temperature does not agree with variation for the case of Schoenborn's data if the four values recommended by Schoenborn are considered. However, if the experimental value of 0.34 cm^2/sec at 39°C is used instead of the lower value of 0.30 cm^2/sec at 41.6°C, the slopes of the straight lines through both sets of data are parallel. The diffusivities calculated by use of Arnold's equation are 1.8 to 1.9 times the values reported by Schoenborn. If the Schoenborn data are accepted as being correct then the abnormality factor for the Arnold equation should have been about 2.08, a value which compares very favorably with the abnormality factors for methanol or ethanol. However, this value would not be predicted by the correlation of the abnormality factors in Figure 51. Therefore it is believed that the experimental values reported by Schoenborn should not be accepted without some question about their validity.

In order to correlate the carbon dioxide-cyclohexanol and carbon dioxide-water data by use of the two sets of diffusivity data in Figure 52, the values of $k_L\bar{a}$ at F-factor equals 1.0 in Figures 47 and 49 were used. These values are tabulated in Table XIII. The correlating equation in this case is as follows,

$$k_L\bar{a} = \beta\ (\text{F-factor})^{0.575} \tag{131}$$

where

$$\beta = f(D_L) \text{ or } f(D_L, \mu_L, \rho_L)$$

Diffusivities from the two correlations in Figure 52 were used to calculate the ratios, $k_L\bar{a}/D_L^{1/2}$ at F-factor = 1.0, which are presented in Table XIII also. If the diffusivity to the one-half power were the only variable required, the resulting ratios should be about the same regardless of the liquid viscosity and density. However, the results in Table

TABLE XIII

CORRELATION OF LIQUID-PHASE MASS TRANSFER COEFFICIENTS

System	T_L, °C	ρ_L, lb/ft^3	μ_L, $\frac{lb}{ft\text{-}hr}$	$\frac{\mu_L}{\rho_L}$, $\frac{ft^2}{hr}$	$k_L\bar{a}$, sec^{-1} @ F-Factor = 1.0	$D_L \times 10^5$, ft^2/hr	$\frac{k_L\bar{a}}{D_L^{\frac{1}{2}}} \times 10^{-2}$	$\frac{k_L\bar{a}}{\left(\frac{D_L\rho_L}{\mu_L}\right)^{\frac{1}{2}}} \times 10^{-2}$	$D_L \times 10^5$ ft^2/hr	$\frac{k_L\bar{a}}{D_L^{\frac{1}{2}}} \times 10^{-2}$	$\frac{k_L\bar{a}}{\left(\frac{D_L\rho_L}{\mu_L}\right)^{\frac{1}{2}}} \times 10^{-2}$
Carbon dioxide-water	25.0	62.2	2.16	0.0347	0.486	7.68 (3)	0.554	0.103			
Carbon dioxide-cyclohexanol	38.0	58.4	58.4	1.0	0.125	1.96 (1)	0.282	0.282	1.10 (2)	0.378	0.378
Carbon dioxide-cyclohexanol	25.5	58.9	123	2.09	0.079	1.40 (1)	0.210	0.304	0.814 (2)	0.276	0.399
Carbon dioxide-cyclohexanol	14.5	59.4	235	3.96	0.042	0.905 (1)	0.141	0.280	0.558 (2)	0.180	0.358

(1) Liquid diffusivity by use of Arnold equation, see Figure 52.

(2) Liquid diffusivity - recommended by Schoenborn; experimentally determined; see Figure 52.

(3) Liquid diffusivity by use of experimental data in Figure 50.

XIII indicate that the ratios, $k_L\bar{a}/D_L^{1/2}$, decrease with increasing liquid viscosity. These results suggested the correlation in Figure 53 where $k_L\bar{a}/D_L^{1/2}$ at F-factor equals 1.0 is plotted versus kinematic viscosity.

Although the data point for the carbon dioxide-water system is over one and one-half log scales separated from the carbon dioxide-cyclohexanol system, a smooth curve through the latter set of data can be extrapolated to the data point for the water system. Unfortunately, no data are available in the intermediate range of kinematic viscosity. However, the data obtained by Fairbrother are included in Figure 53 to indicate the small effect of kinematic viscosity on the mass transfer coefficient in the low viscosity range, 0.035 - 0.14. Fairbrother's data are for the desorption of carbon dioxide from water and water-glycerol solutions at a constant gas velocity and liquid rate. The values of $k_L\bar{a}$ were calculated by use of Equation (21). Fairbrother used a five-inch square column containing four plates with one 3-1/2 inch bubble cap on each plate. The diffusivities of carbon dioxide in glycerol-water solutions were determined by use of Jordan's data[49] for the diffusivity of oxygen in glycerol-water. These data were obtained at 25°C, the temperature used by Fairbrother in his studies. A correction was made for the difference between the molal volumes of oxygen and carbon dioxide by use of Wilke-Chang correlation.

The results in Figure 53 suggest that the effect of kinematic viscosity on the mass transfer coefficient, $k_L\bar{a}$, excluding the effect on liquid diffusivity, is a function of kinematic viscosity itself. Thus the correlation of β in Equation (131) is,

$$\beta = \beta' \, D_L^{1/2} \, (\mu_L/\rho_L)^{\alpha} \qquad (132)$$

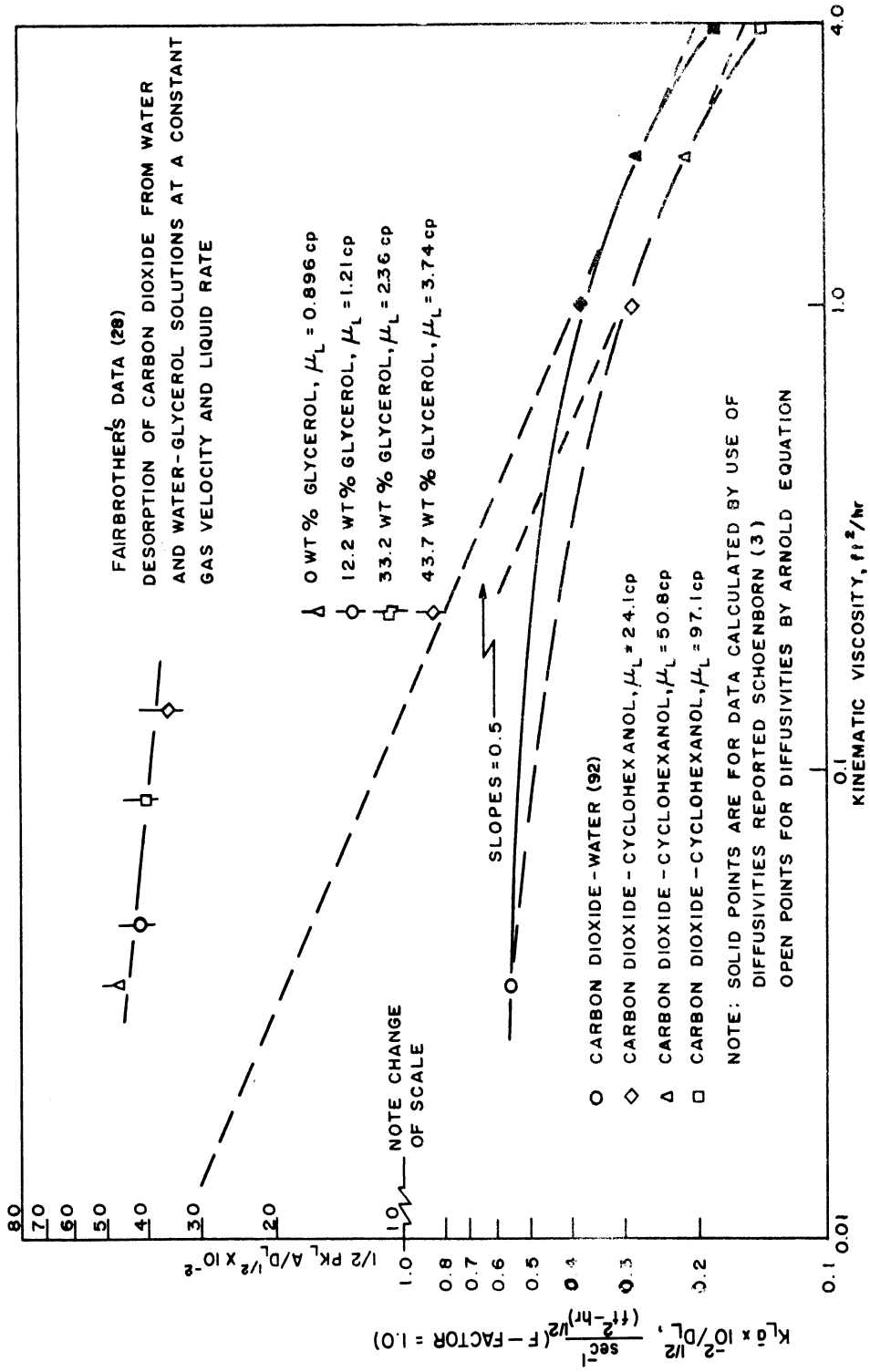

Figure 53. Correlation of the Ratios of the Liquid Mass Transfer Coefficients and Diffusivities at a Constant F-Factor with Liquid Kinematic Viscosity - Data for Water and Cyclohexanol Systems and Water-Glycerol Solutions

TABLE XIV

FAIRBROTHER'S DATA FOR DESORPTION OF CARBON DIOXIDE FROM WATER AND WATER-GLYCEROL MIXTURES

Wt. % Glycerol	$k_L a$	$D_L \times 10^5$, ft^2/hr Oxygen	$D_L \times 10^5$, ft^2/hr Carbon Dioxide	$\frac{k_L \bar{a}}{D_L^{\frac{1}{2}}} \times 10^{-2}$	μ_L/ρ_L, $\frac{ft^2}{hr}$	$\frac{k_L \bar{a}}{\left(\frac{D_L \rho_L}{\mu_L}\right)^{\frac{1}{2}}} \times 10^{-2}$
0	125	16.63	17.85	93.5	0.0349	17.5
12.2	99	13.20	14.21	83	0.0468	18.0
33.2	76	8.02	8.64	81.8	0.0866	24.1
43.7	57	6.04	6.50	70.7	0.134	25.8

where

β' and α are functions of μ_L/ρ_L.

The data for the cyclohexanol can be correlated by use of $\alpha = -0.5$, however. This is shown in Figure 53 and in Table XIII where $k_L\bar{a}/(D_L\rho_L/\mu_L)^{1/2}$ equals 0.29 or 0.38 depending on which diffusivity values are used.

Etherington[27] reported a correlation of liquid-phase mass transfer coefficients which is similar to the one presented in Figure 53. The data obtained by Walters[90], Horton[44], and Fairbrother plus some data obtained by Etherington were used in the correlation. The viscosity range covered by these data is 0.4 to 13 centipoises. Hydraulic data were not obtained in conjunction with the mass transfer data so that the mass transfer coefficients were not determined by use of Equation (39a). Instead, Equation (21) was used and the height, h, was determined by summation of the following terms,

h_c = crest of liquid over top of weirs.

h_L = vertical distance from top of bubble cap slots to top of weir.

$h_s/2$ = vertical length of slots open to weir.

Etherington also arbitrarily used the liquid diffusivity to the two-third power in the correlation which is represented by Equation (91). Other correction factors were also included in the correlation to correct for such variables as liquid density, slot width, surface tension and concentration. An analysis similar to those made by Geddes[34] and Chu[17] was used to determine how most of the factors should be included in the correlating equation. The final correlation of the data indicates that the mass transfer coefficient corrected for diffusivity to the two-thirds power is proportional to the liquid viscosity to the 0.17 power

in the range below liquid viscosity equal to 3.0 centipoises. Above this viscosity the coefficient is proportional to the liquid viscosity to the 0.73 power. It is difficult to make a detailed comparison of Etherington's correlation and the correlation in Figure 53 because of the different exponent on liquid diffusivity and other factors in the correlating equation. The results as presented by Etherington indicate that the transition from a small effect of viscosity to a large effect occurs at about 3 centipoises instead of about 25 centipoises in Figure 53. Maybe this difference could be resolved by use of some recent diffusivities for the systems used by Etherington and by use of diffusivity to the one-half power.

Mixing Studies

Several relationships between point and plate efficiency have been developed mathematically but have not been tested thoroughly by use of experimental data. In the mathematical development of these relationships one common procedure has been used to relate the point and plate efficiency by use of a mixing parameter. This procedure is best described by Equations (99) through (103) and the solution to the differential equations which describes the liquid concentration as a function of position on the tray. The basic differential equations which include a mixing term (see Table II) have been solved by use of appropriate boundary conditions at the terminal positions on the tray. Then the resulting relations have been used in Equation (103) to obtain the relationship between point and plate efficiency. The final relationships include a mixing parameter in every case.

In the present studies, liquid concentrations at four different points on the tray were determined experimentally and were used to calculate an average liquid concentration on the tray. The average liquid concentration was then used in Equation (98) to calculate a point efficiency. This point efficiency was considered as an experimental value which could be compared with the values determined by use of some of the relationships presented in Table II. The four relationships which were used in this comparison included the equations developed by Warzel[92], Crozier[18], Robinson[72], and Lewis.[53] The point efficiencies for the carbon dioxide-cyclohexanol system determined by use of each of these relationships are presented in Table VI-G in Appendix G. In addition, the number of ideal mixing stages for the Gautreaux and O'Connell equation are included in Table VI-G. The calculation of the number of ideal mixing stages was performed by use of the following equation and a trial-and-error procedure.

$$\frac{E_{MV}}{E_{OG}} = \frac{1}{\lambda E_{OG}} \left[\left(1 + \frac{E_{OG}\lambda}{n}\right)^n - 1\right] \tag{70}$$

The point efficiencies determined by use of the Warzel and Crozier equations are within $\pm$ 10 percent of the values calculated by use of the average liquid concentration on the tray. In the majority of the cases, the agreement is within $\pm$ 5 percent. The values predicted by use of the following equation suggested by Robinson[72] do not agree as well with the experimentally determined point efficiencies, however.

$$\frac{E_{MV}}{E_{OG}} = \frac{e^{\eta}-1}{\eta} \tag{133}$$

where η is determined by the slope of the straight line through the concentration at various points on the tray when the data are plotted $\ell n \frac{x - x^*}{x_o - x^o}$ vs W, the fraction of distance across the tray.

The deviations are in some cases as high as 35 percent but the majority of the values are within $\pm$ 10 percent of the experimental values. Robinson[72] has more recently recognized that Equation (133) is not valid for the general case since improper boundary conditions were used in the solution of the differential equation. Equation (133) was obtained by use of the boundary conditions; (1) $\frac{dx}{dW} = 0$ at $W = \infty$ and (2) $x = x_o$ at $W = 1$. The relationship for the boundary conditions, $\frac{dx}{dW} = 0$ at $W = 1$ and $x = x_o$ at $W = 1$, is presented in Table II and is believed to be correct solution to the differential equation.

The excellent agreement between the experimental values of point efficiencies in Table VI-G and the values predicted by use of the equations developed by Warzel, Crozier, and Robinson is probably due partly to the lack of sensitivity to changes in the mixing parameter at the values of λE_{OG} for the cyclohexanol system. The sensitivity of Equation (67) to changes in the mixing parameter "C" at five different values of λE_{OG} is shown in Table XV. The results in Table XV indicate that for a value of λE_{OG} equal to 0.5 the change in the ratio, E_{MV}/E_{OG}, is 1.136 to 1.050 for a change in the mixing parameter of 2.0 to 5.0. The corresponding changes in the ratio, E_{MV}/E_{OG}, at λE_{OG} equals 1.0 is 1.298 to 1.108 and at λE_{OG} equals 2.0 is 1.728 to 1.229. The value of λE_{OG} in the majority of the data for carbon dioxide-cyclohexanol system is in the range of 0.3 to 1.3. Therefore, the mixing parameter in Equation (67) could be in error considerably and still not cause an appreciable error in the point efficiency

TABLE XV

SENSITIVITY OF EQUATION 67 TO CHANGES
IN THE PARAMETER "C" AT VARIOUS VALUES OF λE_{OG}

	"C"	$\frac{E_{MV}}{E_{OG}}$ (1)
$\lambda E_{OG} = 0.5$	1.0	1.298
	2.0	1.136
	5.0	1.050
	10.0	1.027
$\lambda E_{OG} = 1.0$	1.0	1.728
	2.0	1.298
	5.0	1.108
	10.0	1.050
$\lambda E_{OG} = 2.0$	1.0	3.20
	2.0	1.728
	5.0	1.229
	10.0	1.108
$\lambda E_{OG} = 5.0$	1.0	29.4
	2.0	4.480
	5.0	1.728
	10.0	1.293

(1) $E_{MV}/E_{OG} = \frac{e^{\lambda E_{OG}/C} - 1}{\lambda E_{OG}/C}$

predicted by use of this relationship. The relationships developed by Crozier(21) and Robinson(72) are of similar form to the one by Warzel(92) and the sensitivity to errors in the mixing parameter would be expected to be similar to that shown in Table XV.

The results in Table VI-G do however indicate that the liquid mixing can be satisfactorily accounted-for by use of the relationships developed by Warzel and Crozier and possibly the one developed by Robinson if λE_{OG} is in the range below a value of 2.0. It is possible that at higher values of λE_{OG} these relationships would not be valid. In any event,

the use of these equations to calculate point efficiency from plate efficiency would simplify the experimental procedure since only one concentration on the tray would be required instead of concentrations at several points. The studies by Robinson and Gerster[3] indicate that the relationship between point and plate efficiency is more complex than those developed by Warzel and Crozier. Robinson and Gerster used an eddy diffusivity to describe the liquid mixing and develop the following equation,

$$\frac{E_{MV}}{E_{OG}} = \frac{1 - e^{-(\eta+M)}}{(\eta+M)\left(\frac{2\eta+M}{\eta}\right)} + \frac{e^{\eta} - 1}{\left(\frac{2\eta+M}{\eta+M}\right)} \qquad (77)$$

where

$$\eta = -\frac{M}{2} + \sqrt{\frac{M^2}{4} + \lambda E_{OG} M}$$

$$M = \frac{LS}{D_E Z_c B \rho_{ML}} = \frac{S^2}{D_E t_L}$$

Equation (77) is more fundamental than the equations developed by Warzel and Crozier and reveals how the complex empirical parameters in the latter equations can be expressed in terms of a more fundamental parameter, D_E, the tray dimensions, S and B; liquid and gas rate, L and G; the slope of the equilibrium line, and point efficiency. In fact, Robinson[3] has developed the relationship between the Warzel mixing parameter, "C", and the basic parameters in Equation (77). That is,

$$C = f(M, \lambda E_{OG}) \qquad (134)$$

Therefore, in using Equation (67) to determine point efficiency from plate efficiency, the mixing parameter must be determined experimentally in conjunction with the experimental determination of plate efficiency

or a correlation of "C" must be available for use in predicting the point efficiency by a trial-and-error procedure.

Warzel determined the mixing parameters for the ammonia-water system used in his studies but made the mistake of applying the same mixing parameters to the carbon dioxide-water system. In order to estimate the point efficiencies for the carbon dioxide-water system used in the present studies, the mixing parameters for several systems were correlated by Equation (135).

$$\text{"C"} = A \frac{\left(\frac{Z_c}{Z_f} V_f \rho_L B\right)^a}{\mu_L} \left(\frac{BU_s \rho_G}{\mu_L}\right)^b \left(\frac{\rho_L}{\rho_G}\right)^c (\lambda E_{OG})^d \qquad (135)$$

The correlation of "C" for the ammonia-water and carbon dioxide-cyclohexanol systems and for four different systems studied by Schoenborn, et al.[2] is presented in Table XVI. Although the standard deviation for this correlation is 1.33 which indicates that the scatter in the data is appreciable, the predicted values of point efficiency for the carbon dioxide-cyclohexanol system agree very well with the experimental values as shown in Figure 54. This is another indication of the lack of sensitivity in Equation (67) due to changes in the mixing parameter in the low range of λE_{OG}.

The values of the point efficiencies for the carbon dioxide-water system predicted by use of the "C" correlation in Table XVI and the values predicted by use of the parameters for the ammonia-water system as correlated by Warzel are compared in Figure 55. The results in Figure 55 indicate that the point efficiencies predicted by Warzel are in error as much as 14 percent at the higher values of λE_{OG}. The value of 14 percent error in point efficiency is small however, compared to the error in the

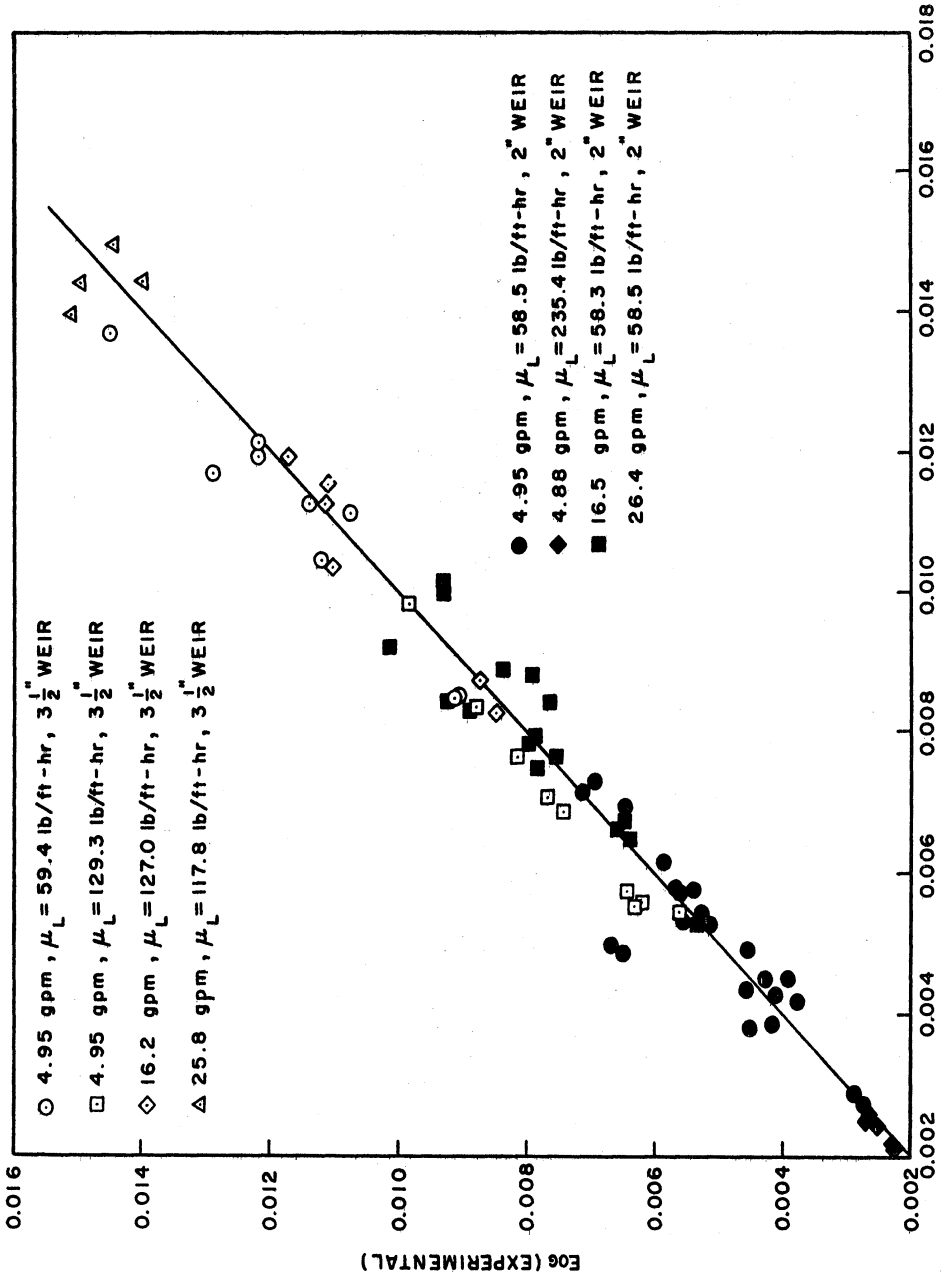

Figure 54. Comparison of Point Efficiencies Predicted by use of "c" Correlation and Warzel's Mixing Equation with Experimental Point Efficiencies

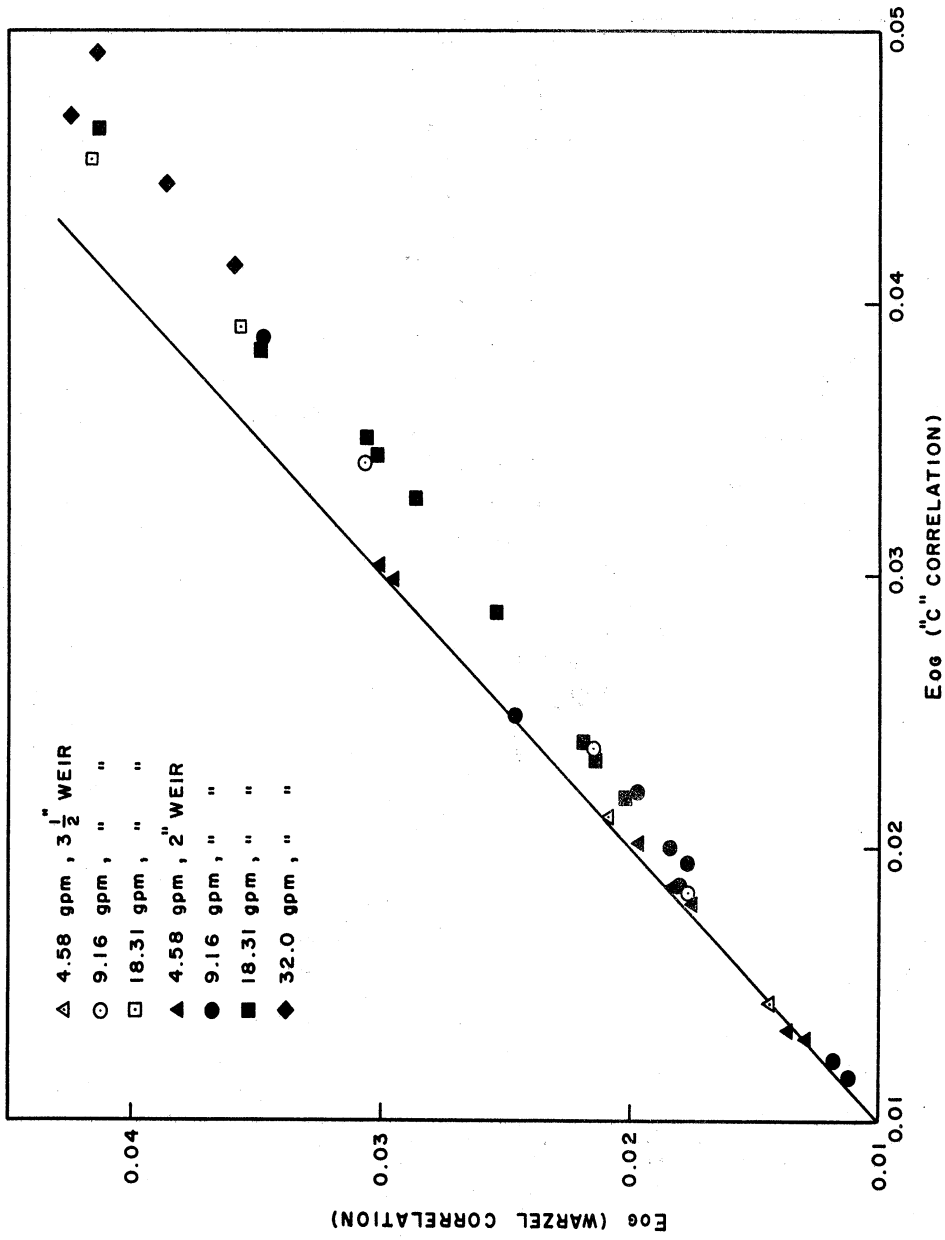

Figure 55. Comparison of Point Efficiencies Predicted by use of Warzel's "C" Correlation and Point Efficiencies Predicted use of New "C" Correlation

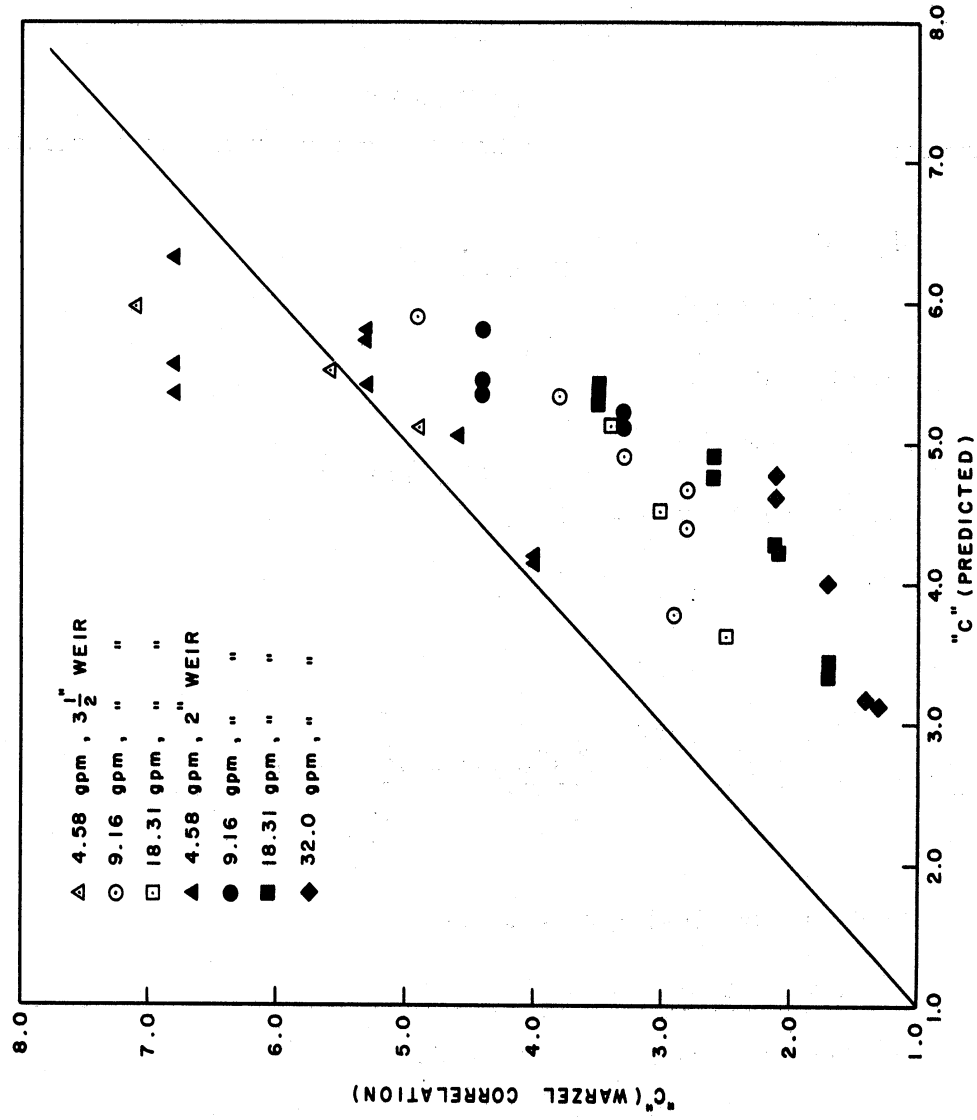

Figure 56. Comparison "C" Values Used by Warzel and Values Predicted by "C" Correlation CO_2 - H_2O System

TABLE XVI

CORRELATION OF MIXING PARAMETER "C"

Data Used: NH_3-H_2O, CO_2-Cyclohexanol } Michigan Data

Methanol-Toluene, Acetone-Water, Cyclohexane-n-Heptane, Mek-H_2O } NCS Data[2]

Correlation:

$$C = 1.063 \underbrace{\left(\frac{Z_c}{Z_f} \frac{V_f \rho_L B}{\mu_L}\right)^{-0.082}}_{\text{I}} \underbrace{\left(\frac{Bu_s \rho_L}{\mu_L}\right)^{0.262}}_{\text{II}} \underbrace{\left(\frac{\rho_L}{\rho_G}\right)^{-0.176}}_{\text{III}} \underbrace{(\lambda E_{OG})^{0.162}}_{\text{IV}}$$

Absolute Avg. Deviation = 0.969

Standard Deviation = 1.328

Standard Deviations for Exponents

Group I	0.037
II	0.036
III	0.037
IV	0.026

values of the parameter "C" as shown in Figure 56. The percentage error in "C" as predicted by the correlation presented by Warzel is greater than 100 in some cases. The point efficiencies predicted by Warzel's correlation of "C" and by the correlation presented in Table XVI are listed in Table V-G in Appendix G. The efficiencies predicted by the latter correlation were used in the correlation of the liquid-phase mass transfer data.

The ratios of plate efficiency and point efficiency which were determined experimentally in the absorption studies can be used to determine the effect of different system properties and tray variables on the basic parameters as defined by the mathematical developments by Robinson and Gerster.(3)

This can be described by use of Equation (98) and (77).

$$\frac{E_{MV}}{E_{OG}} = \frac{x_{avg} - x^*}{x_o - x^*} \tag{98}$$

$$\frac{E_{MV}}{E_{OG}} = \frac{x_{avg} - x^*}{x_o - x^*} = \frac{1 - e^{-(\eta+M)}}{(\eta+M)\left(\frac{2\eta+M}{\eta}\right)} + \frac{e^{\eta} - 1}{\eta\left(\frac{2\eta+M}{\eta+M}\right)} \tag{77a}$$

Therefore, in functional notation,

$$\frac{x_{avg} - x^*}{x_o - x^*} = f(M, \lambda E_{OG}) \tag{136}$$

In Figure 57, the correlation between the logarithm of $\frac{x_{avg} - x^*}{x_o - x^*}$ and λE_{OG} is presented. The data scatter appreciably but there is definite correlation with λE_{OG}. In fact, the slope of the best straight line through the data as determined by "eye" is 0.12. In Figure 58 the ratio, $\frac{x_{avg} - x^*}{x_o - x^*} / E_{OG}^{0.12}$, is plotted versus F-factor. The deviations from the straight line through the data is less than 10 percent in the majority of cases with no apparent trend due to variables such as weir height, liquid rate, or liquid viscosity. In addition, the total effect of F-factor on the ratio, $\frac{x_{avg} - x^*}{x_o - x^*}/(\lambda E_{OG})^{0.12}$, over the range of 0.2 to 2.0 is less than 10 percent. Since the F-factor and the parameter, M, in Equation (77) are related, the results in Figure 58 indicate that the effect of this parameter is very small in the range of λE_{OG} covered by data.

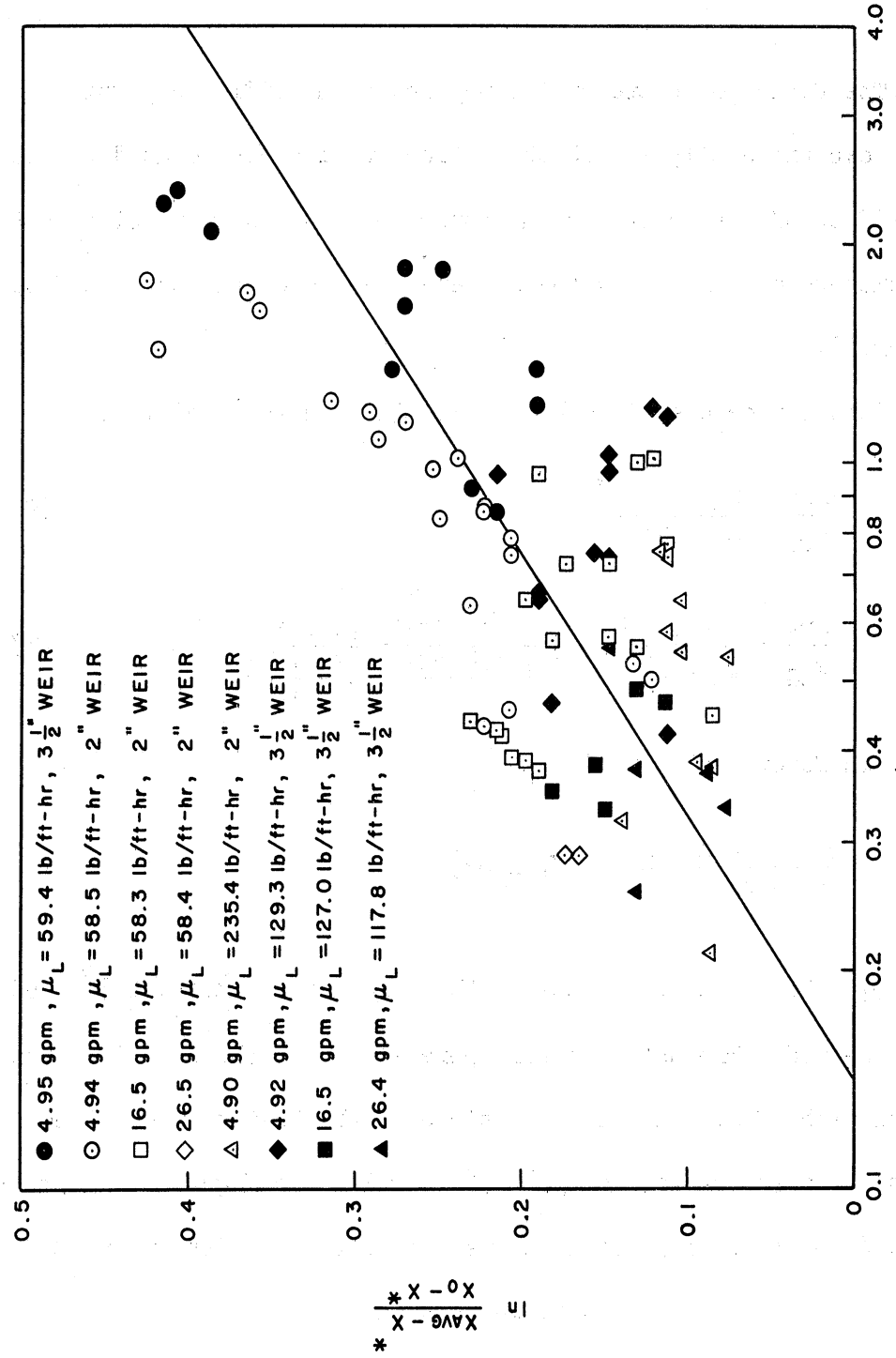

Figure 57. Correlation of the Average Liquid Concentration on the Tray with λE_{OG}

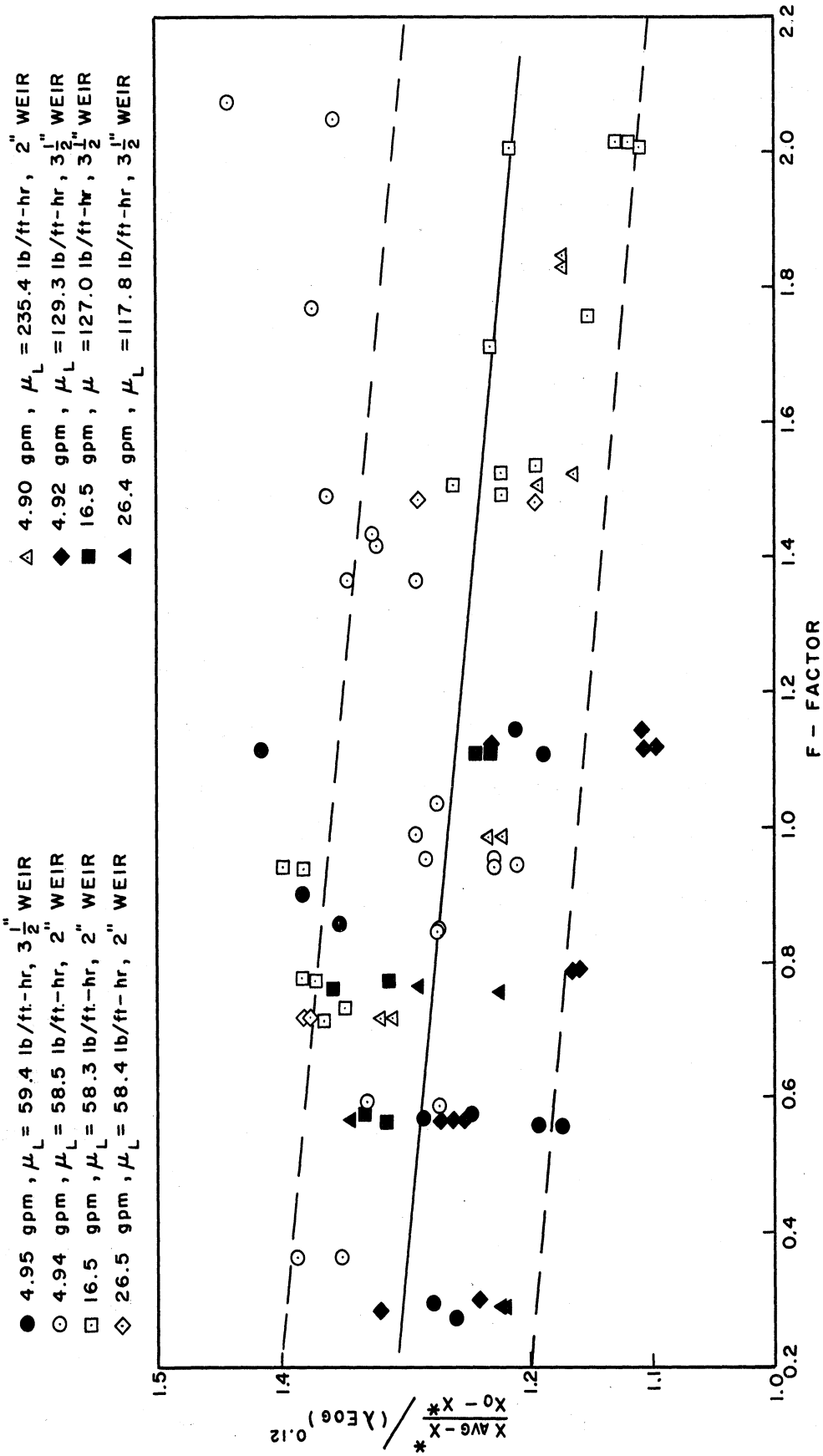

Figure 58. Variation of $\frac{X_{avg} - X^*}{X_o - X^*}/(\lambda E_{OG})^{0.12}$ with F-Factor

This observation agrees very well with the predictions which may be made by examination of any of the point and plate efficiency relationships. Furthermore, the results presented herein indicate that the investigator should choose a system which would have a value of λE_{OG} above 2.0 in order to perform a critical analysis of the point and plate efficiency relationships. Some of the systems where the resistances are distributed between the gas and liquid phases would most likely fall in this range.

In Figure 59, the point efficiencies for the carbon dioxide-cyclohexanol system are compared with the efficiencies predicted by use of the plug flow equation (Lewis equation) and the plate efficiency which would be the point efficiency if complete mixing were assumed. For the solid points in Figure 59, the ordinate should be considered the point efficiency predicted by use of the plug flow equation. For the open points, the ordinate is $E_{OG} = E_{MV}$. The point efficiencies for the 3-1/2 inch weir height are about centrally located between the values for plug flow and complete mixing except possibly at the higher liquid rates. In the case of data for the 2 inch weir height, the point efficiencies are more in agreement with the values predicted by use of the plug flow equation. The only major differences between the conditions on the tray with the 2 inch weir and the 3-1/2 inch weir are the liquid viscosity and the liquid holdup. The data at comparable viscosities in Figure 59 indicate that the mixing on the tray was greater for the case of 3-1/2 inch weir than for the 2 inch weir. In other words, the mixing increases with increased liquid holdup. This is in agreement with the predictions which can be made by examination of Equation (77). That is, as the liquid holdup is increased, M decreases if D_E does not change and in the limit as M

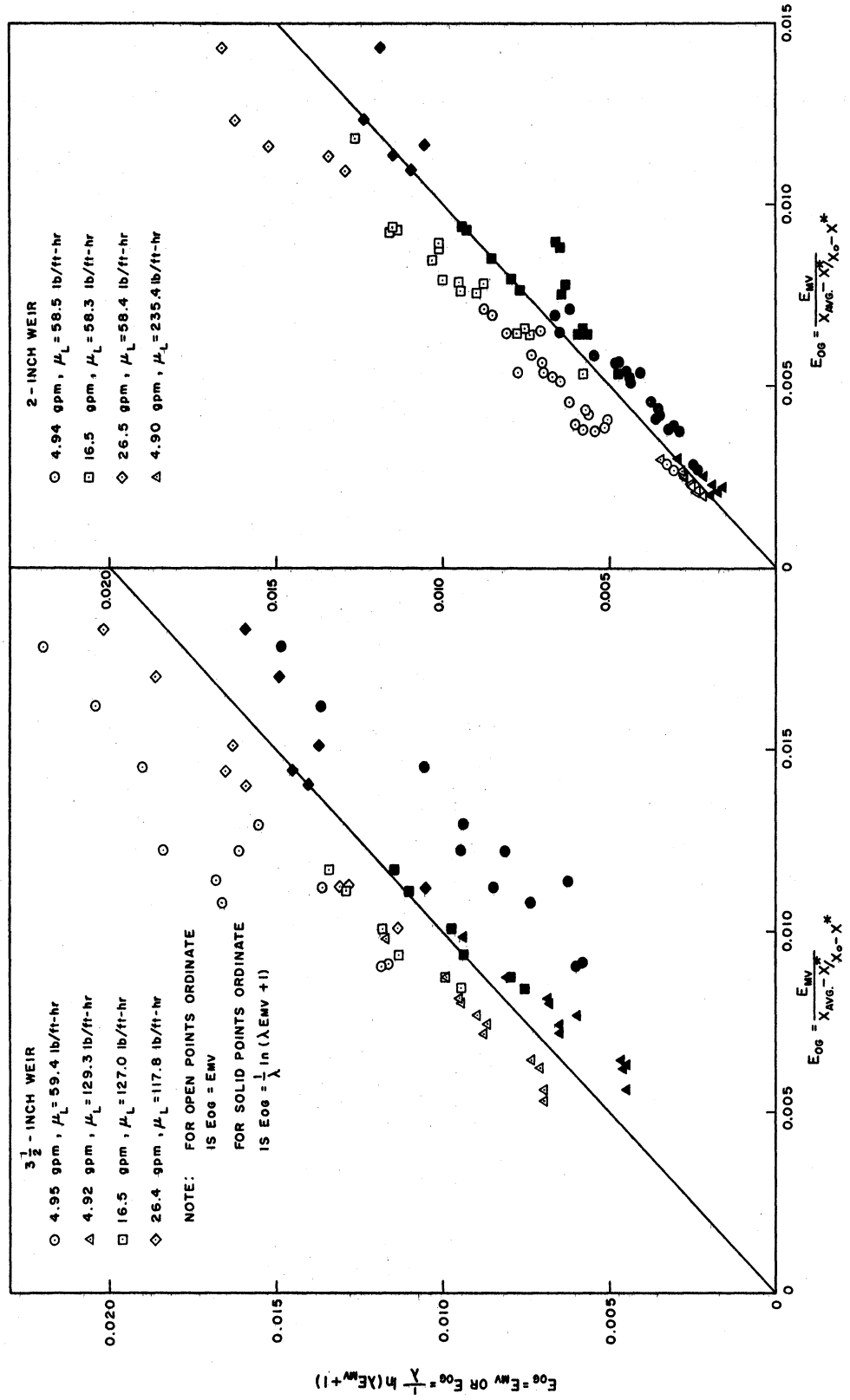

Figure 59. Comparison of Experimental Point Efficiencies With Point Efficiencies for Complete Mixing and Plug Flow.

approaches zero, the ratio, $\frac{E_{MV}}{E_{OG}}$, approaches 1.0. Thus the mixing increases as the liquid holdup increases until the liquid diffusivity is affected appreciably. Thereafter the liquid mixing would be expected to decrease with liquid holdup.

DISCUSSION OF RESULTS

Vaporization Studies

The most satisfactory correlation of the vaporization data which was obtained by the detailed analysis is represented by Equation (123).

$$N_G = 523.9 \frac{D_G^{0.526} \rho_G^{1/2}}{\rho_L^{0.834}} (\text{F-Factor})^{n-1} (Z_f - Z_c)^{0.72} \quad (123)$$

where $$n = 0.852 \left(\frac{\mu_L}{\rho_L}\right)^{0.238}$$

Using Equation (23a) as the mathematical model to define the relationship between N_G, $k_G a$, gas holdup, and superficial gas velocity, Equation (123) may be converted to an expression relating the mass transfer coefficient and the independent variables. That is,

$$N_G = k_G' a \frac{(Z_f - Z_c)}{u_s} \quad (23a)$$

Therefore,

$$k_G' a = 523.9 \frac{D_G^{0.526}}{\rho_L^{0.834}} \frac{(\text{F-Factor})^n}{(Z_f - Z_c)^{0.28}} \quad (123a)$$

Several important points in regards to this correlation are worthy of discussion in relation to previous and future investigations. These are: (1) the effect of gas holdup; (2) the exponent on gas diffusivity; (3) the use of F-factor as a correlating variable; and (4) the variable exponent on F-factor.

It should be remembered that the coefficient, $k_G' a$, is a product of two separate but not completely independent factors. The coefficient, k_G, is related to the flow characteristics of the gas phase within the confines of the liquid. The flow characteristics are however dependent on

the shape and size of the vapor space in the liquid. The average shape and size of the vapor space determines the value of a, the interfacial area per unit volume of gas. Thus the two factors are related and it would be desirable for academic reasons at least to be able to study each of these factors separately. Several attempts have been made to perform this type of study. The problems involved in a study of this type are principally describing the geometry of the vapor bubbles or spaces in the liquid and the mechanism of mass transfer within the gas phase. In the present study data for gas-phase and liquid-phase mass transfer were obtained and by use of both sets of data it is possible to make some qualitative observations as to the effect of such variables as gas rate, liquid and gas holdup, and liquid and gas physical properties upon each factor, k_G and a.

The relationship between the mass transfer coefficient and gas holdup on the tray as represented by Equation (123a) indicates a decrease in the coefficient with increased gas holdup. It should be mentioned that the variable, gas holdup, is not unique since liquid holdup plus gas holdup, or variables such as liquid rate and weir height could have been used to correct for gas and liquid holdup on the tray. The successful correlation of the data by use of gas holdup alone is attributed to the fact that the gas holdup and liquid holdup are related and that the gas holdup is independent of the means by which liquid holdup is varied, i.e., by varying the liquid rate at a constant weir height or vice versa. The correlation might have been performed by arbitrarily assuming that the effect of gas holdup is in accordance with Equation (23a). Then any variations of the mass transfer coefficient with the holdup on the tray could have

been accounted for by use of the liquid holdup on the tray. The degrees of freedom in the system of variables which define the holdup on the tray can be enumerated by writing the relationship between gas holdup, froth height and clear liquid height.

$$Z_f \left(1 - \frac{Z_c}{Z_f}\right) = Z_f - Z_c \qquad (137)$$

If the liquid holdup and F-factor on the tray are fixed then the froth height and gas holdup are defined. By fixing the gas holdup and F-factor, the total holdup on the tray is fixed since the froth density, Z_c/Z_f, is almost totally dependent on F-factor. Therefore, the number of degrees of freedom is two and if any two of the variables, liquid holdup, total holdup (froth height), gas holdup, and F-factor, are specified, the hydraulics of the system are defined. Gas holdup was used in present analysis for sake of simplicity since the use of liquid holdup would have required a complete regression analysis. This would not have been simple due to the non-linearity of Equation (123a).

The decrease in the mass transfer coefficient with increased gas holdup can be rationalized as a variation in the specific interfacial area and the coefficient, k_G. Crozier[21] suggested two different types of bubbling regimes as a possible explanation for the difference between the gas-phase data obtained by Ashby[7] at 1-1/2 inch weir height and similar data by Warzel[92] at 2 and 3-1/2 inch weir heights. Since these two sets of data were satisfactorily correlated by Equation (123) or (123a), there would have to be a continuous transition from one bubbling regime to the other as the liquid holdup is varied in order to be able to correlate the data from the two separate regimes. Chu, et al.[19], have suggested

that the mass transfer coefficient as determined by Equation (23a) can be related to the individual coefficients in the separate froth zones on the tray.

$$k_G'a\ t_G = k_{G_1}'a_1\ \ t_{G_1} + k_{G_2}'a_2\ \ t_{G_2} \qquad (138)$$

where

$k_{G_1}'a_1$ = the coefficient for the bubble formation zone.

t_{G_1} = the gas contact time in the bubble formation zone.

$k_{G_2}'a_2$ = the coefficient for the froth and entrainment zones.

t_{G_2} = the gas contact time in the froth and entrainment zones.

By use of high-speed motion pictures, Chu, et al.[19] studied the effect of the variables, slot submergence, slot area, skirt clearance, liquid viscosity, and surface tension, on the average interfacial area per unit volume of vapor, a_1, and the total contact time, t_G. The studies were conducted by use of a single slot in two different bubble caps. The majority of the tests were conducted using an aluminum cap with the following dimensions: 1-1/2 inch diameter, 1-1/2 inch high and 1/16 inch wall thickness. The slot size was varied between 1/8 by 5/8 to 1/2 by 1-1/4 inches. One set of runs was made by use of a commercial 3 inch-diameter cast iron cap with a single 1-1/4 by 5/8 inch triangular slot. Slot submergence was varied between 0.5 and 4.0 inches; the liquid surface tension between 30 and 72 dynes/cm; and liquid viscosity between 0.4 and 1.0 centipoises. The effect of vapor rate was studied over the range of 15 to 50 ft/sec, superficial slot velocity, while the liquid rate was varied over the range of 0.5 to 12.0 gal/min per inch of free plate width. It was

found that both the average interfacial area per unit volume of vapor, a_1, and the total contact time, t_G, were primarily affected by the head of liquid on the slot. Below a slot submergence of approximately 2.5 inches of liquid, interfacial area was shown to decrease with increasing submergence and increasing slot area. Above 2.5 inches submergence, interfacial area was found to be independent of submergence but a function of skirt clearance, liquid viscosity, and surface tension. No significant effect of air rate on the interfacial area was found. The effects of weir height and liquid rate were satisfactorily correlated by use of slot submergence which is directly related to these variables. Although the viscosity was varied over the narrow range of 0.4 to 1.0 centipoises, the interfacial area at slot submergences greater than 2.5 inches increased approximately 27.5 percent as viscosity was increased over this range.

The foregoing results apply to the effect of the several variables on the interfacial area and contact time in the bubble formation zone. The extent of this zone was found to vary with slot submergence and is the cause for the decrease in interfacial per unit volume of vapor with increase in submergence. At low slot submergence the growth period was fairly short and the bubbles reached the liquid surface while they were still relatively small. A bubble emerging from the slot continued to grow until its top reached the liquid surface. At higher slot submergences the mode of formation changed and a second growth period occurred after a bubble broke away from the slot. In this case a thin channel connected the bubble and the slot, and the bubble continued to expand until the channel became unstable and broke. Because of the channel, larger bubbles

were formed at the higher submergences with a subsequent reduction in area per unit volume of gas. Continued increase in slot submergence above a value of about 3 inches resulted in no change in the average time required for the channel to collapse and consequently bubble size then ceased to be a function of slot submergence.

Calderbank[10] studied the effect of submergence on the efficiencies for the adiabatic vaporization of water, ethyl alcohol, and isopropyl alcohol on a 12 inch-diameter plate equipped with a single 3 inch commercial steel bubble cap and a 6 inch sieve plate. Slot submergence was varied over the range 0.25 to 3.5 inches. Gas holdup data were not obtained during these studies. However, the values of the number of mass transfer units, N_G, were found to be linear with submergence above a value of one inch. At lower values of submergence, the values of N_G decreased very rapidly with decreased submergence. Calderbank extrapolated the straight line portion of the curves to zero submergence to obtain values of the N_G for the bubble formation zone. The results by Chu, et al., indicate that this is an incorrect analysis since the extent of the bubble formation zone varies with submergence. Unfortunately, gas holdup data were not reported so that the data by Calderbank cannot be analyzed in a manner similar to that used in the present study.

The variation in the mass transfer coefficient with weir height found in the present study corresponds with the variation in interfacial area reported by Chu, et al. For the nitrogen-cyclohexanol system, the mass transfer coefficients at the 1-1/2 inch weir height or slot submergence of about one inch are more than one and one-half times the values for the 2 inch weir (slot submergence about 1.5 inches) and about two times

the values for the 3-1/2 inch weir (slot submergence about 2.5 inches). For the nitrogen-ethylene dibromdie system, the mass transfer coefficients at the 1-1/2 inch weir height are about one and one-half times the values at the 3-1/2 inch weir height. Thus it appears that the effect of slot submergence varies with liquid properties or possibly with combined effect of gas and liquid properties. It should be mentioned that the majority of data used in the correlation represented by Equations (123) and (123a) were obtained in the range of slot submergence, one to three inches, where Chu, et al., observed a continuous bubble growth until the surface of the liquid was reached. It is doubtful that this phenomenon occurred in systems used in the present study since froth height was in some cases greater than ten inches. It is very likely, however, that there was a bubble formation zone wherein the bubble was growing continuously until it became dislodged from the slot. In fact, visual observation under some conditions, particularly when high liquid viscosities were used, suggested a bubble formation zone. In this case, the mass transfer coefficients determined by use of Equation (23a) might be shown to be related to the coefficients for the separate zones on the tray as follows,

$$k_G'a\ t_G = k_{G_1}'a_1\ t_{G_1} + k_{G_2}'a_2\ t_{G_2} \qquad (138)$$

If the gas contact time in each zone is defined as follows,

$$t_{G_1} = \beta_1/u_s$$

$$t_{G_2} = \beta_f/u_s$$

where

β_1 = gas holdup in bubble formation zone.

β_f = gas holdup in froth zone.

β = total gas holdup.

Then substituting in Equation (138)

$$\frac{k_G' a \beta}{u_s} = k_{G_1}' a_1 \left(\frac{\beta - \beta f}{u_s}\right) + k_{G_2}' a_2 \frac{\beta f}{u_s} \qquad (139)$$

$$k_G' a = k_{G_1}' a_1 \left(1 - \frac{\beta f}{\beta}\right) + k_{G_2}' a_2 \frac{\beta f}{\beta} \qquad (140)$$

Therefore, at any fixed gas rate, the value of $k_G'a$ depends on the ratio of the gas holdup in froth zone and the total holdup. As the gas holdup in the froth zone becomes a large fraction of the total gas holdup, the value of $k_G'a$ approaches the value of $k_{G_2}'a_2$, the mass transfer coefficient for the froth zone. If the froth zone is small compared to the bubble formation zone, the mass transfer coefficient approaches $k_{G_1}'a_1$. The data from the present study indicate that $k_{G_1}'a_1$ is greater than $k_{G_2}'a_2$ since the value $k_G'a$ decreased as total gas holdup increased. In the case of the nitrogen-cyclohexanol system, $k_{G_1}'a_1$ is greater than two times the value of $k_{G_2}'a_2$.

Equation (140) applies to the case where both the bubble formation and froth zones exist on the tray. At low submergence of the slots, the coefficient, $k_{G_1}'a_1$, accounts for a large percentage of the total coefficient, $k_G'a$. At very low slot submergence, it is very probable that the bubbles do not develop fully before they break through the froth. Thus the maximum bubble size which Spells and Bakowski[83,84] and Chu et al.[19] observed would not be obtained. In any event, the total coefficient, $k_G'a$, would probably be better correlated by use of a relationship such as Equation (140). If the results reported by Chu et al. are accepted as being applicable for the case of multiple slots, then the interfacial area in $k_{G_1}'a_1$ would be independent of gas rate. The coefficient, k_G, in

$k_{G_1}'a_1$ would be expected to be a function of gas rate however. The maximum bubble size or the interfacial area in the froth zone would be a function of gas rate if the results of Spell and Bakowski are accepted as being applicable. Therefore, the total coefficient, $k_G'a$ could be represented by the sum of two terms but each term would be a different function of gas rate. That is for any system,

$$k_G'a = A\ (\text{F-factor})^a\left(1 - \frac{\beta f}{\beta}\right) + B(\text{F-factor})^b\ \frac{\beta f}{\beta} \qquad (141)$$

One of the uncertainties in an analysis of this type is the extent of the bubble formation zone. If this zone is not fully developed in all cases of submergence then $k_{G_1}'a_1$ becomes a function of submergence and the present analysis is not valid.

The dependence of the mass transfer in the gas phase upon the physical properties of the gas has been a major cause of investigation since the advent of the Whitman film theory. According to this theory the mass transfer coefficient should be proportional to the first power of diffusivity. The effects of physical properties such as viscosity and density are not readily apparent unless it is rationalized that these variables affect the thickness of the film across which the transfer is occurring. Chilton and Colburn[15] used an analogy to heat transfer to derive the following relationship between the mass transfer coefficient and the friction factor, f, which is calculated using the skin friction.

$$j_D = \frac{k_G P_{BM}}{G_M}\ \left(\frac{\mu_G}{\rho_G D_G}\right)^{2/3} = 1/2\ f \qquad (142)$$

Sherwood and Pigford[78] suggest the use of the Schmidt number to the minus one-half power by analogy with results from packed and wetted-wass columns.

The mass transfer coefficients for wetted-wall columns have been correlated by the following equation,

$$\frac{k_G D p_{BM}}{D_G P} = 0.023 \left(\frac{DG}{\mu_G}\right)^{0.83} \left(\frac{\mu_G}{\rho_G D_G}\right)^{0.44} \qquad (143)$$

For dilute mixture of solute gas at 1 atmosphere total pressure, Equation (143) reduces to

$$k_G = 0.023 \frac{D_G^{0.56}}{\mu_G^{0.39}} \frac{G^{0.83}}{D^{0.17}} \frac{1}{\rho_G^{0.44}} \qquad (144)$$

or

$$k_G = 0.023 \frac{D_G^{0.56}}{\mu_G^{0.39} \rho_G^{0.02}} \frac{(\text{F-factor})^{0.83}}{D^{0.17}} \qquad (145)$$

The important point to emphasize in regards to Equation (145) is that when F-factor is used as a correlating variable, k_G is proportional to the gas diffusivity to the 0.56 power and not necessarily the Schmidt number to the minus one-half power. It is also interesting to compare Equation (145) with Equation (123a). The dependence of k_G and $k_G'a$ on F-factor differ, which might be expected, but the dependence on gas diffusivity is about the same in both cases.

The effect of the gas physical properties on the mass transfer in packed towers has been studied by several investigators. However, the results have not been consistent. Mehta and Parekh[12] vaporized water, methanol, benzene, and toluene and found that H. T. U. was proportional to the gas diffusivity to the 0.17 power. Smosky and Dodge[82] used water, methanol, benzene and ethyl butyrate to study vaporization of these liquids and correlated their data by use of gas diffusivity to the 0.15 power. Johnstone and Singh[48] found that rates of absorption of sulfur dioxide in sodium hydroxide solution; absorption of ammonia in aqueous acetic acid;

and evaporation of water into air from wood grids varied according to the Schmidt number to the minus two-thirds power. The data of Simkin[80] and Chrisney[16] on the vaporization of solids and liquids from packed beds in the absence of liquid flow indicate that the H. T. U. is proportional to gas diffusivity to the -0.36 power. More recently Lynch and Wilke[54] vaporized water into air, helium, and Freon-12 in a 12 inch-diameter packed tower to study the influence of gas properties on the rate of mass transfer. When these data were correlated by use of Reynolds number, DG/μ_G, H. T. U. was found to be proportional to Schmidt number to the 0.90 power. However, when the same data were correlated by use of F-factor, the values of H. T. U. at a constant liquid rate was found to be proportional to Schmidt number to the 0.47 power. Lynch and Wilke also correlated psychrometric data from several sources[54] and found that the data could be correlated suitably by use of Schmidt number to the 0.5 power. On the basis of the similarity between the two types of data, psychrometric and packed column, Lynch and Wilke preferred the correlation of the packed column by use of F-factor and Schmidt number to the 0.47 power. It was also emphasized by these investigators that the transfer of mass and momentum might be expected to be functions of the same properties of the flow field. Furthermore, they pointed out that the drag coefficient at high values of Reynolds number is independent of Reynolds number and the pressure drop is dependent only upon the inertia of the gas stream, $\rho_G u^2$. Since it was postulated that the rate of mass transfer will depend on the same flow properties as for the case of pressure drop, Lynch and Wilke concluded that the mass transfer coefficient would be a function of the gas inertia and not Reynolds number at high flow rates.

The results reported by Lynch and Wilke[54] are very similar to the results from the analysis of the vaporization data in the present study. When a Reynolds number was used as one of the dimensionless groups to correlate the values of N_G, the exponent on the Schmidt number was found to be -0.89 when all the data were used in the correlation. However, when F-factor was used as a correlating variable, the number of mass transfer units was found to be proportional to the gas diffusivity to the 0.53 power. The number of mass transfer units might have been correlated by use of Schmidt number to the minus one-half power. However, the fundamental variable, $k_G'a$, would definitely not be correlated by use of Schmidt number since the gas density is eliminated when Equation (123) is converted to a correlation of the mass transfer coefficient. It should be mentioned that the variation of gas viscosity in the data obtained by Lynch and Wilke was not great and the correlation would probably not be changed significantly by either including or excluding gas viscosity. The important point is that the $k_G'a$ is not a function of Schmidt number although the data in the form of H. T. U. for packed towers and N_G for bubble cap plates may be shown to be a function of Schmidt number.

It has not been widely recognized that the penetration theory proposed by Higbie[42] or Danckwerts[22] may be used to relate the gas-phase mass transfer coefficient and gas diffusivity. However, the results of the present study suggest that this theory is applicable for the gas phase. The penetration theory is based on a periodic renewal of fluid elements at the interface and it is not difficult to visualize such a process in view of the turbulence in the gas phase in the bubble formation zone. In the froth zone, this renewal could be caused by the

circulation of the gas in the bubbles due to drag at the interface. Rybczynski[74] and Hadamard[40] applied Stoke's method to "creeping" motion of a fluid sphere of zero surface tension to derive a relationship between the rate of circulation inside a fluid drop, the velocity of the drop, and the ratio of the viscosities of the inner and outer phases.

$$q_i = \frac{\pi d_b^2}{32} \frac{V_b}{1 + \mu_o/\mu_i} \tag{146}$$

Hughes and Gilliland[45] used this relation to show that for a bubble the circulation has a great effect on the drag. Or vice versa, the drag on the bubble has a large effect on the circulation inside the bubble. Hughes and Gilliland concluded that bubbles of gas in liquids at high Reynolds number are always circulating. Garner and Hammerton[33] used ammonium chloride to observe the circulation inside bubbles. They concluded that bubbles greater than 0.03 cm in diameter in water tend to have internal circulation and that the energy caused by skin friction must be greater than the surface energy before circulation can persist. The skin friction would be expected to be a function of liquid viscosity. Thus the rate of circulation would be expected to vary with liquid viscosity.

The use of F-factor to correlate the gas-phase mass transfer coefficient is believed to be justified on the basis of the discussion presented by Lynch and Wilke. However, in the case of the gas flowing through the liquid on the tray, the rate of momentum transfer is not related to the total pressure drop across the tray but the pressure drop due to drag between the gas and liquid. An energy balance on the gas between a point below and above the tray may be used to indicate the different causes for dissipation of energy.

$$- \sum F - W = \Delta Z + \frac{\Delta u^2}{2g} + \int_1^2 V \, d \, P \tag{147}$$

If the work term is neglected and the vapor density is assumed to be constant, then

$$\frac{P_1 - P_2}{\rho_G} = \frac{u_2^2 - u_1^2}{2g} + \frac{(Z_2 - Z_1)\rho_L}{\rho_G} + \sum F \tag{148}$$

If the kinetic energy above and below the tray are not significantly different, then

$$\Delta P_T = Z_c \rho_L + \rho_G \sum F \tag{149}$$

where

ΔP_T = total pressure drop.

Z_c = slot submergence.

$\sum F$ = frictional energy losses, ft.-lb/lb.

ρ_L = liquid density, lb/ft^3.

ρ_G = gas density, lb/ft^3.

The term, $\sum F$, is the total energy loss due to the gas flowing through the caps and the liquid. The energy loss due to the gas flowing through the liquid is the term which is related to the momentum transfer. Since this energy loss is probably small, an accurate measurement of the total pressure drop, the pressure drop across the caps, and slot submergence would be required before the energy loss in the liquid could be determined accurately. It would be of interest to see a study of this type performed in the future since the rate of mass transfer and pressure drop in the liquid might be related by use of the present theories of mass and momentum transfer.

The gas-phase and liquid-phase data from the present study may be used to amplify the foregoing discussions in regard to the effect of liquid viscosity on the drag between gas and liquid and the relationship

between pressure drop and mass transfer. In the case of the mass transfer data for the gas phase the coefficients were correlated by Equation (123a) wherein the relationship between the coefficient and F-factor was found to be a function of the liquid viscosity. However, the liquid-phase mass transfer coefficients were correlated by use of Equation (131) wherein the relationship between the coefficient and F-factor was found to be independent of liquid viscosity. Since the relationship between the coefficient and F-factor was found to be a function of liquid viscosity in the case of the gas-phase data and not in the case of the liquid phase data, this is good reason to believe that viscosity affects the drag between the liquid and gas and consequently the mass transfer in the gas phase. If the effect of liquid viscosity were an effect on interfacial area then liquid viscosity should appear in the correlations of the gas and liquid phase data in identical form.

Absorption Studies

The correct correlation of the liquid-phase mass transfer coefficients is somewhat uncertain due to the uncertainty in the diffusivities for carbon dioxide in cyclohexanol. However, in view of the failure of the Wilke and Chang correlation to predict diffusivity data in systems of high liquid viscosities, it is believed that the correlation obtained by use of the diffusivities predicted by the Wilke and Chang relationship is not a correct representation of the data. Although Schoenborn et al.[3] determined experimental diffusivities for carbon dioxide, it was pointed out in a previous section that there is good reason to doubt the validity of these data. Arnold's equation was used to predict diffusivities for the carbon dioxide-cyclohexanol system which were 1.8 to 1.9 times the

values reported by Schoenborn. The form of the correlation equation is as follows when either the Schoenborn data or the data predicted by Arnold's equation are used.

$$k_L\bar{a} = \beta' D_L^{1/2} (\mu_L/\rho_L)^{\alpha} (\text{F-factor})^{0.575} \qquad (131a)$$

where β' and α are functions of μ_L/ρ_L.

The absolute value of β' depends upon which diffusivity data are used as shown in Figure 53. However, since the same form for the correlating equation is obtained by use of diffusivity data from the two separate sources it is believed that Equation (131a) is the correct correlating equation if it is assumed that the penetration theory proposed by Highbie[42] and Danckwerts[22] is applicable. The important points to consider in regards to Equation (131a) is the variation of α with the kinematic liquid viscosity, the dependence of the coefficient on F-factor, and the relationship between the coefficient and liquid diffusivity.

The same problem is confronted with the liquid-phase mass transfer coefficient as in the case of the gas-phase coefficient. That is, the coefficient is a product of two separate but not unrelated terms. However, for the case of the liquid-phase coefficient, it is possible to predict the combined effect of the liquid properties and the gas rate if it is assumed that the gas flows through the liquid in a form approximating a bubble and that Higbie's[42] equation describing the coefficient is applicable. This could not be done for the case of the gas-phase coefficient because of the inability to describe k_G in terms of the fluid dynamics and physical properties of the system. Highbie's equation relates the liquid-phase diffusivity and the bubble characteristics as follows:

$$k_L = 2\sqrt{\frac{D_L}{\pi t_b}} \tag{15a}$$

where

D_L = the liquid-phase diffusivity.

t_b = bubble contact time, d_b/V_b.

d_b = bubble diameter.

V_b = bubble velocity.

Van Krevelen and Hoftijzer[88] used data from several sources to perform a study of the characteristics of bubbles formed at orifices. Bubble diameter and velocity were correlated with liquid properties by use of the following dimensionless relationship.

$$\frac{g\ d_b\ \Delta\rho}{V_b^2\ \rho_L} = M\left(\frac{V_b\ d_b\ \rho_L}{\mu_L}\right)^m \tag{150}$$

In the streamline region of flow the above relationship was found to be as follows:

$$\frac{g\ d_b\ \Delta\rho}{V_b^2\ \rho_L} = 18\ \left(\frac{V_b\ d_b\ \rho_L}{\mu_L}\right)^{-1} \tag{150a}$$

Therefore the expression for bubble contact time becomes,

$$t_b = \frac{d_b}{V_b} = \frac{18}{g}\ \frac{1}{d_b}\ \frac{\mu_L}{\rho_L} \tag{151}$$

if $\Delta\rho$ is approximately equal to ρ_L. The maximum bubble diameter may be related to the volumetric gas rate and bubble frequency.

$$Q_G = N_s n_b \frac{\pi d_b^3}{6} \tag{152}$$

where

n_b = bubble frequency.

N_s = number of bubble sources.

$$\text{and} \quad d_b = \left(\frac{6Q_G}{\pi N_S n_b}\right)^{1/3} \tag{152a}$$

$$\text{or} \quad 1/d_b = \left(\frac{\pi N_S n_b}{6Q_G}\right)^{1/3} \tag{152b}$$

The interfacial area per unit volume of gas is equal to the reciprocal of the bubble diameter, i.e., $a = 1/d_b$. If Equations (151) and (152a) are substituted in Equation (15a), an expression is obtained which relates the mass transfer coefficient, liquid diffusivity, liquid kinematic viscosity, and volumetric gas rate. That is,

$$k_L a = 1.51 \left(\frac{\pi N_S n_b}{6Q_G}\right)^{1/6} D_L^{1/2} \left(\frac{\mu_L}{\rho_L}\right)^{-1/2} \tag{153}$$

Two points in regards to Equation (153) are significant: (1) The mass transfer coefficient is proportional to the liquid kinematic viscosity to the minus one-half power in the range of high liquid viscosities and (2) The mass transfer coefficient based on interfacial area per unit volume of gas is not highly dependent on gas rate. The above observations are valid only when the bubble frequency is independent of gas rate and liquid properties. Calderbank used a special technique to study the frequency of bubbles found at slots and orifices. Over the range of flow rates normally used in industrial practice, it was found that bubble frequency was constant at 20 per second and independent of gas flow rate, slot dimensions, spacing between slots, physical properties of gas and liquid and slot submergence. If the value of 20 per sec for the bubble frequency is substituted in Equation (153), the expression for the liquid-phase mass transfer coefficient in the high range of liquid viscosities becomes,

$$k_L a = 2.23 \left(\frac{N_S}{Q_G}\right)^{1/6} D_L^{1/2} \left(\frac{\mu_L}{\rho_L}\right)^{-1/2} \tag{153a}$$

In the low range of liquid viscosities, van Krevelen and Hoftijzer found that the relationship between bubble diameter and velocity became,

$$\frac{g\, d_b\, \Delta\rho}{V_b^2\, \rho_L} = 2 \qquad (150b)$$

Thus the expression for the bubble contact time is,

$$t_b = \frac{d_b}{V_b} = \frac{2V_b}{g} \qquad (154)$$

and the expression for the mass transfer coefficient becomes,

$$k_L a = 2\left(\frac{g}{2}\right)^{1/4} d_b^{3/4}\, D_L^{1/2} \qquad (155)$$

If Equation (152a) is substituted in Equation (155) the dependence of the mass transfer coefficient on the gas rate is found to be

$$k_L a = 2.23\, \left(\frac{Q_G}{N_s}\right)^{1/4} D_L^{1/2} \qquad (155a)$$

Therefore in the low range of liquid viscosity, the coefficient is dependent on liquid diffusivity and gas rate but independent of liquid kinematic viscosity. By comparison of Equations (153) and (155a), it might be predicted that the dependence of the coefficient upon the gas rate in the low range of liquid viscosity differs from the dependence in the high range of liquid viscosity. The interfacial area in these two equations is the specific area based on the gas holdup while the specific area in the correlation represented by Equation (131a) is based on the liquid holdup. The latter equation may be converted to a basis of area per volume of gas by multiplying by the ratio of liquid and gas holdup as follows:

$$k_L a = k_L \bar{a}\, \frac{Z_c}{Z_f - Z_c} \qquad (156)$$

In the preliminary examination of the data for the carbon dioxide-cyclohexanol system it was found that the ratio, $\frac{Z_c}{Z_f - Z_c}$, could be correlated by use of F-factor to the minus 0.75 power. For the case of the carbon dioxide-water system, the ratio was found to vary with F-factor to the minus 0.6 power. The ratio in both cases however was found to be a function of weir height and liquid rate. As shown in Figure 49 the mass transfer coefficient for this system varies with F-factor to the 0.72 power while the coefficients for the air-water system are a function of F-factor to the 0.575 power. If the foregoing information is used with Equations (131a) and (156) then the expression for the mass transfer coefficient becomes,

$$k_L a = \beta'' \, D_L^{1/2} \, (\mu_L/\rho_L)^{\alpha} \qquad (157)$$

where

β'' is a function of weir height and liquid, or possibly more directly a function of slot submergence and μ_L/ρ_L.

The variation of the exponent on the F-factor or gas rate with liquid kinematic viscosity as predicted by Equations (153a) and (155a) cannot be verified by the experimental data. However, it is believed to be significant that the exponent on the F-factor or gas rate was predicted to be in the range of 0.25 to -0.167 and was found to be about zero.

The results in Figure 53 indicate that the transition region for the exponent on the kinematic viscosity in Equation (131a) is in the range of 0.05 to 1.0 ft^2/hr. It is of interest to see if this range can be predicted by use of the results reported by van Krevelen and Hoftijzer.(88) From the correlation for the characteristics of bubbles

in series, the point where the characteristics become independent of liquid viscosity may be described as follows,

$$\frac{V_b \, d_b \, \rho_L}{\mu_L} = 100 \tag{158}$$

$$\frac{g \, d_b \, \Delta\rho}{V_b^2 \, \rho} = 2 \tag{159}$$

By combining these equations with the relationship between flow rate, bubble diameter, and bubble frequency, it is possible to derive an equation which may be used to solve for the kinematic viscosity.

$$\mu_L/\rho_L = 36 \, (3gQ_G/\pi N_s n_b)^{1/2} \tag{160}$$

where

μ_L/ρ_L = liquid kinematic viscosity, $ft^2/hr.$

At a superficial gas velocity of 6 ft/sec., the value of μ_L/ρ_L according to Equation (160) is 6.38. Therefore, it appears that the predicted value of μ_L/ρ_L is too high by a factor of about ten. The most likely reason for this discrepancy is the value of the Reynolds number used in Equation (158). If in place of 100, the value of 1000 for the Reynolds number is used in Equation (158) the predicted value of μ_L/ρ_L then becomes 0.638. The possibility of an error in the bubble frequency being the cause for the discrepancy is unlikely since a factor of ten in the liquid kinematic viscosity would mean a factor of 100 in the frequency because of the square root relationship in Equation (160).

It should be pointed out that the foregoing analysis is based on the premise that gas flows through the liquid on the tray in a form approximating a bubble. At low gas rates, i.e., below F-factor equals

1.0, this model is probably a very naive representation of a complicated process. The model does serve however to explain on a semi-quantitative basis the results represented by Equation (131a). At high gas rates or at intermediate gas rates and slot submergence the gas flows through the liquid in a nondescript form. In this case, it would be difficult to think of an appropriate shape to use in describing the relationship between the mass transfer coefficient, interfacial area, and rate of surface renewal. In both cases, the times of surface contact are probably randomly distributed, and the model proposed by Danckwerts[22] would most likely describe the mass transfer coefficient better than the model proposed by Higbie.[42]

Similar studies directed toward determining the effects of liquid properties on the liquid-phase mass transfer in the two-phase system on a bubble-cap tray are not numerous. In addition the studies which have been performed have not yielded conclusive results regarding the effects of liquid properties. The correlation reported by Etherington[27] and represented by Equation (91) includes data from several sources[28,44,64] and is similar to the correlation of the data from the present study. However, as mentioned previously, the transition from a small effect of liquid viscosity to a large effect occurred at 3 instead of 25 centipoises as found in the present study. The data used by Etherington covered the range of viscosity from 0.4 to 13 centipoises. Diffusivities were estimated by use of Arnold's equation but the abnormality factors were unknown. In view of the correlation presented in Figure 51 it is predicted that the diffusivities for the hydrocarbon systems used by Etherington were in error considerable. In addition, Etherington arbitrarily assumed that the

liquid diffusivity should be included in the correlation equation to the two-thirds power. Therefore, it is believed the data used by Etherington should be correlated again before a direct comparison is made with the results from the present study.

The studies of liquid-phase mass transfer in other types of gas-liquid contacting devices have been more conclusive with respect to the effects of liquid properties than the studies concerned with bubble-cap trays. For the case of wetted-wall columns, Hatta and Katori[41] derived the following equation to describe the mass transfer coefficient,

$$k_L = \sqrt{\frac{6}{\pi}} \sqrt{\frac{D_L \Gamma}{\rho_L B_F Z}} \qquad (161)$$

where

Z = the length of the wetted surface.

$\frac{\Gamma}{\rho_L B_F}$ = mean velocity of flow.

Equation (161) has been used to accurately predict experimental data obtained from wetted-wall columns where the time of contact between the gas and liquid was small.[76] Extensive data for packed towers have been obtained by Sherwood and Holloway.[77] Below the gas velocity where loading begins, the H. T. U.'s were found to be independent of gas velocity. These data were satisfactorily correlated by use of the following equation,

$$H_L = \frac{1}{\alpha} \left(\frac{L}{\mu_L}\right)^n \left(\frac{\mu_L}{\rho_L D_L}\right)^{0.5} \qquad (162)$$

where

α = constant which varied from 80 to 550 for different packings.

n = constant which varied between 0.22 and 0.46.

L = liquid rate.

It is believed to be significant that in both cases, wetted-wall tower and packed tower, the mass transfer data were correlated by use of liquid diffusivity to the one-half power. In both cases, the time of interfacial contact between the gas and liquid is short and the equations by Danckwerts and Higbie seem to apply. It is logical to expect the same equations to apply for the case of mass transfer on a bubble cap tray. However, it should be pointed out that a recent study by Toor and Marchello[86] indicates that the penetration theory is a limiting case of a more general theory which embraces the penetration and film theories. The study by Toor and Marchello consisted of a mathematical treatment of the problem of mass transfer to a surface which is periodically renewed. They conclude that at low Schmidt numbers a steady-state gradient is set up very rapidly in any new surface element so that unless the rate of renewal is great enough, steady-state transfer takes place through a film. The rate of mass transfer in this case would be expected to be proportional to the diffusivity. At high Schmidt numbers, Toor and Marchello state that the time necessary to set up the steady gradient is increased and even low rates of surface renewal are sufficient to keep most of the elements from being penetrated. The transfer then follows the penetration theory. For the intermediate cases Toor and Marchello derived equations to indicate the relationship between the rate of mass transfer and the diffusivity. Judging from the results of this study it would not be surprising to find that data from any one type of contacting device might be correlated by diffusivity to the exponents between 0.5 and 1.0 if the physical properties of the system are varied over a wide range.

CONCLUSIONS

Hydraulic Characteristics

1. Liquid density, viscosity, and surface tension were not found to have a significant effect upon the hydraulic characteristics of the tray used in the present study. Data from the literature plus data from the present study were used to determine the effects of the foregoing variables upon froth height, clear liquid height, and gas holdup over the following ranges:

   viscosity: 0.6 - 97.3 cp

   density: 0.78 - 2.15 gm/cc

   surface tension: 21.5 - 70 dynes/cm.

   Minor variations of the hydraulic characteristics with liquid properties were noted. However, these variations are believed to be within the range of deviations expected with the measurement techniques used in the present and previous studies.

2. The major variables which may affect the hydraulic characteristics of the bubble-cap tray used in the present study are: gas rate, liquid rate, weir height, splash baffle height, and gas density. The hydraulic characteristics at a constant weir height and liquid rate and variable gas rate and gas density may be satisfactorily correlated by use of F-factor, $u_s \sqrt{\rho_G}$.

Gas-Phase Mass Transfer

1. The coefficients for mass transfer in the gas phase as defined by Equation (23a) were correlated as follows:

$$k_G'a = 523.9 \frac{D_G^{0.526}}{\rho_L^{0.834}} \frac{(\text{F-Factor})^n}{(Z_f - Z_c)^{0.28}} \qquad (123a)$$

where $n = 0.852 \, (\mu_L/\rho_L)^{0.238}$

The data from several systems used in the present and previous studies were predicted by use of Equation (123a) with an average absolute percent deviation of 14.59 between the experimental and predicted data. The range of variables represented by the data used in the above correlation are as follows:

gas density, ρ_G	:	0.0130 - 0.2737 lb/ft^3
gas viscosity, μ_G	:	0.0351 - 0.0485 lb/ft-hr
gas diffusivity, D_G	:	0.210 - 4.22 ft^2/hr
liquid density, ρ_L	:	0.78 - 2.15 gm/cc
liquid viscosity, μ_L	:	0.6 - 24 cp
F-factor, $u_s \sqrt{\rho_G}$	:	0.2 - 1.2
gas holdup, $Z_f - Z_c$	:	2 - 10 inches
liquid rate	:	4.6 - 32.0 gpm
weir height	:	1-1/2 - 3-1/2 inches

2. From the results represented by Equation (123a), the following conclusions are possible:

   (a) When correcting the mass transfer coefficients for differences in gas properties between two

different systems, the use of Schmidt number to the minus one-half power is not justified.

(b) The relationship between the mass transfer coefficient and F-factor varies with changes in liquid kinematic viscosity.

(c) The mass transfer coefficient decreases as the gas holdup on the tray increase due to increase of weir height at a constant liquid rate or increase of liquid rate at a constant weir height.

Liquid-Phase Mass Transfer

1. The complete correlation of the liquid-phase mass transfer coefficients is uncertain because of the questionable diffusivity data available for the carbon dioxide-cyclohexanol system. However, the form of the correlation equation is believed to be as follows:

$$k_L\bar{a} = \beta' D_L^{1/2} (\mu_L/\rho_L)^{\alpha} (\text{F-Factor})^{0.58} \qquad (131a)$$

where β' and α are functions of μ_L/ρ_L .

In the range of kinematic viscosity greater than 1.0 ft^2/hr, the value of α is minus 0.5. Below the value of 1.0 $ft^2/hr.$, α decreases and approaches zero as kinematic viscosity approaches the value of 0.01. The constant, β', varies with kinematic viscosity as shown in Figure 53. However, the absolute value of β' at any level of kinematic viscosity can not be specified because of the uncertainty in the

diffusivity data for the carbon dioxide-cyclohexanol system. The range of variables represented by the data used in the above correlation are as follows:

liquid viscosity, μ_L	:	2 - 235 lb/ft-hr
liquid density, ρ_L	:	58 - 62.4 lb/ft^3
F-factor, $u_s \sqrt{\rho_G}$	:	0.3 - 2.2
liquid rate	:	4.6 - 32.0 gpm
weir height	:	2 - 3-1/2 inches

2. By use of a simple model which assumes that the gas flows through the liquid or froth on the tray in form of bubbles, the correlation between bubble characteristics and liquid properties suggested by Van Krevelen and Hoftijzer(88) and the penetration model proposed by Higbie, the effects of the liquid properties on the mass transfer coefficient were predicted to be in accordance with Equation (131a). This model gives some insight into the effects of liquid properties upon the individual terms, k_L and a. The principal conclusion is that the interfacial area and the coefficient are not unrelated terms. In addition, when liquid viscosity is increased, the interfacial area approaches a linear dependence on viscosity but the coefficient approaches a square-root relationship with viscosity so that the combined effect is the square root of viscosity. As viscosity is decreased in the range of kinematic viscosity below 1.0 ft^2/hr., the interfacial area and consequently k_L become independent of viscosity.

Comparison Between Gas- and Liquid-Phase Mass Transfer

When the liquid-phase mass transfer coefficient, $k_L a$, was converted to $k_L a$, where the interfacial area is based on the gas holdup per unit volume, the coefficient was found to be practically independent of gas rate. A common factor between the liquid- and gas-phase coefficients is the interfacial area. Therefore, the ratio of the two coefficients may be related to F-factor as follows:

$$\frac{k_G}{k_L} = f\left(\frac{D_G}{D_L}, \frac{\mu_L}{\rho_L}, Z_f - Z_c\right) (\text{F-Factor})^n \qquad (163)$$

On the basis of the simple model used to describe k_L, it is believed that this coefficient is almost independent of F-factor. It is therefore concluded that the variable coefficient of F-factor which is a function of liquid kinematic viscosity is due to an effect on k_G and can be attributed to the variation in circulation or turbulence in the gas phase as liquid viscosity is varied.

Liquid Mixing

Experimental point efficiencies were compared with point efficiencies predicted by use of the relationships suggested by Warzel[92], Crozier[21], and Robinson.[72] It is concluded that these relationships may be used to satisfactorily predict point efficiencies when the data are in the range of λE_{OG} below 2.0. In addition, a more critical analysis of the relationships between point and plate efficiency would require data in the range of λE_{OG} above 2.0.

RECOMMENDATIONS

Gas-Phase Mass Transfer

In the present study, the gas-phase viscosity was not varied over a significant range. Consequently, the effect of this variable on gas-phase mass transfer is unknown. It is recommended that future studies be performed by use of systems with widely different gas viscosities. Because of the limited range of gas viscosity which may be covered by gases such as nitrogen, carbon dioxide, helium, etc., the effect of this variable would have to be studied by use of distillation systems or vaporization systems where the temperature is varied over a large range.

The correlation of the gas-phase mass transfer data as represented by Equation (123a) is not a least-squares fit of the data. This probably accounts for some of the deviation between the predicted and experimental data. It would be of interest to recorrelate the vaporization data by use of a non-linear regression program wherein the correlation equation is the form of Equation (123a). By use of the non-linear regression program confidence limits could be established for the various coefficients in the correlating equation. In addition, it might be possible to separate the effects of gas holdup and slot submergence on the mass transfer coefficient.

The results of the present study indicate that liquid properties significantly affect the gas-phase mass transfer coefficient. It is believed that the liquid properties should also affect the energy loss in the gas phase and that there should be some relation between the energy loss and the mass transfer coefficient. It is recommended that in future studies accurate pressure drop measurements across the tray and the

bubble caps be made. These data plus an accurate measurement of liquid holdup or clear liquid height could be used to predict the energy loss due to the gas flowing through the froth on the tray. It would then be of interest to compare the rate of mass transfer and the energy loss in the case of the bubble-cap tray with similar data from other contacting devices such as packed towers and wetted-wall towers.

Liquid-Phase Mass Transfer

The results of the liquid-phase mass transfer study indicates a variable effect of the kinematic viscosity upon the mass transfer coefficient. However, additional investigation of this effect should be performed in the range of 0.1 to 1.0 ft^2/hr for the liquid kinematic viscosity. Possibly data in the literature could be used for this investigation. Specifically, Etherington's data which covers the range of viscosity between 0.4 to 13 centipoises or 0.022 to 0.72 ft^2/hr should be recorrelated using diffusivities determined by use of recent data reported in the literature.

In order to completely establish the correlation of the data from the present study, additional data for the diffusivity of carbon dioxide in cyclohexanol are necessary.

APPENDIX A

DESCRIPTION OF APPARATUS

The apparatus used in this investigation was designed by personnel of the Chemical and Metallurgical Engineering Department of the University of Michigan. Warzel[92] and Ashby[7] used this equipment during the course of their investigations of plate efficiencies. These investigators have given a detailed description of the equipment. However, the test tray and the flow schemes will be described herein in enough detail to enable another investigator to repeat the same or similar studies.

The apparatus was used by Ashby[7] just prior to the present studies and except for a few modifications the equipment is identical to that used by the preceding investigator. The modifications were as follows:

1. Installation of a third blower in parallel with one of the previously installed blowers to increase the range of gas velocity through the test tray.
2. Fabrication and installation of a small heat exchanger between one of the recirculating pumps and the inlet to the test tray to remove heat from the liquid and maintain adiabatic conditions on the tray during the vaporization studies.
3. The rope-type packing glands in both centrifugal pumps (Model 40, Series WS7RD-74 Durcopumps, with 7-1/2 inch open empellers) were replaced by mechanical seals. This was done to eliminate packing gland grease as a

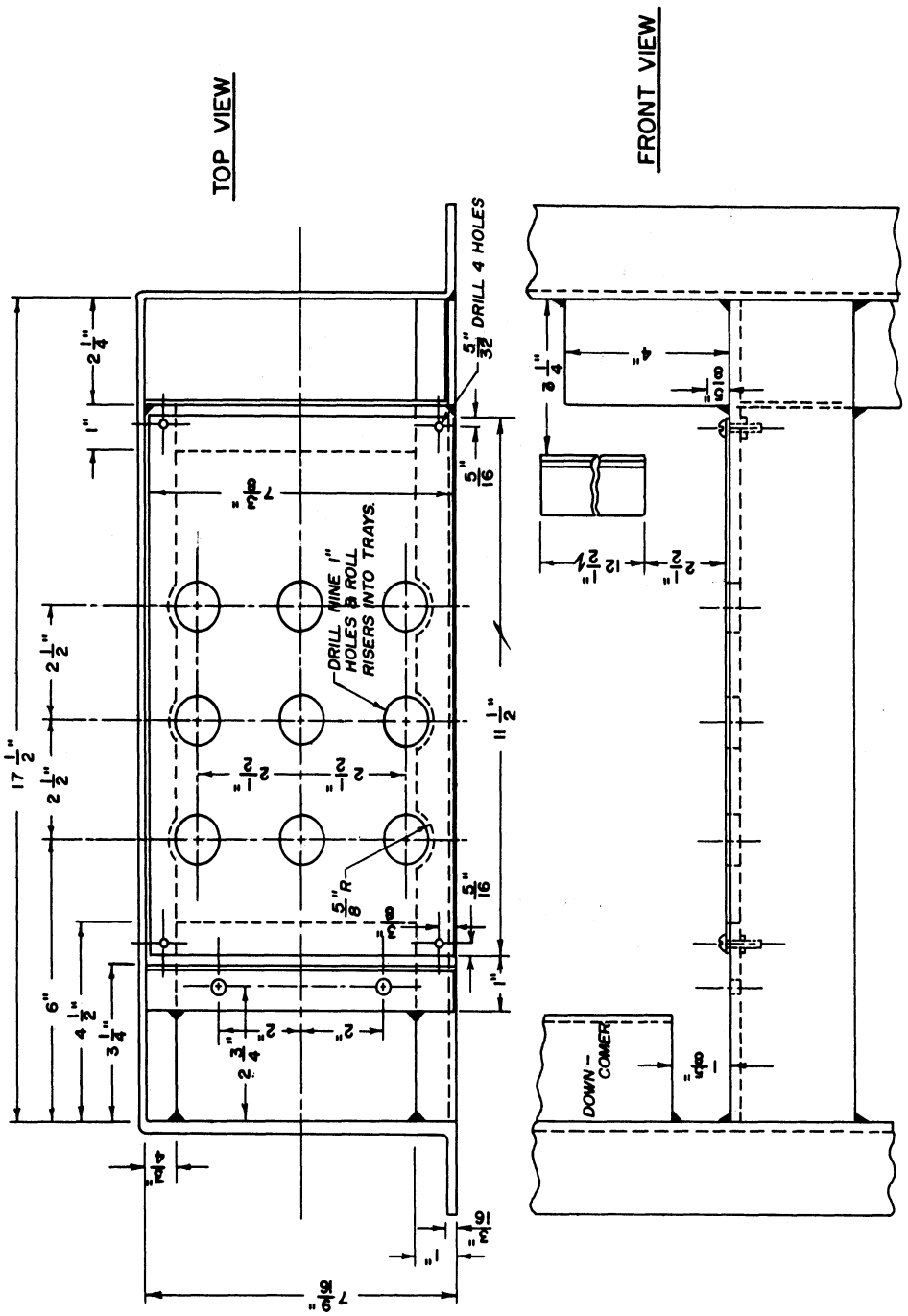

Figure 1A. Bubble Cap Plate Layout

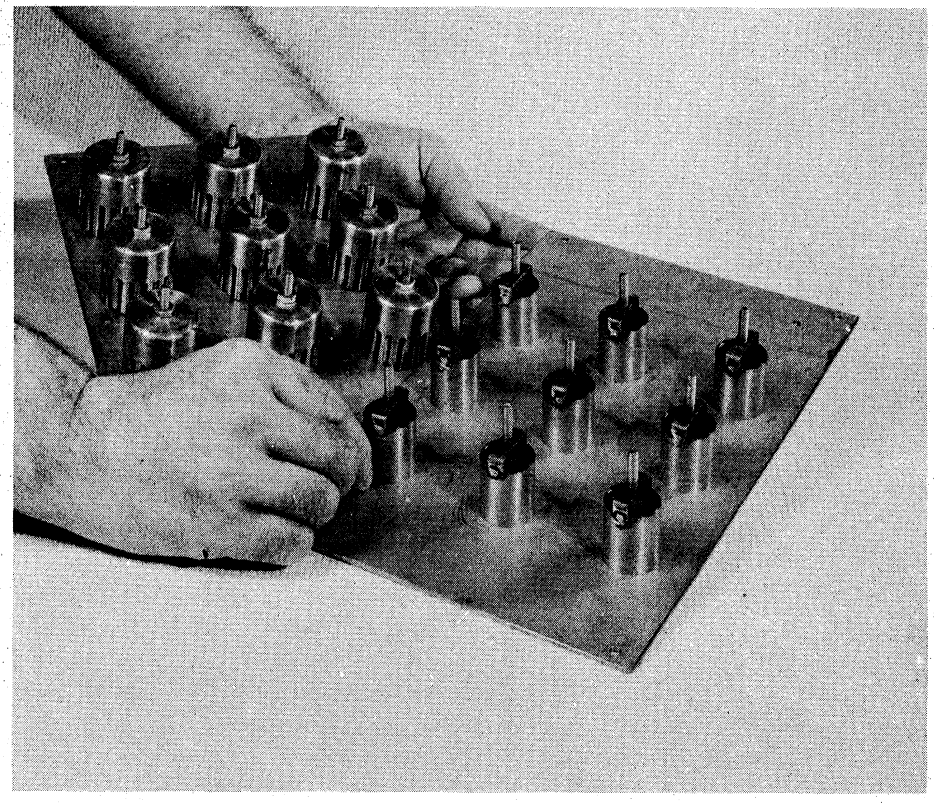

Figure 2a. Removable Trays, Showing Bubble-Caps and Risers for Absorber.

possible source of contamination in the liquids being used in the studies.

4. Fabrication and installation of new windows on the front of the column which could be sealed by use of Teflon tape and Epoxy resin, Shell No. 828, materials which were not affected appreciably by the liquids used in the studies.
5. Installation of froth sampling probes above the test tray and liquid sampling devices on the floor of the test tray.

Test Tray

A general view of the equipment is shown in Figure 2. The test column was designed for five bubble-cap trays but in the present investigation only the first and second trays from the bottom of the column were used. The first tray was used for the test tray. A detailed drawing of this tray is presented in Figure 1A and the detailed dimensions are given in Table VI. The tray contained nine 1-1/2 inch bubble caps arranged on a 2-1/2 inch square pitch. Figure 2A shows two removable trays, one equipped with the caps and the other one with the risers on the removable tray.

The outlet weir on the tray was designed to be adjustable and in the present investigation three different weir heights were used. These were: 1-1/2, 2, and 3-1/2 inch. To eliminate a large hydraulic gradient on the tray an adjustable splash baffle was used. The bottom of the splash baffle in all studies in this investigation was one-half inch above the top of the weir and one-inch in front of the weir.

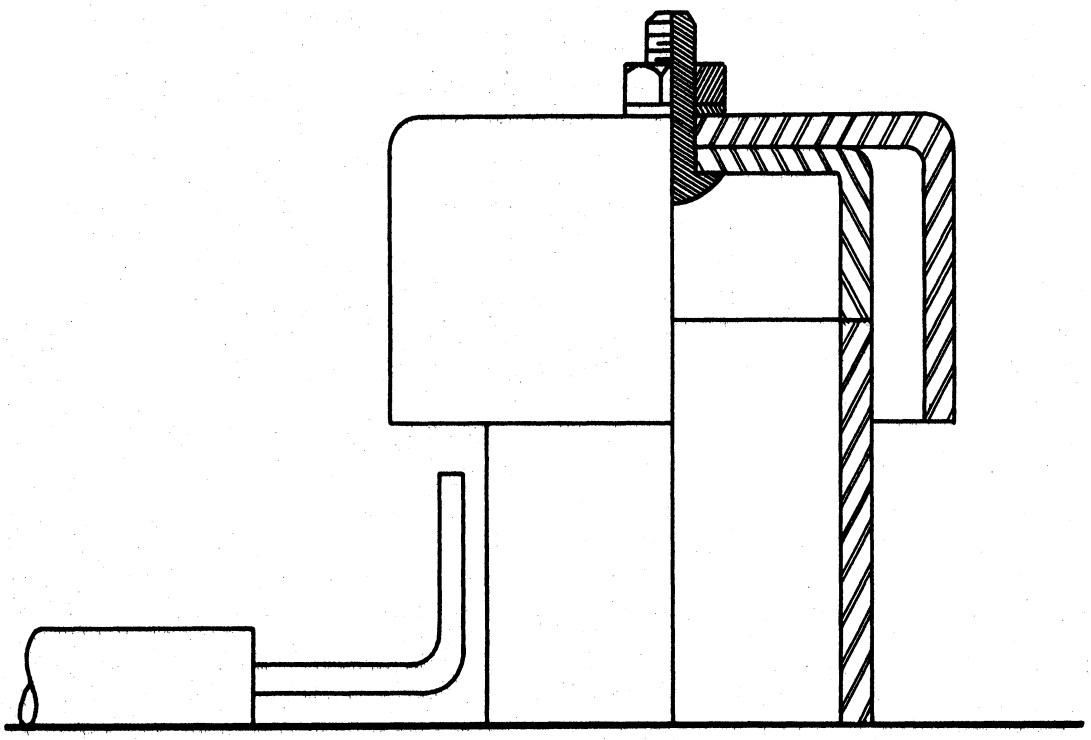

Figure 3A. Position of Probe for Outlet Vapor Sample

In Figure 5 the location of the liquid sampling points are shown. Figure 6 shows the liquid sumps below the sampling points. The liquid sumps were made by first cutting the tops from four risers and then welding these into holes in the tray floor and covering the holes with No. 8 mesh wire gauze. In the bottom of the sumps, 1/4-inch tubing fittings were welded. Stainless steel tubing (thick walled) was fitted to the 1/4-inch fittings and the tubing was run through compression fittings in the stainless steel panel below the test tray to the outside of the column. By the use of 1/4-inch ells, tees, and valves arrangements were made so that the liquid samples could be taken by use of a hypodermic syringe and needle or by use of a valve. In addition, arrangements were made so that the liquid sampling points on the tray could be used to measure the hydrostatic head of liquid above each point.

The tray above the test tray was used to complete the approximation of the boundaries which exist for any tray in a column. It also served the purpose of an entrainment separator and provided a method for obtaining a vapor sample without the entrained droplets. Ashby[7] designed this tray and found that if the vapor sampling device shown in Figure 3A was used, vapor samples devoid of entrainment could be obtained. The caps on this tray were modified by removing the teeth or slots. Ashby's reasoning on this problem was that the entrained droplets from the tray below would impinge on the inside of the caps and flow down the sides. Therefore, if the small sample probe was located in the annulus between the inside of the cap and the riser, a representative vapor sample could be obtained. It does

seem likely that there is a certain probability of a liquid droplet hitting the probe under certain conditions. However, the fact that the data obtained under conditions of high entrainment for certain systems could be correlated with the data for another system (nitrogen-ethylene dibromide) at the same operating conditions but with little or no entrainment would seem to prove this sampling method. This will be discussed further in the Discussion of Results.

The liquid sampling probes used to sample the froth are shown in Figure 4 and consisted of a 1/2-inch piece of 3/8-inch stainless steel tubing welded to the end of a 1/8-inch, thin-walled, stainless steel tubing. The end of the 1/8-inch tubing was bent upward so that the piece of 3/8-inch tubing served as a liquid collector. The 1/8-inch tubing extended through the plate above the test tray where a connection was made to 1/4-inch polyethylene tubing. The polyethylene tubing was taken through compression fittings in the wall of the column to the outside of the column where syringe stoppers were attached to the end of the tubing. Liquid samples were withdrawn through the syringe stoppers by use of a hypodermic syringe and needle.

Three sample probes in the froth were used. The horizontal positions of these probes were as follows: one probe was located near the inlet downcomer approximately above the first sample point on the floor of the tray; another probe was positioned above the center row of caps; and the third probe was approximately located above the last sample point on the tray. The vertical positions of these probes were made adjustable by attaching a bracket to the 1/8-inch tubing on the second tray and then attaching a single rod to this bracket. The rod was run

to the top of the column and through a compression fitting to the outside of the column. By loosening the compression fitting, the rod could be used to adjust the vertical position of the probes on the test tray.

Windows

The column was originally designed to have glass panels on the front side of each of the five trays. Thus the hydraulic action of the column could be observed when the column was in operation. Ashby[7] used Tygon tubing and partially-polymerized styrene to make a seal between the glass panels and the face of the column. Since it was planned to use ethylene dibromide, a very good solvent for many materials, in the present study, it was realized that a different type of material would have to be used to form a seal. Teflon was found to be resistant to the solvent power of ethylene dibromide. But the Teflon was not resilient enough to form a seal when used with the glass panels as originally designed. Therefore, a new design of the windows was made. In this design, a 3/8-inch thick, stainless steel, plate was used to make a frame which would provide a flat surface to make a seal at the face of the column. One of the carbon steel window frames used by Ashby[7] and Warzel[92] was welded to one face of the stainless steel frame. The open area in the stainless steel frame was smaller than that in the former frame. Thus when the carbon steel frame was welded to the stainless steel frame, the difference in the areas of the two openings was represented by a small rectangular annulus around the inside of the carbon steel frame. Teflon tape and Epoxy resin (Shell No. 828) was used to form a seal between

a piece of 2-ply safety glass and the surface of the small rectangular annulus. The whole assembly was bolted to the face of the column. The seal between the stainless steel frame and the finished (ground) surface of the column face was also made by use of Teflon tape and Epoxy resin (Shell No. 828). A good seal was obtained in most cases by first painting the Teflon tape and the areas of contact on the column and the frame with Epoxy resin. The window was then put in place on the column and bolt pressure was used to distribute the resin smoothly. After the resin hardened, the tray was ready for operation.

Windows of the type described above were used on the test tray and the first tray above the test tray. Stainless steel panels, 1/8-inch thick, were used on the other trays of the column. The panels were of the same over-all dimensions as the carbon steel frames used by Ashby and Warzel. In fact, these frames were used to back-up the thin stainless-steel panel and the two pieces were bolted to the column. The seal between the stainless steel panel and the face of the column was also made by use of Teflon tape and Epoxy resin.

Arrangements for Liquid Sampling, Hydrostatic Head and Pressure Drop Measurement

The hydrostatic head was measured at four points on the tray floor by use of the liquid sampling points shown in Figure 4. In Figure 4A a schematic diagram is presented for the arrangement of the valves and tees on the outside of the column which made it possible to use these points for obtaining liquid samples and for measuring the hydrostatic head. The liquid line from each of the four points on the tray were connected to a tee fitting (No. 1) on the outside of the

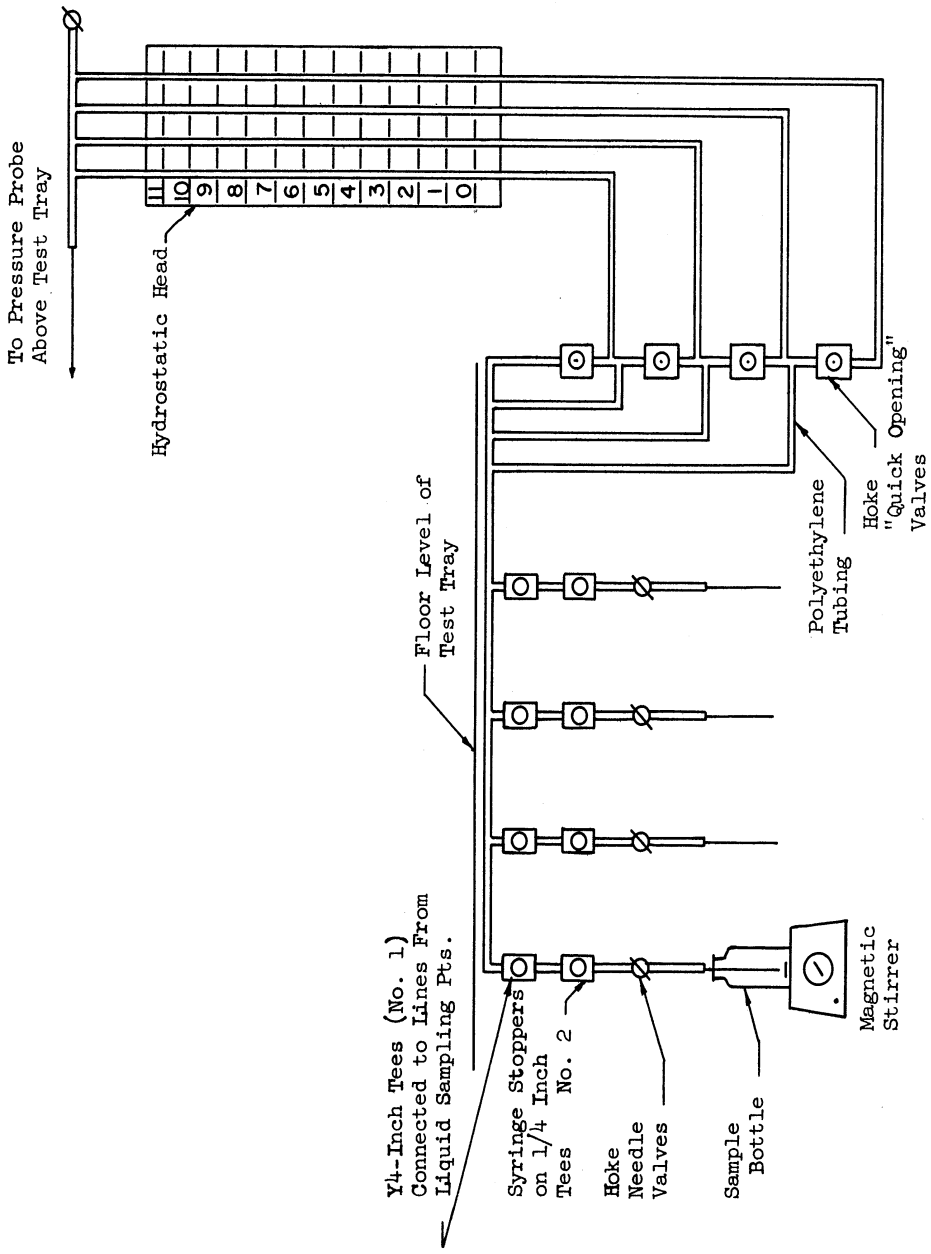

Figure 4A. Apparatus Used to Obtain Liquid Samples and Measure Hydrostatic-head at Four Points on Tray Floor.

column. One side of each tee fitting (No. 1) was used to connect a line to tee fitting, No. 2, and other side of No. 1 was used to connect a line to one side of a Hoke, quick-opening valve. The other side of the Hoke valve was connected to glass tubing mounted on a backboard. The glass tubing was mounted in a vertical position and the top of each tube was connected to a pressure probe above the test tray. A scale in 0.2-inch graduations on the backboard was used to measure the hydrostatic head above each point on the tray. The zero point of the scale on the backboard was carefully adjusted to the tray floor level. Therefore, the liquid level in each glass tube as indicated by the scale was equal to the hydrostatic head at the particular point on the test tray.

The No. 2 tee fittings were used to obtain liquid samples by use of a hypodermic syringe or a small Hoke valve. A syringe stopper over one side of the fitting was used to obtain the samples by use of a hypodermic syringe. The other side of the tee fitting was connected to a Hoke needle valve. A 1/4-inch line from the needle valve was fitted to a piece of 1/4-inch, stainless-steel, tubing. This piece of tubing was ground on one end to form a sharp edge which could be used to puncture the syringe stopper in the sample bottles. Therefore, the tubing could be used to obtain liquid samples by first inserting it into the sample bottle and then closing the quick-opening valve in the line to the glass tubing and opening the small needle valve.

The pressure above the test tray was determined by use of a 1/4-inch probe connected to a 30-inch mercury-filled manometer. The pressure drop across the test plate was measured by a water-filled manometer.

Gas Recirculation - Vaporization Studies

The flow diagrams for the vaporization and absorption studies are shown schematically in Figures 5A and 6A, respectively. In the vaporization studies, the gas plus the cyclohexanol or ethylene dibromide vapors and entrained droplets passed to an entrainment separator where part of the entrained droplets were removed. From the entrainment separator the gas and vapors plus any entrainment remaining in the gas flowed to blower #1. On the suction side of the blower nitrogen was added to make up for leakage and maintain the pressure in the system. Also an orifice plate with one, two, three, or five, 5/8-inch holes was used in a pipe flange on the suction side of the blower to maintain a positive pressure in the test column. At low flow rates the orifice plate with one hole was used but as the flow rate was increased the number of holes in the orifice plate was increased so that the capacity of the blower was not decreased and so that the pressure in the test column did not become greater than that considered safe for the glass windows. After leaving blower #1 the gas entered the bottom of a 12-inch diameter, 4-plate, sieve tray column where it contacted either cyclohexanol or ethylene dibromide, the liquid being used at the time. The liquid in the sieve tray column was maintained at a temperature approaching that of the tap water in the Chemical and Metallurgical Engineering Departmental Laboratories. Thus part of the vapors in the gas was condensed and the gas returned to the test tray with the vapor content appreciably reduced. Before returning to the test tray, the gas was metered by use of a Fischer and Porter Flowrator (Size 12, Tube No. 12-LL25, Serial No. D8-1609, Figure No. 26P-E, Chemical and

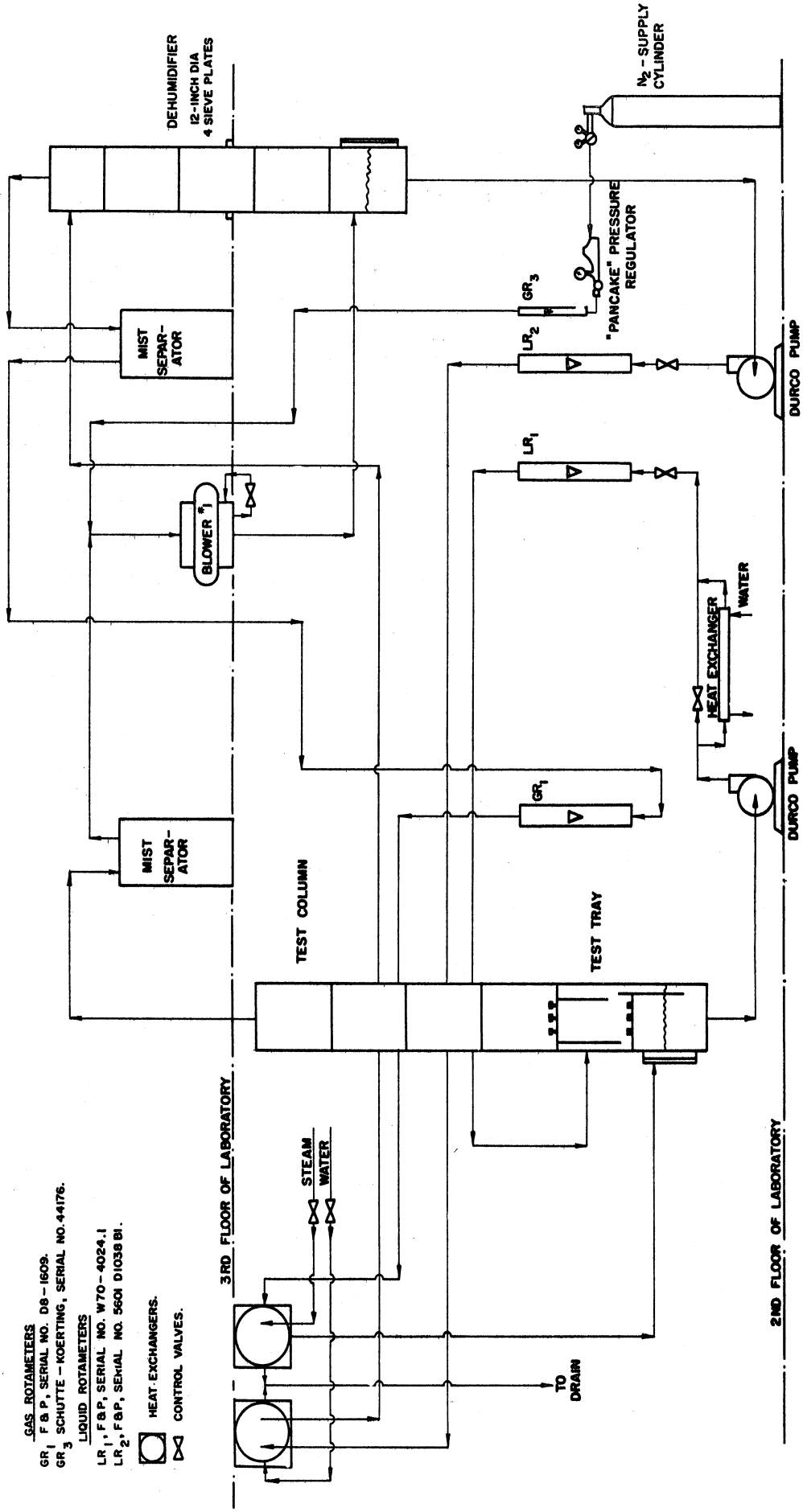

Figure 5-A. Flow Diagram for Vaporization Studies

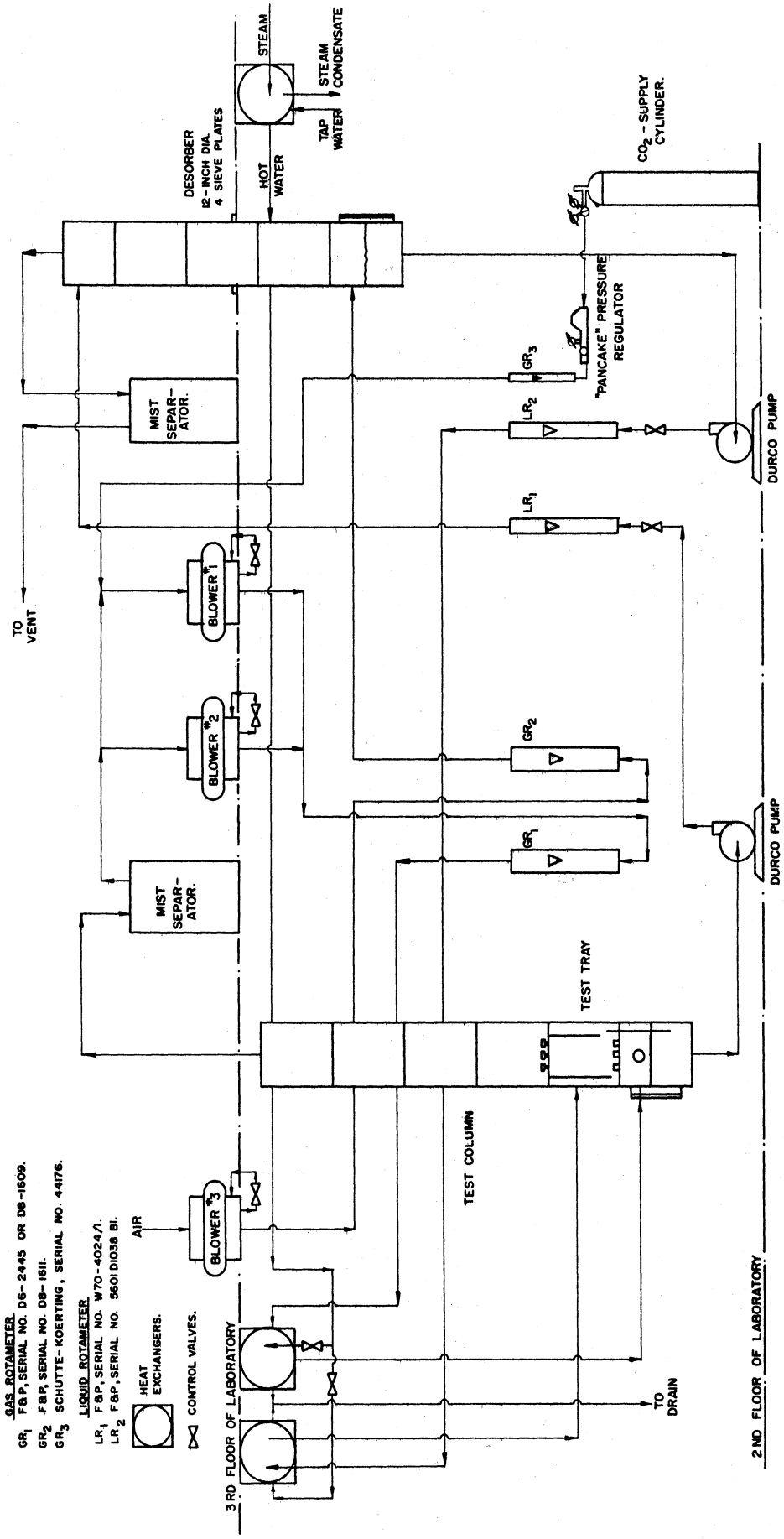

Figure 6-A. Flow Diagram for Absorption Studies

Metallurgical Engineering Department No. C17-200). Scale graduations were in increments of 2 cubic feet per minute and the tube was calibrated by the manufacturer from 0 to 200 cubic feet per minute for a gas of 0.877 gravity at 14.7 psia and 60°F. Warzel[92] checked the calibration of this flowrator and found the scale calibration to be sufficiently accurate for this type of study.

In order to maintain constant conditions at the test tray, an 8-inch diameter Ross heat exchanger (Type "SSCF", No. 804) was used to heat the dehumidified gas after being metered. The heat in the exchanger was supplied by condensing steam at atmospheric pressure.

Liquid Recirculation - Vaporization Studies

Two separate liquid recirculating streams were used in the vaporization studies. These were: (1) The liquid recirculated to the test tray and (2) the liquid recirculated to the dehumidifier. The liquid left the test column at the bottom and was recirculated by a centrifugal pump (Model 40, Series WS7RD-84 Durcopump, with 7-1/2 inch open impeller and mechanical seal, Serial No. DU-3151/52). This mechanical seal is manufactured by the Durametallic Corporation, Kalamazoo, Michigan. Between the pump and the test tray, the liquid was metered by use of a Fischer and Porter Flowrator (Size 8, Series 700, Serial No. W70-4024/1, Tube No. B9-27-10/70-G and Float No. BSVT-93). A portion of the liquid from the pump was by-passed to a small heat exchanger where heat was removed by cooling water. Considerable heat was gained by the liquid in the pump. This was especially true for the cyclohexanol at a high viscosity, i.e., low temperature. Thus,

the small heat exchanger was used to aid in the maintenance of adiabatic conditions on the test tray.

The liquid to the dehumidifier was also circulated by a Durco centrifugal pump equipped with a mechanical seal. A Ross heat exchanger similar to that used in the gas recirculation system was used to remove heat from the liquid and maintain the lower temperature in the dehumidifier.

Gas Recirculation - Absorption Studies

The gas recirculation system in the absorption studies was somewhat simpler than in the case of the vaporization studies. The mixture of carbon dioxide, air, cyclohexanol vapors and cyclohexanol entrained droplets flowed from the test column to the entrainment separator and then to either one or two blowers. When two blowers were used in parallel to increase the range of gas velocity at the test tray, part of the gas from the entrainment separator flowed to Blower #1 and the remainder to Blower #2. Orifice plates in a pipe flange on the suction side of each blower were used to regulate the level of pressure in the test column. Carbon dioxide gas was added to the system on the suction side of Blower #1. The rate of carbon dioxide fed to the system was dictated by the absorption rate on the test tray and by the leakage rate at the pressure in the system. The addition of carbon dioxide was controlled by a "pancake" pressure regulator which is distributed by the Mathieson Company, Joliet, Illinois.

After being compressed at the blowers, the gas was metered. One of two rotameters was used to meter the gas: (1) When the absorption studies were being conducted in the low range of velocity a Fischer

and Porter Flowrator, Size 12, Tube No. 12-LL25, Serial No. D8-1609, Figure No. 26P-E, Chemical and Metallurgical Engineering Department No. C17-200, was used and (2) For the high range of velocity, a Fischer and Porter Flowrator, Size 12, Tube No. 12LL-25, Serial No. D6-2445, Figure No. 26P-E, Chemical and Metallurgical Engineering Department No. C17-235, with a type 347 stainless steel float, No. D8-1617, was used. The latter rotameter was calibrated by use of a Roots-connersville rotary meter using a natural gas at the "J" Station of the Michigan Consolidated Gas Company, Detroit, Michigan. The calibration data are presented in Table IID in Appendix D.

The gas mixture passing through the flowrator was in most cases at a higher temperature than the temperature desired at the test tray. This is because of the heat of compression and the heat gained from the blowers which usually were hot to the "touch" when running. Consequently, the gas stream had to be cooled in the Ross heat exchanger used in the vaporization studies. The cooling water in this case was tap water which had been heated by steam in an auxiliary heat exchanger. Water from the same source was used to maintain the temperature of the liquid to the test tray.

Liquid Recirculation - Absorption Studies

In the absorption studies, one of the centrifugal pumps was used to feed cyclohexanol to the test column and the other one was used to pump the liquid from the bottom of the test column to the top of the desorber (the dehumidifier in the vaporization studies). In the desorber the liquid was contacted with air from the laboratory and the

carbon dioxide was desorbed in order to maintain a low concentration in the feed to the test tray. Before returning to the test tray, the liquid was metered in a Fischer and Porter Flowrator (Size 8, Series No. 700, Serial No. 5601D1038B1, Tube No. B9-27-10/70-G and Float No. BSVT-93). The calibration data for this meter are given in Table IIID, Appendix D. After being metered, the liquid flowed through a Ross heat exchanger where the liquid was either heated or cooled before returning to the test tray.

APPENDIX B

LABORATORY TECHNIQUES

Vaporization Studies

The two factors which were important in obtaining reproducible and accurate data in the vaporization studies were as follows: (1) Adjusting the temperature of the gas and liquid at the test tray to adiabatic conditions and (2) obtaining representative samples of the gas entering and leaving the tray.

Adiabatic Conditions

Theoretically, adiabatic conditions are obtained by setting the inlet gas temperature at the value desired and then controlling the heat added to, or removed from, the liquid so that the temperature of liquid entering the tray is equal to the temperature of the liquid leaving the tray. When the temperature of the liquid ceases to change as it flows across the tray, adiabatic conditions have been established. This is essentially the procedure used in the present studies. However, in the present case the liquid temperature, i.e., the adiabatic saturation temperature of the gas, was the known factor and the gas temperature was adjusted to the point where the liquid temperature did not change significantly as it flowed across the tray. In order to eliminate the time required to search for the adiabatic conditions by trial and error adjustment of the temperatures at the test tray, humidity charts for cyclohexanol and ethylene dibromide in nitrogen were prepared. These charts are presented in Figures 1B and 2B. The following equations were used in the preparation of these charts,

$$T = (\mathcal{H}_{as} - \mathcal{H})\lambda_{T_{as}} + T_{as} \qquad (1B)$$

$$\mathcal{H} = \mathcal{H}_{\omega} - \frac{h_G}{k_G M_G P \lambda_{T_w}} (T - T_w) \qquad (2B)$$

$$\frac{h_G}{k_G M_G P} = C_p \left(\frac{\mu_G \rho_G D_G}{C_p \mu_G / k_q} \right)^{2/3} \qquad (3B)$$

where

$\mathcal{H}$ = humidity of the gas, lb vapor/lb dry nitrogen

$\mathcal{H}_{as}$ = humidity of saturated gas at T_{as}, lb vapor/lb dry nitrogen

$\mathcal{H}_{w}$ = saturated humidity at the wet bulb temperature T_w.

T_{as} = adiabatic saturation temperature, °F

T_w = wet bulb temperature, °F

T = gas temperature, °F

$\lambda_{T_{as}}$ = latent heat of vaporization at the temperature T_{as}, BTU/lb

λ_{T_w} = latent heat of vaporization at the temperature T_w, BTU/lb

h_G = heat transfer coefficient, BTU/hr/°F/ft^2

k_G = mass transfer coefficient, lb moles/hr/ft^2/atm.

P = total pressure, atm.

M_G = molecular weight of gas, lb/lb mole

C_p = specific heat of gas, BTU/lb/mole/°F

S = specific humid heat capacity of the gas, BTU/lb dry gas/°F.

$\mu_G/\rho_G D_G$ = Schmidt Number

$C_p \mu_G / k_q$ = Prandtl Number

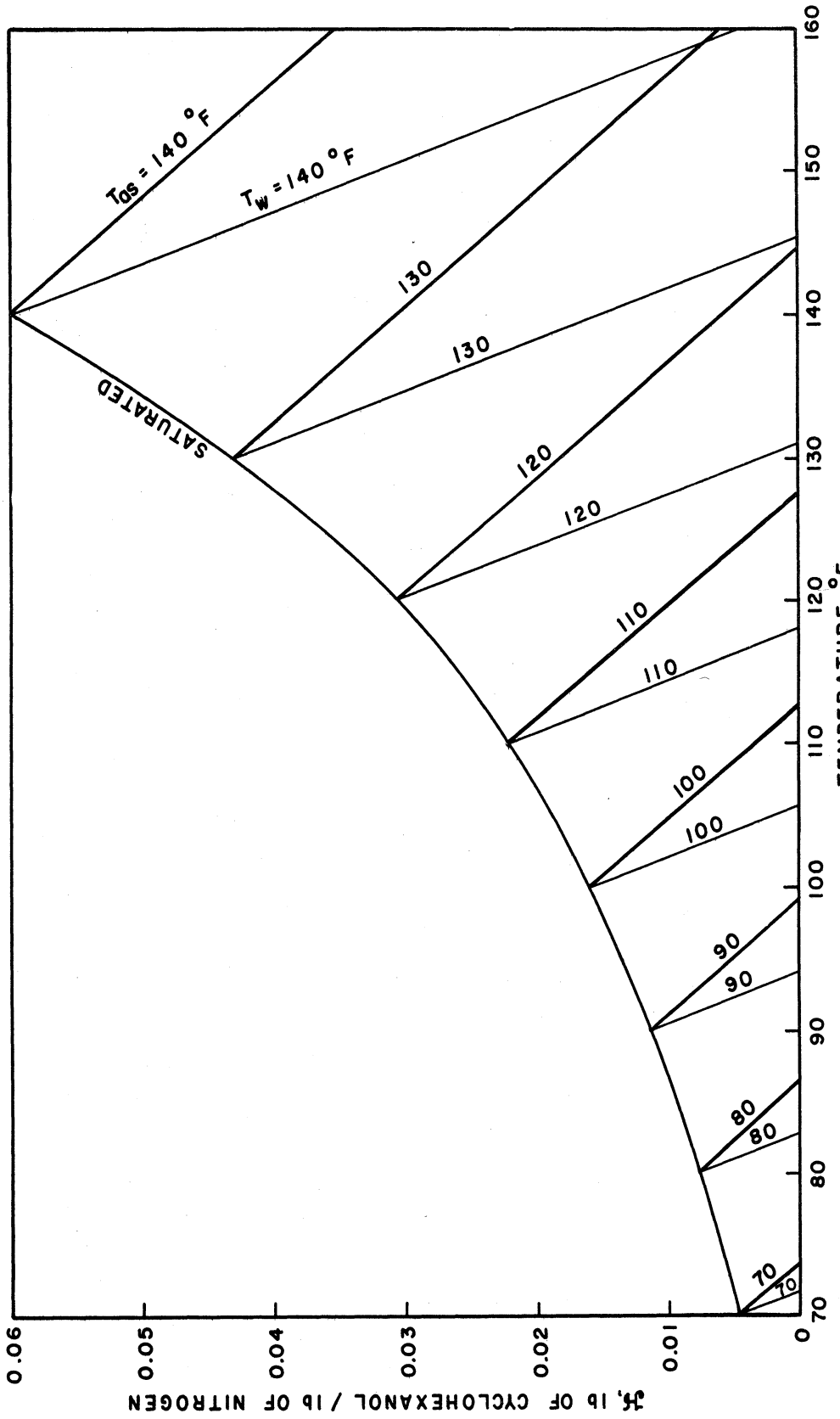

Figure 1-B. Humidity Chart for the Nitrogen-Cyclohexanol System Prepared by C.H. Wu

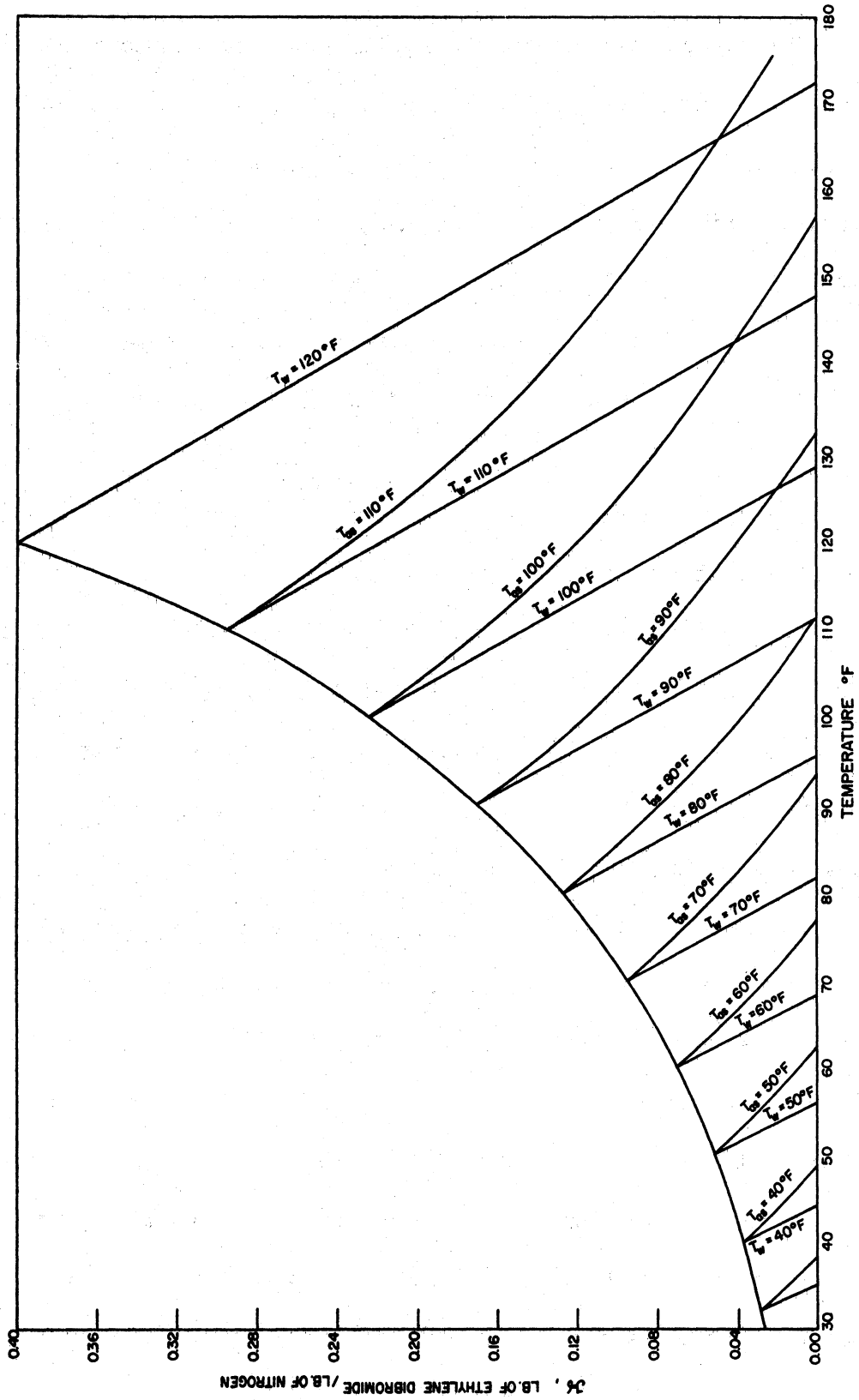

Figure 2-B. Humidity Chart for the Nitrogen - Ethylene Dibromide System
Prepared by C. H. Wu

The vapor pressure data for cyclohexanol and ethylene dibromide which were used in the preparation of these charts are presented in Tables IVE and VE. The term, $h_G/k_G M_G P$, was estimated by Equation (3B) wherein the physical properties, k_q, C_p, ρ_G, and λ were taken from the literature and D_G was calculated using the equation developed by Wilke and Lee[97]. For cyclohexanol in nitrogen, the term, $h_G/k_G M_G P$, was estimated to be 0.540, and for ethylene dibromide in nitrogen, $h_G/k_G M_G P$, was found to be 0.505.

By knowing the liquid temperature desired and then estimating the inlet gas humidity, the inlet gas temperature was determined by use of the adiabatic cooling curves in Figure 1B or Figure 2B. Usually the inlet humidity of the gas was estimated from a preceding run. The adiabatic conditions estimated by use of the humidity charts were in most cases very good estimates judging from the difference between the inlet and outlet liquid temperatures. Occasionally these temperatures differed by as much as 0.3°C but this difference could be decreased by changing the inlet gas temperature. In the majority of the runs made, the difference between the inlet and outlet liquid temperatures did not differ by more than 0.1°C during sampling. There were exceptions however where this difference was as high as 0.2°C. Some difficulty was experienced in obtaining adiabatic conditions at high gas rates but this was thought to be due to inadequate controls on the equipment. The liquid temperatures were measured by calibrated mercury-in-glass thermometers with 0.1°C scale graduations from -1 to 51°C. The gas temperature below the tray was measured by a calibrated mercury-in-glass thermometer with 0.1°C scale graduations from -1 to 101°C.

Sampling

The amount of organic vapor in the inlet and outlet gas was determined by withdrawing the samples from the column through heated sample lines into U-tubes filled with glass beads and immersed in ice baths. Three U-tubes in series were used for each sample. Because both cyclohexanol and ethylene dibromide have freezing points above 0°C, the first U-tube in the series of three was immersed in a chilled water bath. If too much ice was added to this bath a large fraction of the total vapor in the gas sample was condensed in this U-tube and the liquid (cyclohexanol or ethylene dibromide) would freeze and block the flow of gas from the column. The second and third U-tubes in the series were immersed in "dry" ice-acetone baths. In these tubes the vapors were condensed and frozen. Thus the vapor content of the gas leaving the last tube approached the concentration corresponding to saturation at the vapor pressure of cyclohexanol or ethylene dibromide crystals. In all runs, less than 0.5 percent of the total vapor in the samples was collected in the third U-tube and in some cases, particularly for the outlet gas samples, this was as low as 0.1 percent. These results were thought to be sufficient evidence that more than three U-tubes in series were not necessary for sufficient accuracy in the determination of the vapor in the gas samples.

The gas after leaving the U-tubes was saturated with water vapor in a bubbler and then metered by use of wet-test meters. These meters were calibrated in the CM-16 Laboratory in the Chemical and Metallurgical Engineering Department. The calibration data are given in Table IV-D.

The weight of vapor condensed in the U-tubes was determined by weighing the U-tubes before and after sampling. A Christian-Becker projectomatic analytical balance and class S, stainless steel, weights were used to weigh the tubes before and after sampling. Ashby checked the weights against weights which had been calibrated by the Bureau of Standards and found that they were accurate within $\pm$ 0.2mg.

In preparing the U-tubes for the samples, air was passed through the tubes until the cyclohexanol or ethylene dibromide from the preceding samples was completely evaporated. The glass-ground, tapered, stopcocks were then cleaned and a low-temperature stopcock grease was used to seal the tubes. The external surface of each tube was then cleaned by wiping with clean cloths. The tubes were ready for samples after weighing.

Absorption Studies

In the vaporization studies, the mass transfer or plate efficiency was determined by analyzing the composition of the gas entering and leaving the test tray. There are two principle reasons why this experimental technique could not be used for the study of carbon-dioxide absorption by cyclohexanol. These are: (1) The change in the gas composition across the test tray was not great enough to be measured accurately by available methods, and (2) The concentration of carbon dioxide in the liquid varied along the length of the tray. Therefore, liquid samples on the test tray were required to determine an average concentration to be used in the mathematical relationship between overall plate efficiency and point efficiency. Even if it had been possible

to measure the change in gas composition across the test tray, the liquid samples on the tray would have been required in addition to calculate the point efficiency using the measured over-all plate efficiency. Therefore, for each run the following samples were obtained: (1) A sample of the gas above the tray which could be used to determine the equilibrium concentration at the temperature and pressure on the test tray, (2) Samples of the liquid in the entrance and exit downcomers, and (3) Samples of the liquid at four different points on the floor of the test tray.

Test Conditions

In order to eliminate the possibility of cooling or heating the gas-liquid interface, the temperature of the gas entering the tray was adjusted so that adiabatic conditions existed. Thus the equilibrium liquid concentration was determined by the bulk liquid temperature. The gas was recirculated to the test tray after being compressed in the blower and heated or cooled in an exchanger. Since the gas was not dehumidified except for some condensation in the circuit, its cyclohexanol vapor content was approximately equal to the saturation composition corresponding to the liquid temperature on the test tray. Therefore, the gas and liquid temperatures at the test tray were approximately equal. The difference in liquid temperature at the entrance and exit of the tray were never greater than 0.2°C when samples were being obtained.

Sampling

The liquid samples taken during the studies at 3-1/2 inch weir height were obtained by use of a calibrated hypodermic syringe. The lines from each sample point on the tray was fitted with a syringe stopper. A liquid sample was obtained as follows: The hypodermic needle was pushed through the syringe stopper and the plunger of the syringe was slowly withdrawn to fill the syringe. If the vacuum created by the withdrawal of the plunger became too great the liquid began to degas or air leaked into the line through the hole in the stopper. Therefore, the rate at which the sample could be obtained was necessarily slow in order to avoid loss of carbon dioxide in the sample or contamination by air leakage. The sample line and the syringe were flushed by liquid from each point by withdrawing 50 to 100 cc of liquid and rejecting it. A small volume of air from the needle was usually trapped in the syringe as sampling began. This was rejected as the liquid volume in the syringe was being adjusted to the desired volume.

Samples taken from the tray floor by use of the syringe were completely devoid of entrained gas bubbles. A few bubbles were obtained in the samples taken in the inlet and outlet downcomers and in the samples from the froth. These were rejected as the liquid volume in the syringe was adjusted.

The use of hypodermic syringe to obtain liquid samples proved too time consuming. Also, a health hazard was created by skin contact with the cyclohexanol and by breathing the cyclohexanol vapors. Therefore, arrangements were made so that samples could be taken through

needle valves directly into the sample bottles. This arrangement is shown in Figure 4A. The volume of the liquid sample was determined by weighing the sample bottle on a 3000 gram precision balance before and after sampling. A six-inch piece of 1/4-inch, stainless steel, tubing attached to the polyethylene line from each needle valve was pushed through the syringe stopper in the top of the sample bottle. The 1/4-inch tubing was long enough to reach the bottom of the sample bottle so that the tip could be immersed in the barium hydroxide solution. The sample bottle contained a magnetic stirring bar so that a magnetic stirrer could be used to mix the cyclohexanol with the barium hydroxide solution as the sample was being withdrawn. A blank sample was used to indicate the approximate sample volume desired. In order to compare this method of sampling with the method using the hypodermic syringe, each method was used to take consecutive samples from the same sample point during several runs. The concentration of carbon dioxide in these samples are compared in Table I-B. With exception of the samples at a concentration of about 0.5×10^{-5} gm-mol/cc, the concentrations in the samples taken by the two methods agreed within ± 5 percent.

The gas sample from above the test tray was obtained as follows: A 250-millimeter gas sample bulb with stopcocks on both ends was first evacuated to less than 0.2 inches of mercury. This bulb was then attached to the sample line from the test tray. An ice trap in the line was used to remove cyclohexanol vapors. Before the liquid sampling was started, flushing of the gas sample bulb was started by first opening the stopcock on the end of the bulb nearest to the connection to the sample line and then opening the stopcock on the other end.

The bulb was flushed during the time that liquid samples were being taken. This was usually 15 to 20 minutes.

TABLE I-B

COMPARISON OF SAMPLING METHODS

Sample Taken by Syringe	Sample Taken Through Valve
Carbon Dioxide Conc., gm-mol/cc x 10^5	
0.530	0.482
0.982	1.030
1.475	1.425
1.560	1.552
1.650	1.700
2.105	2.080
2.130	2.125
2.245	2.250

Preparation of Sample Bottles

The sample bottles used to receive the liquid samples from the test tray were 8-ounce Boston round bottles made by the Libby-Owens Glass Company. Syringe stoppers were used to seal the top of each bottle. In preparing the bottles for samples, the procedure was as follows:

(1) The bottles were flushed with nitrogen and then sealed with syringe stoppers.

(2) 50 ml. of 0.1N barium hydroxide was added to each

bottle directly from a 50 ml. calibrated, Kimble EXAX, burette.

(3) When the samples were taken by use of needle valves in the sample lines, a stirring bar was added to each bottle.

(4) The bottles were finally weighed on a 3000-gram analytical balance.

Analytical Technique

A 0.1N barium hydroxide solution was used to precipitate the carbon dioxide in barium carbonate when the liquid samples were added to the sample bottles. An excess of barium hydroxide was contained in each bottle. The amount of carbon dioxide in the liquid samples was determined by titration of the excess barium hydroxide with 0.1N hydrochloric acid. The volume of 0.1N barium hydroxide added to each sample bottle was 50 ml. in all cases. In order to minimize the errors which were inherent in the sampling methods and in the titration, the size of the liquid sample was as large as could be conveniently handled in the 8-ounce bottles. Usually the sample size was near 100 cc.

Precautions were taken to avoid contact of the samples with air. This was accomplished by titrating the excess barium hydroxide directly in the sample bottles. The tip of the acid burette (Kimble NORMAX No. 8275 or Kimble EXAX) was pushed through the syringe stopper and the acid was added as the contents of the bottle were agitated by use of a magnetic stirring bar and a magnetic stirrer. A 10 ml. sample of saturated barium chloride was added to each sample to suppress the solubility of the barium carbonate when the samples were titrated.

Cyclohexanol is not miscible with water. Therefore, the sample bottles contained two phases. If these two phases were mixed by the magnetic stirrer, a pink opulescent mixture was formed when the indicator, phenolphthalein, was added. As the 0.1N hydrochloric acid was added, the mixture became white. When the stirrer was stopped, the two phases separated but the aqueous phase was still pink in cases where the end point had not been reached or passed. The titration was continued from this point by adding two to three drops of acid solution, stirring the contents for approximately thirty seconds, and then allowing the two phases to separate. This procedure was continued until the pink color of the aqueous phase disappeared.

In order to check the accuracy of the titrometric method, synthetic samples were prepared by accurately weighing samples of sodium carbonate which were then added to a sample bottle containing 50 ml. of 0.1N barium hydroxide and 100 ml. of cyclohexanol which had been degassed by refluxing under a vacuum. The sodium carbonate reacted with the barium hydroxide according to the following equation,

$$Na_2CO_3 + Ba(OH)_2 \rightarrow \underline{BaCO_3} + 2NaOH$$

Thus the contents of the bottle were identical to that of the samples from the test tray except for the presence of the sodium ions. The synthetic samples were titrated with 0.1N HCl and the milliequivalents of acid were compared with the milliequivalents of barium hydroxide added initially. The two values should have been equal if the titration method was perfect. The average of the differences between

the milliequivalents of barium hydroxide and acid for several samples was about 0.084 milliequivalents. This value represents about 1.8 percent of the milliequivalents of barium hydroxide added to the sample bottles originally. In an attempt to estimate the error in the determination of the milliequivalents of carbon dioxide in the samples from the test tray, it was assumed that the same percentage of error, 1.8, could be applied to the barium hydroxide in the samples before titration. The amount of barium hydroxide remaining varied depending on whether the sample was taken near the inlet or the outlet of the tray. Normally this variation was between 1.5 and 3.5 milliequivalents. Since the milliequivalents of barium hydroxide used in each sample bottle was about 5.0, the error in the milliequivalents of carbon dioxide varied between 0.027 and 0.063 or 0.77 and 4.2 percent, respectively. This error is significantly reduced when it is considered that the liquid sample size was 100 cc.

In concentration units of lb-mol/ft^3, an error of 0.063 milliequivalents in the carbon dioxide determination represents an absolute error of 1.96×10^{-5} lb-mol/ft^3 for a 100 cc liquid sample. This would be the absolute error for the sample at the tray inlet where the concentration of carbon dioxide was 30 to 40×10^{-5} lb-mol/ft^3. In other words, the error in the determination of the inlet sample concentration was of the order of 5-6 percent. For the outlet samples, the absolute error was of the order of 0.85×10^{-5} lb-mol/ft^3 or approximately 0.5 to 1.0 percent on the average. A more detailed evaluation of the experimental error for the absorption studies is presented in Appendix C.

APPENDIX C

ESTIMATE OF EXPERIMENTAL ERROR

Vaporization Studies

An accurate estimate of the absolute error in experimental data of the type obtained in these studies is almost impossible. However, it is important in the interpretation of the data to estimate the experimental error as well as possible. This is particularly important in experimental studies where the error may vary with the conditions or the materials used in the studies. Such is the case in the present investigation, i.e., the percent of error in the value of E_G or N_G may vary depending on the liquid and conditions used in the vaporization studies.

Ashby[7], who studied the vaporization of several liquids, has presented a summary of the types of errors to be expected and has estimated the percentage of error in N_G for each of these inaccuracies. Ashby concludes that the error in N_G can be considerable (20-30%) if the estimated errors for the individual sources of errors existed and were additive. The probability that the errors are additive and not partially compensating, is probably small.

Ashby divided the errors into the following three categories: (1) errors in the determination of the correct equilibrium composition for the gas on the test tray, (2) errors in the determination of the correct inlet and outlet compositions of the gas, and (3) miscellaneous errors. Since approximately the same technique was used in the present investigation, the foregoing categories are applicable. However, it should be realized that each of these categories includes several

types of error. These are the errors due to inaccuracies in calibration data, the errors in fundamental data such as physical properties, etc., and random errors which depend on the operator or observer as well as the technique used in taking the data and operating the equipment. The sources of possible errors in each of the factors, y, y_1, and y*, are listed in the following tables.

Possible Errors in the Gas Equilibrium Composition, y*

1. Measurement of the average bulk liquid temperature on the test tray.
2. Assumption that the surface temperature of the liquid was equal to its bulk temperature.
3. Vapor pressure data.
4. Influence of impurities on the vapor pressure of the liquid.
5. Measurement of the pressure above the test tray.

Possible Errors in the Inlet and Outlet Gas Compositions

1. Weighing of the U-tubes or drying tubes.
2. Correction for change in weight due to atmospheric changes in the balance room.
3. Failure to remove all vapor from the gas samples.
4. Inaccuracy of the wet test meters.

In order to show how the percentage of error in E_G and N_G may vary depending on the system being studied, Table IC has been prepared wherein one percent of error in y*, y_o, and y, was assumed. The following equations were used in the calculations of percentage

errors in E_G and N_G

$$dE_G = \frac{\partial E_G}{\partial y} dy + \frac{\partial E_G}{\partial y_1} dy_1 + \frac{\partial E_G}{\partial y^*} dy^* \qquad (1C)$$

where $$E_G = \frac{y - y_1}{y^* - y_1}$$

$$dE_G = \frac{1}{y^* - y_1} (dy - dy_1 + E_G\, dy_1 - E_G\, dy^*) \qquad (2C)$$

For the maximum error,

$$dE_G = \frac{1}{(y^* - y_1)} (y\epsilon + y_1\epsilon_1 + E_G y_1 \epsilon_1 + E_G y^* \epsilon^*) \qquad (3C)$$

where ϵ = fractional error

$$dN_G = \frac{dN_G}{dE_G} dE_G \qquad (4C)$$

where $$N_G = - \ln (1 - E_G) \qquad (5C)$$

$$dN_G = \frac{dE_G}{1 - E_G} \qquad (6C)$$

The results in Table IC indicate the variation of experimental error with the system studied and explains why the scatter or reproducibility of the data varied where the same technique was used for all systems. Actually to obtain the same reproducibility in the data for the several different systems, the technique should have been varied somewhat. It was necessary to do this in the case of cyclohexanol. In order to approach the reproducibility in E_G which Ashby had obtained in his studies, the volume of gas samples was increased to 2 cubic feet. Ashby took gas samples of 0.5 cubic feet or less. In the ethylene dibromide vaporization studies, good reproducibility of the data was obtained in most cases by taking gas samples of 1 cubic feet. On the basis of the results in Table IC the increase in the reproducibility

TABLE I-C

PERCENTAGE ERROR IN E_G AND N_G RESULTING FROM 1% ERRORS IN y^*, y_1, and y

System	% Error in E_G	% Error in N_G
He-Water*	4.1	13.0
Air-Water*	3.7	17.5
Freon 12-Water*	2.8	15.2
He-i C_4H_9OH*	3.7	9.5
N_2-i C_4H_9OH*	3.52	9.8
He-MIBK*	3.8	10.4
N_2-Cyclohexanol (E_G = 0.55)	6.6	10.2
N_2-$C_2H_4Br_2$(E_G = 0.55)	3.6	5.2

*System studied by Ashby[7].

of the efficiency data with increase in sample volume can be explained by the increase in the reproducibility of determining y and y_1. But why the reproducibility in y and y_1 increased as the sample volume increased is not known. It would seem that somewhere in the technique of taking the samples or weighing the samples a random error in the amount of condensate was introduced but was minimized by taking a larger sample volume. However, this would mean that the absolute value of the error did not increase with the volume of gas sample. This type of error could be introduced by improper handling or treatment of the condensate sample tubes. Another possibility is that there could have been fluctuations in the composition of the gas to or from the test tray. However, since the minimum sampling

time was 15 minutes, the frequency of the fluctuations would have had to be greater than 1 cycle per 15 minutes in order to show up in the analysis of the gas entering and leaving the test tray.

TABLE II-C

RELATIVE MAGNITUDE OF THE TERMS IN EQUATION 3C

Run No.	Gas Sample Volumes, Ft^3	y	y	y*	y*-y	E_G,%
H-14-A	1.0	0.002291	0.003115	0.00413	0.001839	44.93
H-14-B	1.0	0.002197	0.003153	0.00412	0.001923	49.71
H-12-A	1.0	0.00234	0.00282	0.00417	0.00183	26.20
H-12-B	1.0	0.002008	0.002813	0.00413	0.002122	37.90
H-13-A	1.0	0.002227	0.00309	0.004066	0.001839	46.90
H-13-B	1.0	0.002260	0.00280	0.00408	0.00182	29.60
H-15-A	1.0	0.002184	0.003440	0.00416	0.001976	63.60
H-17-A	1.0	0.001920	0.002756	0.00351	0.001590	52.60
H-17-B	1.0	0.00191	0.00293	0.003526	0.001616	63.10
H-21-A	1.0	0.001891	0.00314	0.003990	0.002099	59.50
H-21-B	1.0	0.001828	0.00319	0.00401	0.002182	62.50
H-11-A	1.0	0.002436	0.00315	0.00412	0.001684	42.30
H-11-B	1.0	0.002428	0.00300	0.00408	0.001652	34.50
H-10-A	1.0	0.002420	0.00312	0.00413	0.00171	41.00
H-10-B	1.0	0.00258	0.00334	0.00429	0.00171	44.40
H-37-A	2.0	0.001526	0.003095	0.004081	0.002555	61.41
H-37-B	2.0	0.001505	0.003057	0.004054	0.002549	60.89
H-38-A	2.0	0.001371	0.002960	0.004151	0.00278	57.16
H-38-B	2.0	0.001348	0.002931	0.004151	0.002803	56.47
H-39-A	2.0	0.001498	0.003207	0.004162	0.002664	64.15
H-39-B	2.0	0.001509	0.003197	0.004184	0.002675	63.10

*Runs A and B are duplicates.

Table II-C has been prepared to show the relative magnitude of the terms in Equation 3C and to show the improvement in reproducibility by increase of gas sample size.

Absorption Studies

The experimental errors in the efficiency and mass transfer data for the absorption studies are more uncertain than for similar data in the vaporization studies. This is primarily due to the uncertainties in method of obtaining liquid samples and the method of analyzing for the carbon dioxide in the samples. The possible sources of error in the efficiency are those associated with the concentrations, xo, xi and x* and are tabulated below.

Possible Sources of Error in the Liquid Concentrations, xo and xi

1. Obtaining samples of the liquid from the two-phase system. The factors involved here are: (a) Withdrawing liquid samples devoid of gas bubbles from the system and (b) Transferring the samples to the sample bottles without loss of the carbon dioxide in the samples.
2. Determination of the volume of liquid sample withdrawn from the tray.
3. Analysis of the amount of carbon dioxide in the liquid samples.

Possible Sources of Error in the Equilibrium Liquid Concentration, x*

1. Analysis of the amount of carbon dioxide in the gas sample from above the test tray.
2. Measurement of the pressure above the tray.
3. Measurement of the bulk liquid temperature.
4. The possibility that the gas-liquid interface can be cooled or heated and not necessarily equal to the bulk liquid temperature.
5. Solubility data for carbon dioxide in cyclohexanol.

In the experimental procedure, every effort was made to minimize each of the errors in the foregoing tabulation. In order to obtain an accurate estimate of the maximum possible error, a detailed study of each of the variables would be required. Therefore, for the present evaluation only the effect of the error in the analyses of carbon dioxide will be considered. The percentage error in the plate efficiency, E_{ML}, may be determined by use of Equation (12C) which was derived as follows:

$$dE_{ML} = \frac{\partial E_{ML}}{\partial x_o} dx_o + \frac{\partial E_{ML}}{\partial x_1} dx_1 + \frac{\partial E_{ML}}{\partial x^*} dx^* \qquad (7C)$$

$$\frac{\partial E_{ML}}{\partial x_o} = \frac{1}{x^* - x_1} \qquad (8C)$$

$$\frac{\partial E_{ML}}{\partial x_o} = -\frac{1}{x^* - x_1} + \frac{E_{ML}}{x^* - x_1} \qquad (9C)$$

$$\frac{\partial E_{ML}}{\partial x^*} = - \frac{(x_o - x_1)}{(x^* - x_1)^2} \tag{10C}$$

$$dE_{ML} = \frac{1}{(x^* - x_1)} (dx_o - dx_1) + \frac{E_{ML}}{(x^* - x_1)} (dx_1 - dx^*) \tag{11C}$$

In the section describing the laboratory techniques it was shown that the percentage error in the concentrations, x_o and x_1 differed significantly due to the variation of the error in the analysis with the amount of excess barium hydroxide in the sample. The error in x_o was one percent or less while the possible error in x_1 was determined to be as high as six percent. Equation (11C) has been rewritten in the following form

$$dE_{ML} = (E_{ML} - 1) \frac{dx_1}{(x^* - x_1)} + \frac{(dx_o - E_{ML} dx^*)}{(x^* - x_1)} \tag{12C}$$

$$= (E_{ML} - 1) \frac{x_1 \epsilon_{x_1}}{(x^* - x_1)} + \frac{(\epsilon_{x_o} - E_{ML} x^* \epsilon)}{(x^* - x_1)} \tag{13C}$$

$$\frac{dE_{ML}}{E_{ML}} = \frac{(E_{ML} - 1)}{E_{ML}} \frac{x_1 \epsilon_{x_1}}{(x^* - x_1)} + \frac{(x_o \epsilon_{x_o} - E_{ML} x^* \epsilon_{x^*})}{(x^* - x_1)} \tag{14C}$$

$$\text{Max. \% Error in } E_{ML} = \frac{100}{E_{ML}(x^* - x_1)} [x_o \epsilon_{x_o} + E_{ML} x^* \epsilon_{x^*} - x_1 \epsilon_{x_1} (E_{ML} - 1)] \tag{15C}$$

From the results in Table III-C, it is concluded that the maximum error in the plate efficiency, E_{ML}, may vary between a minimum of 1.5 and a maximum of 11 percent depending on the value of the plate efficiency and the equilibrium liquid concentration. In terms

of absolute error, the results in Table III-C indicate that the efficiency data are accurate within ± 2.5 efficiency percent.

TABLE III-C

VARIATION OF THE PERCENTAGE ERROR IN PLATE EFFICIENCY, E_{ML}, WITH THE FOLLOWING ERRORS IN x_o, x_1 AND x^*.

Absolute Error in x_o and $x^* = 2 \times 10^{-5}$

Absolute Error in $x_1 = 4 \times 10^{-5}$

$(x^* - x_1) \times 10^5$	E_{ML}	% Error in E_{ML}	Absolute Error in E_{ML}, %
200	0.50	5	2.5
300	0.50	3.3	1.65
400	0.50	2.5	1.25
200	0.75	3.0	2.25
300	0.75	2.0	1.50
400	0.75	1.5	1.12
200	0.25	11	2.75
300	0.25	7.4	1.85
400	0.25	5.5	1.37

APPENDIX D

CALIBRATION DATA

TABLE I-D

CALIBRATION DATA FOR ROTAMETER NO. D6-2445 WITH FLOAT NO. D8-1617, STAINLESS STEEL TYPE 347; CALIBRATION BY USING WATER (*)

Rotameter Scale Reading (**)	C_R (***)
42	2.567
57	2.032
64	1.891
72	1.751
94	1.542
112	1.422
117	1.404
130	1.337
147	1.273
155	1.245
165	1.220
187	1.182
186	1.179
202	1.158
219	1.147
232	1.125
264	1.104
264	1.075

(*) Calibration obtained as follows: The rate of water flowing through the rotameter at each rotameter reading was determined by collecting and weighing the water for a certain time interval. These data were corrected to volumetric rate of a gas with a gravity of 0.877 at 14.7 psia and 60°F by use of the rotameter equation, $W = C_R \sqrt{\rho(\rho_f - \rho)}$. Data obtained by Dennis Ward[91].

(**) Ft^3/min. of a gas with a gravity of 0.877 at 14.7 psia and 60°F.

(***) Actual flow rate, $ft^3/min = C_R$(rotameter scale reading)$\sqrt{\rho_1/\rho_2}$

where ρ_1 = density of a gas with a gravity of 0.877 at 14.7 psia and 60°F.

ρ_2 = density of gas being used.

TABLE II-D

CALIBRATION DATA FOR ROTAMETER NO. D6-2445 WITH FLOAT NO. D8-1617, STAINLESS STEEL TYPE 347; CALIBRATION BY ROTARY METER (*)

Rotameter Scale Reading (**)	C_R (***)
50	2.0814
60	1.8307
100	1.3744
100	1.3842
150	1.1414
150	1.1612
200	1.0490
200	1.0593
200	1.0626
250	1.0092
250	1.0076
250	1.0193
300	0.9625
300	0.9800
300	0.9900
350	0.9525
350	0.9510
350	0.9597
400	0.9394
400	0.9412
400	0.9347
400	0.9344

(*) Rotameter calibrated using natural gas and a Roots-Connersville rotary meter; Serial No. 59433, Size, 5 x 15; ft^3/revolution, 0.5144; ft^3/hr at 1" H_2O differential, 23,000; meter located at "J" Station, Michigan Consolidated Gas Co., Detroit, Michigan. Natural gas gravity, 0.618.

(**) Ft^3/min of a gas with a gravity of 0.877 at 14.7 psia and 60°F.

(***) Actual flow rate, $ft^3/min = C_R$ (rotameter scale reading) $\sqrt{\rho_1/\rho_2}$ where ρ_1 = density of a gas with a gravity of 0.877 at 14 psia and 60°F. ρ_2 = density of gas being used.

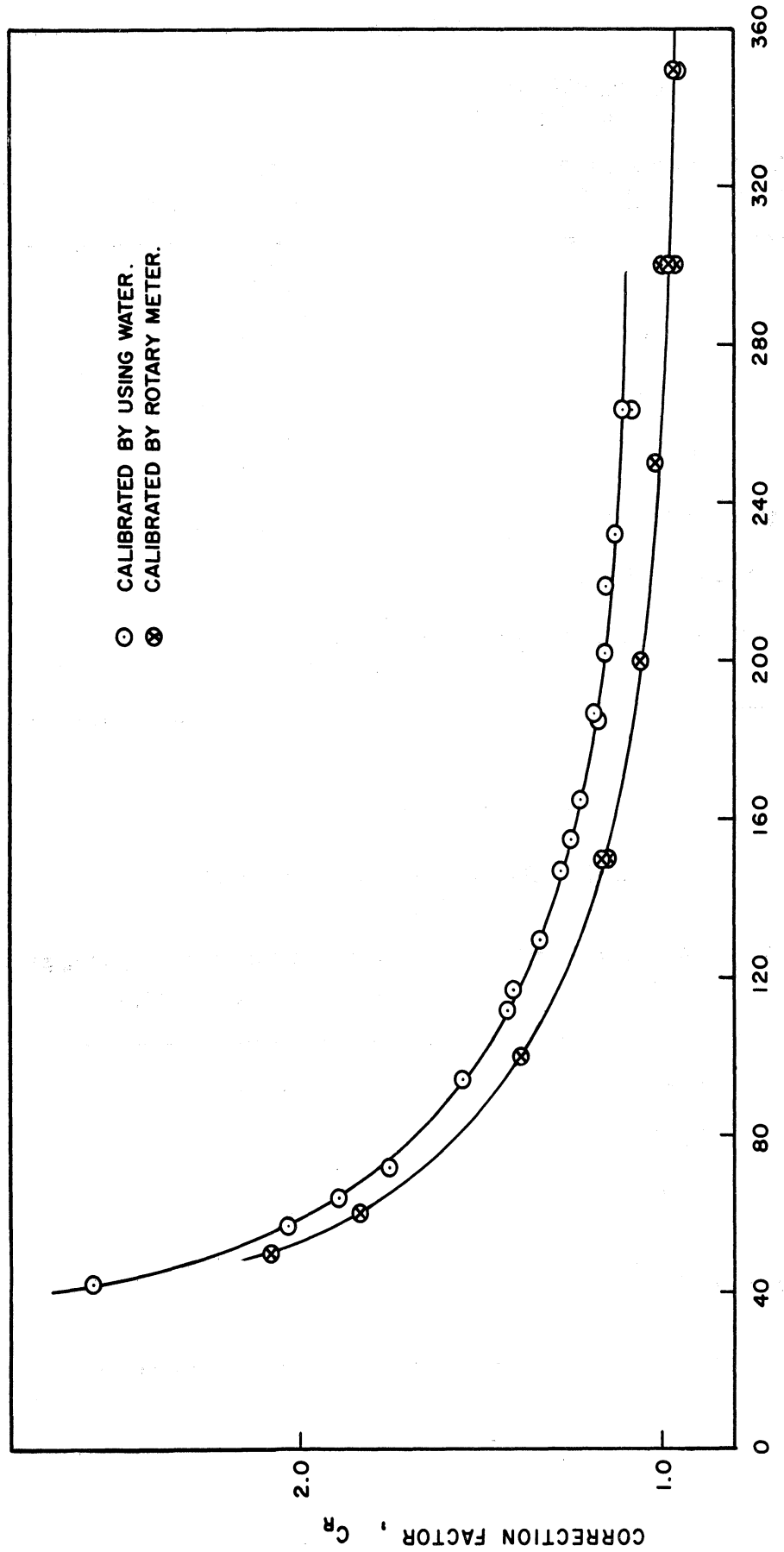

Figure 1-D. Calibration of Rotameter D6-2445

TABLE III-D

CALIBRATION DATA FOR ROTAMETER W70-4024/1;
CALIBRATION BY USING WATER (*)

Scale Reading (**)	Water Rate, $ft^3/sec.$
20	0.01422
40	0.02845
60	0.04265
80	0.05693

(*) Date obtained by Ashby[7]. Water temperature 54°F; float density, 7.85 gm/cc.

(**) Percent of maximum flow (32.0 gal/min).

TABLE IV-D

CALIBRATION DATA FOR WET-TEST METERS,
H9SS AND J5SS

Meter No.	Meter Correction Factor
H9SS	0.986
H9SS	0.9835*
J5SS	1.003

* Value used by Ashby[7].

APPENDIX E

PHYSICAL PROPERTIES

TABLE I-E

VISCOSITY OF CYCLOHEXANOL*

Temperature, °C.	Viscosity c_P
20.40	70.30
21.00	67.10
21.05	66.50
23.80	55.00
25.20	49.20
28.30	42.90
31.30	35.60
35.80	27.20
38.20	23.82
39.00	22.85
40.15	21.40
42.86	17.63
42.90	17.58
46.50	14.49

*Determined by use of ASTM Method D

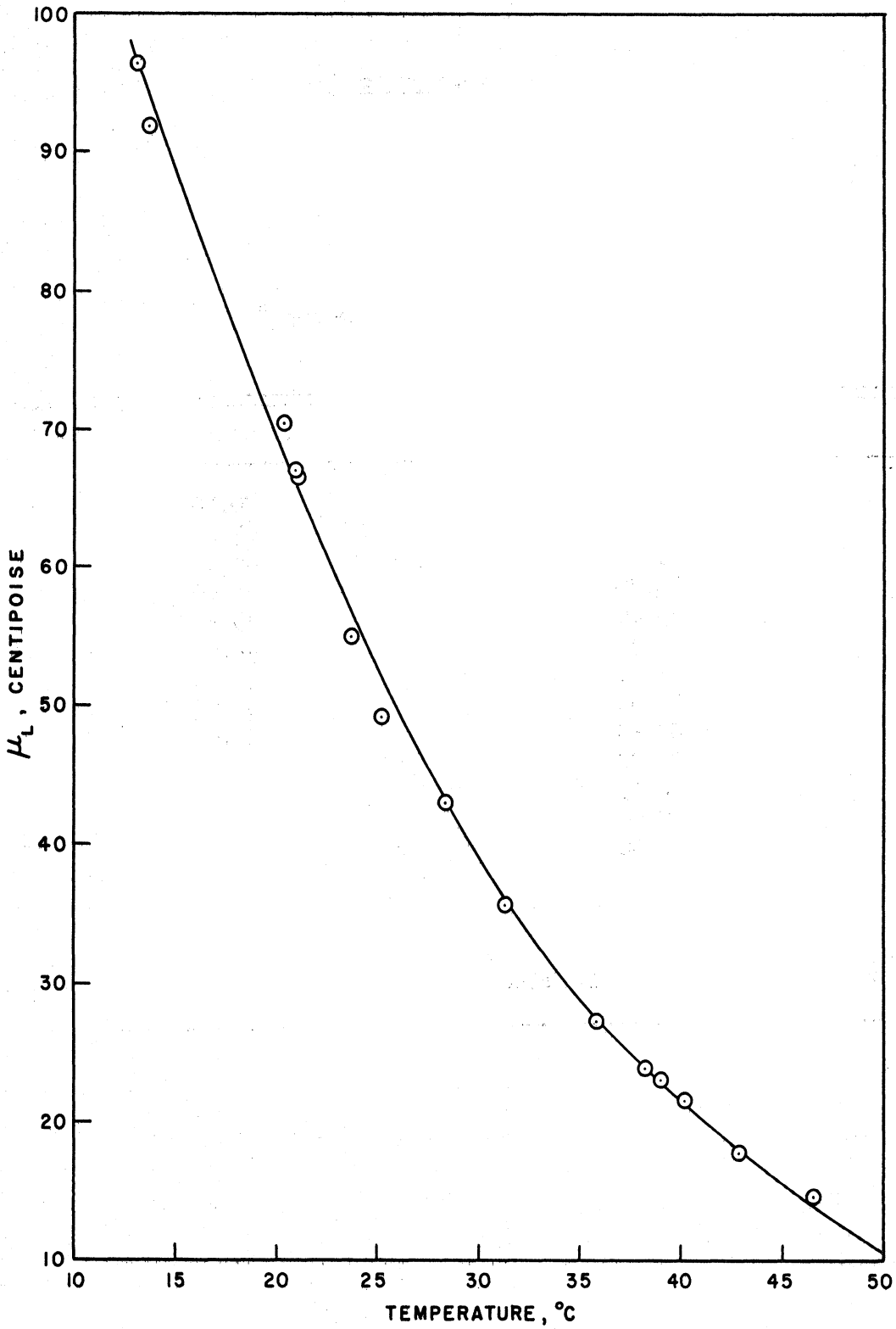

Figure 1-E. Viscosity of Cyclohexanol

TABLE II-E

DENSITY OF CYCLOHEXANOL*

Temperature, °C.	Density, gm/cc
46.1	0.9290
47.1	0.9284
46.6	0.9288
45.4	0.9299
42.0	0.9320
41.6	0.9320
41.1	0.9323
40.3	0.9331
39.7	0.9337
38.9	0.9339
37.7	0.9360
36.1	0.9362
35.9	0.9363
35.8	0.9366
35.4	0.9378
34.3	0.9391
30.8	0.9403
30.6	0.9405
30.0	0.9409
29.4	0.9413
28.9	0.9418
28.2	0.9421
27.1	0.9431
26.5	0.9435
25.1	0.9443
23.5	0.9459

*Determined by use of a hydrometer, checked by use of a pycnometer.

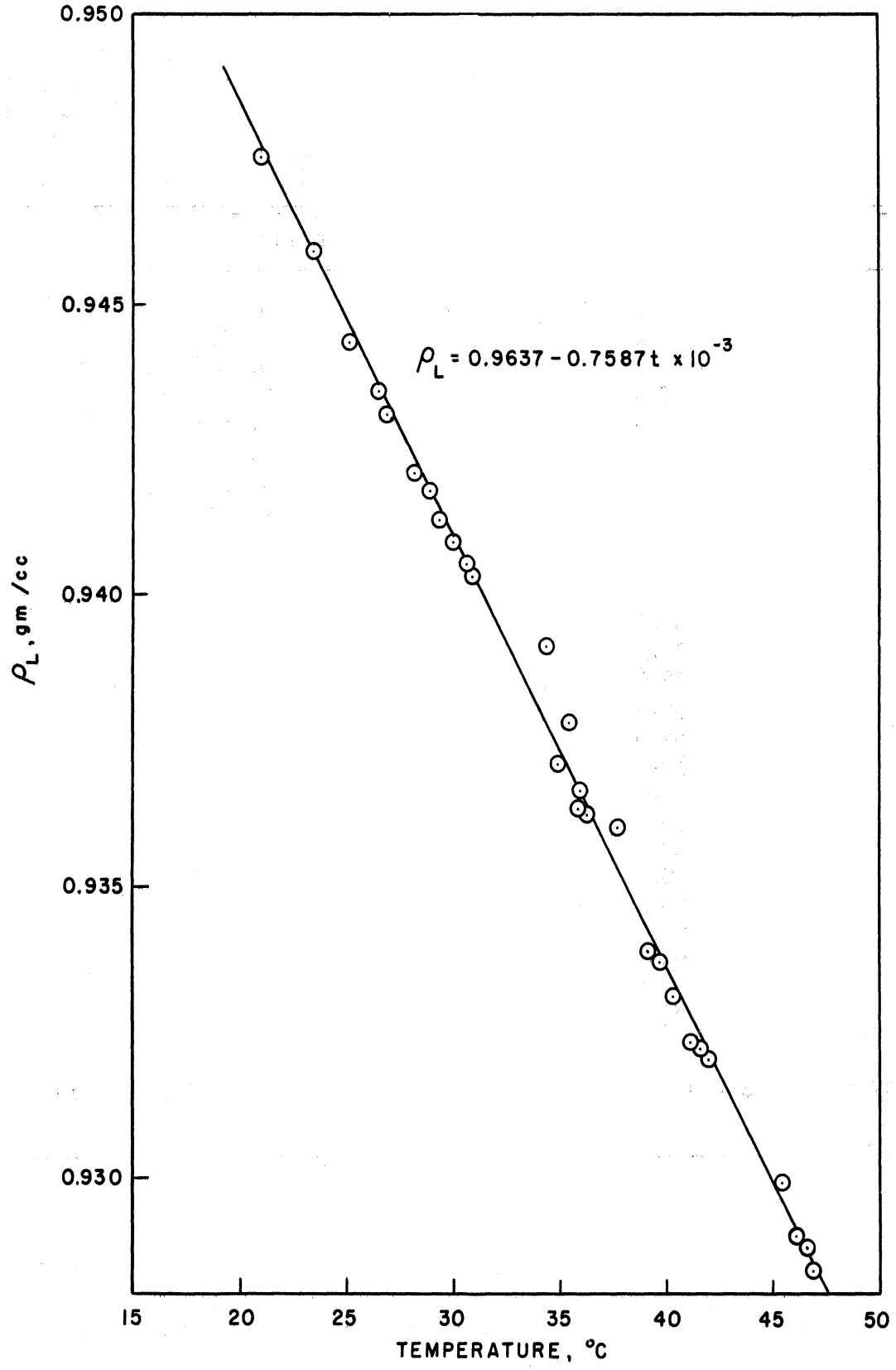

Figure 2-E. Density of Cyclohexanol

TABLE III-E

SOLUBILITY DATA FOR CARBON DIOXIDE IN CYCLOHEXANOL (55)

Temperature °C	$H \times 10^{-2}$ $\frac{\text{atm. ft}^3}{\text{lb. mol}}$	$H \times 10^{-2}$ $\frac{\text{atm}}{\text{mol fraction}}$
25.1	3.830	2.258
28.3	3.975	2.337
30.8	4.048	2.377
33.6	4.181	2.448
36.3	4.362	2.549
39.4	4.475	2.608
41.8	4.624	2.690
47.8	5.120	2.910

TABLE IV-E

VAPOR PRESSURE OF CYCLOHEXANOL (67)

Temperature °C	Vapor Pressure, mm Hg
21.0	1
44.0	5
56.0	10
68.8	20
83.0	40
91.8	60

TABLE V-E

VAPOR PRESSURE OF ETHYLENE DIBROMIDE (67)

Temperature °C	Vapor Pressure, mm Hg
20	10.14
25	13.18
30	16.98
35	21.68
40	27.48
45	34.59
50	43.25

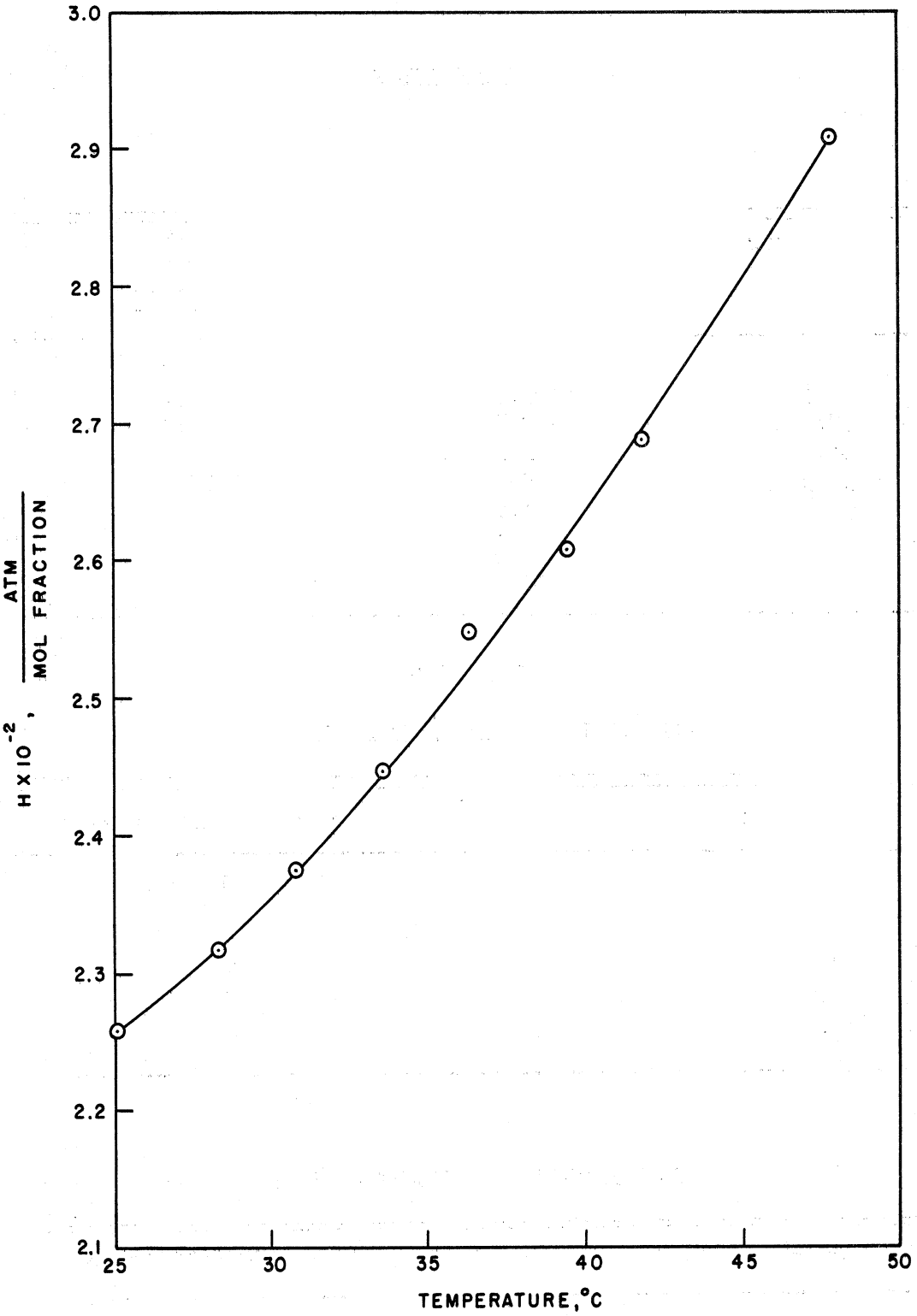

Figure 3-E. Henry's Law Constants for Carbon Dioxide-Cyclohexanol System

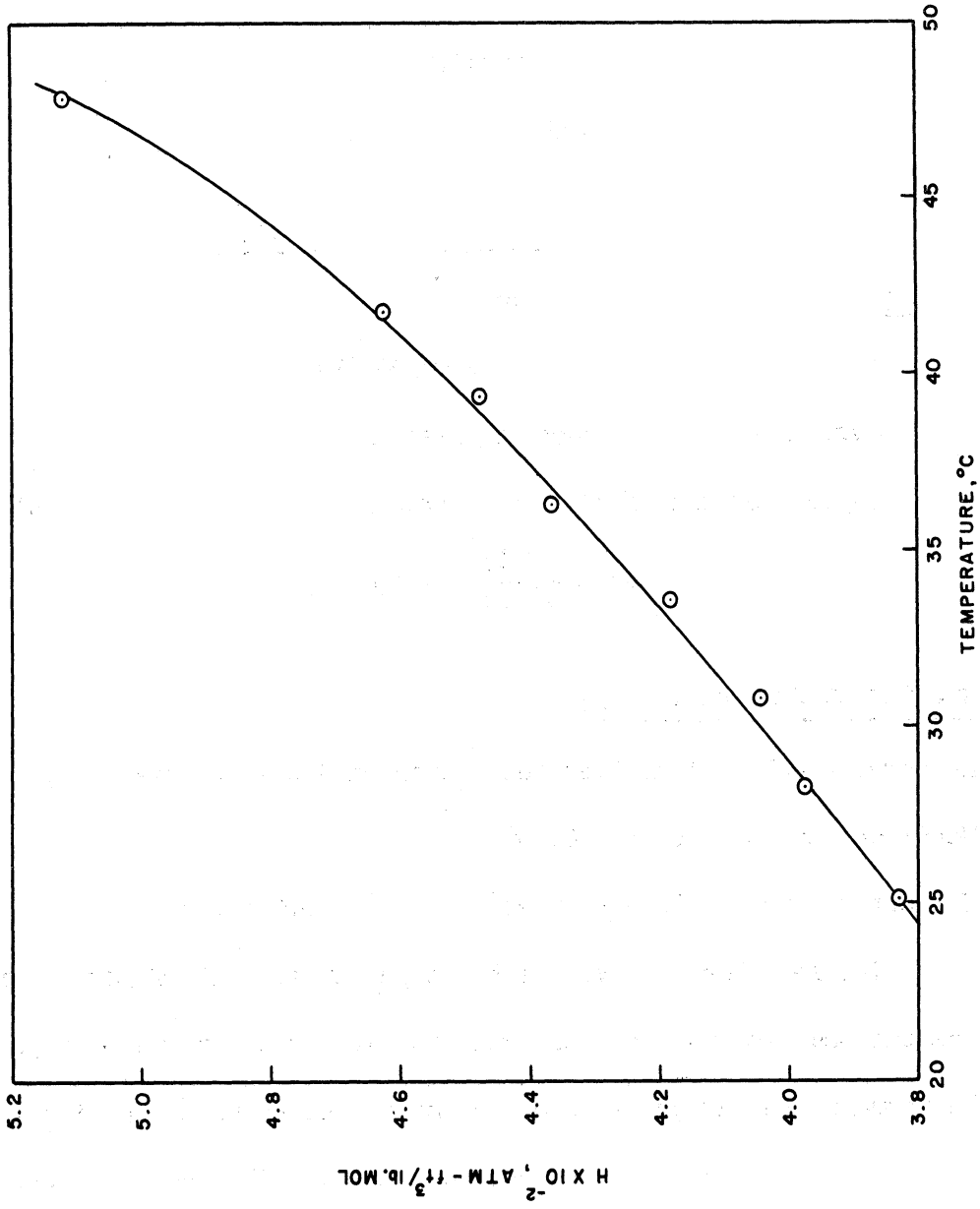

Figure 4-E. Henry's Law Constants for Carbon Dioxide-Cyclohexanol System

APPENDIX F

SAMPLE CALCULATIONS

Vaporization Data - Run No. E-10-A

1. Gas Equilibrium Composition, y*

Pressure above test plate = 30.33 "Hg

Avg. liquid temperature on test tray = 33.15°C

Vapor pressure of liquid at avg. liquid temperature = 0.780 "Hg

$$y^* = \frac{0.780}{30.33} = 0.02572$$

2. Gas Outlet Composition, y_1

Measured sample volume (wet test meter rdg) = 1.000 ft^3

Meter correction factor = 0.986

Corrected sample volume = (0.986)(1.000) = 0.986 ft^3

The lb moles of dry, inert gas per cubic foot of gas metered were calculated assuming that the gas was saturated with water vapor at the temperature and pressure of the meter and assuming the ideal gas law. In this case, the meter temperature was 82.9°F; the meter pressure was 29.08 in. Hg; and the lb-mole of air per cubic foot of gas metered was 235.77×10^{-5}.

Amount of air in sample = $(0.986)(235.77 \times 10^{-5})$

$= 232.47 \times 10^{-5}$ lb mole

Weight of ethylene dibromide condensed in U-tubes = 3.4727 grams

$= 4.0748 \times 10^{-5}$ lb mole

Total moles of inert gas plus ethylene dibromide vapor

$$= \frac{232.47 \times 10^{-5} \text{ lb moles} \\ 4.0748 \times 10^{-5} \text{ lb moles of } C_2H_4Br_2}{236.5448 \times 10^{-5} \text{ lb moles}}$$

$$y_1 = \frac{4.0748 \times 10^{-5}}{236.54 \times 10^{-5}} = 0.017227$$

3. Gas Inlet Composition, y_o

The method used to determine the gas inlet composition was identical to that used to determine the outlet composition shown above.

$$y_o = 0.008166$$

4. Point Vapor Efficiency

The point and plate efficiencies were assumed to be identical for these runs, i.e. $E_{OG} = E_{MV}$.

Therefore, $$E_{OG} = \frac{y_1 - y_o}{y^* - y_o}$$ from Equation

$$E_{OG} = \frac{1.7227 - 816.7}{2572.0 - 816.7} = \frac{906.0}{1755.3} = .5162 \text{ or } 51.62\%$$

5. Number of Individual Gas Transfer Units per Plate, N_G

$$N_G = \frac{1}{1 - y^*} \ln \frac{(1 - y_1)(y^* - y_o)}{(1 - y_o)(y^* - y_1)}$$ according to Equation (31)

$$N_G = \frac{1}{1 - 0.02572} \ln \frac{(1 - 0.017227)(0.02572 - 0.008166)}{(1 - 0.008166)(0.02572 - 0.017227)}$$

$$N_G = 0.745$$

$$N_G = - \ln (1 - E_{OG})$$ according to Equation (96)

$$N_G = - \ln (1 - 0.5162) = 0.7262$$

6. Gas Flow Rate

The gas rotameter calibration in Table III-D was applied gases with different densities according to the following equation:

$$Q_1 = Q_2 \sqrt{\frac{\rho_2}{\rho_1}}$$

where

Q_1 = volumetric flow rate of fluid 1 at a given meter reading, ft^3/min,

Q_2 = volumetric flow rate of fluid 2 at the same meter reading, ft^3/min,

ρ_1 = density of fluid 1, lb/ft^3, and

ρ_2 = density of fluid 2, lb/ft^3.

The actual gas flowing through the rotameter is nitrogen containing a little ethylene dibromide vapor. Its composition is the same as the inlet gas composition, y_o.

Average molecular weight of gas flowing through meter

$$= y_o M_{C_2H_4Br_2} + (1 - y_o) M_{N_2}$$

$$= (0.008166)(159.884) + (1 - 0.008166)(28) = 29.306$$

Gas rotameter scale reading = 80.5

Temperature of gas in meter = 541.3°R

Pressure in meter = 31.08 in. Hg

$$Q_o = 80.5\sqrt{\frac{(0.877)(28.9)(29.92)(541.3)}{(29.306)(31.08)(520)}} = 75.29 \text{ ft}^3/\text{min}.$$

The flow rate may be converted to lb-moles per minute as follows:

$$V = \frac{(75.29)(31.08)}{(21.82)(541.3)} = 0.1961 \text{ lb-moles/min}.$$

This is the same as the inlet gas flow rate, V_o, since no vapor is gained or lost between the rotameter and the test column inlet. Therefore $V_o = 0.1961$ lb-moles/min.

The flow rate of gas above the test plate, V_1, is obtained as follows:

$$V_1 = V_o \frac{(1 - y_o)}{(1 - y_1)} = \frac{(0.1961)(0.991834)}{(0.9828)} = 0.1978 \text{ lb moles/min.}$$

The average gas flow rate through the froth on the test plate is taken as the arithmetic average of V_1 and V_o.

$$V_{avg} = 0.1970$$

7. Average Gas Temperature

The temperature of the gas leaving the tray was calculated with the following relation:

$$T_1 = T_o - E_{OG} (T_o - T_s)$$

T_1 = outlet temperature of gas, °F,

T_o = inlet temperature of gas, °F, and

T_s = adiabatic saturation temperature (temperature of liquid on the test plate), °F.

The inlet gas temperature, T_o, was 122.0°F.

$T_1 = 122.0 - 0.5162 (122.0 - 91.7) = 106.9°F$

The average gas temperature = 114.4°F or 574.4°R

8. Superficial Velocity

If the active plate area is taken as the area between the splash baffle and the inlet downcomer (.615 ft^2) and the average pressure is taken as the pressure above the plate (30.33 in. Hg), V_{avg} can be converted to gas superficial velocity as follows:

$$\text{Superficial velocity, } v_s = \frac{(0.181)(359)(29.92)(574.4)}{(60)(0.615)(30.33)(492)}$$

$$= 2.209 \text{ ft/sec.}$$

9. Average Gas Density, ρ_G

M_{avg} = 29.3 lbs/lb-mole

T_{avg} = 574.4°R

P_1 = 30.33 in. Hg

$$\rho_G = \frac{(28.7)(30.33)(492)}{(359)(29.92)(574.4)} = 0.0709 \text{ lbs/ft}^3$$

10. F-Factor

$$F = v_s\sqrt{\rho_G}$$

$$F = 2.209\sqrt{0.0709} = 0.5876$$

11. Gas Contact Time

Froth height, Z_f, = 4.2 inches

Average clear liquid height, Z_c = 1.82 inches

Gas holdup = $Z_f - Z_c$ = 2.38 inches

$$\text{Gas contact time} = \frac{Z_f - Z_c}{(12)(v_s)} = \frac{2.38}{(12)(2.209)} = 0.08978 \text{ sec.}$$

12. Mass Transfer Coefficient, k_Ga

$$k_Ga = \frac{N_G}{t_G}$$

where t_G = gas contact time

$$k_Ga = \frac{0.7262}{0.08978} = 8.095$$

TABLE I-F

LABORATORY DATA SHEET - VAPORIZATION DATA

Date June 10, 1957

Run No. E-10-A System N_2 - $C_2H_4Br_2$ Operator Begley - Salesin

Weir Height 1-1/2" Splash baffle height 2"
Gas rotameter rdg. 80.5 Liquid rotameter rdg. 40

Barometer	29.08	"Hg at 80.9°F
Pressure in gas rotameter	2.00	"Hg
Pressure above 1st plate	1.25	"Hg
Pressure drop across 1st plate	3.60	"H_2O
Froth height	4.20"	
Clear liquid height, inches	(1) 2.00 (2) 1.68 (3) 1.78 (4) 1.80	

Temperatures:

Position	°C	TC	mv	°F
Liquid on plate No. 1 of rect. col. (in)	33.20			
Liquid on plate No. 1 of rect. col. (out)	33.10			
Liquid in liquid rotameter No. 1		L-9	1.182	85.1
Gas below plate No. 1 of rect. col.	49.85	L-3	1.863	114.6
Gas above plate No. 1 of rect. col.		G-2	1.213	86.7
Gas in gas rotameter No. 1	27.40			

	Out	In
Meter No.	H9SS	J5SS
Temperature of meter, °F	82.9	82.5
Pressure in meter, "H_2O	0.0	0.0
Final meter rdg, cu. ft.	1.000	1.000
Initial meter rdg, cu. ft.	0.000	0.000
Total flow, cu. ft.	1.000	1.000
Meter factor	0.986	1.003

Drying tube number	T-26	T-12	T-3	S-12	S-23	S-20
Final tube wt., gms	119.6720	125.4782	144.6585	114.0492	120.4477	115.2178
Initial tube wt., gms	116.3810	125.2994	144.6556	112.5727	120.2642	115.2164
Condensate, gms	3.2910	0.1788	0.0029	1.4765	0.1835	0.0014

Sample delivered, cu. ft.	0.2	0.4	0.6	0.8	1.0
Liquid on plate No. 1 (in), °C	33.20	33.20	33.20	33.20	33.20
Liquid on plate No. 1 (out), °C	33.10	33.10	33.10	33.10	33.10
Gas Temperature, (in), °C	49.85	50.00	50.10	50.10	50.20

Avg. Liquid temperature, 33.15 °C, 91.67 °F
Avg. Gas temperature (in), 50.05 °C, 122.09 °F

Inlet sample condensate 1.6614 grams
Outlet sample condensate 3.4727 grams

TABLE II-F

LABORATORY DATA SHEET - ABSORPTION DATA

Date December 10, 1956

Run # 15-A System CO_2 - Cyclohexanol Operator Begley - Salesin

Weir height 3-1/2" Splash baffle height 4"

Gas rotometer rdg. 41 Liquid rotometer rdg. 82

Barometer	29.18 "Hg at 70.0°F
Pressure in gas rotometer	1.5 "Hg
Pressure above 1st plate	1.1 "Hg
Pressure drop across 1 plate	1.0 " H_2O
Froth height	8.8"
Clear liquid height, inches	(1) 6.01 (2) 5.4 (3) 5.5 (4) 5.9

Temperatures:

Position	°C	TC	mv	°F
Liquid on plate #1 of rect. col. (in)				
Liquid on plate #1 of rect. col. (out)		L-4	0.951	75.1
Liquid entering bottom of rect. col.				
Liquid in liquid rotometer #2		L-9	0.970	76.0
Gas below plate #1 of rect. col.		L-3	0.982	
Gas below plate #1 of rect. col. (wet bulb)				
Gas above plate #1 of rect. col. (dry bulb)		G-2	0.903	
Gas in gas rotometer #1		G-3	1.184	

Spl. bottle no.	106	105	106A	107	108	109		
Vol. of $Ba(OH)_2$, c.c.	50	50	50	50	50	50		
Spl. position	1	2	3	4	5	6		
Vol. of liquid spl., c.c.	100	100	100	100	100	100		

Gas Sample Bulb No. 2

Absorption Data - Run No. 15-A

1. Concentration of Carbon Dioxide in Entering Liquid, X_1

Volume of 0.09575N $Ba(OH)_2$ = 50 ml.

Volume of 0.09510N HCL = 36.53 ml

Milliequivalent of $Ba(OH)_2$ = 4.788

Milliequivalent of HCl = 3.475

Milliequivalent of carbon dioxide = 1.313

Syringe volume of liquid sample = 100 cc

Correction factor = 0.9957

Actual volume of liquid sample = 99.57 cc

Concentration of carbon dioxide = $\frac{1.313}{2} \times 99.57$

$= 0.659 \times 10^{-5} \frac{\text{gm. moles}}{\text{cc}}$

$= 41.0 \times 10^{-5} \frac{\text{lb. moles}}{\text{ft}^3}$

lb. moles of cyclohexanol/ft^3 = 0.5880

Mol fraction of carbon dioxide = $41.0 \times 10^{-5}/0.5876$

$X_1 = 69.7 \times 10^{-5}$

2. Concentration of Carbon Dioxide in Outlet Liquid Samples, x_5 and x_6

Calculation similar to that for x_1.

$x_5 = 111.2 \times 10^{-5}$

$x_6 = 127.0 \times 10^{-5}$

3. Equilibrium Concentration of Carbon Dioxide in Liquid

Average liquid temperature = 24.0°C

Pressure above the tray = 1.012 atm.

Mole fraction of carbon dioxide

in gas above the tray = 0.9005

Partial pressure of carbon dioxide

above the tray = 0.9113 atm.

Henry's Law Constant = 224.0 $\frac{\text{atm.}}{\text{mol fraction}}$

Equilibrium mol fraction = $\frac{p}{H} = \frac{0.9113}{224.0} = 406.8 \times 10^{-5}$

4. Murphree Liquid Efficiency, E_{ML}

$$E_{ML_{15}} = \frac{x_5 - x_1}{x^* - x_1}$$

$$= \frac{111.2 - 69.7}{406.8 - 69.7} = 0.1231 \text{ or } 12.31\%$$

$$E_{ML_{16}} = \frac{x_6 - x_1}{x^* - x_1} = \frac{127.0 - 69.7}{406.8 - 69.7} = 17.0\%$$

5. Calculation of Liquid Rate, GPM and L_M

Ashby(7) used water to calibrate the liquid rotameter. These data are presented in Table III-D and were used to calculate the flow rates for cyclohexanol by use of the following equation:

$$\frac{Q_1}{Q_2} = \sqrt{\frac{\rho_2(\rho_F - \rho_1)}{\rho_1(\rho_F - \rho_2)}}$$

where

Q_1 = volumetric flow rate of fluid 1 at a given meter reading,

Q_2 = volumetric flow rate of fluid 2 for the same reading,

ρ_1 = density of fluid 1,

ρ_2 = density of fluid 2,

ρ_F = density of the rotameter float.

Rotameter reading = 82.0

Q_2 = 0.0582 (Table III-D)

ρ_1 = 0.945

ρ_2 = 0.99949

ρ_F = 7.85

$$\text{Liquid rate} = 0.0582\sqrt{\frac{0.99949\ (7.85 - 0.9450)}{0.9450\ (7.85 - 0.99949)}}$$

$= 0.059946\ ft^3/sec$

$= 0.059946 \times 7.48 \times 60 = 26.904$ GPM.

$$L_M = \frac{(0.05995)(0.9450)(62.4)(60)}{100.2} = 2.1167 \text{ lb-moles/min.}$$

6. Gas Rate, u_s, F-Factor, and G_m

Gas rotameter reading (Rotameter No. D8-1609) = 41.0

Mol fraction of carbon dioxide = 0.902

Mol fraction of cyclohexanol in gas (assuming gas to be saturated at plate liquid temperature and pressure)

Vapor pressure of cyclohexanol at 24.4°C = 0.051" Hg

Pressure above plate = 30.28" Hg

Mol fraction cyclohexanol $= \frac{0.051}{30.28} = 0.001684$

Mol fraction air = 1 - 0.902 - 0.001684 = 0.096

Molecular weight of gas =

(100.2)(0.001684) + 44 (0.902) + (28.9)(0.096)

0.1687 + 39.688 + 2.7744 = 42.631

Pressure at rotameter = 30.68" Hg

Temperature at rotameter = 85.1°F.

$$\underline{Q} = 41\sqrt{\frac{(1.458)(T)}{(M)\ (P)}} = 41\sqrt{\frac{(1.458)(545.1)}{(42.63)(30.68)}} = 31.96\ ft^3/min$$

$$\underline{G_m} = \frac{(Q)\ (P)}{(21.82)(T)} = 0.08244 \text{ lb mole/min}$$

Superficial Gas Velocity

Pressure above tray = 30.28" Hg

Temperature above tray = 75.92°F

$$u_s = \frac{(G_m)(RT)}{(0.615)(60)(P)} = \frac{(0.08244)(535.9)}{(1.689)(30.28)} = 0.8638 \text{ ft/sec.}$$

$$\rho_G = \frac{(P)\ \ (M)}{(21.82)(T)} \qquad \frac{(30.28)(42.63)}{(21.82)(535.9)} = 0.1104 \text{ lb/ft}^3$$

F-Factor

$$\text{F-Factor} = 0.8638\ \sqrt{0.1104} = 0.2870$$

7. Murphree Vapor Plate Efficiency, E_{MV}

$$E_{MV_{15}} = \frac{E_{ML_{15}}}{E_{ML_{15}} + \frac{HG_m}{PL_m}(1 - E_{ML_{15}})}$$

$$\frac{0.1231}{0.1231 + \frac{(224.0)(0.08244)}{(1.012)(2.1167)}(1 - 0.1231)}$$

$$\frac{0.1231}{0.1231 + (8.62)(0.8769)} = 0.01603 \text{ or } 1.603\%$$

8. Murphree Vapor Point Efficiency, E_{OG}

$$\frac{E_{MV_{15}}}{E_{OG}} = \frac{x_{avg} - x^*}{x_5 - x^*}$$

$$x_{avg} = \frac{C_2 + C_3 + C_4 + C_5}{4(\rho_m)}$$

$$= \frac{(41.45 + 41.0 + 63.5 + 65.5)}{4\ (0.5885)} \times 10^{-5}$$

$$= \frac{(52.862)}{0.5885} \times 10^{-5} = 89.8 \times 10^{-5}$$

$$x^* = 406.8 \times 10^{-5}$$

$$x_5 = 111.2 \times 10^{-5}$$

$$\frac{E_{MV15}}{E_{OG}} = \frac{89.8 - 406.8}{111.2 - 406.8} = \frac{317.0}{295.6} = 1.073$$

$$E_{OG} = \frac{E_{MV15}}{1.073} = \frac{0.01603}{1.073} = 0.01493 \text{ or } 1.493\%$$

9. Number of Over-All Gas-Phase Mass Transfer Units

$$N_{OG} = - \ln (1 - E_{OG})$$

$$N_{OG} = - \ln (1 - 0.01493)$$

$$N_{OG} = 0.0151$$

10. Number of Liquid-Phase Mass Transfer Units

$$\frac{1}{N_{OG}} = \frac{1}{N_G} + \frac{\lambda}{N_L}$$

$$\frac{1}{N_G} = 0$$

$$N_L = N_{OG} = (8.62)(0.0151) = 0.130$$

11. Liquid Contact Time

Liquid rate $= \frac{26.904 \text{ GPM}}{7.48 \times 60} = 0.05991 \text{ ft}^3/\text{sec}$

Froth height $= 9.01$ inches

Equivalent cap height $= 0.27$ inches

Relative froth density $= 0.648$

Contact time $= \frac{(9.01 - 0.27)(0.615)(0.648)}{(12)(0.05991)} = 4.843$ sec.

12. Mass Transfer Coefficient

$$N_L = k_L \bar{a} t_L$$

$$k_L\bar{a} = \frac{N_L}{t_L} = \frac{0.130}{4.843} = 0.02685$$

APPENDIX G

EXPERIMENTAL AND CALCULATED DATA

TABLE I-C

PLATE EFFICIENCIES IN RECTANGULAR COLUMN AT UNIVERSITY OF MICHIGAN
(ORIGINAL DATA FOR N_2-ETHYLENE DIBROMIDE SYSTEM)
1.50-IN. WEIR, 2.0-IN. SPLASH BAFFLE

RUN NO.		E-6-A		E-6-B		E-2-A		E-2-B		E-1-A		E-1-B		E-3-A	
1.	GAS ROT. RDG.	34		36		46		46		77		77		77	
2.	LIQ. ROT. RDG.	40		40		40		40		38		38		39	
3.	BAROMETRIC PRESSURE, IN Hg	29.27		29.27		29.32		29.32		29.36		29.36		29.32	
4.	PRESSURE IN GAS ROT., IN Hg	2.10		2.10		1.70		1.80		2.10		1.20		2.05	
5.	PRESSURE ABOVE PLATE, IN Hg	1.60		1.65		1.20		1.30		1.40		1.10		1.40	
6.	PRESSURE DROP ACROSS PLATE, IN H_2O	3.10		3.10		3.20		3.20		3.60		3.60		3.60	
7.	FROTH HEIGHT, IN.	3.5		3.5		3.55		3.7		4.2		4.2		4.2	
8.	CLEAR LIQUID HT. AT POSITION 2, IN	1.90		1.95		1.90		1.95		1.90		1.90		1.95	
9.	3	1.80		1.80		1.80		1.80		1.60		1.60		1.65	
10.	4	1.82		1.82		1.80		1.80		1.75		1.75		1.80	
11.	5	1.80		1.80		1.80		1.80		1.75		1.75		1.80	
12.	AVG. CLEAR LIQ. HT. IN.	1.83		1.83		1.83		1.84		1.75		1.75		1.80	
13.	AVG. LIQ. TEMP. ON PLATE, °F	93.1		92.98		93.31		93.07		93.02		93.34		92.88	
14.	LIQ. TEMP. IN ROT. °F	84.9		85.0		85.3		84.5		80.8		82.4		90.77	
15.	TEMP. OF GAS BELOW PLATE, °F	135.3		135.2		131.3		130.9		129.2		130.6		137.0	
16.	TEMP. IN GAS ROT. °F	77.0		77.0		78.6		78.0		75.58		76.1		79.0	
17.	SAMPLING POINT	OUTLET	INLET	OUTLET	INLET	OUTLET	INLET	OUTLET	INLET	OUTLET	INLET	OUTLET	INLET	OUTLET	INLET
18.	TEMP. OF GAS SAMPLE METER, °F	79.0	78.5	79.5	77.8	77.5	77.3	77.5	77.2	72.4	71.5	73.4	72.5	78.5	79.0
19.	PRESSURE IN METER, IN H_2O	--	--	--	--	--	--	--	--	--	--	--	--	--	--
20.	METERED SAMPLE VOL. FT^3	1.2000	1.0000	1.101	1.0000	1.0004	1.0000	0.7933	0.8518	1.003	1.0000	0.7765	0.9055	1.0000	1.0000
21.	METER CORRECTION FACTOR	0.986	1.003	0.986	1.003	0.986	1.003	0.986	1.003	0.986	1.003	0.985	1.003	0.986	1.003
22.	CORRECTED SAMPLE VOLUME FT^3	1.183	1.003	1.0856	1.003	0.9864	1.003	0.7822	0.8544	0.9863	1.003	0.7656	0.9082	0.986	1.003
23.	LB. MOL OF GAS PER FT^3 MET. $X\ 10^5$	240.24	240.62	239.89	241.11	241.76	241.90	241.75	241.98	245.69	246.32	245.00	245.60	241.06	240.62
24.	LB. MOL OF GAS IN SAMPLE $X\ 10^5$	284.25	241.34	260.42	241.83	238.47	242.63	189.09	206.75	242.32	247.06	187.57	233.05	237.69	241.34
25.	ETHYLENE DIBROMIDE ABS. IN TUBES, gm	4.4036	2.3035	4.0436	1.5231	3.8569	1.4533	3.4407	1.7695	4.5938	2.3813	3.6164	2.1744	3.6965	1.5330
26.	ETHYLENE DIBROMIDE ABS. IN TUBES, LB. MOL $X\ 10^5$	5.167	2.703	4.745	1.787	4.5256	1.7053	4.0372	2.0763	5.390	2.794	4.243	3.255	4.2307	1.7988
27.	TOT. MOLS IN SAMPLE LB.MOL $X\ 10^5$	289.42	244.04	265.17	243.62	243.0	244.33	193.13	208.83	247.71	249.85	191.81	226.31	241.916	243.14
28.	y_o, y_1	0.01784	* 0.01108	0.01789	0.007335	0.01862	0.006980	0.02090	0.009943	0.02176	0.01118	0.02212	0.01438	0.01748	0.007398
29.	VAPOR PRES. OF LIQ. ON PLATE IN Hg	0.80"		0.80		0.82		0.805		0.80		0.81		0.80	
30.	y^*	0.02592		0.2587		0.02687		0.02629		0.02601		0.02659		0.02604	
31.	E_{OG} %	* 56.58		56.95		58.43		67.03		71.34		59.71		54.12	
32.	$N_{OG} = -\ell n\ (1-E_{OG})$	* 0.835		0.844		0.878		1.11		1.250		0.908		0.779	
33.	v_s, FT/SEC	0.9458		1.006		1.301		1.284		2.141		2.144		2.157	
34.	ρ_G LB/FT^3	0.07109		0.07016		0.0694		0.07106		0.07197		0.07213		0.06995	
35.	$F = v_s\sqrt{\rho_G}$	0.2522		0.2668		0.3432		0.3422		0.5742		0.5724		0.5705	
36.	t_G, SEC	0.1471		0.1375		0.1102		0.1210		0.09536		0.09523		0.09272	
37.	k'_Ga, SEC^{-1}	* 5.68		6.14		7.97		9.17		13.11		9.535		8.40	

* INLET SAMPLE DATA TAKEN FROM E-6-B.

TABLE I-G (CONTINUED)

PLATE EFFICIENCIES IN RECTANGULAR COLUMN AT UNIVERSITY OF MICHIGAN
(ORIGINAL DATA FOR N_2-ETHYLENE DIBROMIDE SYSTEM)
1.50-IN. WEIR, 2.0-IN. SPLASH BAFFLE

RUN NO.		E-3-B		E-4-A		E-4-B		E-5-A		E-5-B		E-11-A		E-11-B	
1.	GAS ROT. RDG.	77		114		114		161		161		46.5		46.5	
2.	LIQ. ROT. RDG.	36		39		40		40		40		40		40	
3.	BAROMETRIC PRESSURE, IN Hg	29.32		29.30		29.30		29.15		29.15		28.87		28.87	
4.	PRESSURE IN GAS ROT., IN Hg	2.20		2.20		2.05		2.60		2.60		1.45		1.60	
5.	PRESSURE ABOVE PLATE, IN Hg	1.45		1.22		1.10		1.05		1.05		0.90		1.00	
6.	PRESSURE DROP ACROSS PLATE, IN H_2O	3.60		4.48		4.33		6.10		6.10		3.15		3.15	
7.	FROTH HEIGHT, IN.	3.9		5.2		5.2		6.5		6.5		3.7		3.7	
8.	CLEAR LIQ. HT. AT POSITION 2, IN	1.90		2.0		2.00		2.05		2.05		2.00		2.00	
9.	3	1.60		1.5		1.50		1.45		1.40		1.83		1.83	
10.	4	1.75		1.7		1.70		1.40		1.40		1.83		1.85	
11.	5	1.75		1.8		1.80		1.70		1.70		1.80		1.80	
12.	AVG. CLEAR LIQ. HT. IN.	1.75		1.75		1.75		1.65		1.64		1.86		1.87	
13.	AVG. LIQ. TEMP. ON PLATE, °F	93.02		93.81		94.25		94.73		94.57		92.8		92.98	
14.	LIQ. TEMP. IN ROT. °F	90.7		91.7		92.0		90.2		90.0		86.5		86.5	
15.	TEMP. OF GAS BELOW PLATE, °F	137.0		134.3		136.2		139.1		138.4		118.9		119.4	
16.	TEMP. IN GAS ROT. °F	78.8		78.0		78.1		76.5		76.5		82.5		82.9	
17.	SAMPLING POINT	OUTLET	INLET	OUTLET	INLET	OUTLET	INLET	OUTLET	INLET	OUTLET	INLET	OUTLET	INLET	OUTLET	INLET
18.	TEMP. OF GAS SAMPLE METER, °F	79.5	79.0	79.2	78.7	80.3	79.9	78.0	77.6	78.2	80.3	80.1	80.5	80.7	80.5
19.	PRESSURE IN METER, IN H_2O	--	--	--	--	--	--	--	--	--	--	--	--	--	--
20.	METERED SAMPLE VOL. FT^3	1.0000	1.0000	1.0000	1.0000	1.0000	1.0000	1.0000	1.0000	1.0000	1.0000	1.002	1.000	1.000	1.000
21.	METER CORRECTION FACTOR	0.986	1.003	0.986	1.003	0.986	1.003	0.986	1.003	0.986	1.003	0.986	1.003	0.986	1.003
22.	CORRECTED SAMPLE VOLUME, FT^3	0.986	1.003	0.986	1.003	0.986	1.003	0.986	1 003	0.986	1.003	0.988	1.003	0.986	1.003
23.	LB. MOL OF GAS PER FT^3 MET.X 10^5	240.32	240.84	240.36	240.70	239.56	239.86	239.93	240.24	239.80	240.08	235.92	236.06	235.61	235.76
24.	LB. MOL OF GAS IN SAMPLE X 10^5	236.96	241.56	236.99	241.42	236.21	240.58	236.57	240.96	236.44	240.80	233.10	236.77	233.01	236.47
25.	ETHYLENE DIBROMIDE ABS. IN TUBES, gm	3.6502	1.5202	3.7102	1.4884	3.7779	1.4594	3.8830	1.6178	3.8521	1.6851	3.7141	1.6530	3.7667	1.7303
26.	ETHYLENE DIBROMIDE ABS. IN TUBES, LB. MOL X 10^5	4.2831	1.7838	4.3535	1.7465	4.4329	1.7512	4.5562	1.8983	4.5200	1.9773	4.3580	1.9396	4.4198	2.0303
27.	TOT. MOLS IN SAMPLE LB.MOL X 10^5	240.24	243.34	241.34	243.17	240.64	242.33	241.126	242.86	240.96	242.78	237.46	238.71	237.43	238.5
28.	y_o, y_1	0.01775	0.007330	0.01804	0.007182	0.01842	0.007227	0.01890	0.007817	0.01876	0.008145	0.018353	0.008125	0.018615	0.008513
29.	VAPOR PRES. OF LIQ. ON PLATE IN Hg	0.80		0.825		0.830		0.840		0.835		0.810		0.810	
30.	y^*	0.02600		0.02703		0.02730		0.02782		0.02765		0.027209		0.027118	
31.	E_{OG} %	55.84		54.70		55.75		55.40		54.42		53.59		54.30	
32.	$N_{OG} = -\ln (1-E_{OG})$	0.819		0.886		0.815		0.807		0.786		0.7678		0.783	
33.	v_s, FT/SEC	2.1676		3.227		3.206		4.638		4.665		1.2896		1.288	
34.	ρ_G LB/FT^3	0.06963		0.0695		0.06923		0.06865		0.06881		0.06929		0.07022	
35.	$F = v_s\sqrt{\rho_G}$	0.5722		0.8502		0.8448		1.2150		1.2222		0.3410		0.3418	
36.	t_G, SEC	0.08266		0.09186		0.08968		0.08804		0.08682		0.11826		0.1184	
37.	k'_Ga, SEC^{-1}	9.908		9.645		9.088		9.17		9.053		6.492		6.613	

* INLET SAMPLE DATA TAKEN FROM E-6-B.

TABLE I-G (CONTINUED)

PLATE EFFICIENCIES IN RECTANGULAR COLUMN AT UNIVERSITY OF MICHIGAN
(ORIGINAL DATA FOR N_2-ETHYLENE DIBROMIDE SYSTEM)
1.50-IN. WEIR, 2.0-IN. SPLASH BAFFLE

RUN NO.	E-7-A		E-7-B		E-10-A		E-10-B		E-9-A		E-9-B		E-8-A		E-8-B	
1. GAS ROT. RDG.	78		78		80.5		80.7		119		119		158		158	
2. LIQ. ROT. RDG.	39.4		39.9		40		40		39		40		40		39	
3. BAROMETRIC PRESSURE, IN Hg	28.92		28.92		29.08		29.08		29.09		29.09		29.13		29.13	
4. PRESSURE IN GAS ROT., IN Hg	3.70		3.40		2.00		2.05		2.25		2.25		2.65		2.65	
5. PRESSURE ABOVE PLATE, IN Hg	1.50		1.30		1.25		1.30		1.25		1.25		1.20		1.20	
6. PRESSURE DROP ACROSS PLATE, IN H_2O	3.50		3.25		3.60		3.60		4.45		4.45		5.77		5.77	
7. FROTH HEIGHT, IN.	4.0		4.0		4.2		4.2		5.3		5.3		6.2		6.4	
8. CLEAR LIQ. HT. AT POSITION 2, IN	2.00		2.00		2.00		2.00		2.05		2.02		2.10		2.05	
9. 3	1.72		1.75		1.68		1.68		1.50		1.50		1.40		1.40	
10. 4	1.80		1.80		1.78		1.80		1.70		1.70		1.45		1.45	
11. 5	1.80		1.80		1.80		1.80		1.78		1.80		1.75		1.75	
12. AVG. CLEAR LIQ. HT. IN.	1.83		1.84		1.82		1.82		1.76		1.76		1.73		1.66	
13. AVG. LIQ. TEMP. ON PLATE, °F	87.44		87.35		91.67		91.49		92.48		92.39		94.06		94.06	
14. LIQ. TEMP. IN ROT. °F	86.2		85.9		85.1		85.0		85.8		85.9		91.1		91.3	
15. TEMP. OF GAS BELOW PLATE, °F	121.3		120.9		114.6		114.6		114.4		114.7		116.2		116.2	
16. TEMP. IN GAS ROT. °F	151.5		151.3		81.3		81.1		79.2		79.3		76.5		76.7	
17. SAMPLING POINT	OUTLET	INLET	OUTLET	INLET	OUTLET	INLET	OUTLET	INLET	OUTLET	INLET	OUTLET	INLET	OUTLET	INLET	OUTLET	INLET
18. TEMP. OF GAS SAMPLE METER, °F	83.50	83.30	83.10	83.0	82.9	82.5	82.7	82.5	81.1	80.8	81.9	81.4	74.7	81.4	75.0	74.3
19. PRESSURE IN METER, IN H_2O	--	--	--	--	--	--	--	--	--	--	--	--	--	--	--	--
20. METERED SAMPLE VOL. FT^3	1.200	1.200	1.2111	1.000	1.000	1.000	1.000	1.000	1.000	1.000	1.000	1.000	1.0002	1.0000	0.9998	1.0000
21. METER CORRECTION FACTOR	0.986	1.003	0.986	1.003	0.986	1.003	0.986	1.003	0.986	1.003	0.986	1.003	0.986	1.003	0.986	1.003
22. CORRECTED SAMPLE VOLUME, FT^3	1.1832	1.2036	1.1941	1.003	0.986	1.003	0.986	1.003	0.986	1.003	0.986	1.003	0.9862	1.003	00.9918	1.003
23. LB. MOL OF GAS PER FT^3 MET. X 10^5	233.98	234.13	234.27	234.35	235.77	236.06	235.93	236.06	236.18	237.45	236.60	236.96	242.14	242.6	241.94	242.39
24. LB. MOL OF GAS IN SAMPLE X 10^5	276.85	281.80	279.74	235.05	232.47	236.77	232.63	236.77	232.87	238.16	233.29	237.67	238.80	243.33	241.89	243.12
25. ETHYLENE DIBROMIDE ABS. IN TUBES, gm	3.6217	2.3206	3.6603	1.6900	3.4727	1.6614	3.4409	1.6769	3.5071	1.6493	3.6396	1.6204	3.7795	1.8531	3.8491	1.9707
26. ETHYLENE DIBROMIDE ABS. IN TUBES, LB. MOL X 10^5	4.250	2.723	4.295	1.983	4.0748	1.9495	4.0375	1.9676	4.1152	1.9353	4.2706	1.9013	4.4348	2.1744	4.5164	2.3124
27. TOT. MOLS IN SAMPLE LB.MOL X 10^5	281.10	279.08	284.04	237.03	236.54	238.72	236.67	238.74	236.99	240.09	237.56	239.57	243.24	245.50	246.41	245.43
28. y_o, y_1	0.015119	0.009757	0.015121	0.008366	0.017227	0.008167	0.017356	0.008242	0.017364	0.008060	0.017977	0.007936	0.018233	0.008857	0.018329	0.009422
29. VAPOR PRES. OF LIQ. ON PLATE IN Hg	0.699		0.695		0.780		0.78		0.800		0.800		0.835		0.835	
30. y^*	0.02298		0.02300		0.02572		0.025675		0.026368		0.026368		0.02753		0.027531	
31. E_{OG} %	40.55		46.02		51.62		52.28		50.82		54.48		50.21		49.19	
32. $N_{OG} = -\ln(1-E_{OG})$	0.520		0.6166		0.7262		0.7402		0.7095		0.7974		0.7324		0.677	
33. v_s, FT/SEC	2.064		2.0712		2.209		2.211		3.290		3.304		4.387		4.400	
34. ρ_G LB/FT^3	0.07142		0.07064		0.07092		0.07109		0.07085		0.07090		0.07136		0.07156	
35. $F = v_s\sqrt{\rho_G}$	0.5490		0.5509		0.5876		0.5897		0.8751		0.8787		1.1735		1.177	
36. t_G, SEC	0.0876		0.08691		0.08976		0.09347		0.08967		0.08930		0.08491		0.08977	
37. k'_Ga, SEC^{-1}	5.936		7.095		8.089		7.53		7.921		8.929		8.20		7.54	

* INLET SAMPLE DATA TAKEN FROM E-6-B.

TABLE I-G (CONTINUED)

PLATE EFFICIENCIES IN RECTANGULAR COLUMN AT UNIVERSITY OF MICHIGAN
(ORIGINAL DATA FOR N_2-ETHYLENE DIBROMIDE SYSTEM)
3.50-IN. WEIR, 4-IN. SPLASH BAFFLE

RUN NO.	E-15-A		E-15-B		E-12-A		E-12-B		E-17-A		E-17-B	
1. GAS ROT. RDG.	41		41		45		45		61		62	
2. LIQ. ROT. RDG.	40		40		40		40		44		39	
3. BAROMETRIC PRESSURE, IN Hg	29.20		29.20		28.87		28.87		29.16		29.16	
4. PRESSURE IN GAS ROT., IN Hg	1.36		2.20		1.50		1.85		2.10		2.15	
5. PRESSURE ABOVE PLATE, IN Hg	1.00		1.30		0.70		1.05		1.25		1.25	
6. PRESSURE DROP ACROSS PLATE, IN H_2O	6.60		6.45		6.35		6.30		6.15		6.13	
7. FROTH HEIGHT, IN.	6.9		6.9		6.7		6.6		6.8		6.9	
8. CLEAR LIQ. HT. AT POSITION 2, IN	4.00		3.90		3.68		3.73		3.60		3.60	
9. 3	3.55		3.50		3.25		3.28		3.10		3.05	
10. 4	3.55		3.50		3.30		3.35		3.20		3.15	
11. 5	3.65		3.60		3.38		3.40		3.50		3.25	
12. AVG. CLEAR LIQ. HT. IN.	3.69		3.63		3.40		3.44		3.30		3.26	
13. AVG. LIQ. TEMP. ON PLATE, °F	93.88		93.92		92.9		93.0		93.72		94.51	
14. LIQ. TEMP. IN ROT. °F	86.5		86.10		83.4		83.8		88.9		89.5	
15. TEMP. OF GAS BELOW PLATE, °F	132.9		133.2		130.8		131.0		131.4		132.0	
16. TEMP. IN GAS ROT. °F	91.9		92.0		82.0		83.0		87.4		88.0	
17. SAMPLING POINT	OUTLET	INLET	OUTLET	INLET	OUTLET	INLET	OUTLET	INLET	OUTLET	INLET	OUTLET	INLET
18. TEMP. OF GAS SAMPLE METER, °F	90.5	90.0	91.1	90.3	79.5	79.5	80.4	80.0	85.2	85.0	86.5	86.4
19. PRESSURE IN METER, IN H_2O	--	--	--	--	--	--	--	--	--	--	--	--
20. METERED SAMPLE VOL. FT^3	1.0000	1.0000	1.0000	1.0000	1.0000	1.0000	1.0000	1.0000	1.0000	1.0000	0.9998	0.9998
21. METER CORRECTION FACTOR	0.986	1.003	0.986	1.003	0.986	1.003	0.986	1.003	0.986	1.003	0.986	1.003
22. CORRECTED SAMPLE VOLUME, FT^3	0.986	1.003	0.986	1.003	0.986	1.003	0.986	1.003	0.986	1.003	0.9858	1.0027
23. LB. MOL OF GAS PER FT^3 MET. X 10^5	230.93	230.6	230.4	231.15	236.49	236.49	235.84	236.13	224.7	234.9	233.9	233.9
24. LB. MOL OF GAS IN SAMPLE X 10^5	227.70	231.29	227.0	232.0	233.18	237.20	232.54	236.84	221.5	235.6	230.5	234.5
25. ETHYLENE DIBROMIDE ABS. IN TUBES gm	4.0816	2.0864	4.1365	1.9319	3.8936	1.7640	4.0137	1.7317	4.1086	2.1495	4.1913	2.0557
26. ETHYLENE DIBROMIDE ABS. IN TUBES, LB. MOL X 10^5	4.7893	2.4481	4.850	2.27	4.5687	2.0698	4.7096	2.0319	4.829	2.517	4.91	2.41
27. TOT. MOLS IN SAMPLE LB. MOL X 10^5	232.49	233.74	231.85	234.3	237.75	239.27	237.25	238.87	226.3	238.1	235.41	236.9
28. y_o, y_1	0.02060	0.010473	0.02095	0.00969	0.019217	0.008651	0.019851	0.008506	0.021338	0.01057	0.020858	0.010173
29. VAPOR PRES. OF LIQ. ON PLATE IN Hg	0.830		0.830		0.817		0.82		0.835		0.85	
30. y^*	0.027438		0.0272		0.27513		0.027406		0.027458		0.027951	
31. E_{OG}%	59.83		64.31		56.02		60.02		63.76		60.10	
32. $N_{OG} = -\ell n\ (1-E_{OG})$	0.914		1.0303		0.821		0.917		1.0143		0.92	
33. v_s, FT/SEC	1.113		1.125		1.295		1.260		1.669		1.681	
34. ρ_G LB/FT^3	0.0708		0.0705		0.0692		0.06925		0.07139		0.07109	
35. $F = v_s\sqrt{\rho_G}$	0.289		0.299		0.3419		0.3325		0.4460		0.4480	
36. t_G, SEC	0.241		0.250		0.2122		0.2090		0.17475		0.1804	
37. k'_Ga, SEC^{-1}	3.79		4.121		3.869		4.390		5.958		5.099	

* INLET SAMPLE DATA TAKEN FROM E-6-B.

TABLE I-G (CONTINUED)

PLATE EFFICIENCIES IN RECTANGULAR COLUMN AT UNIVERSITY OF MICHIGAN
(ORIGINAL DATA FOR N_2-ETHYLENE DIBROMIDE SYSTEM,
3.50-IN. WEIR, 4-IN. SPLASH BAFFLE

RUN NO.	E-13-A		E-13-B		E-14-A		E-14-B		E-16-A		E-16-B	
1. GAS ROT. RDG.	79		79		116		116		144		143	
2. LIQ. ROT. RDG.	40		40		40		41		40		40	
3. BAROMETRIC PRESSURE, IN Hg	28.84		28.84		28.92		28.91		29.12		29.12	
4. PRESSURE IN GAS ROT., IN Hg	2.55		2.45		2.20		2.20		2.60		2.80	
5. PRESSURE ABOVE PLATE, IN Hg	1.55		1.45		0.93		0.93		0.90		1.00	
6. PRESSURE DROP ACROSS PLATE, IN H_2O	7.00		7.00		8.20		8.05		10.00		9.60	
7. FROTH HEIGHT, IN.	8.0		8.0		10.0		10.0		11.65		11.7	
8. CLEAR LIQ. HT.AT POSITION 2, IN	3.81		3.82		4.00		4.00		4.15		3.95	
9. 3	3.33		3.30		3.65		3.30		3.35		3.15	
10. 4	3.37		3.35		3.30		3.30		3.20		3.00	
11. 5	3.50		3.50		3.60		3.55		3.80		3.45	
12. AVG. CLEAR LIQ. HT. IN.	3.50		3.49		3.46		3.54		3.63		3.39	
13. AVG. LIQ. TEMP. ON PLATE, °F	93.2		93.1		93.38		93.42		93.2		92.13	
14. LIQ. TEMP. IN ROT. °F	84.3		83.3		87.2		87.7		84.7		85.0	
15. TEMP. OF GAS BELOW PLATE, °F	131.0		131.0		131.7		132.0		129.0		132.0	
16. TEMP. IN GAS ROT. °F	82.7		83.0		81.8		82.0		84.9		84.2	
17. SAMPLING POINT	OUTLET	INLET	OUTLET	INLET	OUTLET	INLET	OUTLET	INLET	OUTLET	INLET	OUTLET	INLET
18. TEMP. OF GAS SAMPLE METER, °F	83.0	82.5	83.5	83.2	84.5	84.2	85.5	84.8	91.7	91.5	91.5	91.0
19. PRESSURE IN METER, IN H_2O	--	--	--	--	--	--	--	--	--	--	--	--
20. METERED SAMPLE VOL. FT^3	1.0000	1.0000	1.0000	1.0000	1.0000	1.0000	1.0000	1.0000	1.0000	1.0000	1.0000	1.0000
21. METER CORRECTION FACTOR	0.986	1.003	0.986	1.003	0.986	1.003	0.986	1.003	0.986	1.003	0.986	1.003
22. CORRECTED SAMPLE VOLUME, FT^3	0.986	1.003	0.986	1.003	0.986	1.003	0.986	1.003	0.986	1.003	0.986	1.003
23. LB. MOL OF GAS PER FT^3 MET.X 10^5	233.67	234.04	233.31	233.54	233.25	233.47	232.41	232.93	229.4	229.6	229.5	230.0
24. LB. MOL OF GAS IN SAMPLE X 10^5	230.40	234.75	230.04	234.24	229.93	234.17	229.15	233.63	226.18	230.3	226.2	230.7
25. ETHYLENE DIBROMIDE ABS. IN TUBES, gm	4.0598	1.7750	4.0253	1.7738	4.0933	1.7824	4.1316	1.7961	4.0104	1.9660	3.9965	1.9870
26. ETHYLENE DIBROMIDE ABS. IN TUBES, LB. MOL X 10^5	4.7637	2.0593	4.7232	2.0802	4.8030	2.0914	4.8479	2.1075	4.705	2.306	4.690	2.330
27. TOT.MOLS IN SAMPLE LB.MOL X 10^5	235.16	236.81	234.77	236.32	234.78	236.26	234.00	235.74	230.88	232.6	230.89	233.0
28. y_o, y_1	0.020257	0.008691	0.020119	0.008802	0.020457	0.008852	0.020718	0.008940	0.020378	0.009914	0.020312	0.0100
29. VAPOR PRES.OF LIQ.ON PLATE IN Hg	0.82		0.817		0.82		0.823		0.82		0.82	
30. y*	0.026983		0.027017		0.027471		0.027663		0.027315		0.027315	
31. E_{OG}%	63.23		62.13		62.33		62.90		60.13		59.55	
32. $N_{OG} = -\ell n\ (1-E_{OG})$	1.037		1.031		1.0125		1.028		0.92		0.906	
33. v_s, FT/SEC	2.20		2.20		3.250		3.255		4.036		4.3608	
34. ρ_G LB/FT^3	0.0705		0.0703		0.0694		0.0696		0.0704		0.07035	
35. $F = v_s\sqrt{\rho_G}$	0.585		0.585		0.858		0.862		1.0655		1.155	
36. t_G, SEC	0.1705		0.1704		0.168		0.1655		0.1656		0.1588	
37. k'_{Ga}, SEC^{-1}	6.080		6.070		6.025		6.210		5.555		5.705	

* INLET SAMPLE DATA TAKEN FROM E-6-B.

TABLE I-G (CONTINUED)

PLATE EFFICIENCIES IN RECTANGULAR COLUMN AT UNIVERSITY OF MICHIGAN
(ORIGINAL DATA FOR N_2-ETHYLENE DIBROMIDE SYSTEM)
3.50-IN. WEIR, 4-IN. SPLASH BAFFLE

RUN NO.	E-18-A		E-18-B		E-19-A		E-19-B		E-20-A		E-20-B	
1. GAS ROT. RDG.	60		60		81		82		115		116	
2. LIQ. ROT. RDG.	80		80		79.5		79		79.5		79.5	
3. BAROMETRIC PRESSURE, IN Hg	29.10		29.10		29.03		29.03		29.00		29.00	
4. PRESSURE IN GAS ROT., IN Hg	2.60		2.60		2.50		2.60		3.40		3.00	
5. PRESSURE ABOVE PLATE, IN Hg	1.50		1.55		1.30		1.30		1.70		1.60	
6. PRESSURE DROP ACROSS PLATE, IN H_2O	8.25		6.90		9.10		8.80		11.00		10.10	
7. FROTH HEIGHT, IN.	9.0		8.5		10.1		10.1		11.4		11.4	
8. CLEAR LIQ. HT. AT POSITION 2, IN	4.60		4.5		4.90		4.70		5.50		4.90	
9. 3	4.00		3.95		4.10		4.40		4.40		4.05	
10. 4	4.10		4.05		4.20		4.10		4.70		4.20	
11. 5	4.25		4.10		4.30		4.20		4.90		4.30	
12. AVG. CLEAR LIQ. HT. IN.	4.24		4.15		4.37		4.35		4.88		4.425	
13. AVG. LIQ. TEMP. ON PLATE, °F	93.56		93.88		93.60		94.21		93.0		92.8	
14. LIQ. TEMP. IN ROT. °F	86.0		87.4		91.80		93.0		90.4		90.4	
15. TEMP. OF GAS BELOW PLATE, °F	130.8		132.5		131.1		132.5		130.8		130.6	
16. TEMP. IN GAS ROT. °F	82.4		82.4		81.5		81.5		81.8		81.68	
17. SAMPLING POINT	OUTLET	INLET	OUTLET	INLET	OUTLET	INLET	OUTLET	INLET	OUTLET	INLET	OUTLET	INLET
18. TEMP. OF GAS SAMPLE METER, °F	80	79.75	80.2	80.0	80.0	79.8	79.5	79.5	82.2	82.0	82.6	82.3
19. PRESSURE IN METER, IN H_2O	--	--	--	--	--	--	--	--	--	--	--	--
20. METERED SAMPLE VOL. FT^3	1.0000	1.0000	1.0000	1.0000	1.0000	1.0000	1.0000	1.0000	1.0000	1.0000	1.0000	1.0000
21. METER CORRECTION FACTOR	0.986	1.003	0.986	1.003	0.986	1.003	0.986	1.003	0.986	1.003	0.986	1.003
22. CORRECTED SAMPLE VOLUME, FT^3	0.986	1.003	0.986	1.003	0.986	1.003	0.986	1.003	0.986	1.003	0.986	1.003
23. LB. MOL OF GAS PER FT^3 MET. X 10^5	238.1	238.3	238.1	238.1	237.6	237.6	237.9	237.9	235.7	235.7	235.4	235.40
24. LB. MOL OF GAS IN SAMPLE X 10^5	234.7	239.0	234.7	238.8	234.2	238.2	234.5	237.9	232.4	235.7	232.1	236.11
25. ETHYLENE DIBROMIDE ABS. IN TUBES, gm	4.0602	1.9829	4.1501	2.2425	4.1460	1.9727	4.1936	1.9579	4.0114	2.0009	3.9966	1.9404
26. ETHYLENE DIBROMIDE ABS. IN TUBES, LB. MOL X 10^5	4.76	2.326	4.87	2.63	4.86	2.31	4.40	2.29	4.706	2.340	4.689	2.276
27. TOT. MOLS IN SAMPLE LB. MOL X 10^5	239.46	241.33	239.57	241.43	239.06	240.51	239.40	240.19	237.10	238.04	236.79	236.10
28. y_o, y_1	0.019870	0.09639	0.020328	0.010893	0.020329	0.0096	0.020487	0.009537	0.019848	0.00983	0.01980	0.009639
29. VAPOR PRES. OF LIQ. ON PLATE IN Hg	0.823		0.824		0.82		0.835		0.81		0.81	
30. y*	0.026895		0.026884		0.027035		0.027530		0.0263		0.026470	
31. E_{OG}%	59.46		59.0		61.53		60.74		60.82		60.37	
32. $N_{OG} = -\ell n\ (1-E_{OG})$	0.899		0.8878		0.9795		0.9315		0.933		0.9269	
33. v_s, FT/SEC	1.2107		1.2076		2.2509		2.2826		3.192		3.214	
34. ρ_G LB/FT^3	0.07218		0.07259		0.07084		0.07069		0.07181		0.07145	
35. $F = v_s\sqrt{\rho_G}$	0.3245		0.3254		0.598		0.607		0.855		0.8597	
36. t_G, SEC	0.3278		0.3001		0.2119		0.2135		0.1703		0.1747	
37. $k'_G a$, SEC^{-1}	2.7425		2.958		4.613		4.362		5.4785		5.305	

* INLET SAMPLE DATA TAKEN FROM E-6-B.

TABLE I-G (CONTINUED)

PLATE EFFICIENCIES IN RECTANGULAR COLUMN AT UNIVERSITY OF MICHIGAN
(ORIGINAL DATA FOR N_2-CYCLOHEXANOL SYSTEM)
1.50 IN. WEIR, 4-IN. SPLASH BAFFLE

RUN NO.	H-1-B		H-2-A		H-3-A		H-3-B	
1. GAS ROT. RDG.	120		120		80		80	
2. LIQ. ROT. RDG.	25		25		25		25	
3. BAROMETRIC PRESSURE, IN Hg	29.23		29.14		29.23		29.23	
4. PRESSURE IN GAS ROT., IN Hg	2.55		2.65		2.20		2.25	
5. PRESSURE ABOVE PLATE, IN Hg	1.80		2.05		1.87		1.90	
6. PRESSURE DROP ACROSS PLATE, IN H_2O	--		--		2.00		2.10	
7. FROTH HEIGHT, IN.	5.3		5.3		4.10		4.2	
8. CLEAR LIQUID HT. AT POSITION 2, IN	1.95		1.95		2.00		2.00	
9. 3	1.35		1.35		1.50		1.55	
10. 4	1.35		1.35		1.60		1.60	
11. 5	1.70		1.70		1.70		1.70	
12. AVG. CLEAR LIQ. HT. IN.	1.59		1.59		1.70		1.71	
13. AVG. LIQ. TEMP. ON PLATE, °F	114.4		114.0		115.9		115.7	
14. LIQ. TEMP. IN ROT., °F	113.1		109.1		113.2		102.9	
15. TEMP. OF GAS BELOW PLATE, °F	114.0		109.8		117.4		115.9	
16. TEMP. IN GAS ROT., °F	77.6		75.4		81.1		81.1	
17. SAMPLING POINT	OUTLET	INLET	OUTLET	INLET	OUTLET	INLET	OUTLET	INLET
18. TEMP. OF GAS SAMPLE METER, °F	78.50	79.00	78.6	78.8	81.5	81.6	81.5	82.0
19. PRESSURE IN METER, IN H_2O	--	--	--	--	--	--	--	--
20. METERED SAMPLE VOL. FT^3	0.9999	0.9997	0.6001	0.7365	0.0231	1.0000	1.0000	1.0008
21. METER CORRECTION FACTOR	0.986	1.003	1.003	0.986	1.003	0.986	1.003	0.986
22. CORRECTED SAMPLE VOLUME, FT^3	0.986	1.003	0.6019	0.7262	0.6250	0.986	1.003	0.9868
23. LB. MOL. OF GAS PER FT^3 MET. X 10^5	240.1	239.7	239.6	239.8	238.3	238.2	238.3	237.6
24. LB. MOL. OF GAS IN SAMPLE X 10^5	236.8	240.4	144.0	174.0	149.0	235.0	239.0	234.0
25. CYCLOHEXANOL ABSORBED IN TUBES, gm	0.5708	0.2922	0.3642	0.2035	0.3750	0.3191	0.7149	0.3174
26. CYCLOHEXANOL ABS. IN TUBES, LB. MOL. X 10^5	1.240	0.644	0.803	0.450	0.825	0.702	1.351	0.699
27. TOT. MOL. IN SAMPLE, LB.MOL.X 10^5	238.04	241.044	144.80	174.45	149.825	235.7	240.351	234.7
28. y_o, y_1, MOLS. CYCLOHEXANOL/MOL.GAS	0.00521	0.00267	0.00555	0.00258	0.00351	0.00298	0.00562	0.002979
29. VAPOR PRES. OF LIQ. ON PLATE, IN Hg	0.2165		0.204		0.2244		0.2205	
30. y^*	0.00697		0.00681		0.00721		0.00705	
31. E_{OG}%	35.8		70.3		59.9		65.0	
32. $N_{OG} = -\ell n\ (1-E_{OG})$	0.445		1.225		0.922		1.061	
33. v_s, FT/SEC	3.332		3.32		2.21		2.18	
34. ρ_G LB/FT^3	0.0701		0.0702		0.0698		0.0707	
35. $F = v_s\sqrt{\rho_G}$	0.884		0.882		0.584		0.580	
36. t_G, SEC	0.0928		0.0932		0.0999		0.0951	
37. k'_Ga, SEC-1	4.80		13.14		9.24		11.17	

TABLE I-G (CONTINUED)

PLATE EFFICIENCIES IN RECTANGULAR COLUMN AT UNIVERSITY OF MICHIGAN
(ORIGINAL DATA FOR N_2-CYCLOHEXANOL SYSTEM)
1.50-IN. WEIR, 2-IN. SPLASH BAFFLE

RUN NO.		H-4-A		H-4-B		H-5-A		H-5-B		H-6-A		H-7-A	
1.	GAS ROT. RDG.	120		120		120		120		160		80	
2.	LIQ. ROT. RDG.	25		25		25		25		25		25	
3.	BAROMETRIC PRESSURE, IN Hg ABS.	29.30		29.30		29.40		29.4		29.5		29.065	
4.	PRESSURE IN GAS ROT., IN Hg	1.85		2.00		2.45		2.80		3.30		2.00	
5.	PRESSURE ABOVE PLATE, IN Hg	2.50		2.60		1.85		2.00		2.20		1.60	
6.	PRESSURE DROP ACROSS PLATE, IN H_2O	3.00		2.80		2.90		2.80		3.90		2.00	
7.	FROTH HEIGHT, IN.	5.50		5.5		5.7		5.7		7.0		4.4	
8.	CLEAR LIQ. HT., POSITION 2, IN.	1.90		1.85		2.10		2.10		2.15		2.15	
9.	3	1.50		1.55		1.55		1.55		1.50		1.70	
10.	4	1.50		1.55		1.55		1.55		1.50		1.80	
11.	5	1.90		1.90		2.30		2.30		2.10		1.90	
12.	AVG. CLEAR LIQ. HT. IN.	1.70		1.71		1.81		1.81		1.81		1.89	
13.	AVG. LIQ. TEMP. ON PLATE, °F	101.35		101.44		100.76		100.78		99.77		100.63	
14.	LIQ. TEMP. IN ROT. °F	95.5		95.4		97.7		97.9		95.3		100.0	
15.	TEMP. OF GAS BELOW PLATE, °F	108.0		108.5		106.5		107.0		105.0		106.0	
16.	TEMP. IN GAS ROT., °F	78.0		78.1		76.6		76.5		95.4		77.1	
17.	SAMPLING POINT	OUTLET	INLET	OUTLET	INLET	OUTLET	INLET	OUTLET	INLET	OUTLET	INLET	OUTLET	INLET
18.	TEMP. OF GAS SAMPLE METER, °F	83.8	83.2	83.8	84.2	78.2	78.2	78.4	78.4	71.0	71.0	72.5	72.5
19.	PRESSURE IN METER IN H_2O	--	--	--	--	--	--	--	--	--	--	--	--
20.	METERED SAMPLE VOL. FT^3	1.000	1.000	1.0325	1.0000	1.0000	1.0000	1.0000	1.000	1.0000	1.0000	1.0000	1.0000
21.	METER CORRECTION FACTOR	1.003	0.986	1.003	0.986	1.003	0.986	1.003	0.986	0.986	1.003	0.986	1.003
22.	CORRECT SAMPLE VOL. FT^3	1.003	0.986	1.038	0.986	1.003	0.986	1.003	0.986	0.986	1.003	0.986	1.003
23.	LB.MOL.OF GAS/FT^3 MET.X 10^5	237.15	237.75	237.15	236.65	241.6	241.6	241.6	241.6	243.3	243.8	243.0	243.0
24.	LB.MOL.OF GAS IN SAMPLE X 10^5	238.0	234.0	246.0	234.0	242.0	238.0	242.0	238.0	239.9	244	240.0	244.0
25.	CYCLOHEXANOL ABSD.IN TUBE, gm	0.5057	0.3174	0.4618	0.3147	0.4325	0.2976	0.4335	0.2925	0.4205	0.2402	0.4932	0.3011
26.	CYCLOHEXANOL ABSD.IN TUBE, LB. MOL. X 10^5	1.115	0.699	1.015	0.694	0.952	0.655	0.954	0.645	0.925	0.53	0.889	0.663
27.	TOT.MOLS.IN SAMPLE LB.MOL.X 10^5	239.115	234.699	247.015	234.7	242.4	238.3	242.4	238.65	240.83	244.5	240.9	244.7
28.	y_o, y_1 MOLS.CYCLOHEXANOL/MOL.GAS	0.01678	0.00298	0.00412	0.002952	0.00392	0.00274	0.00392	0.00270	0.00384	0.002168	0.00369	0.00271
29.	VAPOR PRES. OF LIQ.ON PLATE, IN Hg	0.138		0.138		0.134		0.135		0.128		0.132	
30.	y^*	0.00434		0.00433		0.00428		0.00430		0.00404		0.00427	
31.	E_{OG}%	124.1		84.8		76.7		76.3		89.3		62.8	
32.	$N_{OG} = -\ell n\ (1-E_{OG})$	--		1.882		1.436		1.440		2.24		0.995	
33.	v_s, FT/SEC	--		--		3.28		3.288		4.19		2.165	
34.	ρ_G LB/FT^3	--		--		0.0716		0.0716		0.0725		0.0708	
35.	$F = v_s\sqrt{\rho_G}$	--		--		0.877		0.878		1.130		0.576	
36.	t_G, SEC	--		--		0.0989		0.0986		0.103		0.0966	
37.	$k'_G a$, SEC^{-1}	--		--		14.52		14.60		21.5		10.3	

TABLE I-G (CONTINUED)

PLATE EFFICIENCIES IN RECTANGULAR COLUMN AT UNIVERSITY OF MICHIGAN
(ORIGINAL DATA FOR N_2-CYCLOHEXANOL SYSTEM)
1.50-IN. WEIR, 2-IN. SPLASH BAFFLE

RUN NO.	H-7-B		H-8-A		H-8-A		H-9-A		H-9-B	
1. GAS ROT. RDG.	80		40		40		160		160	
2. LIQ. ROT. RDG.	25		25		25		25		25	
3. BAROMETRIC PRESSURE, IN Hg ABS.	29.065		29.07		29.07		28.86		28.86	
4. PRESSURE IN GAS ROT., IN Hg	2.20		2.10		2.00		2.65		2.65	
5. PRESSURE ABOVE PLATE, IN Hg	1.85		1.80		1.80		1.60		1.60	
6. PRESSURE DROP ACROSS PLATE, IN H_2O	2.10		1.60		1.55		4.00		4.00	
7. FROTH HEIGHT, IN.	4.35		3.5		3.5		7.1		7.0	
8. CLEAR LIQ.HT. POSITION 2, IN.	2.15		2.00		2.05		2.15		2.15	
9. 3	1.70		1.80		1.80		1.45		1.50	
10. 4	1.80		1.85		1.85		1.40		1.45	
11. 5	1.90		1.90		1.90		2.15		2.15	
12. AVG. CLEAR LIQ. HT. IN.	1.89		1.89		1.90		1.79		1.81	
13. AVG. LIQ. TEMP. ON PLATE, °F	100.62		102.2		102.3		99.9		99.9	
14. LIQ. TEMP. IN ROT. °F	99.4		99.6		99.5		92.0		91.8	
15. TEMP. OF GAS BELOW PLATE, °F	106.2		107.9		109.0		104.5		104.5	
16. TEMP. IN GAS ROT., °F	77.5		79.7		80.0		73.0		73.0	
17. SAMPLING POINT	OUTLET	INLET	OUTLET	INLET	OUTLET	INLET	OUTLET	INLET	OUTLET	INLET
18. TEMP. OF GAS SAMPLE METER, °F	74.3	74.2	78.0	78.0	78.7	78.5	80.8	80.7	81.8	81.8
19. PRESSURE IN METER IN H_2O	--	--	--	--	--	--	--	--	--	--
20. METERED SAMPLE VOL. FT^3	1.000	1.000	1.0000	1.0000	1.0000	1.0000	1.000	1.000	1.000	1.000
21. METER CORRECTION FACTOR	0.986	1.003	0.986	1.003	0.986	1.003	0.986	1.003	0.986	1.003
22. CORRECT SAMPLE VOL. FT^3	0.986	1.003	0.986	1.003	0.986	1.003	0.986	1.003	0.986	1.003
23. LB.MOL.OF GAS/FT^3 MET. X 10^5	242.8	242.8	244.5	244.5	241.3	241.3	232.7	232.7	234.5	234.5
24. LB.MOL.OF GAS IN SAMPLE X 10^5	239.4	244.0	241.3	245.5	238.0	242.0	229.5	234.0	231.5	236.0
25. CYCLOHEXANOL ABSD.IN TUBE, gm	0.3681	0.2934	0.4016	0.3229	0.3960	0.3314	0.3929	0.3022	0.3906	0.2876
26. CYCLOHEXANOL ABSD.IN TUBE, LB. MOL. X 10^5	0.811	0.646	0.844	0.712	0.871	0.730	0.866	0.666	0.860	0.633
27. TOT.MOLS.IN SAMPLE LB.MOL.X 10^5	239.77	244.65	242.1	246.2	238.4	242.73	230.37	234.67	232.36	236.63
28. y_o, y_1 MOLS.CYCLOHEXANOL/MOL.GAS	0.003385	0.002648	0.003665	0.00290	0.003662	0.00302	0.00378	0.002845	0.003715	0.002685
29. VAPOR PRES. OF LIQ. ON PLATE, IN Hg	0.132		0.133		0.134		0.122		0.122	
30. y^*	0.00427		0.004308		0.004309		0.004000		0.004000	
31. E_{OG}%	45.5		54.5		50.0		80.9		78.3	
32. $N_{OG} = -\ell n\ (1-E_{OG})$	0.612		0.794		0.696		1.659		1.535	
33. v_s, FT/SEC	2.17		1.088		1.082		4.44		4.44	
34. ρ_G LB/FT^3	0.0703		0.0705		0.0704		0.0700		0.0698	
35. $F = v_s\sqrt{\rho_G}$	0.575		0.289		0.288		1.177		1.173	
36. t_G, SEC	0.0944		0.1232		0.1232		0.0997		0.0972	
37. k'_Ga, SEC^{-1}	6.49		6.43		5.65		16.65		15.70	

TABLE I-G (CONTINUED)

PLATE EFFICIENCIES IN RECTANGULAR COLUMN AT UNIVERSITY OF MICHIGAN
(ORIGINAL DATA FOR N_2-CYCLOHEXANOL SYSTEM)
3.50-IN. WEIR, 4-IN. SPLASH BAFFLE

RUN NO.	H-31-A		H-31-B		H-32-A		H-32-B		H-33-A		H-33-B		H-34-A		H-34-B	
1. GAS ROT. RDG.	80		80		118		118		149		149		46		44	
2. LIQ. ROT. RDG.	25		25		25		25		25		25		26		25	
3. BAROMETRIC PRESSURE, IN Hg ABS.	29.18		29.18		29.24		29.24		29.24		29.24		29.19		29.19	
4. PRESSURE IN GAS ROT., IN Hg	2.30		2.40		2.35		2.20		2.62		2.50		2.40		2.50	
5. PRESSURE ABOVE PLATE, IN Hg	1.90		1.90		1.60		1.50		1.60		1.50		2.15		2.20	
6. PRESSURE DROP ACROSS PLATE, IN H_2O	3.80		3.80		4.40		4.40		5.15		5.20		3.30		3.30	
7. FROTH HEIGHT, IN.	7.7		7.7		8.8		9.0		100		10		6.7		6.7	
8. CLEAR LIQ. HT. POSITION 2, IN.	4.00		4.00		3.90		3.95		3.75		3.80		3.90		3.90	
9. 3	3.20		3.20		2.90		2.90		2.70		2.75		3.35		3.35	
10. 4	3.40		3.40		3.00		3.00		2.65		2.70		3.50		3.45	
11. 5	3.97		3.97		3.55		3.55		3.30		3.55		3.80		3.80	
12. AVG. CLEAR LIQ. HT. IN.	3.64		3.64		3.34		3.35		3.10		3.15		3.64		3.63	
13. AVG. LIQ. TEMP. ON PLATE, °F	122.0		122.0		122.0		122.0		121.8		121.5		121.7		122.0	
14. LIQ. TEMP. ON ROT. °F	113.0		113.8		118.7		118.9		118.4		118.2		118.2		118.5	
15. TEMP. OF GAS BELOW PLATE, °F	139.5		140.5		140.5		140.2		140.0		140		139.0		140.7	
16. TEMP. IN GAS ROT., °F	65.1		65.2		71		71.3		70.7		71.1		71.5		71.3	
17. SAMPLING POINT	OUTLET	INLET	OUTLET	INLET	OUTLET	INLET	OUTLET	INLET	OUTLET	INLET	OUTLET	INLET	OUTLET	INLET	OUTLET	INLET
18. TEMP. OF GAS SAMPLE METER, °F	73.0	73.2	72.9	73.0	71.0	71.5	71.3	71.7	70.5	71.5	70.5	71.2	72.0	72.0	72.2	72.5
19. PRESSURE IN METER IN H_2O	--	--	--	--	--	--	--	--	--	--	--	--	--	--	--	--
20. METERED SAMPLE VOL. FT^3	2.0000	2.0000	2.0000	2.0000	2.0000	2.0000	2.0000	2.0000	2.0000	2.0000	2.0000	2.0000	2.0000	2.0000	2.0000	2.0000
21. METER CORRECTION FACTOR	0.986	1.003	0.986	1.003	0.986	1.003	0.986	1.003	0.986	1.003	0.986	1.003	0.986	1.003	0.986	1.003
22. CORRECT SAMPLE VOL. FT^3	1.972	2.006	1.972	2.006	1.972	2.006	1.972	2.006	1.972	2.006	1.972	2.006	1.972	2.006	1.972	2.006
23. LB. MOL. OF GAS/FT^3 MET. X 10^5	242.95	242.95	244.0	244.0	245.3	245.3	245.3	245.3	245.4	245.4	254.4	254.4	244.2	244.2	243.5	243.5
24. LB. MOL. OF GAS IN SAMPLE X 10^5	479.5	488.0	482.0	490.0	484.0	492.0	484.0	492.0	484.0	492.0	484	492	482	490	480	488
25. CYCLOHEXANOL ABSD. IN TUBE, gm	1.3691	0.5604	1.3594	0.5545	1.4043	0.418	1.4339	0.4092	1.4367	0.4160	1.4513	--	1.2449	0.5239	1.2392	0.5246
26. CYCLOHEXANOL ABSD. IN TUBE, LB. MOL. X 10^5	3.01	1.235	2.99	1.22	3.10	0.92	3.16	0.900	3.16	0.915	3.30	--	2.74	1.15	2.72	1.153
27. TOT. MOLS. IN SAMPLE LB. MOL.X 10^5	482.51	489.2	484.99	491.22	487.10	492.92	287.16	492.9	487.16	492.92	487.2	--	484.74	491.15	482.72	489.15
28. y_o, y_1 MOLS.CYCLOHEXANOL/MOL. GAS	0.00624	0.002524	0.00617	0.002482	0.00635	0.001867	0.00650	0.001829	0.0065	0.00186	0.00657	0.00186*	0.00565	0.002346	0.00565	0.00236
29. VAPOR PRES. OF LIQ. ON PLATE, IN Hg	0.282		0.282		0.282		0.282		0.28		0.278		0.28		0.282	
30. y^*	0.00908		0.00908		0.00914		0.00919		0.00907		0.00905		0.00895		0.009000	
31. E_{OG}%	57.5		56.0		61.6		64.3		64.3		65.5		50.0		49.6	
32. $N_{OG} = -\ln(1-E_{OG})$	0.859		0.822		0.956		1.03		1.109		1.064		0.094		0.69	
33. v_s, FT/SEC	2.31		2.32		3.42		3.44		4.34		4.34		1.31		1.262	
34. ρ_G LB/FT^3	0.0675		0.0671		0.067		0.0667		0.067		0.0666		0.0682		0.0676	
35. $F = v_s\sqrt{\rho_G}$	0.60		0.601		0.885		0.886		1.123		1.12		0.343		0.328	
36. t_G, SEC	0.146		0.1454		0.133		0.137		0.1327		0.132		0.195		0.2024	
37. $k'_G a$, SEC^{-1}	5.88		5.65		7.19		7.52		8.35		8.08		3.54		3.4	

* BORROW FROM RUN H-33-A.

TABLE I-G (CONTINUED)

PLATE EFFICIENCIES IN RECTANGULAR COLUMN AT UNIVERSITY OF MICHIGAN
(ORIGINAL DATA FOR N_2-CYCLOHEXANOL SYSTEM)
2-IN. WEIR, 2.50-IN. SPLASH BAFFLE

RUN NO.	H-28-A		H-28-B		H-27-A		H-27-B		H-29-A		H-29-B	
1. GAS ROT. RDG.	40		40		80		78		120		120	
2. LIQ. ROT. RDG.	25		25		25		25		25		25	
3. BAROMETRIC PRESSURE, IN Hg ABS.	29.38		29.38		29.37		29.37		29.2		29.3	
4. PRESSURE IN GAS ROT., IN Hg	1.90		2.20		2.50		2.50		2.40		2.55	
5. PRESSURE ABOVE PLATE, IN Hg	1.70		1.90		2.10		2.10		1.64		1.84	
6. PRESSURE DROP ACROSS PLATE, IN H_2O	1.80		1.90		2.45		2.50		3.10		3.28	
7. FROTH HEIGHT, IN.	4.3		4.2		5.7		5.7		6.5		6.8	
8. CLEAR LIQ. HT. POSITION 2, IN.	2.45		2.50		2.60		2.60		2.55		2.60	
9. 3	2.20		2.20		2.05		2.10		1.95		1.95	
10. 4	2.30		2.30		2.20		2.20		1.90		1.95	
11. 5	2.35		2.35		2.40		2.40		2.40		2.4	
12. AVG. CLEAR LIQ. HT. IN.	2.38		2.34		2.31		2.33		2.20		2.23	
13. AVG. LIQ. TEMP. ON PLATE, °F	121.55		121.55		121.37		--		121.1		122.61	
14. LIQ. TEMP. ON ROT. °F	118.6		119.1		119.0		118.5		119.7		119.0	
15. TEMP. OF GAS BELOW PLATE, °F	134.0		135.2		133.9		135.9		141.2		139	
16. TEMP. IN GAS ROT., °F	80.3		80.4		78.0		78.3		76.2		76.0	
17. SAMPLING POINT	OUTLET	INLET	OUTLET	INLET	OUTLET	INLET	OUTLET	INLET	OUTLET	INLET	OUTLET	INLET
18. TEMP. OF GAS SAMPLE METER, °F	81.6	81.5	81.2	81.5	76.0	76.4	77.3	77.5	76.2	77.2	78.0	78.9
19. PRESSURE IN METER IN H_2O	--	--	--	--	--	--	--	--	--	--	--	--
20. METER CORRECTION FACTOR	2.0205	2.0000	2.0183	2.0000	2.0000	2.0000	2.0016	2.0000	2.2511	2.0011	2.0047	2.0000
21. METER CORRECTION FACTOR	0.986	1.003	0.986	1.003	0.986	1.003	0.986	1.003	0.986	1.003	0.986	1.003
22. CORRECT SAMPLE VOL. FT^3	1.972	2.000	1.9900	2.006	1.972	2.006	1.977	2.006	2.196	2.0071	1.9766	2.006
23. LB. MOL. OF GAS/FT^3 MET. X 10^5	238.75	238.75	238.7	238.7	242.6	242.1	241.87	241.85	241.0	241.0	241.1	241.1
24. LB. MOL. OF GAS IN SAMPLE X 10^5	472.0	479.0	474.0	479	479	486.0	477.6	484	535	484	476.4	484
25. CYCLOHEXANOL ABSD. IN TUBE, gm	1.2619	0.5700	1.2437	0.5797	1.3126	0.5502	1.3402	0.5647	1.6166	0.4417	1.3964	0.4537
26. CYCLOHEXANOL ABSD. IN TUBE, LB. MOL. X 10^5	2.780	1.255	2.74	1.276	2.993	1.212	2.954	1.24	3.56	0.971	3.076	0.997
27. TOT. MOLS. IN SAMPLE LB.MOL. X 10^5	474.78	480.255	476.74	480.3	482.3	487.2	480.55	485.24	538.56	484.97	479.48	485
28. y_o, y_1 MOLS.CYCLOHEXANOL/MOL. GAS	0.00585	0.00262	0.00575	0.00266	0.00600	0.002492	0.00614	0.00256	0.00663	0.002000	0.00641	0.00206
29. VAPOR PRES. OF LIQ. ON PLATE, IN Hg	0.278		0.278		0.274		0.274		0.29		0.289	
30. y*	0.00894		0.00893		0.00870		0.00870		0.00939		0.00931	
31. E_{OG}%	51.1%		49.3%		56.5		58.5		62.7		60.0	
32. $N_{OG} = -\ell n\ (1-E_{OG})$	0.715		0.68		0.834		0.90		0.985		0.917	
33. v_s, FT/ SEC	1.110		1.136		2.26		2.19		3.42		3.44	
34. ρ_G LB/FT^3	0.0676		0.0678		0.0687		0.069		0.068		0.0674	
35. $F = v_s\sqrt{\rho_G}$	0.2886		0.296		0.5925		0.575		0.891		0.895	
36. t_G, SEC	0.148		0.1365		0.125		0.128		0.1063		0.103	
37. $k'_G a$, SEC^{-1}	4.82		4.98		6.67		7.000		9.35		8.91	

TABLE I-G (CONTINUED)

PLATE EFFICIENCIES IN RECTANGULAR COLUMN AT UNIVERSITY OF MICHIGAN
(ORIGINAL DATA FOR N_2-CYCLOHEXANOL SYSTEM)
2-IN. WEIR, 2.50-IN. SPLASH BAFFLE

RUN NO.		H-30-A		H-30-B		H-14-A		H-14-B		H-25-A		H-25-B	
1.	GAS ROT. RDG.	150		150		40		40		40		40	
2.	LIQ. ROT. RDG.	25		25		25		25		25		25	
3.	BAROMETRIC PRESSURE, IN Hg ABS.	29.10		29.10		29.26		29.26		29.51		29.51	
4.	PRESSURE IN GAS ROT., IN Hg	2.65		2.70		1.60		1.70		2.40		2.20	
5.	PRESSURE ABOVE PLATE, IN Hg	1.64		1.74		1.50		1.55		2.15		2.05	
6.	PRESSURE DROP ACROSS PLATE, IN H_2O	4.18		4.05		2.00		2.00		2.00		1.95	
7.	FROTH HEIGHT, IN.	7.5		7.5		4.6		4.7		4.6		4.60	
8.	CLEAR LIQ. HT. POSITION 2, IN.	2.50		2.60		2.50		2.50		2.50		2.50	
9.	3	1.95		1.95		2.20		2.20		2.15		2.20	
10.	4	1.90		1.95		2.27		2.30		2.25		2.25	
11.	5	2.55		2.60		2.33		2.35		2.30		2.30	
12.	AVG. CLEAR LIQ. HT. IN.	2.25		2.28		2.33		2.34		2.30		2.31	
13.	AVG. LIQ. TEMP. ON PLATE, °F	121.82		122.36		99.32		99.1		101.0		100.9	
14.	LIQ. TEMP. ON ROT. °F	119.0		119.5		95.9		95.2		99.7		99.0	
15.	TEMP. OF GAS BELOW PLATE, °F	138.1		138.2		102.6		102.6		106.7		104.2	
16.	TEMP. IN GAS ROT., °F	75.1		75.7		75.8		75.6		75.0		75.5	
17.	SAMPLING POINT	OUTLET	INLET	OUTLET	INLET	OUTLET	INLET	OUTLET	INLET	OUTLET	INLET	OUTLET	INLET
18.	TEMP. OF GAS SAMPLE METER, °F	74.1	75.5	75.1	76.9	76.8	76.2	76.8	76.2	71.0	70.9	71.5	72.0
19.	PRESSURE IN METER IN H_2O	--	--	--	--	--	--	--	--	--	--	--	--
20.	METERED SAMPLE VOL. FT^3	2.006	2.0000	2.0000	2.0000	1.0000	1.0000	1.0000	1.0000	2.0000	2.0000	2.0000	2.0000
21.	METER CORRECTION FACTOR	0.986	1.003	0.986	1.003	0.986	1.003	0.986	1.003	1.003	0.986	0.986	1.003
22.	CORRECT SAMPLE VOL. FT^3	1.980	2.006	1.972	2.006	0.986	1.003	0.986	1.003	2.006	1.972	1.972	2.006
23.	LB. MOL. OF GAS/FT^3 MET. X 10^5	242.7	240.7	241.3	232.05	242.1	242.3	242.1	242.3	248.0	248.0	247.0	247.
24.	LB. MOL. OF GAS IN SAMPLE X 10^5	481	484	476	466	287.3	243.0	238.7	243.0	497.0	489.5	487.7	495
25.	CYCLOHEXANOL ABSD. IN TUBE, gm	1.3998	0.4688	1.3999	0.4454	0.3385	0.2535	0.3426	0.2424	0.7650	0.4942	0.7494	0.4964
26.	CYCLOHEXANOL ABSD. IN TUBE, LB. MOL. X 10^5	3.08	1.031	3.08	0.98	0.746	0.558	0.755	0.535	1.683	1.089	1.65	1.092
27.	TOT. MOLS. IN SAMPLE LB. MOL. X 10^5	484.08	485.031	479.1	466.98	239.45	243.6	239.5	243.5	298.7	490.6	489.35	496.1
28.	y_o, y_1 MOLS. CYCLOHEXANOL/MOL. GAS	0.00636	0.002134	0.00644	0.0021	0.003115	0.002291	0.003153	0.002197	0.00338	0.00222	0.003375	0.00201
29.	VAPOR PRES. OF LIQ. ON PLATE, IN Hg	0.28		0.282		0.127		0.127		0.137		0.135	
30.	y^*	0.00911		0.00915		0.00413		0.00412		0.00435		0.0043	
31.	E_{OG}%	60.6		61.5		44.93		49.71		54.5		59.6	
32.	$N_{OG} = -\ln (1-E_{OG})$	0.933		0.955		0.613		0.730		0.789		0.91	
33.	v_s, FT/SEC	4.36		4.35		1.107		1.082		1.08		1.084	
34.	ρ_G LB/FT^3	0.0667		0.067		0.0705		0.0708		0.0718		0.0718	
35.	$F = v_s\sqrt{\rho_G}$	1.127		1.128		0.294		0.288		0.2898		0.2904	
36.	t_G, SEC	0.103		0.10		0.1711		0.1815		0.1775		0.176	
37.	$k'_G a$, SEC^{-1}	9.30		9.55		3.58		4.022		4.44		5.17	

TABLE I-G (CONTINUED)

PLATE EFFICIENCIES IN RECTANGULAR COLUMN AT UNIVERSITY OF MICHIGAN
(ORIGINAL DATA FOR N_2-CYCLOHEXANOL SYSTEM)
2-IN. WEIR, 2.50-IN. SPLASH BAFFLE

RUN NO.	H-12-A		H-12-B		H-13-A		H-13-B		H-15-A		H-17-A	
1. GAS ROT. RDG.	80		80		80		80		80		80	
2. LIQ. ROT. RDG.	25		25		25		25		25		25	
3. BAROMETRIC PRESSURE, IN Hg ABS.	28.84		28.84		29.27		29.27		29.37		29.66	
4. PRESSURE IN GAS ROT., IN Hg	2.15		2.20		2.35		2.35		2.25		2.58	
5. PRESSURE ABOVE PLATE, IN Hg	1.80		1.90		1.95		1.85		1.85		2.25	
6. PRESSURE DROP ACROSS PLATE, IN H_2O	2.60		2.40		2.65		2.40		2.40		2.65	
7. FROTH HEIGHT, IN.	4.3		4.5		5.3		5.2		5.50		5.1	
8. CLEAR LIQ. HT. POSITION 2, IN.	2.65		2.60		2.65		2.62		2.60		2.60	
9. 3	2.10		2.05		2.10		2.07		2.10		2.05	
10. 4	2.20		2.20		2.25		2.21		2.20		2.10	
11. 5	2.40		2.40		2.40		2.39		2.40		2.4	
12. AVG. CLEAR LIQ. HT. IN.	2.34		2.31		2.35		2.32		2.33		2.29	
13. AVG. LIQ. TEMP. ON PLATE, °F	99.97		99.3		99.5		99.32		100.1		94.1	
14. LIQ. TEMP. ON ROT. °F	97.2		97.0		91.0		90.5		90.9		95.2	
15. TEMP. OF GAS BELOW PLATE, °F	104.8		105.2		103.7		102.1		105.4		98.6	
16. TEMP. IN GAS ROT., °F	73.0		73.2		68.2		68.0		66.9		69.9	
17. SAMPLING POINT	OUTLET	INLET	OUTLET	INLET	OUTLET	INLET	OUTLET	INLET	OUTLET	INLET	OUTLET	INLET
18. TEMP. OF GAS SAMPLE METER, °F	69.0	69.0	69.0	69.0	75.2	74.0	75.8	74.7	70.6	70.7	69.0	69.4
19. PRESSURE IN METER IN H_2O	--	--	--	--	--	--	--	--	--	--	--	--
20. METERED SAMPLE VOL. FT^3	1.0000	1.0000	1.0000	1.0000	1.000	1.000	1.0000	1.0000	1.0000	1.0000	1.0000	1.0000
21. METER CORRECTION FACTOR	0.986	1.003	0.986	1.003	0.986	1.003	0.986	1.003	0.986	1.003	0.986	1.003
22. CORRECT SAMPLE VOL. FT^3	0.986	1.003	0.986	1.003	0.986	1.003	0.986	1.003	0.986	1.003	0.986	1.003
23. LB. MOL. OF GAS/FT^3 MET. X 10^5	243.8	243.8	243.8	243.8	247.3	248.5	246.9	248.35	246.6	246.6	251.1	251.0
24. LB. MOL. OF GAS IN SAMPLE X 10^5	240.5	244.5	240.5	244.5	243.8	249.2	243.8	249.6	243.2	247.9	247.9	252
25. CYCLOHEXANOL ABSD. IN TUBE, gm	0.3077	0.2599	0.3064	0.2225	0.3439	0.2528	0.3150	0.2570	0.3813	0.2469	0.3112	0.2261
26. CYCLOHEXANOL ABSD. IN TUBE, LB. MOL. X 10^5	0.678	0.572	0.676	0.491	0.756	0.556	0.694	0.566	0.84	0.544	0.685	0.486
27. TOT. MOLS. IN SAMPLE LB. MOL. X 10^5	241.2	245.07	241.2	246.0	244.6	249.1	244.5	250.2	244.0	248.4	248.6	252.2
28. y_o, y_1 MOLS. CYCLOHEXANOL/MOL. GAS	0.00282	0.00234	0.002813	0.002008	0.00309	0.002227	0.00280	0.00226	0.003440	0.002184	0.002756	0.001920
29. VAPOR PRES. OF LIQ. ON PLATE, IN Hg	0.128		0.127		0.127		0.127		0.130		0.112	
30. y^*	0.00417		0.00413		0.004066		0.00408		0.00416		0.00351	
31. E_{OG}%	26.2		37.9		46.9		29.6		63.6		42.6	
32. $N_{OG} = -\ell n\ (1-E_{OG})$	0.300		0.476		0.659		0.35		1.011		0.746	
33. v_s, FT/SEC	2.15		2.11		2.177		2.18		2.18		2.142	
34. ρ_G LB/FT^3	0.0704		0.0704		0.0715		0.0713		0.0715		0.0733	
35. $F = v_s\sqrt{\rho_G}$	0.570		0.558		0.581		0.583		0.583		0.580	
36. t_G, SEC	0.0665		0.0766		0.1132		0.11		0.1213		0.109	
37. k'_Ga, SEC^{-1}	4.51		6.21		5.82		3.18		8.34		6.85	

TABLE I-G (CONTINUED)

PLATE EFFICIENCIES IN RECTANGULAR COLUMN AT UNIVERSITY OF MICHIGAN
(ORIGINAL DATA FOR N_2-CYCLOHEXANOL SYSTEM)
2-IN. WEIR, 2.50-IN. SPLASH BAFFLE

RUN NO.		H-17-B		H-21-A		H-21-B		H-15-B		H-11-A		H-11-B		H-18-A	
1.	GAS ROT. RDG.	80		80		80		120		120		120		120	
2.	LIQ. ROT. RDG.	25		25		25		25		25		25		25	
3.	BAROMETRIC PRESSURE, IN Hg ABS.	29.66		29.4		29.4		29.37		29.22		29.22		29.56	
4.	PRESSURE IN GAS ROT., IN Hg	2.20		2.55		2.40		2.70		2.50		2.60		3.05	
5.	PRESSURE ABOVE PLATE, IN Hg	1.80		2.17		2.10		3.20		1.90		1.90		2.30	
6.	PRESSURE DROP ACROSS PLATE, IN H_2O	2.50		2.43		2.40		2.00		3.10		3.10		3.10	
7.	FROTH HEIGHT, IN.	5.1		5.3		5.4		6.2		6.3		6.4		6.1	
8.	CLEAR LIQ. HT. POSITION 2, IN.	2.60		2.60		2.60		2.40		2.50		2.50		2.50	
9.	3	2.05		2.05		2.10		1.80		1.85		1.85		1.80	
10.	4	2.20		2.20		2.20		1.80		1.85		1.85		1.80	
11.	5	2.35		2.40		2.40		2.30		2.35		2.30		2.30	
12.	AVG. CLEAR LIQ. HT. IN.	2.30		2.31		2.32		2.08		2.14		2.12		2.10	
13.	AVG. LIQ. TEMP. ON PLATE, °F	95.8		98.9		99.9		100.3		99.7		99.7		96.2	
14.	LIQ. TEMP. ON ROT. °F	94.9		96.9		98.1		90.8		97.8		97.6		96.1	
15.	TEMP. OF GAS BELOW PLATE, °F	101.2		103.1		103.3		105.8		102.5		104.9		103.1	
16.	TEMP. IN GAS ROT., °F	71.8		72.2		73.3		66.0		73.5		74.3		70.4	
17.	SAMPLING POINT	OUTLET	INLET	OUTLET	INLET	OUTLET	INLET	OUTLET	INLET	OUTLET	INLET	OUTLET	INLET	OUTLET	INLET
18.	TEMP. OF GAS SAMPLE METER, °F	69.0	69.0	71.5	67.7	68.8	71.8	71.7	71.5	67.9	67.9	67.9	67.9	68.4	68.3
19.	PRESSURE IN METER IN H_2O	--	--	--	--	--	--	--	--	--	--	--	--	--	--
20.	METERED SAMPLE VOL. FT^3	1.0000	1.0000	1.0000	1.0025	1.0000	0.9975	1.010	1.000	1.0000	1.0000	1.0000	1.0000	1.0000	1.0000
21.	METER CORRECTION FACTOR	0.986	1.003	1.003	0.986	0.986	1.003	0.986	1.003	0.986	1.003	0.986	1.003	0.986	1.003
22.	CORRECT SAMPLE VOL. FT^3	0.986	1.003	1.003	0.990	0.986	1.000	0.996	1.003	0.986	1.003	0.986	1.003	0.986	1.003
23.	LB. MOL. OF GAS/FT^3. MET. X 10^5	251.1	251.1	256.3	249.5	248.4	246.2	245.5	245.5	248.0	248.0	248.0	248.0	250	250
24.	LB. MOL. OF GAS IN SAMPLE X 10^5	247.9	252	247	246.6	245.2	246.2	244.2	246	244.2	248.6	244.2	248.6	246.2	250.0
25.	CYCLOHEXANOL ABSD. IN TUBE, gm	0.3312	0.2198	0.3530	0.2122	0.3562	0.2051	0.3858	0.2376	0.3506	0.2755	0.3339	0.2751	0.3298	0.2098
26.	CYCLOHEXANOL ABSD. IN TUBE, LB. MOL. X 10^5	0.729	0.484	0.776	0.468	0.785	0.451	0.849	0.522	0.773	0.606	0.735	0.605	0.725	0.461
27.	TOT. MOLS. IN SAMPLE LB. MOL. X 10^5	248.6	252.5	247.8	247.1	246.0	246.7	245.05	246.5	244.97	249.2	244.9	249.2	246.9	250.5
28.	y_o, y_1 MOLS. CYCLOHEXANOL/MOL. GAS	0.00293	0.00191	0.00314	0.001891	0.00319	0.001828	0.00346	0.00212	0.00315	0.002436	0.00300	0.002428	0.00294	0.00184
29.	VAPOR PRES. OF LIQ. ON PLATE, IN Hg	0.111		0.126		0.128		0.130		0.128		0.127		0.120	
30.	y*	0.003526		0.003990		0.00401		0.00415		0.00412		0.00408		0.00376	
31.	E_{OG}%	63.1		59.5		62.5		66.0		42.3		34.5		57.3	
32.	$N_{OG} = -\ell n\ (1-E_{OG})$	0.996		0.905		0.981		1.079		0.548		0.424		0.851	
33.	v_s, FT/SEC	2.146		2.13		2.15		3.28		3.28		3.30		3.24	
34.	ρ_G LB/FT^3	0.0725		0.0725		0.0721		0.0719		0.0713		0.0710		0.073	
35.	$F = v_s\sqrt{\rho_G}$	0.576		0.574		0.577		0.879		0.876		0.880		0.875	
36.	t_G, SEC	0.1087		0.117		0.1191		0.1050		0.106		0.108		0.1029	
37.	k'_Ga, SEC^{-1}	9.19		7.74		8.25		10.29		5.19		3.93		8.28	

TABLE I-G (CONTINUED)

PLATE EFFICIENCIES IN RECTANGULAR COLUMN AT UNIVERSITY OF MICHIGAN
(ORIGINAL DATA FOR N_2-CYCLOHEXANOL SYSTEM)
2-IN. WEIR, 2.50-IN.SPLASH BAFFLE

RUN NO.	H-19-A		H-19-B		H-20-A		H-20-B		H-22-A		H-22-B		H-10-A	
1. GAS ROT. RDG.	120		120		120		120		120		120		160	
2. LIQ. ROT. RDG.	25		25		25		25		25		25		25	
3. BAROMETRIC PRESSURE, IN Hg ABS.	29.33		29.33		29.4		29.4		29.2		29.2		29.1	
4. PRESSURE IN GAS ROT., IN Hg	2.70		2.50		2.40		2.50		2.40		2.40		3.00	
5. PRESSURE ABOVE PLATE, IN Hg	2.10		1.90		1.70		1.90		1.70		1.70		1.90	
6. PRESSURE DROP ACROSS PLATE, IN H_2O	3.00		2.10		2.20		2.30		2.90		2.90		4.20	
7. FROTH HEIGHT, IN.	6.6		6.5		6.4		6.5		6.5		6.5		7.40	
8. CLEAR LIQ. HT. POSITION 2, IN.	2.50		2.50		2.50		2.50		2.50		2.50		2.50	
9. 3	1.90		1.90		1.80		1.80		1.80		1.80		1.80	
10. 4	1.90		1.90		1.80		1.80		1.80		1.80		1.80	
11. 5	2.35		2.30		2.30		2.30		2.30		2.30		2.40	
12. AVG. CLEAR LIQ. HT. IN.	2.16		2.15		2.10		2.10		2.10		2.10		2.13	
13. AVG. LIQ. TEMP. ON PLATE, °F	99.0		99.9		99.3		99.9		99.6		99.7		99.9	
14. LIQ. TEMP. ON ROT.,°F	91.8		92.4		97		97.9		95.1		95.3		96.8	
15. TEMP. OF GAS BELOW PLATE, °F	104.5		104.9		104.8		105.3		105.1		106.5		111.6	
16. TEMP. IN GAS ROT., °F	72		71.9		71.7		71.8		71.4		71.8		67.8	
17. SAMPLING POINT	OUTLET	INLET	OUTLET	INLET	OUTLET	INLET	OUTLET	INLET	OUTLET	INLET	OUTLET	INLET	OUTLET	INLET
18. TEMP. OF GAS SAMPLE METER, °F	84.6	84.1	85. 4	85.0	73.0	71.1	73.4	71.5	76.3	76.1	76.3	76.4	73.8	73.8
19. PRESSURE IN METER IN H_2O	--	--	--	--	--	--	--	--	--	--	--	--	--	--
20. METERED SAMPLE VOL. FT^3	1.100	1.100	1.0000	1.0000	1.0000	1.0100	1.0000	1.0000	1.7000	1.7000	1.7000	1.7032	1.0000	1.0000
21. METER CORRECTION FACTOR	0.986	1.003	0.986	1.003	1.003	0.986	1.003	0.986	0.986	1.003	0.986	1.003	0.986	1.003
22. CORRECT SAMPLE VOL, FT^3	1.0846	1.103	0.986	1.003	1.003	0.996	1.003	0.986	1.078	1.707	1.678	1.706	0.986	1.003
23. LB. MOL. OF GAS/FT^3 MET. X 10^5	246.3	246.3	235.7	236.5	245.2	246.8	244.9	246.5	241.2	241.5	241.2	241.4	241.4	242.75
24. LB MOL OF GAS IN SAMPLE X 10^5	267.1	271.7	232.0	237.5	246	246.0	245.8	243	404.0	412	404.0	425	240	244
25. CYCLOHEXANOL ABSD. IN TUBE, gm	0.3972	0.2413	0.3603	0.1941	0.3751	0.2133	0.3587	0.2292	0.6219	0.3519	0.6184	0.3545	0.3409	0.2699
26. CYCLOHEXANOL ABSD. IN TUBE, LB. MOL. X 10^5	0.874	0.531	0.795	0.428	0.825	0.47	0.79	0.505	1.370	0.774	1.360	0.78	0.75	0.593
27. TOT. MOLS. IN SAMPLE LB. MOL. X 10^5	267.97	272.2	232.8	237.9	246.8	246.5	246.6	243.5	405.4	412.8	405.4	425.8	240.75	244.6
28. y_o, y_1, MOLS. CYCLOHEXANOL/MOL. GAS	0.00326	0.001944	0.003418	0.00180	0.003342	0.001902	0.00320	0.002074	0.003380	0.001872	0.003360	0.001833	0.003120	0.002420
29. VAPOR PRES. OF LIQ. ON PLATE, IN Hg	0.128		0.129		0.127		0.129		0.127		0.128		0.128	
30. y^*	0.00414		0.00416		0.00408		0.00412		0.004110		0.00414		0.00413	
31. E_{OG}%	55.5		68.5		66.2		55.0		67.5		66.1		41.0	
32. $N_{OG} = -\ell n\ (1-E_{OG})$	0.809		1.154		1.085		0.799		1.126		1.082		0.529	
33. v_s, FT/SEC	3.32		3.32		3.28		3.26		3.29		3.28		4.48	
34. ρ_G LB/FT^3	0.07075		0.071		0.0714		0.0716		0.071		0.0709		0.0702	
35. $F = v_s\sqrt{\rho_G}$	0.881		0.885		0.876		0.872		0.875		0.872		1.10	
36. t_G, SEC	0.1113		0.109		0.1092		0.1122		0.1115		0.1118		0.098	
37. $k'_G a$, SEC^{-1}	10.0		10.6		9.93		7.11		10.1		9.70		5.46	

TABLE I-G (CONTINUED)

PLATE EFFICIENCIES IN RECTANGULAR COLUMN AT UNIVERSITY OF MICHIGAN
(ORIGINAL DATA FOR N_2-CYCLOHEXANOL SYSTEM)
2-IN. WEIR, 2.50-IN. SPLASH BAFFLE

RUN NO.	H-10-B		H-23-A		H-23-B		H-24-A		H-37-A		H-37-B		H-36-A	
1. GAS ROT. RDG.	160		160		160		160		51		51		96	
2. LIQ. ROT. RDG.	25		25		25		25		50		50		50	
3. BAROMETRIC PRESSURE, IN Hg ABS.	29.1		29.21		29.21		29.53		29.50		29.50		29.38	
4. PRESSURE IN GAS ROT., IN Hg	2.80		3.20		3.10		3.00		2.90		2.85		2.80	
5. PRESSURE ABOVE PLATE, IN Hg	1.70		2.10		2.05		1.95		2.60		2.57		2.30	
6. PRESSURE DROP ACROSS PLATE, IN H_2O	4.20		4.45		4.45		4.20		2.90		2.85		3.60	
7. FROTH HEIGHT, IN.	7.5		7.8		7.8		7.8		6.2		6.4		7.8	
8. CLEAR LIQ. HT. POSITION 2, IN.	2.50		2.40		2.50		2.50		3.40		3.40		3.55	
9. 3	1.80		1.75		1.80		1.85		2.80		2.80		2.65	
10. 4	1.80		1.70		1.80		1.80		2.95		2.95		2.70	
11. 5	2.50		2.40		2.45		2.50		3.20		3.20		3.30	
12. AVG. CLEAR LIQ. HT. IN.	2.15		2.06		2.14		2.16		3.09		3.09		3.05	
13. AVG. LIQ. TEMP. ON PLATE, °F	100.5		99.9		99.2		99.5		100.5		100.2		100.2	
14. LIQ. TEMP. ON ROT., °F	90.8		95.3		95.1		97.8		99.8		99.5		99.6	
15. TEMP. OF GAS BELOW PLATE, °F	113.0		105.5		105.0		105.5		109.58		110.1		110.3	
16. TEMP. IN GAS ROT., °F	68.1		72.7		72.5		71.2		76.06		76.1		72.5	
17. SAMPLING POINT	OUTLET	INLET	OUTLET	INLET	OUTLET	INLET	OUTLET	INLET	OUTLET	INLET	OUTLET	INLET	OUTLET	INLET
18. TEMP. OF GAS SAMPLE METER, °F	73.8	73.8	76.0	75.8	77.0	77.5	64.5	64.0	98.1	77.0	98.3	77.0	75.3	75.0
19. PRESSURE IN METER IN H_2O	--	--	--	--	--	--	--	--	--	--	--	--	--	--
20. METERED SAMPLE VOL. FT^3	1.0000	1.0000	2.0000	2.0000	2.0000	2.0000	2.0007	2.0000	2.0000	2.0000	2.0018	2.0040	2.0014	2.0000
21. METER CORRECTION FACTOR	0.986	1.003	0.986	1.003	1.003	0.986	1.003	0.986	0.986	1.003	0.986	1.003	0.986	1.003
22. CORRECT SAMPLE VOL. FT^3	0.986	1.003	1.972	2.006	2.006	1.972	2.016	1.972	1.972	2.006	1.974	2.0100	1.973	2.006
23. LB. MOL. OF GAS/FT^3 MET. X 10^5	242.75	242.75	241.7	241.8	241.2	240.8	252.8	252.9	242.86	243.65	242.7	243.7	243.8	244.0
24. LB. MOL. OF GAS IN SAMPLE X 10^5	240	244	476.2	484.6	484	476	510.0	499.0	478.92	488.76	479.1	489.7	481.1	504.5
25. CYCLOHEXANOL ABSD. IN TUBE, gm	0.3656	0.2867	0.7887	0.4698	0.8194	0.4651	0.8404	0.4567	0.6756	0.3393	0.6673	0.3352	0.7938	0.3439
26. CYCLOHEXANOL ABSD. IN TUBE, LB. MOL. X 10^5	0.804	0.631	1.734	1.003	1.80	1.022	1.85	1.004	1.487	0.747	1.4692	0.738	1.7477	0.7572
27. TOT. MOL. IN SAMPLE LB. MOL. X 10^5	240.8	244.6	477.9	485.6	485.8	477	511.85	500.0	480.4	489.5	480.53	490.5	482.85	505.29
28. y_o, y_1 MOLS. CYCLOHEXANOL/MOL. GAS	0.00334	0.00258	0.00363	0.002128	0.00371	0.002142	0.00362	0.00201	0.003095	0.001526	0.003057	0.001505	0.003620	0.001500
29. VAPOR PRES. OF LIQ. ON PLATE, IN Hg	0.132		0.128		0.127		0.128		0.131		0.130		0.131	
30. y^*	0.00429		0.004118		0.00406		0.00402		0.004081		0.004054		0.004135	
31. E_{OG}%	44.4		75.5		81.7		80.2		61.41		60.89		80.44	
32. $N_{OG} = -\ell n\ (1-E_{OG})$	0.588		1.406		1.70		1.62		0.951		0.937		1.631	
33. v_s, FT/SEC	4.77		4.37		4.24		4.30		2.73		2.75		3.641	
34. ρ_G LB/FT^3	0.0698		0.0715		0.072		0.073		0.0755		0.07539		0.07457	
35. $F = v_s\sqrt{\rho_G}$	1.261		1.167		1.136		1.161		0.754		0.755		0.994	
36. t_G, SEC	0.0935		0.1093		0.111		0.114		0.0950		0.1005		0.1087	
37. $k'_G a$, SEC^{-1}	6.29		12.85		15.31		14.2		10.01		9.32		15.01	

TABLE I-G CONTINUED)

PLATE EFFICIENCIES IN RECTANGULAR COLUMN AT UNIVERSITY OF MICHIGAN
(ORIGINAL DATA FOR N_2-CYCLOHEXANOL SYSTEM)
2-IN. WEIR, 2.50-IN. SPLASH BAFFLE

RUN NO.	H-36-B		H-35-A		H-35-B		H-38-A		H-38-B		H-39-A		H-39-B	
1. GAS ROT. RDG.	96		100		100		100		100		147		147	
2. LIQ. ROT. RDG.	50		50		50		50		50		50		50	
3. BAROMETRIC PRESSURE, IN Hg ABS.	29.38		29.29		29.29		29.50		29.50		29.30		29.30	
4. PRESSURE IN GAS ROT.,IN Hg	2.80		3.00		3.00		2.80		2.85		3.30		3.30	
5. PRESSURE ABOVE PLATE, IN Hg	2.25		2.50		2.40		2.30		2.30		2.20		2.22	
6. PRESSURE DROP ACROSS PLATE, IN H_2O	3.60		3.80		3.70		3.60		2.70		4.60		4.65	
7. FROTH HEIGHT, IN.	7.8		7.7		7.7		7.8		7.6		9.5		9.5	
8. CLEAR LIQ. HT. POSITION 2, IN.	3.55		3.55		3.55		3.55		3.55		3.40		3.40	
9. 3	2.65		2.62		3.62		2.65		2.60		2.45		2.45	
10. 4	2.70		2.65		3.65		2.65		2.65		2.30		2.30	
11. 5	3.30		3.25		3.30		3.25		3.25		3.20		3.20	
12. AVG. CLEAR LIQ. HT. IN.	3.05		3.02		3.03		3.03		3.03		2.84		2.84	
13. AVG. LIQ. TEMP. ON PLATE, °F	100.4		100.3		100.4		100.4		100.4		100.4		100.4	
14. LIQ. TEMP. ON ROT. °F	99.7		97.9		98.2		99.7		99.5		98.0		97.9	
15. TEMP. OF GAS BELOW PLATE, °F	109.85		106.5		104.0		113.5		113.7		109.1		108.5	
16. TEMP. IN GAS ROT., °F	72.7		72.4		72.4		71.6		71.3		75.6		75.6	
17. SAMPLING POINT	OUTLET	INLET	OUTLET	INLET	OUTLET	INLET	OUTLET	INLET	OUTLET	INLET	OUTLET	INLET	OUTLET	INLET
18. TEMP. OF GAS SAMPLE METER, °F	75.6	75.3	78.0	77.9	78.0	78.8	77.5	76.0	77.1	76.0	80.5	80.5	80.5	80.5
19. PRESSURE IN METER, IN H_2O	--	--	--	--	--	--	--	--	--	--	--	--	--	--
20. METERED SAMPLE VOL. FT^3	1.9989	2.0000	2.0000	2.0083	2.0000	1.9917	2.0000	2.0000	2.0140	2.2002	2.0000	2.0000	2.0010	2.0000
21. METER CORRECTION FACTOR	0.986	1.003	0.986	1.003	0.986	1.003	0.986	1.003	0.986	1.003	0.986	1.003	0.986	1.003
22. CORRECT SAMPLE VOL, FT^3	1.971	2.006	1.972	2.015	1.972	2.0000	1.972	2.006	1.9858	2.2036	1.972	2.006	1.973	2.006
23. LB. MOL. OF GAS/FT^3 MET. X 10^5	243.6	243.8	244.5	244.5	241	241.0	243.3	244.4	243.58	244.36	239.2	239.2	239.2	239.2
24. LB. MOL. OF GAS IN SAMPLE X 10^5	480.0	489.0	482	493	476	482.0	479.8	490.2	483.70	539.70	471.7	479.8	472.0	479.8
25. CYCLOHEXANOL ABSD. IN TUBE, gm	0.7059	0.3330	0.7577	0.3123	0.6467	0.3038	0.6479	0.3056	0.6457	0.3309	0.6898	0.3272	0.6881	0.3296
26. CYCLOHEXANOL ABSD. IN TUBE, LB. MOL. X 10^5	1.554	0.7332	1.67	0.688	1.423	0.6685	1.4265	0.6728	1.422	0.7285	1.5177	0.7199	1.5139	0.7252
27. TOT. MOLS. IN SAMPLE LB. MOL. X 10^5	481.55	489.73	482.76	493.7	477.4	482.7	481.23	490.87	485.12	540.43	473.22	480.52	473.5	480.53
28. y_o, y_1	0.003227	0.001500	0.003470	0.001395	0.002978	0.001385	0.002960	0.001371	0.002931	0.001348	0.003207	0.001498	0.003197	0.001505
29. VAPOR PRES. OF LIQ. ON PLATE, IN Hg	0.132		0.130		0.130		0.132		0.132		0.130		0.130	
30. y^*	0.004173		0.00408		0.00410		0.004151		0.004151		0.004162		0.004184	
31. E_{OG}%	64.65		77.3		58.7		57.16		56.47		64.15		63.10	
32. $N_{OG} = -\ell n\ (1-E_{OG})$	1.040		1.484		0.885		0.8475		0.8303		1.026		0.9955	
33. v_s, FT/SEC	3.646		3.662		3.675		3.717		3.72		4.616		4.62	
34. ρ_G LB/FT^3	0.0744		0.0751		0.0748		0.07402		0.0741		0.0741		0.0740	
35. $F = v_s\sqrt{\rho_G}$	0.9917		1.007		1.003		1.007		1.007		1.251		1.256	
36. t_G, SEC	0.1086		0.1066		0.1059		0.1071		0.1026		0.1203		0.1203	
37. $k'_G a$, SEC^{-1}	9.576		13.93		8.357		7.913		8.095		8.53		8.28	

TABLE II-G

PREDICTION OF VAPORIZATION DATA

System	Run No.	Weir Height Inches	Liquid Rate, gpm	N_G Experimental	N_G Predicted by Equation (123)	Percent Deviation Equation (123)	N_G Predicted by Equations (114)+(124)	Percent Deviation Equations (114)+(124)	N_G Predicted by Equation (109)	Percent Deviation Equation (109)	N_G Predicted by Equation (108)	Percent Deviation Equation (108)
N_2-$C_2H_4Br_2$												
	E-7A	1-1/2	7.9	0.489	0.565	13.53	0.533	8.25	0.794	62.40	0.627	28.35
	E-7B			0.588	0.560	- 5.06	0.529	-11.21	0.785	33.55	0.618	5.06
	E-8A			0.696	0.586	-18.84	0.557	-24.97	0.793	14.98	0.672	3.43
	E-8B			0.677	0.610	-10.95	0.580	-16.71	0.818	20.90	0.694	2.53
	E-9A			0.678	0.596	-13.79	0.566	-19.80	0.810	19.40	0.667	1.57
	E-9B			0.752	0.594	-26.63	0.564	-33.33	0.808	7.42	0.665	11.51
	E-10A			0.692	0.578	-19.80	0.548	-26.27	0.800	15.59	0.635	8.20
	E-10B			0.672	0.595	-13.00	0.564	-19.16	0.818	21.73	0.630	3.34
	E-11A			0.734	0.676	- 8.61	0.644	-14.06	0.910	23.95	0.685	6.72
	E-11B			0.754	0.679	-11.07	0.645	-16.86	0.915	21.42	0.691	8.30
	E-12A	3-1/2	7.9	0.821	1.036	20.76	0.986	16.71	1.261	53.60	0.944	15.00
	E-12B			0.917	1.023	10.33	0.973	5.75	1.250	36.30	0.934	1.85
	E-13A			1.037	0.924	-12.29	0.877	-18.25	1.144	10.29	0.904	12.84
	E-13B			1.031	0.926	-11.36	0.879	-17.30	1.146	11.12	0.906	12.10
	E-14A			1.012	0.939	- 7.82	0.893	-13.32	1.143	12.97	0.933	7.79
	E-14B			1.028	0.930	-10.52	0.885	-16.19	1.136	10.49	0.928	9.69
	E-15A			0.914	1.127	18.92	1.070	14.55	1.355	48.25	1.007	10.16
	E-15B			1.070	1.160	7.76	1.101	2.84	1.384	29.30	1.027	4.02
	E-16A			0.920	0.946	2.79	0.899	- 2.32	1.147	24.65	0.956	3.94
	E-16B			0.906	0.928	2.36	0.881	- 2.88	1.129	24.65	0.952	5.04
	E-17A			1.014	0.924	- 9.78	0.876	-15.77	1.153	13.73	0.893	11.90
	E-17B			0.920	0.947	2.85	0.899	- 2.35	1.175	27.67	0.910	1.08
	E-18A		15.9	0.899	1.405	36.00	1.333	32.55	1.598	77.80	1.185	31.78
	E-18B			0.888	1.324	32.94	1.255	29.26	1.530	72.40	1.140	28.35
	E-19A			0.978	1.084	9.75	1.028	4.91	1.292	32.01	1.022	4.51
	E-19B			0.932	1.089	14.46	1.036	9.99	1.295	38.90	1.024	9.86
	E-20A			0.933	0.953	2.07	0.902	- 3.46	1.165	24.80	0.956	2.42
	E-20B			0.927	0.972	4.59	0.920	- 0.73	1.181	27.40	0.969	4.52

TABLE II-G (CONT'D)

PREDICTION OF VAPORIZATION DATA

System	Run No.	Weir Height Inches	Liquid Rate, gpm	N_G Experimental	N_G Predicted by Equation (123)	Percent Deviation Equation (123)	N_G Predicted by Equations (114)+(124)	Percent Deviation Equations (114)+(124)	N_G Predicted by Equation (109)	Percent Deviation Equation (109)	N_G Predicted by Equation (108)	Percent Deviation Equation (108)
N_2-Cyclohexanol												
	H-3A	1-1/2	8.0	0.921	1.020	9.70	0.966	4.70	0.948	2.90	0.932	1.20
	H-3B			1.061	0.780	-36.03	0.736	-44.15	0.777	26.80	0.769	27.55
	H-7A			0.995	0.727	-36.88	0.690	-44.29	0.786	21.00	0.753	24.38
	H-7B			0.612	0.714	14.33	0.679	9.92	0.776	26.70	0.742	21.19
	H-8A			0.794	0.594	-33.78	0.563	-41.01	0.877	10.50	0.789	0.63
	H-8B			0.696	0.592	-17.49	0.562	-23.83	0.878	26.10	0.790	13.49
	H-28A	2	8.0	0.715	0.819	12.75	0.782	8.60	0.972	35.95	0.912	27.60
	H-28B			0.680	0.789	13.80	0.750	9.40	0.943	38.65	0.893	31.33
	H-27A			0.884	0.997	11.33	0.947	6.66	0.911	3.02	0.917	3.70
	H-27B			0.900	1.000	10.06	0.949	5.23	0.923	2.54	0.924	2.66
	H-29A			0.985	1.049	6.14	1.003	1.82	0.829	15.88	0.862	12.44
	H-29B			0.917	1.045	12.28	0.998	8.16	0.830	9.53	0.871	4.98
	H-30A			0.933	1.133	17.80	1.087	14.17	0.824	11.70	0.881	5.55
	H-30B			0.955	1.135	15.80	1.083	12.00	0.823	13.82	0.882	7.66
	H-25A			0.789	0.764	- 3.29	0.720	- 9.53	1.076	36.40	0.963	22.10
	H-25B			0.910	0.761	-19.56	0.718	-26.74	1.072	17.75	0.959	5.35
	H-21A			0.905	0.823	- 9.94	0.776	-16.64	0.876	3.16	0.835	7.77
	H-22A			1.126	1.016	-10.85	0.965	-16.72	0.858	23.80	0.846	24.81
	H-22B			1.082	1.017	- 6.42	0.966	-12.02	0.860	20.50	0.848	21.60
	H-31A	3-1/2	8.0	0.859	1.130	23.96	1.078	20.31	0.994	15.90	1.002	16.63
	H-31B			0.822	1.141	27.95	1.083	24.13	1.006	22.40	1.017	23.80
	H-32A			0.956	1.252	23.67	1.198	20.18	0.955	0.05	0.997	4.31
	H-32B			1.030	1.279	19.45	1.225	15.89	0.968	5.98	1.009	1.99
	H-33A			1.109	1.385	19.94	1.325	16.30	0.960	13.45	1.023	7.78
	H-33B			1.064	1.375	22.59	1.317	19.22	0.954	10.31	1.015	4.63

TABLE II-G (CONT'D)

PREDICTION OF VAPORIZATION DATA

System	Run No.	Weir Height Inches	Liquid Rate, gpm	N_G Experimental	N_G Predicted by Equation (123)	Percent Deviation Equation (123)	N_G Predicted by Equations (114)+(124)	Percent Deviation Equations (114)+(124)	N_G Predicted by Equation (109)	Percent Deviation Equation (109)	N_G Predicted by Equation (108)	Percent Deviation Equation (108)
Freon-12 H_2O												
	87	1-1/2	8.0	2.780	2.818	1.34	2.600	- 6.93	2.665	4.12	2.738	1.49
	88			2.780	2.817	1.32	2.598	- 6.99	2.666	4.12	2.739	1.49
	89			3.400	3.530	3.69	3.255	- 4.45	3.198	5.93	3.066	9.83
	90			3.620	3.530	- 2.53	3.257	-11.16	3.197	11.68	3.065	15.33
	91			2.430	2.837	14.36	2.608	- 6.83	2.669	9.85	2.850	17.27
	92			2.790	2.837	1.67	2.607	- 7.01	2.669	4.32	2.850	2.16
	93			2.940	2.804	- 4.84	2.579	-13.99	2.620	10.89	2.859	2.76
	94			3.250	2.798	-16.12	2.574	-26.25	2.614	19.59	2.850	12.30
He-iC_4H_9OH												
	147	1-1/2	8.0	1.660	1.525	- 8.82	1.795	7.53	1.308	21.20	1.782	7.35
	148			1.520	1.503	- 1.12	1.777	14.48	1.370	9.88	1.781	17.13
	149			1.590	1.482	- 7.28	1.756	9.43	1.355	14.80	1.758	10.59
	150			1.820	1.528	-19.10	1.787	- 1.84	1.261	30.70	1.781	2.13
	151			1.630	1.597	- 2.06	1.874	13.00	1.301	20.20	1.831	12.35
	152			1.640	1.683	2.56	1.967	16.62	1.316	19.72	1.901	15.91
	153			1.740	1.741	0.06	2.032	14.39	1.331	23.45	1.925	10.61
	155			1.510	1.496	- 0.91	1.773	14.82	1.286	14.82	1.739	15.15
	156			1.640	1.467	-11.80	1.741	5.79	1.346	17.96	1.743	6.25
	157			1.570	1.462	- 7.38	1.738	9.66	1.343	14.48	1.734	10.46
N_2-iC_4H_9OH												
	134	1-1/2	8.0	1.880	1.550	-21.27	1.540	-22.04	1.184	37.00	1.643	12.59
	135			1.800	1.551	-16.09	1.541	-16.80	1.184	34.20	1.644	8.69
	136			1.880	1.584	-18.69	1.570	-19.77	1.329	29.30	1.716	8.71
	137			1.820	1.552	-17.29	1.537	-18.40	1.309	28.05	1.691	7.10
	138			1.700	1.471	-15.56	1.461	-16.36	1.186	30.25	1.591	6.40
	139			1.730	1.471	-17.61	1.461	-18.43	1.186	31.25	1.591	8.01
	140			1.800	1.642	- 9.61	1.636	-10.05	1.169	35.05	1.692	6.02
	141			1.840	1.700	- 8.23	1.693	- 8.67	1.201	34.75	1.736	5.68

TABLE II-G (CONT'D)

PREDICTION OF VAPORIZATION DATA

System	Run No.	Weir Height Inches	Liquid Rate, gpm	N_G Experimental	N_G Predicted by Equation (123)	Percent Deviation Equation (123)	N_G Predicted by Equations (114)+(124)	Percent Deviation Equations (114)+(124)	N_G Predicted by Equation (109)	Percent Deviation Equation (109)	N_G Predicted by Equation (108)	Percent Deviation Equation (108)
He-MIBK												
	158	1-1/2	8.0	1.740	1.765	1.40	2.154	19.24	1.260	27.55	1.642	5.65
	159			1.750	1.757	0.41	2.152	18.69	1.251	28.50	1.620	7.46
	160			1.870	1.856	- 0.73	2.272	17.70	1.315	29.68	1.635	12.60
	161			1.870	1.856	- 0.74	2.272	17.68	1.315	29.68	1.634	12.60
	162			1.680	1.664	- 0.96	2.031	17.29	1.201	28.50	1.616	3.78
	163			1.680	1.664	- 0.93	2.032	17.31	1.201	28.50	1.617	3.74
	164			1.650	1.736	4.98	2.115	21.98	1.239	24.87	1.712	3.78
	165			1.650	1.731	4.67	2.108	21.72	1.236	25.05	1.706	3.38
He-H_2O												
	115	1-1/2	8.0	1.990	1.783	-11.61	1.899	- 4.76	1.796	9.73	1.696	14.78
	116			1.920	1.783	- 7.69	1.899	- 1.08	1.796	6.44	1.696	11.68
	117			1.880	1.750	- 7.45	1.862	- 0.97	1.761	6.33	1.705	9.30
	118			1.850	1.754	- 5.48	1.866	0.85	1.765	4.60	1.709	7.65
	119			2.140	1.533	-39.61	1.710	-25.16	2.164	1.10	1.937	9.49
	120			2.140	1.533	-39.59	1.710	-25.16	2.163	1.10	1.937	9.49
	121			2.340	1.586	-47.54	1.771	-32.12	2.465	5.36	2.111	9.80
	122			2.370	1.587	049.36	1.772	-33.78	2.465	4.00	2.111	10.92
AIR-H_2O												
	64	1-1/2	8.0	2.380	2.021	-17.78	1.568	-51.81	2.478	4.10	2.525	6.10
	65			2.420	1.962	-23.34	1.523	-58.87	2.420	0.99	2.468	1.98
	66			3.100	2.138	-44.98	1.654	-87.38	3.055	1.45	2.892	6.55
	67			3.180	2.137	-48.84	1.653	-92.39	3.056	3.92	2.892	9.08
	68			2.920	2.135	-36.75	1.652	-76.80	3.056	4.67	2.892	9.62
	69			2.280	2.118	- 7.64	1.641	-38.95	2.330	2.19	2.483	8.91
	70			2.240	2.075	- 7.94	1.608	-39.32	2.294	2.39	2.446	9.19
	71			2.220	1.962	-13.17	1.526	-45.45	2.045	7.88	2.245	11.40
	72			2.280	1.962	-16.22	1.526	-49.38	2.045	10.30	2.245	1.57
	123			2.350	2.116	-11.05	1.651	-42.35	2.319	1.33	2.459	4.62
	124			2.340	2.117	-10.52	1.649	-41.89	2.322	0.76	2.465	5.35
	125			2.220	2.119	- 4.76	1.652	-34.39	2.238	0.82	2.418	8.90
	126			2.110	2.127	0.81	1.660	-27.13	2.242	6.26	2.420	14.67
	127			2.290	2.064	-10.95	1.612	-42.03	2.272	0.78	2.409	5.20

TABLE II-G (CONT'D)

PREDICTION OF VAPORIZATION DATA

System	Run No.	Weir Height Inches	Liquid Rate, gpm	N_G Experimental	N_G Predicted by Equation (123)	Percent Deviation Equation (123)	N_G Predicted by Equations (114)+(124)	Percent Deviation Equations (114)+(124)	N_G Predicted by Equation (109)	Percent Deviation Equation (109)	N_G Predicted by Equation (108)	Percent Deviation Equation (108)
	128			2.440	1.900	-28.39	1.482	-64.63	2.353	3.56	2.398	1.74
	129			2.400	1.901	-26.27	1.482	-61.90	2.353	1.96	2.398	0.91
	130			2.960	2.038	-45.24	1.587	-86.46	2.943	0.57	2.775	6.24
	131			3.140	2.039	-54.02	1.586	-97.92	2.946	6.17	2.780	11.46
	53	2	8.0	2.630	2.283	-15.20	1.764	-49.09	2.723	3.54	2.778	5.61
	54			2.620	2.322	-12.84	1.794	-46.04	2.758	5.28	2.812	7.35
	55			2.570	2.224	-15.54	1.719	-49.47	2.669	3.86	2.724	5.98
	56			2.570	2.466	- 4.24	1.917	-34.09	2.432	5.35	2.654	3.26
	57			2,520	2.483	- 1.48	1.925	-30.91	2.454	2.63	2.681	6.38
	58			2.380	2.491	4.47	1.940	-22.70	2.448	2.87	2.668	12.07
	59			2.730	2.331	-17.14	1.800	-51.65	2.511	8.02	2.679	1.87
	60			2.650	2.351	-12.73	1.816	-45.89	2.517	5.01	2.688	1.44
	61			2.480	2.562	3.20	1.978	-25.35	2.524	1.76	2.769	11.63
	62			4.010	2.425	-65.36	1.864	-115.07	3.372	15.90	3.200	20.20
	63			3.640	2.423	-50.23	1.863	-95.34	3.371	7.39	3.197	12.15
NH_3-H_2O												
	A-32	2	4.58	1.860	2.370	21.54	2.272	18.15	2.269	22.00	2.049	10.12
	A-29			1.700	2.063	17.59	1.974	13.87	1.983	16.65	1.937	13.98
	A-19			1.690	1.887	10.45	1.819	7.11	1.815	7.42	1.848	9.33
	A-21			1.710	1.645	- 3.95	1.575	- 8.54	1.615	5.55	1.723	0.75
	A-31		9.16	1.870	2.622	28.68	2.512	25.57	2.459	31.50	2.183	16.75
	A-28			1.860	2.180	14.77	2.086	10.82	2.067	11.13	1.999	7.50
	A-18			1.760	2.103	16.32	2.017	12.76	1.982	12.62	1.996	13.43
	A-20			1.640	1.911	14.19	1.826	10.16	1.818	10.81	1.929	17.60
	A-30		18.31	2.170	3.118	30.40	2.977	27.11	2.861	28.55	2.450	12.91
	A-22			2.110	2.656	20.56	2.537	16.81	2.422	15.29	2.304	9.19
	A-23			1.970	2.593	24.03	2.471	20.27	2.340	18.78	2.332	18.33
	A-24			1.800	2.406	25.19	2.291	21.42	2.170	20.55	2.270	26.05

TABLE II-G (CONT'D)

PREDICTION OF VAPORIZATION DATA

System	Run No.	Weir Height Inches	Liquid Rate, gpm	N_G Experimental	N_G Predicted by Equation (123)	Percent Deviation Equation (123)	N_G Predicted by Equations (114)+(124)	Percent Deviation Equations (114)+(124)	N_G Predicted by Equation (109)	Percent Deviation Equation (109)	N_G Predicted by Equation (108)	Percent Deviation Equation (108)
	A-26		32.04	2.550	3.794	32.78	3.609	29.35	3.312	29.85	2.884	13.08
	A-25			2.580	3.333	22.59	3.166	18.50	2.893	12.11	2.727	5.69
	A-27			2.560	3.507	26.99	3.327	23.05	2.950	15.23	2.935	14.62
	AD-39		4.58	1.960	2.342	16.31	2.256	13.10	2.211	12.82	2.030	3.57
	AD-40			1.610	1.844	12.70	1.754	8.20	1.788	11.09	1.839	14.24
	AD-45			1.720	1.625	- 5.81	1.540	-11.67	1.601	6.90	1.711	0.51
	AD-38		9.16	2.050	2.539	19.26	2.441	16.01	2.357	14.97	2.153	5.05
	AD-37			1.780	2.027	12.18	1.930	7.76	1.921	7.90	1.975	10.96
	AD-44			1.580	1.641	3.75	1.553	- 1.71	1.620	2.50	1.748	10.60
	AD-34		18.31	2.720	2.968	8.35	2.829	3.85	2.681	1.44	2.450	9.95
	AD-33			2.530	2.667	5.16	2.535	0.21	2.409	4.78	2.360	6.71
	AD-43			2.330	2.647	11.99	2.526	7.75	2.390	2.56	2.327	0.12
	AD-36			2.490	2.497	0.29	2.372	- 4.98	2.259	9.26	2.303	7.51
	AD-41		32.0	2.810	3.626	22.50	3.458	18.74	3.125	11.20	2.838	1.00
	AD-42			2.820	3.523	19.96	3.349	15.81	2.981	5.70	2.897	2.72
	A-2	3-1/2	4.58	2.130	2.699	21.07	2.547	16.36	2.550	19.72	2.285	7.29
	A-9			2.340	2.523	7.27	2.423	3.43	2.322	0.78	2.249	3.88
	A-11			2.470	2.415	- 2.26	2.332	- 5.92	2.190	11.34	2.227	9.84
	A-17			2.550	2.400	- 6.25	2.321	- 9.86	2.174	14.72	2.206	13.50
	A-13			2.390	2.332	- 2.47	2.226	- 7.35	2.112	11.60	2.251	5.85
	A-3		9.16	2.280	3.020	24.51	2.873	20.64	2.753	20.76	2.467	8.22
	A-8			2.640	2.818	6.32	2.702	2.31	2.524	4.40	2.413	8.60
	A-10			2.760	2.729	- 1.14	2.611	- 5.72	2.425	12.12	2.447	11.31
	A-16			2.740	2.710	- 1.09	2.598	- 5.46	2.401	12.38	2.427	11.41
	A-12			2.510	2.700	7.06	2.576	2.57	2.367	5.70	2.494	0.62
	A-4		18.31	2.730	3.358	18.70	3.192	14.47	2.992	9.60	2.645	3.13
	A-5			2.620	3.378	22.43	3.218	18.59	2.997	14.40	2.658	1.45
	A-7			3.270	3.291	0.64	3.140	- 4.15	2.857	12.62	2.699	17.47
	A-15			3.100	3.289	5.74	3.137	1.17	2.854	7.94	2.699	12.92
	A-14		18.31	3.190	3.422	6.77	3.265	2.29	2.888	9.46	2.867	10.11
	A-6		32.0	4.450	4.429	- 0.47	4.191	- 6.17	3.715	16.52	3.304	25.75
			Absolute Average Percent Deviation			14.59		21.08		19.62		11.59
			Standard Deviation			0.389		0.502				

TABLE III-G

PLATE EFFICIENCIES IN RECTANGULAR COLUMN AT UNIVERSITY OF MICHIGAN,
CARBON DIOXIDE-CYCLOHEXANOL SYSTEM
WEIR HEIGHT, 3-1/2 IN; SPLASH BAFFLE HEIGHT, 4 IN.

RUN NO.	2-A	2-B	3-A	3-B	4-A	4-B	21-A	21-B	5-A	5-B	19-A	19-B	8-A	8-B
BAROMETRIC PRESSURE, IN Hg	29.13	29.12	29.19	29.19	28.96	28.96	28.77	28.77	29.04	29.04	29.30	29.30	28.92	28.92
LIQUID FLOW														
ROTAMETER READING	15.0	15.0	15.0	15.0	15.0	15.0	15.0	15.0	15.0	15.0	15.0	15.0	15.0	15.0
LIQUID TEMP. AT ROTAMETER, °F	102.1	102.6	99.7	99.7	99.4	99.9	97.0	97.6	99.9	99.6	100.5	101.4	76.0	76.1
LB. MOL PER MINUTE	0.3840	0.3840	0.3840	0.3840	0.3840	0.3840	0.3849	0.3848	0.3840	0.3840	0.3840	0.3840	0.3860	0.3860
GALLONS PER MINUTE	4.950	4.950	4.950	4.950	4.950	4.950	4.937	4.93	4.950	4.950	4.950	4.950	--	--
GALLONS PER MIN. PER FT. WEIR	7.920	7.920	7.920	7.920	7.920	7.920	7.899	7.899	7.920	7.920	7.920	7.920	--	--
GAS FLOW AT ROTAMETER														
ROTAMETER READING	120	120	160	160	40.0	40.0	80.0	80.0	80.0	80.0	162	162	43.0	40.0
TEMPERATURE AT ROTAMETER, °F	105.1	104.0	105.9	105.9	85.1	87.5	91.8	94.5	91.4	93.5	112.0	112.0	80.0	81.0
PRESSURE AT ROTAMETER, IN Hg	30.73	30.52	32.19	32.19	31.16	31.36	30.27	30.32	31.39	31.44	31.80	31.80	30.82	30.72
LB. MOL PER MINUTE	0.2362	0.2400	0.3220	--	0.0865	--	0.1575	0.1570	0.1610	0.1621	0.3220	0.3220	0.0864	0.0809
CUBIC FEET PER MINUTE	95.0	96.7	123.7	--	--	--	62.60	62.66	62.0	62.30	126.9	126.9	33.04	30.60
GAS FLOW AT TEST TRAY														
SUPERFICIAL GAS VELOCITY, v_s, FT/SEC.	2.680	2.834	3.366	3.256	0.8910	--	1.750	1.743	1.730	1.699	3.670	3.480	0.8910	0.8370
DENSITY, ρ_G, LB. PER CU.FT.	0.1027	0.1014	0.1092	0.1092	0.1089	0.1097	0.1058	0.1062	0.1089	0.1079	0.1080	0.1077	0.1136	0.1133
F-FACTOR, $v_s\sqrt{\rho_G}$	0.859	0.901	1.112	1.112	0.2944	--	0.5693	0.5682	0.5710	0.558	1.207	1.141	0.3004	0.2820
HYDRAULIC DATA														
FROTH HEIGHT, IN.	7.6	7.6	8.4	8.4	5.5	5.5	--	--	6.7	6.7	8.6	8.6	6.0	6.0
CLEAR LIQUID HEIGHT, IN POSITION 2	4.30	3.40	3.30	3.30	3.40	3.34	3.75	3.75	3.75	3.80	3.30	3.30	3.80	3.80
POSITION 3	3.20	3.30	2.50	2.50	3.40	3.0	3.15	3.15	3.10	3.10	2.45	2.45	3.35	3.35
POSITION 4	--	--	2.40	2.40	3.20	3.10	3.25	3.25	3.30	3.30	2.40	2.40	3.50	3.50
POSITION 5	3.0	3.0	3.30	3.30	3.40	3.37	3.70	3.70	3.66	3.56	3.20	3.20	3.70	3.70
PRESSURE DROP ACROSS TRAY, IN H_2O	--	--	4.60	4.60	2.90	2.95	3.50	3.50	3.20	3.50	4.80	4.95	3.10	2.95
GAS COMPOSITION, MOL FR														
y(ENTERING TRAY)	--	--	0.9131	--	0.9110	0.9159	--	--	0.9114	0.8764	--	--	--	--
y(LEAVING TRAY)	0.8294	0.8293	0.9114	0.9114	0.9139	0.9148	0.9321	0.9407	0.9046	0.8702	0.9096	0.9084	0.9428	0.9451
LIQUID COMPOSITION, $\frac{LB.MOL}{FT^3} \times 10^5$ *														
POSITION 1	25.37	24.59	26.7	25.78	27.12	25.36	19.34	19.72	28.93	23.34	18.60	18.05	24.90	25.20
POSITION 2	107.83	114.17	126.12	126.29	83.93	73.44	98.97	100.90	124.22	111.42	117.90	113.5	55.80	56.75
POSITION 3	104.77	116.41	138.04	136.18	98.79	104.91	112.4	114.50	124.90	115.04	129.80	126.9	84.40	81.80
POSITION 4	--	140.38	159.28	174.48	112.28	114.09	123.8	121.06	130.96	124.59	--	--	87.00	84.36
POSITION 5	148.03	149.34	172.54	--	128.44	126.12	134.0	142.50	152.37	136.45	157.0	156.0	100.6	106.1
POSITION 6	153.55	154.93	151.87	180.05	131.82	134.50	148.2	149.60	128.27	149.50	164.9	165.1	113.0	114.0
EQUILIBRIUMS CONDITIONS ON TEST TRAY														
PRESSURE ABOVE TRAY, ATM	1.0037	0.9901	1.039	1.039	1.035	1.041	0.9967	0.9983	1.0346	1.0380	1.0280	1.0260	1.0220	1.0180
TEMPERATURE, °F	100.2	100.2	99.72	99.72	99.41	99.86	99.68	100.13	99.86	99.59	99.64	100.3	72.64	72.75
CO_2 PARTIAL PRESSURE, ATM	0.8324	0.8211	0.9469	0.9469	0.9459	0.9523	0.9352	0.9422	0.9354	0.9033	0.9351	0.9320	0.9635	0.9621
HENRY'S LAW CONSTANT, ATM/MOL FR	257.0	257.0	256.0	256.0	255.5	256.4	256.0	256.8	256.4	255.9	255.9	257.4	222.3	222.3
$\underline{x}$*, MOL FR X 10^5	324.0	319.5	369.8	369.8	370.2	371.4	365.3	366.9	364.8	355.7	365.4	362.1	433.4	432.8
C*, LB.MOL PER CU.FT. X 10^5	188.5	185.8	214.9	214.9	215.1	215.9	212.4	213.3	212.1	205.3	212.5	210.9	258.7	257.9
MURPHREE EFFICIENCY %														
Eml 16	78.60	80.69	66.28	80.40	55.40	57.23	67.18	67.30	54.19	68.66	75.28	79.46	38.20	38.62
Eml 15	75.00	77.30	77.15	--	53.65	52.68	59.60	63.41	67.11	61.41	71.09	71.54	32.83	35.18

* ALL SAMPLES TAKEN BY USE OF HYPODERMIC SYRINGE

TABLE III-G (CONTINUED)

PLATE EFFICIENCIES IN RECTANGULAR COLUMN AT UNIVERSITY OF MICHIGAN,
CARBON DIOXIDE-CYCLOHEXANOL SYSTEM
WEIR HEIGHT, 3-1/2 IN SPLASH BAFFLE HEIGHT, 4 IN.

RUN NO.	7-A	7-B	6-A	6-B	9-A	9-B	16-A	16-B	20-A	20-B	14-A	14-B	12-A	12-B
BAROMETRIC PRESSURE, IN Hg	29.07	29.07	29.40	29.40	28.92	28.92	29.33	29.33	28.77	28.77	29.31	29.31	29.10	29.10
LIQUID FLOW														
ROTAMETER READING	15.0	15.0	15.0	15.0	15.0	15.0	15.0	15.0	15.0	15.0	50.0	50.0	50.0	50.0
LIQUID TEMP. AT ROTAMETER, °F	78.4	79.4	77.7	77.0	81.6	81.9	80.6	81.1	75.0	75.3	77.40	76.40	74.6	75.9
LB. MOL PER MINUTE	0.3860	0.3860	0.3860	0.3860	0.3860	0.3860	0.3860	0.3860	0.3865	0.3864	1.294	1.292	1.295	1.295
GALLONS PER MINUTE	4.920	4.920	4.920	4.920	4.920	4.920	4.920	4.920	4.910	4.910	16.370	16.490	16.450	16.460
GALLONS PER MIN. PER FT. WEIR	7.872	7.872	7.872	7.872	7.872	7.872	7.872	7.872	7.856	7.856	26.19	26.38	26.32	26.34
GAS FLOW AT ROTAMETER														
ROTAMETER READING	80.0	80.0	80.0	80.0	112	112	160	160	162	162	41.0	41.0	80.0	81.0
TEMPERATURE AT ROTAMETER, °F	80.6	81.7	81.0	81.6	85.8	86.6	95.4	96.2	92.0	93.8	84.5	84.5	78.8	80.75
PRESSURE AT ROTAMETER, IN Hg	30.97	30.97	31.20	31.10	31.32	31.32	31.73	31.78	31.32	31.12	30.51	30.51	30.70	30.70
LB. MOL PER MINUTE	0.1610	0.1600	0.1615	0.1616	0.2250	0.2260	0.3220	0.3220	0.3250	0.3239	0.0821	0.0822	0.1621	0.1638
CUBIC FEET PER MINUTE	61.50	61.60	61.20	61.60	85.75	86.30	123.6	123.3	125.2	125.8	31.99	32.00	62.08	62.94
GAS FLOW AT TEST TRAY														
SUPERFICIAL GAS VELOCITY, v_s, FT/SEC.	1.670	1.673	1.675	1.676	2.352	2.364	3.340	3.341	3.428	3.431	0.8631	0.8619	1.707	1.730
DENSITY, ρ_G, LB. PER CU.FT.	0.1128	0.1122	0.1129	0.1121	0.1123	0.1111	0.1122	0.1119	0.1109	0.1103	0.1103	0.1106	0.1095	0.1093
F-FACTOR, $v_s\sqrt{\rho_G}$	0.561	0.561	0.564	0.562	0.7890	0.790	1.120	1.119	1.142	1.139	0.2866	0.2867	0.5648	0.572
HYDRAULIC DATA														
FROTH HEIGHT, IN.	6.6	6.6	6.8	6.8	7.4	7.4	8.6	8.6	8.7	8.7	7.7	7.7	9.6	9.6
CLEAR LIQUID HEIGHT, IN POSITION 2	3.70	3.70	3.60	3.60	3.80	3.80	3.35	3.35	3.40	3.40	4.60	4.60	5.20	5.20
POSITION 3	3.05	3.05	3.20	3.20	2.95	2.95	2.50	2.50	2.55	2.55	4.35	4.35	4.20	4.20
POSITION 4	3.25	3.25	3.30	3.30	3.00	3.00	2.50	2.50	2.80	2.80	4.50	4.50	4.40	4.40
POSITION 5	3.75	3.75	3.80	3.80	3.60	3.60	3.30	3.30	3.60	3.60	4.90	4.90	5.00	5.00
PRESSURE DROP ACROSS TRAY, IN H_2O	--	--	3.6	3.6	4.0	4.0	5.0	5.0	5.0	5.10	4.0	4.1	4.6	4.7
GAS COMPOSITION, MOL FR														
y(ENTERING TRAY)	--	--	--	--	--	--	--	--	--	--	--	--	--	--
y(LEAVING TRAY)	0.9378	0.9474	0.9294	0.9211	0.9395	0.9200	0.9430	0.9144	0.9263	0.9266	0.9056	0.9056	0.8911	0.8942
LIQUID COMPOSITION, $\frac{\text{LB.MOL}}{\text{FT}^3} \times 10^5$ *														
POSITION 1	28.38	28.91	26.84	27.10	30.42	32.14	28.45	26.10	29.95	29.39	32.60	34.55	43.45	46.10
POSITION 2	--	--	--	--	109.8	116.0	85.85	125.7	123.8	121.4	34.33	35.18	53.45	53.90
POSITION 3	104.31	104.8	90.0	--	124.0	119.1	127.6	127.8	128.4	131.4	33.83	38.20	62.70	63.60
POSITION 4	--	--	--	--	137.7	139.9	--	--	--	--	59.00	65.50	87.50	86.50
POSITION 5	132.9	132.9	126.2	--	145.8	145.5	154.7	152.9	151.3	151.1	67.35	--	96.10	97.05
POSITION 6	138.8	141.8	137.8	137.5	153.7	158.1	164.3	163.7	161.7	160.6	74.00	81.95	101.8	104.6
EQUILIBRIUMS CONDITIONS ON TEST TRAY														
PRESSURE ABOVE TRAY, ATM	1.0220	1.0150	1.0260	1.0240	1.0220	1.0217	1.0260	1.0254	1.0084	1.0033	1.0080	1.0130	1.0090	1.0077
TEMPERATURE, °F	75.65	76.01	76.3	76.46	79.16	80.13	77.43	77.99	76.64	77.09	76.91	76.82	77.18	77.76
CO_2 PARTIAL PRESSURE, ATM	0.9584	0.9616	0.9536	0.9432	0.9602	0.9400	0.9710	0.9376	0.9341	0.9297	0.9129	0.9174	0.8991	0.9011
HENRY'S LAW CONSTANT, ATM/MOL FR	224.5	224.7	225.0	225.2	228.2	228.8	226.1	226.7	225.3	225.8	225.6	225.5	225.8	226.4
x*, MOL FR X 10^5	426.9	427.9	423.8	418.8	420.8	410.9	429.0	413.6	414.6	411.7	404.6	406.8	398.2	398.0
C*, LB MOL PER CU.FT. X 10^5	252.8	253.0	250.5	247.6	247.4	241.1	252.5	243.7	242.1	243.1	238.8	240.2	234.8	234.6
MURPHREE EFFICIENCY %														
Eml 16	49.51	50.62	50.05	50.54	56.83	60.16	60.94	63.59	61.74	63.82	17.33	22.35	30.65	31.15
Eml 15	46.90	46.63	44.71	--	53.17	54.15	56.41	58.31	56.19	57.08	16.87	--	27.63	27.02

* ALL SAMPLES TAKEN BY USE OF HYPODERMIC SYRINGE

TABLE III-G (CONTINUED)

PLATE EFFICIENCIES IN RECTANGULAR COLUMN AT UNIVERSITY OF MICHIGAN,
CARBON DIOXIDE-CYCLOHEXANOL SYSTEM
WEIR HEIGHT, 3-1/2 IN; SPLASH BAFFLE HEIGHT, 4 IN.

RUN NO.	10-A	10-B	17-A	17-B	15-A	15-B	13-A	13-B	11-A	11-B	18-A	18-B
BAROMETRIC PRESSURE, IN Hg	29.05	29.05	29.31	29.31	29.18	29.18	29.10	29.10	24.05	29.05	29.31	29.31
LIQUID FLOW												
ROTAMETER READING	50.0	50.0	50.0	50.0	82.0	84.0	80.0	80.0	80.0	80.0	80.0	80.0
LIQUID TEMP. AT ROTAMETER, °F	77.5	77.8	77.0	77.0	76.0	77.3	80.1	80.0	81.3	82.0	77.3	77.6
LB. MOL PER MINUTE	1.292	1.294	1.294	1.294	2.117	2.159	2.068	2.068	2.069	2.068	2.070	2.070
GALLONS PER MINUTE	16.490	16.460	16.455	16.455	26.904	27.583	26.330	26.330	26.36	26.36	26.33	26.34
GALLONS PER MIN. PER FT. WEIR	26.38	26.34	26.33	26.33	43.05	44.13	42.13	42.13	42.18	42.18	42.13	42.14
GAS FLOW AT ROTAMETER												
ROTAMETER READING	108	108	158	158	41.0	41.0	80.0	78.0	107	107	156	156
TEMPERATURE AT ROTAMETER, °F	82.4	83.1	95.8	96.8	85.1	86.9	85.4	85.6	75.9	86.3	98.3	98.7
PRESSURE AT ROTAMETER, IN Hg	31.05	30.95	31.51	31.41	30.68	30.38	30.50	30.35	30.65	30.65	31.31	31.31
LB. MOL PER MINUTE	0.220	0.220	0.3233	0.3235	0.08244	0.08215	0.1620	0.1576	0.2187	0.2171	0.3226	0.3228
CUBIC FEET PER MINUTE	83.8	84.2	124.4	125.1	31.95	32.27	63.22	61.83	83.43	84.42	125.5	125.7
GAS FLOW AT TEST TRAY												
SUPERFICIAL GAS VELOCITY, v_s, FT/SEC.	2.300	2.315	3.387	3.390	0.8638	0.8710	1.742	1.695	2.342	2.331	3.402	3.412
DENSITY, ρ_G, LB. PER CU.FT.	0.1098	0.1085	0.1074	0.1067	0.1104	0.1085	0.1054	0.1050	0.1063	0.1055	0.1033	0.1029
F-FACTOR, $v_s\sqrt{\rho_G}$	0.7620	0.7626	1.110	1.108	0.2870	0.2869	0.5656	0.5493	0.7635	0.7571	1.093	1.0946
HYDRAULIC DATA												
FROTH HEIGHT, IN.	10.5	10.5	10.3	10.7	8.8	8.8	10.8	10.8	11.5	11.5	12.0	12.0
CLEAR LIQUID HEIGHT, IN POSITION 2	5.30	5.30	4.95	4.95	6.01	6.01	6.20	6.20	6.05	6.05	5.90	5.90
POSITION 3	4.15	4.15	3.70	3.70	5.40	5.40	5.10	5.10	4.80	4.80	4.55	4.55
POSITION 4	4.25	4.25	3.65	3.65	5.50	5.50	5.20	5.20	4.80	4.80	4.45	4.45
POSITION 5	5.00	5.00	4.40	4.40	5.90	5.90	5.90	5.90	5.55	5.55	5.10	5.10
PRESSURE DROP ACROSS TRAY, IN H_2O	5.2	5.2	6.1	6.0	--	--	5.5	5.5	5.80	5.95	7.20	7.20
GAS COMPOSITION, MOL FR												
y(ENTERING TRAY)	--	--	--	--	--	--	--	--	--	--	--	--
y(LEAVING TRAY)	0.8699	0.8623	0.8229	0.8059	0.9005	0.8827	0.8389	0.8356	0.8512	0.8389	0.7352	0.7306
LIQUID COMPOSITION, $\frac{\text{LB.MOL}}{\text{FT}^3} \times 10^5$ *												
POSITION 1	46.80	51.50	54.80	52.50	41.0	38.10	43.00	42.78	49.04	25.98	52.30	52.10
POSITION 2	63.00	48.00	85.40	80.40	41.45	39.00	47.22	47.38	54.90	--	66.40	65.30
POSITION 3	71.70	75.50	88.00	84.90	41.00	39.40	55.00	53.50	60.90	63.90	68.30	70.50
POSITION 4	92.50	90.90	111.4	110.1	63.50	62.90	70.10	69.80	77.25	75.50	95.10	92.30
POSITION 5	104.0	104.6	111.3	110.4	65.50	67.30	81.40	81.60	88.00	90.50	96.60	92.00
POSITION 6	109.3	113.0	119.0	119.2	74.60	73.00	90.00	90.10	93.00	94.10	98.60	102.2
EQUILIBRIUMS CONDITIONS ON TEST TRAY												
PRESSURE ABOVE TRAY, ATM	1.0180	1.0110	1.0130	1.0130	1.0120	1.0020	0.9977	0.9977	1.001	0.9993	1.0080	1.0064
TEMPERATURE, °F	77.0	77.63	76.28	76.46	75.20	76.87	82.13	82.22	81.68	82.26	77.18	77.54
CO_2 PARTIAL PRESSURE, ATM	0.8856	0.8718	0.8336	0.8164	0.9113	0.8845	0.8370	0.8337	0.8521	0.8383	0.7411	0.7353
HENRY'S LAW CONSTANT, ATM/MOL FR	225.6	226.3	225.0	225.2	224.0	225.2	231.0	231.0	230.5	231.1	225.8	226.2
x^*, MOL FR X 10^5	392.6	385.2	370.5	362.5	406.8	382.1	362.3	360.9	369.7	362.7	328.2	325.1
C^*, LB. MOL PER CU.FT. X 10^5	232.2	227.0	218.9	214.2	241.1	231.5	212.1	211.1	216.5	212.2	193.5	191.6
MURPHREE EFFICIENCY %												
Eml 16	33.99	35.14	39.38	41.54	17.00	16.57	27.71	28.07	26.11	36.44	32.85	35.97
Eml 15	30.93	30.26	34.54	35.91	12.31	13.91	22.66	22.86	23.21	34.46	31.42	28.66

* ALL SAMPLES TAKEN BY USE OF HYPODERMIC SYRINGE

TABLE III-6 (CONTINUED)

PLATE EFFICIENCIES IN RECTANGULAR COLUMN AT UNIVERSITY OF MICHIGAN,
CARBON DIOXIDE-CYCLOHEXANOL SYSTEM
WEIR HEIGHT, 2 IN; SPLASH BAFFLE HEIGHT, 2-1/2 IN

RUN NO.	26-A	26-B	23-A	23-B	24-A	24-B	27-A	27-B	34-A	34-B	25-A	25-B	49-A	49-B
BAROMETRIC PRESSURE, IN Hg	29.08	29.08	29.12	29.12	29.53	29.53	29.40	29.40	29.09	29.09	29.46	29.46	29.38	29.38
LIQUID FLOW														
ROTAMETER READING	15.0	15.0	15.0	15.0	15.0	15.0	15.0	15.0	15.0	15.0	15.0	15.0	15.0	15.0
LIQUID TEMP. AT ROTAMETER, °F	100.3	100.2	93.6	95.1	101.6	100.7	98.5	99.5	101.4	101.8	99.6	99.1	99.8	100.0
LB. MOL PER MINUTE	0.385	0.385	0.385	0.385	0.387	0.385	0.384	0.384	0.385	0.385	0.385	0.385	0.385	0.385
GALLONS PER MINUTE	4.932	4.932	4.932	4.934	4.936	4.941	4.931	4.931	4.941	4.941	4.932	4.932	4.940	4.940
GALLONS PER MIN. PER FT. WEIR	7.891	7.891	7.891	7.894	7.898	7.906	7.890	7.890	7.906	7.906	7.891	7.891	7.904	7.904
GAS FLOW AT ROTAMETER														
ROTAMETER READING	46	45	83	83	121	121	100	100	103	103	146	146	183	183
TEMPERATURE AT ROTAMETER, °F	83.6	83.6	90.1	92.0	100.4	101.6	144.8	146.5	146.9	147.3	103.7	103.6	145.4	145.9
PRESSURE AT ROTAMETER, IN Hg	31.23	31.28	30.67	30.72	30.77	30.80	31.86	31.96	31.64	31.64	31.79	31.66	32.98	32.85
LB. MOL PER MINUTE	0.1015	0.1021	0.1636	0.1632	0.2363	0.2366	0.2889	0.2962	0.2834	0.2833	0.2890	0.2894	0.4090	0.4086
CUBIC FEET PER MINUTE	38.56	37.46	64.01	63.99	93.90	94.14	119.65	123.03	118.60	118.67	111.8	112.42	163.84	164.4
GAS FLOW AT TEST TRAY														
SUPERFICIAL GAS VELOCITY, v_s, FT/SEC.	1.080	1.091	1.789	1.783	2.548	2.546	3.092	3.173	2.986	2.988	3.096	3.110	4.292	4.300
DENSITY, ρ_G, LB. PER CU. FT.	0.1116	0.1118	0.1091	0.1093	0.1108	0.1108	0.09334	0.0882	0.1019	0.1017	0.1116	0.1011	0.1006	0.1004
F-FACTOR, $v_s\sqrt{\rho_G}$	0.3607	0.3643	0.5909	0.5884	0.8465	0.8483	0.9443	0.9427	0.9529	0.9530	1.034	0.9904	1.362	1.362
HYDRAULIC DATA														
FROTH HEIGHT, IN.	4.0	4.1	4.7	4.7	5.4	5.7	6.0	6.0	5.4	5.4	5.8	5.8	8.0	8.0
CLEAR LIQUID HEIGHT, IN POSITION 2	2.20	2.20	2.10	2.10	2.10	2.10	--	--	2.10	2.10	2.00	2.00	2.00	2.00
POSITION 3	2.00	2.00	1.80	1.80	1.60	1.60	--	--	1.60	1.60	1.45	1.45	1.45	1.45
POSITION 4	2.07	2.07	2.00	2.00	1.60	1.60	--	--	1.60	1.60	1.40	1.40	1.40	1.40
POSITION 5	2.10	2.10	2.10	2.10	2.10	2.10	--	--	2.10	2.10	2.05	2.05	2.05	2.05
PRESSURE DROP ACROSS TRAY, IN H_2O	2.0	1.90	2.30	2.30	2.90	2.90	2.95	2.95	3.10	3.10	3.43	3.40	4.65	4.65
GAS COMPOSITION, MOL FR														
y (ENTERING TRAY)	--	--	--	--	--	--	--	--	--	--	--	--	--	--
y (LEAVING TRAY)	0.9779	0.9766	0.9742	0.9755	0.9768	0.9730	0.5017	0.5017	0.6841	0.6824	0.9715	0.9721	0.6440	0.6391
LIQUID COMPOSITION, $\frac{\text{LB. MOL}}{\text{FT}^3} \times 10^5$	*	*	*	*	*	*					*	*		
POSITION 1	23.94	24.22	26.12	10.60	27.56	27.59	15.11	14.02	13.24	18.19	25.92	25.45	17.52	16.94
POSITION 2	33.09											92.14		
	30.01	31.47	54.37	69.46	79.96	81.31	34.51	34.71	47.56	57.55	91.63	88.88	63.44	62.09
POSITION 3	61.18											102.9		
	64.23	57.46	82.90	83.74	98.77	100.49	42.72	43.80	60.07	69.56	102.7	105.92	76.96	83.53
POSITION 4	76.24	64.59	91.62	89.56	119.93	120.55	44.34	50.10	68.75	89.29	133.0	132.2	99.93	--
POSITION 5	97.36					132.83						140.0		
	97.14	95.99	113.64	114.20	131.36	132.79	52.25	53.58	83.24	95.99	138.6	140.64	101.4	98.89
POSITION 6	109.74	110.24	125.61	125.83	141.98	142.83	60.49	58.77	92.34	101.03	149.6	149.6	104.9	108.9
EQUILIBRIUMS CONDITIONS ON TEST TRAY														
PRESSURE ABOVE TRAY, ATM	1.0354	1.0371	1.0134	1.0150	1.0287	1.0294	1.0414	1.0414	1.0525	1.0515	1.0348	1.0314	1.0568	1.0555
TEMPERATURE, °F	99.9	99.9	100.2	100.5	100.4	99.7	100.9	101.3	100.4	100.3	100.1	100.2	100.4	100.6
CO_2 PARTIAL PRESSURE, ATM	1.0120	1.0127	0.9872	0.9900	1.0055	1.0016	0.5224	0.5225	0.7199	0.7174	1.0050	1.0026	0.6777	0.6743
HENRY'S LAW CONSTANT, ATM/MOL FR	256.3	256.5	256.8	257.6	257.3	256.1	257.3	257.9	257.3	257.5	256.6	257	257.3	257.6
x*, MOL FR X 10^5	394.8	394.8	384.4	384.3	390.8	391.1	203.0	202.6	279.8	278.6	391.7	390.1	263.4	261.8
C*, LB. MOL PER CU. FT. X 10^5	229.6	229.5	223.6	223.5	227.2	227.3	117.6	117.4	162.7	161.9	227.2	226.8	153.2	152.0
MURPHREE EFFICIENCY %														
Eml 16	41.59	41.76	50.24	53.97	57.16	57.46	43.99	42.81	54.47	57.52	61.68	61.46	64.21	67.77
Eml 15	35.60	34.82	44.23	48.54	51.86	52.49	36.02	38.04	47.64	54.04	55.63	56.67	61.68	60.55

* SAMPLES WITHDRAWN BY USE OF HYPODERMIC SYRINGE, OTHER SAMPLES WITHDRAWN THROUGH VALVE INTO SAMPLE BOTTLE

TABLE III-G (CONTINUED)

PLATE EFFICIENCIES IN RECTANGULAR COLUMN AT UNIVERSITY OF MICHIGAN,
CARBON DIOXIDE-CYCLOHEXANOL SYSTEM
WEIR HEIGHT, 2 IN; SPLASH BAFFLE HEIGHT, 2-1/2 IN.

RUN NO.	45-A	45-B	29-A	29-B	42-A	42-B	32-A	32-B	41-A	41-B	47-A	47-B	35-A	35-B
BAROMETRIC PRESSURE. IN Hg	29.12	29.12	29.26	29.26	29.27	29.27	29.06	29.06	29.18	29.18	29.02	29.02	29.02	29.02
LIQUID FLOW														
ROTAMETER READING	15.0	15.0	15.0	15.0	15.0	15.0	15.0	15.0	15.0	15.0	50.0	50.0	50.0	50.0
LIQUID TEMP. AT ROTAMETER, °F	100.8	100.8	101.0	101.7	101.9	101.7	100.6	102.1	99.9	100.2	100.2	100.3	99.0	100.3
LB. MOL PER MINUTE	0.384	0.385	0.385	0.385	0.385	0.385	0.385	0.385	0.385	0.385	1.285	1.285	1.288	1.288
GALLONS PER MINUTE	4.940	4.930	4.929	4.929	4.940	4.946	4.946	4.941	4.940	4.940	16.529	16.530	16.540	16.540
GALLONS PER MIN. PER FT. WEIR	7.904	7.888	7.886	7.886	7.904	7.914	7.914	7.906	7.904	7.904	26.446	26.448	26.464	26.464
GAS FLOW AT ROTAMETER														
ROTAMETER READING	192	190	203	205	253	253	300	300	313	313	50.0	50.0	65	65
TEMPERATURE AT ROTAMETER, °F	133.0	133.0	134.5	135.5	147.0	147.2	161.0	161.3	161.2	161.0	131.3	131.6	130.7	132.9
PRESSURE AT ROTAMETER, IN Hg	31.62	31.57	31.56	31.61	32.67	32.69	33.16	33.16	30.68	30.68	30.92	30.82	31.16	31.16
LB. MOL PER MINUTE	0.4045	0.4017	0.4419	0.4464	0.5183	0.5197	0.6211	0.6294	0.6386	0.6384	0.2062	0.2020	0.2270	0.2272
CUBIC FEET PER MINUTE	165.5	164.7	181.6	183.5	210.1	210.6	253.8	257.3	257.0	256.9	86.0	84.60	93.50	94.50
GAS FLOW AT TEST TRAY														
SUPERFICIAL GAS VELOCITY, v_s, FT/SEC.	4.431	4.408	4.905	4.939	5.632	5.649	6.809	6.902	6.914	6.913	2.248	2.190	2.460	2.468
DENSITY, ρ_G LB. PER CU. FT.	0.1040	0.1032	0.0923	0.09265	0.09850	0.09849	0.0902	0.0901	0.0959	0.0960	0.1062	0.1060	0.1002	0.09946
F-FACTOR, $v_s\sqrt{\rho_G}$	1.4313	1.4149	1.4901	1.503	1.7690	1.7738	2.0460	2.071	2.143	2.143	0.733	0.7140	0.780	0.7790
HYDRAULIC DATA														
FROTH HEIGHT, IN.	8.5	8.5	8.0	8.0	10.0	10.0	10.0	10.0	11.8	11.8	7.0	7.0	7.7	7.7
CLEAR LIQUID HEIGHT, IN POSITION 2	2.00	2.00	2.00	2.00	2.20	2.20	2.15	2.15	2.15	2.15	3.55	3.55	3.55	3.55
POSITION 3	1.40	1.40	1.50	1.50	1.70	1.70	1.80	1.80	1.85	1.85	2.70	2.70	2.65	2.65
POSITION 4	1.35	1.35	1.40	1.40	1.60	1.60	1.70	1.70	1.75	1.75	2.80	2.80	2.75	2.75
POSITION 5	2.00	2.00	2.10	2.10	2.20	2.20	2.20	2.20	2.15	2.15	3.30	3.30	3.25	3.25
PRESSURE DROP ACROSS TRAY, IN H_2O	5.40	5.55	5.50	5.50	6.30	6.2	--	--	--	--	--	--	--	--
GAS COMPOSITION, MOL FR														
y (ENTERING TRAY)	--	--	--	--	--	--	--	--	--	--	--	--	--	--
y (LEAVING TRAY)	0.8416	0.8249	0.5645	0.5645	0.6889	0.6890	0.4783	0.4741	0.5973	0.5987	0.8895	0.7134	0.7134	0.6982
LIQUID COMPOSITION, $\frac{\text{LB. MOL}}{\text{FT}^3} \times 10^5$														
POSITION 1	18.45	16.49	16.06	22.22	14.20	--	3.49	4.50	15.4	13.6	27.48	26.40	26.03	24.29
POSITION 2	76.90	77.91	68.66	40.36	69.68	66.33	48.67	50.70	70.92	69.11	35.01	34.44	34.22	33.95
POSITION 3	101.33	87.45	69.74	86.24	93.68	104.77	68.44	50.26	102.14	95.71	38.80	41.27	35.59	36.22
POSITION 4	130.30	129.36	97.60	106.79	119.19	120.87	84.08	81.28	116.01	115.38	64.90	64.34	57.25	55.92
POSITION 5	125.52	120.46	93.70	--	110.92	111.20	76.64	77.33	105.71	105.52	84.25	81.00	70.18	71.04
POSITION 6	138.35	131.16	102.75	106.00	119.38	119.43	--	85.07	111.80	114.27	95.91	91.13	81.51	80.67
EQUILIBRIUMS CONDITIONS ON TEST TRAY														
PRESSURE ABOVE TRAY, ATM	1.0117	1.0100	1.0030	1.0030	1.0200	1.0204	1.0114	1.0114	1.0241	1.0241	1.0167	1.0201	1.0231	1.0214
TEMPERATURE, °F	100.1	100.0	100.2	100.8	100.4	100.5	100.3	100.4	100.3	100.4	100.3	100.4	100.3	100.4
CO_2 PARTIAL PRESSURE, ATM	0.8513	0.8331	0.5661	0.5661	0.6889	0.6890	0.4849	0.4810	0.6117	0.6130	0.9044	0.8912	0.7299	0.7131
HENRY'S LAW CONSTANT, ATM/MOL FR	256.7	256.6	257	258	257.3	257.5	257.2	257.3	257.2	257.3	257.1	257.3	257.0	257.3
x^*, MOL FR X 10^5	331.6	324.7	220.3	219.4	267.7	267.6	188.5	186.9	237.8	238.2	351.8	346.4	284.0	277.1
C^*, LB. MOL PER CU. FT. X 10^5	192.8	188.9	128.0	127.7	155.7	155.6	109.6	108.7	138.3	138.1	204.4	201.4	165.0	161.2
MURPHREE EFFICIENCY %														
Eml 16	68.56	66.23	77.34	79.19	73.97	74.21	--	77.38	78.23	80.36	38.51	36.90	39.70	41.08
Eml 15	57.89	60.05	69.14	--	68.02	68.56	68.92	69.95	73.26	73.38	31.94	31.09	31.63	34.07

* SAMPLES WITHDRAWN BY USE OF HYPODERMIC SYRINGE, OTHER SAMPLES WITHDRAWN THROUGH VALVE INTO SAMPLE BOTTLE.

TABLE III-G (CONTINUED)

PLATE EFFICIENCIES IN RECTANGULAR COLUMN AT UNIVERSITY OF MICHIGAN,
CARBON DIOXIDE-CYCLOHEXANOL SYSTEM
WEIR HEIGHT, 2 IN; SPLASH BAFFLE HEIGHT, 2-1/2 IN.

RUN NO.	36-A	36-B	30-A	30-B	43-A	43-B	33-A	33-B	44-A	44-B	50-A	50-B	48-A	48-B
BAROMETRIC PRESSURE, IN P_o	29.22	29.22	29.47	29.47	28.88	28.88	29.02	29.02	28.79	28.79	29.33	29.33	29.27	29.27
LIQUID FLOW														
ROTAMETER READING	50.0	50.0	49.5	49.5	50.0	50.0	50.0	50.0	50.0	50.0	50.0	50.0	80.0	80.0
LIQUID TEMP. AT ROTAMETER, °F	100.3	100.1	98.0	97.3	100.7	100.3	101.5	100.3	100.7	100.5	94.9	96.0	100.1	100.1
LB. MOL PER MINUTE	1.288	1.288	1.271	1.270	1.288	1.288	1.288	1.288	1.289	1.289	1.289	1.289	2.062	2.062
GALLONS PER MINUTE	16.540	16.550	16.320	16.320	16.550	16.540	16.547	16.547	16.550	16.55	16.54	16.54	26.484	26.484
GALLONS PER MIN. PER FT. WEIR	26.46	26.48	26.11	26.11	26.48	26.46	26.48	26.48	26.48	26.48	26.46	26.46	42.37	42.37
GAS FLOW AT ROTAMETER														
ROTAMETER READING	100	100	205	205	240	240	290	290	300	300	208	205	50	50
TEMPERATURE AT ROTAMETER, °F	148.0	148.6	131.6	131.6	145.7	--	158.7	158.7	160.0	160.1	137.6	140.7	130.6	130.9
PRESSURE AT ROTAMETER, IN Hg	32.22	32.22	31.87	31.67	32.08	32.08	32.92	32.82	32.99	32.99	33.93	33.53	30.87	30.87
LB. MOL PER MINUTE	0.2828	0.2820	0.4450	0.4420	0.5040	--	0.6150	0.6150	0.6190	0.6200	0.4547	0.4491	0.2056	0.2062
CUBIC FEET PER MINUTE	116.4	116.1	179.8	180.2	207.8	--	252.4	252.6	253.0	254.0	174.8	175.6	85.80	86.11
GAS FLOW AT TEST TRAY														
SUPERFICIAL GAS VELOCITY, v_s, FT/SEC.	2.978	2.970	4.910	4.900	5.590	--	6.810	6.800	6.780	6.840	4.837	4.816	2.254	2.261
DENSITY, ρ_G LB. PER CU. FT.	0.09957	0.1002	0.09562	0.09495	0.09395	--	0.08684	0.08686	0.09222	0.09107	0.1013	0.09993	0.1015	0.1014
F-FACTOR, $v_s\sqrt{\rho_G}$	0.9410	0.9400	1.497	1.506	1.710	--	2.004	2.004	2.060	2.064	1.539	1.522	0.7191	0.7190
HYDRAULIC DATA														
FROTH HEIGHT, IN.	8.0	8.0	--	--	11.7	11.7	13.0	13.0	12.5	12.5	10.5	10.5	9.3	9.3
CLEAR LIQUID HEIGHT, IN POSITION 2	3.5	3.5	3.55	3.70	3.75	3.75	3.80	3.80	3.95	3.95	3.75	3.75	4.60	4.60
POSITION 3	2.55	2.55	2.55	2.65	2.75	2.75	2.95	2.95	3.00	3.00	2.70	2.70	3.60	3.60
POSITION 4	2.50	2.50	2.40	2.50	2.55	2.55	2.75	2.75	2.85	2.85	2.55	2.55	3.65	3.65
POSITION 5	3.18	3.18	3.40	3.90	3.60	3.60	3.75	3.75	3.80	3.80	3.60	3.60	4.25	4.25
PRESSURE DROP ACROSS TRAY, IN H_2O	--	--	--	--	--	--	--	10.0	14.4	14.8	8.40	7.80	4.40	4.40
GAS COMPOSITION, MOL FR														
y (ENTERING TRAY)	--	--	--	--	--	--	--	--	--	--	0.6883	--	0.7756	--
y (LEAVING TRAY)	0.6350	0.6377	0.6372	0.6310	0.6078	0.6088	0.4066	0.4087	0.5366	0.5180	0.6970	0.6817	0.7776	0.7746
LIQUID COMPOSITION, $\frac{\text{LB. MOL}}{\text{FT}^3} \times 10^5$														
POSITION 1	24.83	24.76	31.63	34.48	25.88	23.85	19.33	23.45	26.05	24.89	26.40	26.27	24.70	27.96
POSITION 2	30.05	30.06	55.46	49.58	48.02	53.46	--	46.36	57.89	55.11	47.56	47.87	31.82	33.17
POSITION 3	36.10	36.35	67.16	70.97	65.77	74.51	60.49	48.47	78.77	75.28	63.72	64.47	34.57	35.46
POSITION 4	56.07	56.56	89.47	89.33	--	--	--	--	--	--	--	--	46.83	49.63
POSITION 5	69.46	68.13	77.21	79.34	79.20	78.37	63.81	60.67	79.62	76.50	72.84	79.23	65.70	65.23
POSITION 6	80.61	75.95	87.07	87.83	88.76	86.49	66.24	67.66	91.70	84.83	89.16	84.50	80.36	79.02
EQUILIBRIUMS CONDITIONS ON TEST TRAY														
PRESSURE ABOVE TRAY, ATM	1.0535	1.0535	1.0050	1.0050	0.9987	1.0020	1.0033	1.0033	1.0090	0.9706	1.0421	1.0338	1.0117	1.0117
TEMPERATURE, °F	100.3	99.95	100.3	100.8	100.2	100.1	100.6	100.6	100.4	100.0	100.2	100.2	100.4	100.4
CO_2 PARTIAL PRESSURE, ATM	0.6690	0.6718	0.6426	0.6363	0.6070	0.6100	0.4079	0.4074	0.5414	0.5201	0.7264	0.7047	0.7867	0.7837
HENRY'S LAW CONSTANT, ATM/MOL FR	257.2	256.5	257.1	258.0	257.1	256.7	257.6	257.6	257.3	257.3	257.0	257.0	257.3	257.3
x*, MOL FR X 10^5	260.1	261.9	249.9	246.6	236.1	237.6	158.4	158.2	210.4	202.1	282.6	274.2	305.8	304.6
C*, LB. MOL PER CU. FT. X 10^5	151.2	152.3	145.2	143.4	137.3	138.2	92.08	92.26	122.4	117.5	164.3	160.0	177.8	177.1
MURPHREE EFFICIENCY %														
Eml 16	44.00	40.02	48.82	49.04	56.29	54.65	64.31	64.02	67.95	64.55	45.33	43.56	36.29	34.14
Eml 15	35.22	33.91	40.14	41.26	47.73	47.59	60.94	53.89	55.46	55.58	33.57	39.65	26.69	24.90

* SAMPLES WITHDRAWN BY USE OF HYPODERMIC SYRINGE, OTHER SAMPLES WITHDRAWN THROUGH VALVE INTO SAMPLE BOTTLE.

TABLE III-G (CONTINUED)

PLATE EFFICIENCIES IN RECTANGULAR COLUMN AT UNIVERSITY OF MICHIGAN,
CARBON DIOXIDE-CYCLOHEXANOL SYSTEM
WEIR HEIGHT, 2 IN; SPLASH BAFFLE HEIGHT, 2-1/2 IN.

RUN NO.	28-A	28-B	31-A	31-B	46-A	46-B	37-A	37-B	38-A	38-B	39-A	39-B	40-A	40-B
BAROMETRIC PRESSURE, IN Hg	29.11	29.11	29.55	29.55	28.94	28.94	29.12	29.12	29.22	29.22	28.92	28.92	29.09	29.09
LIQUID FLOW														
ROTAMETER READING	80.0	80.0	80.0	80.0	15.0	15.0	15.0	15.0	15.0	15.0	15.0	15.0	15.0	15.0
LIQUID TEMP. AT ROTAMETER, °F	95.9	96.6	100.6	100.8	64.8	64.7	58.1	58.0	57.8	57.9	58.1	58.1	57.6	57.6
LB. MOL PER MINUTE	2.063	2.062	2.062	2.061	0.3898	0.3898	0.3878	0.3880	0.3875	0.3876	0.3880	0.3880	0.3877	0.3877
GALLONS PER MINUTE	26.410	26.410	26.480	26.48	4.850	4.851	4.890	4.890	4.885	4.887	4.890	4.890	4.887	4.887
GALLONS PER MIN. PER FT. WEIR	42.26	42.26	42.37	42.37	7.760	7.762	7.824	7.824	7.816	7.819	7.824	7.824	7.819	7.819
GAS FLOW AT ROTAMETER														
ROTAMETER READING	107	107	200	200	57.0	57.0	100	100	200	200	250	250	315	315
TEMPERATURE AT ROTAMETER, °F	133.0	133.8	132.9	133.6	115.2	115.7	51.3	51.3	61.8	54.1	50.0	50.0	53.1	53.3
PRESSURE AT ROTAMETER, IN Hg	31.06	31.06	31.70	31.70	31.14	31.14	32.02	32.02	32.72	32.67	32.72	32.12	33.19	33.09
LB. MOL PER MINUTE	0.2928	0.2917	0.4420	0.4439	0.2087	0.2101	0.3026	0.3022	0.4750	0.4790	0.5650	0.5600	0.7082	0.7078
CUBIC FEET PER MINUTE	126.2	125.9	180.4	181.4	84.11	84.76	105.4	105.3	165.2	164.3	192.4	194.2	238.9	239.6
GAS FLOW AT TEST TRAY														
SUPERFICIAL GAS VELOCITY, v_s, FT/SEC.	3.231	3.223	4.880	4.905	2.094	2.108	2.954	2.949	4.660	4.720	5.700	5.740	7.213	7.209
DENSITY, ρ_G LB. PER CU. FT.	0.09173	0.09224	0.09198	0.09127	0.1168	0.1158	0.1109	0.1112	0.1046	0.1040	0.1032	0.1034	0.1002	0.1000
F-FACTOR, $v_s\sqrt{\rho_G}$	0.9787	0.9791	1.4801	1.4817	0.7154	0.7168	0.9834	0.9842	1.508	1.523	1.830	1.843	2.283	2.280
HYDRAULIC DATA														
FROTH HEIGHT, IN.	10.7	10.7	12.0	12.0	5.2	5.2	5.7	5.7	7.5	7.5	9.0	9.0	9.2	9.2
CLEAR LIQUID HEIGHT, IN POSITION 2	4.85	4.85	5.40	5.40	2.35	2.35	2.30	2.30	2.20	2.20	2.20	2.20	2.30	2.30
POSITION 3	3.60	3.60	3.90	3.90	1.95	1.95	1.80	1.80	1.60	1.60	1.75	1.75	2.00	2.00
POSITION 4	3.50	3.50	3.70	3.70	2.00	2.00	1.85	1.85	1.55	1.55	1.60	1.60	1.80	1.80
POSITION 5	4.25	4.25	4.40	4.40	2.20	2.20	2.20	2.20	2.20	2.20	2.25	2.25	2.35	2.35
PRESSURE DROP ACCROSS TRAY, IN H_2O	5.40	5.30	7.6	7.5	2.70	2.70	3.10	3.10	5.40	6.00	6.90	7.0	10.4	11.2
GAS COMPOSITION, MOL FR														
y (ENTERING TRAY)	--	--	--	--	--	--	--	--	--	--	--	--	--	--
y (LEAVING TRAY)	0.5348	0.5504	0.5417	0.5241	0.9416	0.9180	0.7254	0.7312	0.5835	0.5838	0.6693	0.6746	0.5731	0.5696
LIQUID COMPOSITION, $\frac{\text{LB. MOL}}{\text{FT}^3} \times 10^5$														
POSITION 1	27.45	26.15	29.41	27.95	31.77	30.03	29.13	28.89	28.56	25.12	27.20	30.08	26.56	29.71
POSITION 2	26.36	31.02	44.25	44.42	34.49	33.28	60.48	59.69	64.98	67.92	67.78	72.07	66.64	67.02
POSITION 3	34.99	34.26	50.18	46.92	72.90	47.66	71.37	70.76	71.18	70.60	87.47	88.92	85.27	--
POSITION 4	24.27	47.36	--	--	93.16	90.43	81.19	80.73	--	--	--	--	--	--
POSITION 5	108.73	63.59	65.88	68.35	102.82	76.47	87.49	88.62	89.19	85.28	98.89	102.02	93.87	96.28
POSITION 6	67.26	61.90	71.13	74.75	107.30	105.97	94.29	96.90	91.83	89.54	105.26	108.26	101.09	103.40
EQUILIBRIUMS CONDITIONS ON TEST TRAY														
PRESSURE ABOVE TRAY, ATM	1.0077	1.0080	1.0043	1.0043	1.0241	1.0241	1.0501	1.0501	1.0444	1.0424	1.0000	1.0000	1.0057	1.0057
TEMPERATURE, °F	99.9	100.4	100.4	100.8	59.32	59.38	58.08	58.01	57.83	57.92	58.14	58.14	57.61	57.65
CO_2 PARTIAL PRESSURE, ATM	0.5390	0.5548	0.5441	0.5262	0.9642	0.9392	0.7617	0.7678	0.6113	0.6086	0.6693	0.6746	0.5764	0.5728
HENRY'S LAW CONSTANT, ATM/MOL FR	256.4	257.3	257.3	258.0	202.3	202.3	200.5	200.5	200.5	200.5	200.8	200.8	200.0	200.0
x*, MOL FR X 10^5	210.2	215.6	211.5	204.0	476.6	464.3	379.9	382.9	304.9	303.5	333.3	336.0	288.2	286.4
C*, LB. MOL PER CU. FT. X 10^5	122.2	125.4	122.9	118.6	285.7	277.9	227.4	229.2	182.5	181.7	199.8	201.4	172.6	171.5
MURPHREE EFFICIENCY %														
Eml 16	41.88	35.91	44.47	51.49	30.07	30.92	33.16	34.26	41.47	41.54	45.70	46.13	51.54	52.46
Eml 15	35.91	37.61	38.88	44.44	28.25	18.90	29.72	30.07	39.76	38.78	41.98	42.45	46.53	47.40

* SAMPLES WITHDRAWN BY USE OF HYPODERMIC SYRINGE, OTHER SAMPLES WITHDRAWN THROUGH VALVE INTO SAMPLE BOTTLE.

TABLE IV-G

MASS TRANSFER UNITS AND MASS TRANSFER COEFFICIENTS - ABSORPTION STUDIES

Run No.	Weir Height Inches	Liquid Rate gpm	Liquid Viscosity μ_L lb/ft-hr	Gas Velocity u_s ft/sec	F-Factor	λ	$E_{MV_{15}}$	$E_{OG_{15}}$	$N_{OG_{15}}$	$N_{L_{15}}$	Liquid Contact Time t_L sec	$k_L\bar{a}$ sec^{-1}	$D_L \times 10^5$* ft^2/hr	$k_L\bar{a}/D_L^{1/2}$
4A	3-1/2	4.95	60.3	0.89	0.294	55.64	0.02038	0.0162	0.0163	0.907	16.19	0.0560	0.471	0.257
4B		4.95	60.0	0.84	0.276	49.55	0.02195	0.0178	0.0180	0.892	16.13	0.0553	0.478	0.253
21A		4.94	59.8	1.75	0.569	105.1	0.01360	0.0112	0.0113	1.188	16.14	0.0736	0.475	0.338
21B		4.94	58.8	1.74	0.568	104.9	0.01609	0.0122	0.0123	1.290	16.17	0.0798	0.484	0.363
5A		4.95	59.5	1.73	0.571	105.1	0.01904	0.0145	0.0146	1.534	16.17	0.0949	0.478	0.434
5B		4.95	60.0	1.70	0.558	100.9	0.01552	0.0129	0.0130	1.312	16.22	0.0809	0.475	0.371
2A		4.95	58.7	2.68	0.859	176.0	0.01676	0.0114	0.0115	2.024	14.77	0.1370	0.484	0.623
2B		4.95	58.7	2.83	0.901	181.3	0.01844	0.0122	0.0123	2.230	14.51	0.1537	0.484	0.699
3A		4.95	59.7	3.37	1.112	199.7	0.01663	0.0108	0.0108	2.157	13.37	0.1613	0.477	0.739
19A		4.95	59.9	3.67	1.207	208.6	0.01165	0.00910	0.00914	1.907	12.83	0.1486	0.475	0.682
19B		4.95	58.6	3.48	1.141	210.0	0.01183	0.00905	0.00904	1.898	13.20	0.1438	0.486	0.672
8A	3-1/2	4.92	147.1	0.89	0.300	48.7	0.00984	0.00878	0.00883	0.430	16.17	0.0266	0.182	0.197
8B		4.92	145.2	0.84	0.282	45.7	0.01174	0.00982	0.00984	0.450	16.13	0.0279	0.182	0.207
6A		4.92	130.0	1.68	0.564	91.7	0.00874	0.00720	0.00722	0.662	15.65	0.0423	0.209	0.292
7A		4.92	131.9	1.67	0.561	91.9	0.00952	0.00816	0.00823	0.756	15.71	0.0481	0.205	0.336
7B		4.92	131.2	1.67	0.561	91.9	0.00942	0.00809	0.00813	0.747	15.71	0.0475	0.207	0.330
9A		4.92	119.1	2.35	0.789	131.1	0.00865	0.00744	0.00742	0.973	15.18	0.0641	0.231	0.422
9B		4.92	114.4	2.36	0 790	131.0	0.00894	0.00770	0.00772	1.011	15.18	0.0666	0.232	0.438
16A		4.92	124.6	3.34	1.120	184.0	0.00696	0.00562	0.00561	1.032	13.77	0.0749	0.218	0.508
16B		4.92	123.4	3.34	1.119	184.5	0.00732	0.00645	0.00642	1.184	13.77	0.0860	0.222	0.577
20A		4.91	128.3	3.43	1.142	188.2	0.00698	0.00632	0.00631	1.188	13.54	0.0877	0.212	0.603
20B		4.91	126.8	3.43	1.139	188.7	0.00705	0.00627	0.00631	1.191	13.58	0.0877	0.215	0.599
12A	3-1/2	16.45	125.6	1.71	0.565	28.01	0.01345	0.0117	0.0118	0.330	6.39	0.0516	0.215	0.352
12B		16.46	123.7	1.73	0.562	28.41	0.01286	0.0111	0.0112	0.318	6.38	0.0498	0.221	0.335
10A		16.49	127.0	2.30	0.762	37.70	0.01177	0.0101	0.0102	0.384	6.37	0.0603	0.214	0.412
10B		16.46	124.2	2.32	0.763	38.06	0.01127	0.00938	0.00944	0.359	6.36	0.0564	0.219	0.381
17A		16.46	130.0	3.39	1.110	55.49	0.00942	0.00845	0.00843	0.468	6.69	0.0700	0.209	0.484
17B		16.46	129.5	3.39	1.108	55.58	0.00998	0.00879	0.00883	0.491	6.72	0.0731	0.210	0.504

* Diffusivities predicted by Wilke-Chang correlation.(13)

TABLE IV-G (CONT'D)

MASS TRANSFER UNITS AND MASS TRANSFER COEFFICIENTS - ABSORPTION STUDIES

Run No.	Weir Height Inches	Liquid Rate gpm	Liquid Viscosity μ_L lb/ft-hr	Gas Velocity u_s ft/sec	F-Factor	λ	$E_{MV_{15}}$	$E_{OG_{15}}$	$N_{OG_{15}}$	$N_{L_{15}}$	Liquid Contact Time t_L sec	$k_L\bar{a}$ sec^{-1}	$D_L \times 10^5$* ft^2/hr	$k_L\bar{a}/D_L^{1/2}$
15A	3-1/2	26.9	135.0	0.86	0.287	8.62	0.01626	0.0151	0.0152	0.131	4.84	0.0271	0.201	0.192
15B		27.6	127.8	0.87	0.287	8.51	0.01860	0.0170	0.0171	0.146	4.72	0.0309	0.213	0.212
13A		26.3	107.2	1.74	0.566	18.14	0.01590	0.0140	0.0141	0.256	4.67	0.0548	0.258	0.341
13B		26.3	107.0	1.70	0.549	17.65	0.01650	0.0144	0.0145	0.256	4.63	0.0553	0.2 8	0.343
11A		26.4	108.9	2.34	0.764	24.34	0.01277	0.0112	0.0113	0.275	4.52	0.0608	0.254	0.382
11B		26.4	106.8	2.33	0.757	24.28	0.02118	0.0183	0.0185	0.449	4.52	0.0993	0.258	0.617
18A		26.3	125.6	3.40	1.093	34.91	0.01296	0.0112	0.0113	0.394	4.54	0.0868	0.215.	0.592
18B		26.3	124.4	3.41	1.095	35.06	0.01131	0.0101	0.0102	0.358	4.54	0.0789	0.218	0.533
26A	2	4.93	59.4	1.08	0.361	65.5	0.00850	0.00692	0.00692	0.453	9.06	0.0500	0.478	0.229
26B		4.93	59.4	1.09	0.364	65.6	0.00805	0.00644	0.02642	0.421	9.00	0.468	0.478	0.214
23A		4.93	58.9	1.79	0.591	107.7	0.00733	0.00583	0.00581	0.626	8.53	0.0734	0.482	0.334
23B		4.93	58.1	1.78	0.588	107.6	0.00871	0.00710	0.00712	0.766	8.55	0.0896	0.490	0.405
24A		4.94	58.4	2.55	0.847	152.7	0.00700	0.00561	0.00712	0.857	8.05	0.1065	0.487	0.482
24B		4.94	58.4	2.55	0.848	153.1	0.00707	0.00565	0.00561	0.859	8.09	0.1062	0.477	0.481
27A		4.93	57.4	3.09	0.944	185.6	0.00306	0.00270	0.00270	0.501	7.99	0.0627	0.497	0.281
27B		4.93	56.9	3.17	0.943	186.3	0.00323	0.00287	0.02290	0.540	7.99	0.0676	0.503	0.301
34A		4.94	58.4	2.99	0.953	180.1	0.00503	0.00409	0.00410	0.738	7.94	0.0929	0.487	0.420
34B		4.94	58.1	2.99	0.953	180.4	0.00648	0.00510	0.00511	0.922	7.94	0.1161	0.491	0.524
25A		4.93	59.0	3.10	1.03	186.2	0.00670	0.00526	0.00531	0.989	7.84	0.1261	0.482	0.574
25B		4.93	58.8	3.11	0.99	187.5	0.00694	0.00537	0.00541	1.014	7.91	0.1282	0.484	0.584
49A		4.94	58.4	4.29	1.36	259.0	0.00619	0.00453	0.00451	1.168	7.72	0.1513	0.487	0.685
49B		4.94	58.0	4.30	1.36	259.4	0.00568	0.00434	0.00430	1.115	7.72	0.144	0.491	0.653
45A		4.94	59.0	4.43	1.43	267.0	0.00512	0.00385	0.00380	1.015	7.76	0.1308	0.482	0.596
45B		4.93	59.2	4.41	1.42	265.4	0.00563	0.00421	0.00420	1.115	7.73	0.1442	0.480	0.658
29A		4.93	58.7	4.90	1.49	294.2	0.00773	0.00538	0.00541	1.592	7.84	0.2031	0.483	0.925
42A		4.94	58.4	5.63	1.77	339.7	0.00577	0.00380	0.00380	1.291	8.49	0.1521	0.488	0.688
32A		4.95	58.6	6.81	2.05	410.2	0.00539	0.00377	0.00380	1.559	9.50	0.1641	0.484	0.746
32B		4.94	58.4	6.90	2.07	416.2	0.00600	0.00393	0.00390	1.623	9.57	0.1696	0.487	0.767
41A		4.94	58.6	6.91	2.14	417.0	0.00679				9.88		0.486	

* Diffusivities predicted by Wilke-Chang correlation.[13]

TABLE IV-G (CONT'D)

MASS TRANSFER UNITS AND MASS TRANSFER COEFFICIENTS - ABSORPTION STUDIES

Run No.	Weir Height Inches	Liquid Rate gpm	Liquid Viscosity μ_L lb/ft-hr	Gas Velocity u_s ft/sec	F-Factor	λ	E_{MV15}	E_{OG15}	N_{OG15}	N_{L15}	Liquid Contact Time t_L sec	$k_L\bar{a}$ sec^{-1}	$D_L \times 10^5$* ft^2/hr	$k_L\bar{a}/D$ 1/2
46A	2	4.84	227.5	2.09	0.715	105.8	0.00342	0.00298	0.00300	0.317	10.48	0.0302	0.116	0.280
46B		4.85	227.4	2.11	0.717	106.8	0.00216	0.00198	0.00200	0.214	9.13	0.0234	0.116	0.217
37A		4.89	237.3	2.95	0.983	147.0	0.00283	0.00260	0.00260	0.382	9.29	0.0411	0.110	0.391
37B		4.89	237.6	2.95	0.984	148.7	0.00288	0.00262	0.00260	0.387	9.28	0.0417	0.110	0.397
38A		4.88	238.0	4.66	1.51	235.3	0.002802	0.00251	0.00250	0.588	8.76	0.0671	0.109	0.642
38B		4.89	237.9	4.72	1.52	237.8	0.00246	0.00227	0.00230	0.547	8.74	0.0626	0.110	0.599
39A		4.89	236.0	5.70	1.83	292.4	0.00246	0.00222	0.00220	0.643	8.47	0.0759	0.110	0.723
39B		4.89	236.0	5.74	1.84	289.8	0.00255	0.00230	0.00230	0.666	8.43	0.0790	0.110	0.752
40A		4.89	238.4	7.21	2.28	363.3	0.00239	0.00214	0.00210	0.763	8.83	0.0864	0.108	0.831
40B		4.89	238.2	7.21	2.28	363.3	0.00247	0.00207	0.00210	0.763	8.82	0.0865	0.108	0.832
47A		16.53	58.6	2.25	0.733	40.6	0.01148	0.00933	0.00933	0.371	4.10	0.0906	0.484	0.410
47B		16.53	58.4	2.19	0.714	39.6	0.01127	0.00930	0.00930	0.371	4.09	0.0906	0.490	0.410
35A		16.54	58.6	2.46	0.780	44.3	0.01034	0.00848	0.00848	0.379	4.08	0.0928	0.486	0.420
35B		16.54	58.4	2.47	0.979	44.4	0.01147	0.00925	0.00925	0.414	4.08	0.1014	0.486	0.459
36A		16.54	58.6	2.98	0.941	53.6	0.01002	0.00794	0.00794	0.472	3.86	0.1222	0.484	0.555
36B		16.55	59.3	2.97	0.940	53.5	0.00950	0.00766	0.00766	0.412	4.02	0.1025	0.479	0.469
30A		16.32	58.6	4.91	1.50	89.6	0.00739	0.00639	0.00639	0.577	3.98	0.1448	0.484	0.658
30B		16.32	57.6	4.90	1.51	89.3	0.00773	0.00645	0.00645	0.581	3.98	0.1459	0.495	0.656
50A		16.54	58.8	4.84	1.54	87.1	0.00585	0.00535	0.00535	0.465	3.94	0.1181	0.483	0.538
50B		16.54	58.8	4.82	1.52	86.7	0.00752	0.00658	0.00658	0.574	3.93	0.1894	0.483	0.863
43A		16.55	58.7	5.59	1.71	100.7	0.00898	0.00755	0.00755	0.766	4.05	0.1892	0.483	0.862
43B		16.54	59.1	5.72	1.76	102.9	0.00877	0.00783	0.00783	0.811	4.12	0.1967	0.481	0.898
33A		16.55	58.1	6.81	2.00	122.8	0.01255	0.01182	0.00118	1.477	4.37	0.338	0.490	1.525
33B		16.55	58.1	6.80	2.00	122.6	0.00951	0.00788	0.00788	0.970	4.37	0.2218	0.490	1.003
44A		16.55	58.5	6.78	2.06	122.5	0.01010	0.00983	0.00893	1.102	4.47	0.2467	0.486	1.116
44B		16.55	58.4	6.84	2.06	123.3	0.01006	0.00885	0.00885	1.101	4.47	0.2464	0.486	1.115
48A	2	26.48	58.4	2.25	0.719	25.4	0.01344	0.01130	0.0113	0.295	3.46	0.0854	0.486	0.386
48B		26.48	58.4	2.26	0.719	25.4	0.01287	0.01090	0.0109	0.278	3.46	0.0804	0.486	0.364
28B		26.41	58.4	3.22	0.979	36.1	0.01620	0.01230	0.0123	0.453	3.46	0.1308	0.486	0.592
31A		26.48	58.4	4.88	1.480	54.9	0.01660	0.01430	0.0143	0.675	3.61	0.1870	0.486	0.846
31B		26.48	57.6	4.90	1.482	55.3	0.01425	0.01160	0.0116	0.651	3.61	0.1804	0.494	0.811

* Diffusivities predicted by Wilke-Chang correlation.(13)

TABLE V-G

WARZEL'S DATA FOR CARBON DIOXIDE ABSORPTION AND DESORPTION
USING AIR-WATER SYSTEM WITH THE GAS PHASE DILUTE IN CARBON DIOXIDE

Run No.	Weir Height Inches	Liquid Rate gpm	u_s ft/sec	F-Factor	λ	E_{MV}	"C" Warzel Correlation	E_{OG}	t_L sec	"C" by Equation (135)	E_{OG_2} From "C" by Equation (135)	N_{OG} From E_{OG_2}	N_L	$k_L\bar{a}$ sec^{-1}	$\frac{k_L\bar{a} \times 10^{-2}*}{D_L^{1/2}}$
C-116	3-1/2	4.58	1.06	0.29		6.13	4.2		13.63						
C-115			2.13	0.57	159.8	2.99	4.9	0.0209	12.73	5.12	0.0211	0.0214	3.41	0.268	0.292
C-111			3.18	0.86	237.0	1.99	5.6	0.0144	12.66	5.53	0.0144	0.0145	3.44	0.271	0.296
C-109			4.72	1.29	351.7	1.32	7.1	0.0102	13.64	5.97	0.0098	0.0098	3.45	0.253	0.276
C-117		9.16	1.06	0.29	25.81	6.67	2.9	0.0524	12.36	3.78	0.0550	0.0565	1.46	0.118	0.129
C-114			2.15	0.58	80.62	4.57	3.3	0.0307	12.38	4.92	0.0341	0.0347	2.80	0.226	0.247
C-110			3.19	0.86	120.3	3.11	3.7	0.0215	7.73	5.34	0.0236	0.0239	2.87	0.371	0.405
C-108			4.72	1.29	177.08	2.46	4.9	0.0176	8.00	5.91	0.0184	0.0186	3.29	0.412	0.449
C-118		18.31	1.06	0.29	19.88	6.75	2.5	0.0540	4.79	3.62	0.0574	0.0591	1.18	0.246	0.268
C-113			2.15	0.58	40.37	5.57	3.0	0.0416	5.22	4.54	0.0452	0.0463	1.87	0.358	0.391
C-112			3.18	0.86	59.51	4.95	3.4	0.0357	5.26	5.13	0.0391	0.0399	2.37	0.451	0.492
C-119	2.0	32.0	1.06	0.29	10.60	8.20		0.0686	4.11	3.35	0.0729	0.0757	0.80	0.195	0.213
C-100		4.58	1.05	0.29	79.23	4.10	4.0	0.0300	9.80	4.19	0.0304	0.0308	2.44	0.249	0.272
C-98			2.11	0.57	157.2	2.81	4.6	0.0197	8.89	5.05	0.0202	0.0204	3.21	0.361	0.394
C-93			3.16	0.87	235.1	1.75	5.3	0.0130	7.79	5.41	0.0130	0.0131	3.08	0.395	0.431
C-92			4.67	1.29	345.0	0.70	6.8	0.0060	7.15	5.35	0.0058	0.0058	2.00	0.279	0.305
C-106			4.62	1.27	348.5	0.88	6.8	0.0073	7.18	5.56	0.0070	0.0070	2.45	0.341	0.372
C-99		9.16	1.06	0.29	39.84	4.77	2.3	0.0348	13.63	3.85	0.0388	0.0395	1.58	0.116	0.126
C-97			2.11	0.57	78.82	2.41	2.8	0.0184	4.78	4.40	0.0200	0.0202	1.59	0.334	0.364
C-90			3.16	0.87	117.7	2.46	3.3	0.0177	4.77	5.11	0.0195	0.0197	2.32	0.486	0.530
C-89			4.67	1.30	173.8	1.41	4.4	0.0112	4.56	5.36	0.0116	0.0117	2.03	0.445	0.486
C-105			4.62	1.27	174.3	1.50	4.4	0.0118	4.56	5.41	0.0122	0.0123	2.15	0.471	0.514
C-101		18.31	1.05	0.29	19.87	5.31	1.7	0.0413	2.88	3.47	0.0464	0.0475	0.94	0.327	0.351
C-102			2.11	0.57	39.29	4.13	2.1	0.0306	3.08	4.28	0.0350	0.0356	1.40	0.455	0.497
C-94			3.14	0.86	58.56	4.02	2.6	0.0286	3.18	4.93	0.0329	0.0334	1.96	0.615	0.671

* $D_L = 84.09 \times 10^{-6}$ ft^2/hr, by Wilke-Chang correlation.(13)

TABLE WL-G (CONT'D)

WARZEL'S DATA FOR CARBON DIOXIDE ABSORPTION AND DESORPTION
USING AIR-WATER SYSTEM WITH THE GAS PHASE DILUTE IN CARBON DIOXIDE

Run No.	Weir Height Inches	Liquid Rate gpm	u_s ft/sec	F-Factor	λ	E_{MV}	"C" Warzel Correlation	E_{OG}	t_L sec	"C" by Equation (135)	E_{OG_2} From "C" by Equation (135)	N_{OG} From E_{OG_2}	N_L	sec^{-1}	$\frac{k_L\bar{a} \times 10^{-2}*}{D_L^{1/2}}$
C-95			4.71	1.31	87.85	2.63	3.5	0.0202	3.29	5.31	0.0218	0.0221	1.94	0.589	0.643
C-107			4.65	1.27	86.31	2.82	3.5	0.0214	3.21	5.35	0.0232	0.0235	2.03	0.631	0.689
C-103		32.0	1.05	0.29	11.25	5.92	1.3	0.0478	2.40	3.19	0.0538	0.0553	0.62	0.259	0.283
C-104			2.11	0.57	22.59	5.05	1.7	0.0386	2.93	4.02	0.0445	0.0455	1.03	0.350	0.382
C-96			3.15	0.87	33.54	5.88	2.1	0.0415	3.23	4.78	0.0492	0.0505	1.69	0.524	0.572
CD-85	2.0	4.58	1.04	0.28	78.01	3.99	4.0	0.0295	8.40	4.16	0.0298	0.0302	2.36	0.281	0.306
CD-84			3.11	0.84	233.26	2.64	5.3	0.0175	7.90	5.74	0.0179	0.0181	4.22	0.535	0.583
CD-122			3.15	0.85	235.4	2.78	5.3	0.0181	7.90	5.80	0.0186	0.0188	4.42	0.560	0.611
CD-121			4.68	1.28	346.2	1.97	6.8	0.0136	7.61	6.32	0.0134	0.0134	4.66	0.612	0.668
CD-83		9.16	2.08	0.56	78.27	3.54	2.8	0.0246	4.78	4.67	0.0278	0.0282	2.21	0.462	0.504
CD-82			3.11	0.84	117.3	2.86	3.3	0.0197	4.77	5.22	0.0221	0.0223	2.62	0.549	0.599
CD-120			4.71	1.29	175.9	2.24	4.4	0.0160	5.84	5.81	0.0171	0.0173	3.03	0.519	0.566
CD-86		18.31	1.06	0.28	19.71	4.30	1.7	0.0349	3.03	3.34	0.0383	0.0391	0.77	0.254	0.277
CD-80			2.09	0.56	39.07	4.05	2.1	0.0302	3.16	4.25	0.0344	0.0350	1.37	0.434	0.473
CD-79			3.12	0.85	58.47	3.43	2.6	0.0254	3.26	4.79	0.0287	0.0291	1.70	0.521	0.568
CD-81			4.63	1.27	86.73	2.91	3.5	0.0219	3.29	5.38	0.0239	0.0242	2.09	0.637	0.695
CD-87		32.0	1.07	0.29	11.47	5.12	1.3	0.0423	2.40	3.13	0.0469	0.0481	0.55	0.230	0.251
CD-88			3.13	0.85	33.57	4.85	2.1	0.0359	3.23	4.62	0.0416	0.0424	1.42	0.441	0.480

* $D_L = 84.09 \times 10^{-6}$ ft^2/hr, by Wilke-Chang correlation.[13]

TABLE VI-G

COMPARISON OF POINT EFFICIENCY VALUES DETERMINED BY USE OF SEVERAL DIFFERENT RELATIONSHIPS BETWEEN POINT AND PLATE EFFICIENCY

Run No.	Weir Height Inches	Liquid Rate gpm	Liquid Viscosity, cp	u_s ft/sec	C	γ	η	n(4)	$\frac{x_{avg} - x^*}{x_o - x}$	E_{MV}	E_{OG}(1)	E_{OG}(2)	E_{OG}(3)	E_{OG}(5)	E_{OG}(6)
2A	3-1/2	4.95	~ 37.5	2.68	3.05	2.82	1.01	1.86	1.47	0.0168	0.0117	0.0124	0.00972	0.0114	0.00823
2B				2.83	3.55	3.33	.99	1.86	1.52	0.0184	0.0130	0.0137	0.0108	0.0122	0.00810
3A				3.37	3.14	4.65	1.16	1.96	1.55	0.0166	0.0113	0.0131	0.00879	0.0108	0.00734
4A				0.89	2.28	1.95	0.62	2.12	1.26	0.0204	0.0166	0.0172	0.0147	0.0162	0.0136
4B				0.84	1.79	1.57	0.67	1.99	1.24	0.0220	0.0171	0.0183	0.0154	0.0170	0.0148
5A				1.73	4.39	4.15	0.51	-	1.31	0.0190	0.0157	-	0.0145	0.0145	0.0105
5B				1.70	4.52	4.31	0.44	1.50	1.21	0.0155	0.0133	-	0.0123	0.0129	0.00934
19A				3.67	3.47	3.38	0.66	1.50	1.28	0.0116	0.00883	-	0.00676	0.00910	0.00590
19B				3.48	3.24	3.09	0.84	-	1.31	0.0118	0.00879	-	0.00759	0.00905	0.00595
21A				1.75	3.27	3.08	0.55	1.55	1.21	0.0136	0.0113	0.0117	0.0102	0.0112	0.00844
21B				1.74	2.95	2.76	0.69	1.89	1.32	0.0161	0.0127	0.0133	0.0112	0.0122	0.00943
8A	3-1/2	4.92	~ 24	0.89	1.69	1.24	0.52	2.10	1.12	0.00984	0.00866	0.00891	0.00667	0.00878	0.00804
8B				0.84	1.64	1.20	0.52	-	1.20	0.0117	0.0102	-	-	0.00982	0.00940
6A				1.68	-	-	0.43	-	1.21	0.00874	-	-	0.00762	0.00720	0.00642
7A				1.67	1.02	-	0.36	-	1.77	0.00952	0.00687	-	0.00813	0.00816	0.00684
7B				1.67	-	-	0.41	-	1.16	0.00942	-	-	0.00946	0.00809	0.00679
9A				2.35	3.20	2.93	0.39	1.56	1.16	0.00865	0.00741	0.00761	0.00707	0.00744	0.00648
9B				2.36	3.84	3.57	0.39	1.50	1.16	0.00894	0.00780	0.00796	0.00730	0.00770	0.00592
16A				3.34	1.83	1.50	0.56	1.83	1.24	0.00696	0.00527	-	0.00519	0.00562	0.00448
16B				3.34	4.66	4.45	0.49	1.28	1.13	0.00732	0.00643	-	0.00568	0.00645	0.00463
20A				3.43	4.41	4.17	0.54	1.32	1.10	0.00698	0.00611	0.00622	0.00526	0.00632	0.00446
20B				3.43	4.10	3.86	0.52	1.32	1.12	0.00705	0.00611	0.00623	0.00537	0.00627	0.00450
12A	3-1/2	16.4	~ 24	1.71	1.23	0.42		6.40	1.15	0.0134	0.0117	0.0119		0.0117	0.0114
12B				1.73	1.81	0.33		9.78	1.16	0.0129	0.0117	0.0114		0.0111	0.0110
10A				2.30	1.40	0.65		4.81	1.17	0.0118	0.0102	0.0104		0.0101	0.00974
10B				2.32	0.94	-		373	1.20	0.0113	0.00928	-		0.00938	0.00937
17A				3.39	2.18	1.54		-	1.12	0.00942	0.00844	-		0.00845	0.00758
17B				3.39	1.93	1.28		2.12	1.14	0.00998	0.00876	0.00893		0.00879	0.00793
11A	3-1/2	26.4	~ 25	2.34	1.18	-		2.56	1.14	0.0128	0.0108	-		0.0112	0.0105
11B				2.33	-	1.29		2.75	1.16	0.0212	-	0.0180		0.0183	0.0159
13A				1.74	1.12	0.21		130	1.14	0.0159	0.0142	0.0142		0.0140	0.0140
13B				1.70	1.13	0.23		-	1.14	0.0165	0.0147	0.0148		0.0144	0.0145

TABLE VI-G (CONT'D)

COMPARISON OF POINT EFFICIENCY VALUES DETERMINED BY USE OF SEVERAL DIFFERENT RELATIONSHIPS BETWEEN POINT AND PLATE EFFICIENCY

Run No.	Weir Height Inches	Liquid Rate gpm	Liquid Viscosity, cp	V_s ft/sec	λ	γ	η	$n^{(4)}$	$\frac{x_{AVE} - x^*}{x_o - x}$	E_{MV}	$E_{OG}^{(1)}$	$E_{OG}^{(2)}$	$E_{OG}^{(3)}$	$E_{OG}^{(5)}$	$E_{OG}^{(6)}$
15A				0.86	1.02	0.050		-	1.04	0.0165	0.0138	-		0.0151	0.0137
15B				0.87	1.03	-		-	1.09	0.0166	0.0154	-		0.0170	0.0154
16A				3.40	1.47	-		-	1.16	0.0130	0.0125	-		0.0112	0.0126
16B				3.41	1.49	-		-	1.12	0.0113	0.0110	-		0.0101	0.0108
26A	2	4.95	~37	1.08	1.14	0.42	0.52	10.7	1.23	0.0850	0.00693	0.00718	0.00647	0.00692	0.00661
26B				1.09	1.11	0.34	0.50	3.58	1.25	0.00805	0.00659	0.00679	0.00620	0.00644	0.00646
23A				1.80	1.48	1.02	0.53	3.65	1.26	0.00733	0.00536	0.00620	0.00555	0.00583	0.00540
23B				1.76	2.32	2.16	0.48	2.30	1.23	0.00771	0.00732	0.00795	0.00678	0.00710	0.00714
24A				2.55	2.02	1.68	0.58	2.22	1.25	0.00700	0.00562	0.00526	0.00515	0.00561	0.00476
24B				2.55	2.02	1.70	0.58	2.16	1.25	0.00707	0.00567	0.00594	0.00420	0.00565	0.00479
27A				3.09	2.09	1.66	0.34	2.18	1.13	0.00306	0.00270	0.00277	0.00528	0.00270	0.00242
27B				3.17	2.10	1.69	0.56	1.80	1.12	0.00323	0.00284	0.00259	0.00249	0.00287	0.00242
34A				2.99	1.96	1.68	0.50	2.78	1.23	0.00503	0.00414	0.00433	0.00387	0.00409	0.00358
34B				2.99	2.03	1.71	0.64	2.26	1.27	0.00648	0.00462	0.00539	0.00464	0.00510	0.00429
25A				3.10	2.40	2.12	0.61	2.17	1.27	0.00670	0.00539	0.00563	0.00485	0.00526	0.00435
25B				3.11	2.39	2.12	0.64	2.24	1.29	0.00694	0.00520	0.00580	0.00496	0.00537	0.00445
49A				4.29	2.21	1.93	0.76	2.40	1.37	0.00619	0.00466	0.00494	0.00414	0.00453	0.00370
49B				4.30	2.21	1.94	0.67	1.97	1.31	0.00568	0.00435	0.00461	0.00398	0.0434	0.00349
45A				4.43	2.20	1.96	0.54	1.72	1.33	0.00512	0.00398	0.00422	0.00363	0.00385	0.00322
45B				4.41	2.44	2.23	0.70	2.31	1.34	0.00563	0.00438	0.00463	0.00386	0.00421	0.00345
29A				4.90	3.10	2.87	0.72	2.23	1.44	0.00773	0.00580	0.00608	0.00529	0.00538	0.00403
42A				5.63	2.34	2.14	0.75	2.47	1.52	0.00577	0.00419	0.00449	0.00387	0.00400	0.00319
32A				6.81	2.62	2.54	-	2.15	1.43	0.00539	0.00391	0.00419	-	0.00377	0.00284
32B				6.90	2.74	2.65	0.97	2.99	1.53	0.00600	0.00427	0.00457	0.00355	0.00393	0.00300
41A				6.91	2.59	2.38	1.01	2.37	1.01	0.00679	0.00459	0.00493	0.00381		0.00322
41B				6.91	2.52	2.50	1.04	2.11	1.01	0.00657	0.00444	0.00485	0.00373		0.00316
46A	2	4.83	~14.5	2.09	-	0.12	0.28	3.66	1.15	0.00342	-	0.00296	0.00297	0.00298	0.00292
46B				2.11	-	0.17	0.27	4.83	1.09	0.00216	-	0.00197	0.00188	0.00198	0.00194
37A				2.95	2.16	1.68	0.23	1.80	1.09	0.00283	0.00259	0.00263	0.00252	0.00260	0.00237
37B				2.95	2.06	1.58	0.24	1.99	1.10	0.00288	0.00262	0.00267	0.00254	0.00262	0.00238
38A				4.66	2.50	2.06	0.33	1.67	1.12	0.00230	0.00249	0.00254	0.00237	0.00251	0.00218
38B				4.72	3.47	3.10	0.25	1.26	1.06	0.00246	0.00228	0.00230	0.00216	0.00227	0.00193
39A				5.70	2.23	1.90	0.32	1.52	1.11	0.00246	0.00213	0.00220	0.00209	0.00222	0.00157
39B				5.74	2.40	1.98	3.16	1.55	1.11	0.00255	0.00222	0.00228	0.00217	0.00230	0.00191
40A				7.21	2.47	2.07	0.40	1.47	1.12	0.00239	0.00205	0.00210	0.00194	0.00214	0.00172
40B				7.21	2.28	1.83	0.40	2.04	1.19	0.00247	0.00203	0.00215	0.00200	0.00207	0.00176

TABLE VI-G (CONT'D)

COMPARISON OF POINT EFFICIENCY VALUES DETERMINED BY USE OF SEVERAL DIFFERENT RELATIONSHIPS BETWEEN POINT AND PLATE EFFICIENCY

Run No.	Weir Height Inches	Liquid Rate gpm	Liquid Viscosity, cp	u_s ft/sec	c	γ	η	n(4)	$\frac{x_{avg} - x^*}{x_o - x}$	E_{MV}	E_{OG}(1)	E_{OG}(2)	E_{OG}(3)	E_{OG}(5)	E_{OG}(6)
47A	2	16.5	≈38	2.25	1.15	0.37	0.52	-	1.23	0.0115	0.00964	0.00989	0.00873	0.00933	0.00942
47B				2.19	1.18	0.41	0.51	165	1.21	0.0113	0.00956	0.00979	0.00865	0.00930	0.00933
35A				2.46	1.23	0.47	0.51	271	1.22	0.0103	0.00879	0.00901	0.00793	0.00848	0.00851
35B				2.47	1.25	0.54	0.50	86	1.24	0.0115	0.00963	0.00990	0.00887	0.00925	0.00926
36A				2.98	1.13	0.31	0.59	9300	1.26	0.0100	0.00820	0.00840	0.00734	0.00794	0.00802
36B				2.97	1.14	0.32	0.56	232	1.24	0.00950	0.00786	0.00804	0.00707	0.00766	0.00768
30A				4.91	2.10	1.52	0.39	2.07	1.16	0.00739	0.00642	0.00739	0.00606	0.00639	0.00566
30B				4.90	1.50	0.81	0.52	2.68	1.20	0.00773	0.00636	0.00773	0.00589	0.00645	0.00588
50A				4.84	1.84	1.28	0.43	1.74	1.09	0.00585	0.00516	0.00528	0.00468	0.00535	0.00472
50B				4.82	1.74	1.20	0.47	1.96	1.14	0.00752	0.00639	0.00662	0.00588	0.00658	0.00579
43A				5.59	1.71	1.17	0.56	1.95	1.19	0.00898	0.00722	0.00751	0.00670	0.00755	0.00640
43B				5.72	2.19	1.74	0.49	1.46	1.12	0.00877	0.00735	0.00758	0.00682	0.00783	0.00626
33A				6.81	-	-	-	1.10	1.06	0.0126	-	-	-	0.01182	0.00759
33B				6.80	2.60	2.10	0.51	1.79	1.21	0.00951	0.00785	0.00808	0.00730	0.00783	0.00630
44A				6.78	2.47	2.02	0.54	1.36	1.13	0.0101	0.00818	0.00847	0.00761	0.00893	0.00657
44B				6.84	2.41	1.96	0.57	1.38	1.14	0.0101	0.00811	0.00840	0.00747	0.00885	0.00654
48A	2	26.4	~38	2.25	1.21	0.43	0.38	3030	1.19	0.0134	0.0114	0.0120	0.0111	0.0113	0.0116
48B				2.26	1.16	0.32	0.39	-	1.18	0.0129	0.0113	0.0115	0.0106	0.0109	0.0111
28B				3.22	1.15	0.31	0.47	39000	1.31	0.0162	0.0131	0.0134	0.0127	0.0123	0.0127
31A				4.88	1.68	1.02	0.46	9.41	1.16	0.0166	0.0133	0.0137	0.0131	0.0143	0.0118
31B				4.90	1.69	1.06	0.59	2.76	1.22	0.0142	0.0117	0.0121	0.0104	0.0116	0.0105

(1) $E_{OG} = \frac{c}{\lambda} \ln \left(\frac{\lambda}{c} E_{MV} + 1\right)$

(2) $E_{OG} = \frac{1 + \gamma}{\lambda} \ln \left(\frac{1 + \gamma}{\lambda} E_{MV} + 1\right)$

(3) $E_{OG} = \frac{\eta E_{MV}}{e^{\eta} - 1}$

(4) $E_{OG} = \frac{n}{\lambda} \left[(\lambda E_{MV} + 1)^{1/n} - 1\right]$

(5) $E_{OG} = \frac{E_{MV}}{\frac{x_{avg} - x^*}{x_o - x^*}}$

(6) $E_{OG} = \frac{1}{\lambda} \ln (\lambda E_{MV} + 1)$

TABLE VII-G

DATA USED IN THE CORRELATION OF THE AVERAGE LIQUID CONCENTRATION ON THE TRAY

Run No.	Weir Height Inches	Liquid Rate gpm	μ_L, cp	u_s ft/sec	F-Factor	$\frac{x_{avg} - x^*}{x_o - x^*}$	$\ln\frac{x_{avg} - x^*}{x_o - x^*}$	λE_{OG}	$\frac{\frac{x_{avg} - x^*}{x_o - x^*}}{(\lambda E_{OG})^{0.12}}$
4A	3-1/2	4.95	~37.5	0.89	0.294	1.26	0.231	0.901	1.277
4B				0.84	0.276	1.24	0.215	0.883	1.259
5A				1.73	0.571	1.31	0.270	1.524	1.245
5B				1.70	0.558	1.21	0.191	1.302	1.172
21A				1.75	0.569	1.21	0.191	1.177	1.190
21B				1.74	0.568	1.32	0.278	1.281	1.283
2A				2.68	0.859	1.47	0.386	2.006	1.352
2B				2.83	0.901	1.52	0.419	2.212	1.382
3A				3.37	1.112	1.55	0.438	2.157	1.414
19A				3.67	1.207	1.28	0.247	1.898	1.186
19B				3.48	1.141	1.31	0.270	1.900	1.210
8A	3-1/2	4.92	~24	0.89	0.300	1.12	0.113	0.428	1.240
8B				0.84	0.282	1.20	0.182	0.449	1.320
6A				1.68	0.564	1.21	0.191	0.660	1.271
7A				1.67	0.561	1.17	0.157	0.750	1.210
7B				1.67	0.561	1.16	0.148	0.744	1.200
9A				2.35	0.789	1.16	0.148	0.975	1.162
9B				2.36	0.790	1.16	0.148	1.009	1.159
16A				3.34	1.120	1.24	0.215	1.034	1.234
16B				3.34	1.119	1.13	0.122	1.190	1.107
20A				3.43	1.142	1.10	0.095	1.196	1.076
20B				3.43	1.139	1.12	0.113	1.183	1.098
12A	3-1/2	16.4	~24	1.71	0.565	1.15	0.140	0.328	1.315
12B				1.73	0.572	1.16	0.148	0.315	1.332
10A				2.30	0.762	1.17	0.157	0.381	1.312
10B				2.32	0.763	1.20	0.182	0.357	1.359
17A				3.39	1.110	1.12	0.113	0.469	1.228
17B				3.39	1.108	1.14	0.131	0.489	1.242
15A	3-1/2	26.4	~25	0.86	0.287	1.08	0.077	0.367	1.218
15B				0.87	0.287	1.09	0.086	0.413	1.220
13A				1.74	0.566	1.14	0.131	0.253	1.343
13B				1.70	0.549	1.14	0.131	0.253	1.343
11A				2.34	0.764	1.14	0.131	0.393	1.275
11B				2.33	0.757	1.16	0.148	0.639	1.223

TABLE VII-G (CONT'D)

DATA USED IN THE CORRELATION OF THE AVERAGE LIQUID CONCENTRATION ON THE TRAY

Run No.	Weir Height Inches	Liquid Rate gpm	μ_L, cp	u_s ft/sec	F-Factor	$\frac{x_{avg} - x^*}{x_o - x^*}$	$\ln \frac{x_{avg} - x^*}{x_o - x^*}$	λE_{OG}	$\frac{x_{avg} - x^*}{x_o - x^*} / (\lambda E_{OG})^{0.12}$
26A	2	4.95	~ 37	1.08	0.361	1.23	0.207	0.460	1.350
26B				1.09	0.364	1.25	0.223	0.422	1.387
23A				1.80	0.591	1.26	0.231	0.628	1.330
23B				1.78	0.588	1.23	0.207	0.764	1.270
24A				2.55	0.846	1.25	0.223	0.857	1.273
24B				2.55	0.848	1.25	0.223	0.865	1.271
27A				3.09	0.944	1.13	0.122	0.504	1.228
27B				3.17	0.943	1.12	0.113	0.535	1.208
34A				2.99	0.953	1.23	0.207	0.737	1.278
34B				2.99	0.953	1.27	0.239	0.920	1.282
25A				3.10	1.034	1.27	0.239	0.979	1.273
25B				3.11	0.990	1.29	0.254	1.007	1.290
49A				4.29	1.362	1.37	0.315	1.173	1.345
49B				4.30	1.362	1.31	0.270	1.126	1.290
45A				4.43	1.431	1.33	0.286	1.028	1.325
45B				4.41	1.415	1.34	0.292	1.117	1.322
29A				4.90	1.490	1.44	0.365	1.583	1.362
42A				5.63	1.769	1.52	0.419	1.291	1.473
32A				6.81	2.046	1.43	0.358	1.546	1.357
32B				6.90	2.071	1.53	0.425	1.636	1.441
46A	2	4.88	~14.5 cp	2.09	0.715	1.15	0.140	0.315	1.320
46B				2.11	0.717	1.09	0.086	0.213	1.310
37A				2.95	0.983	1.09	0.086	0.385	1.221
37B				2.95	0.984	1.10	0.095	0.390	1.232
38A				4.66	1.508	1.12	0.113	0.591	1.192
38B				4.72	1.523	1.08	0.077	0.540	1.163
39A				5.70	1.830	1.11	0.104	0.649	1.170
39B				5.74	1.843	1.11	0.104	0.666	1.170
40A				7.21	2.283	1.12	0.113	0.778	1.150
40B				7.21	2.280	1.19	0.174	0.752	1.230

TABLE VII-G (CONT'D)

DATA USED IN THE CORRELATION OF THE AVERAGE LIQUID CONCENTRATION ON THE TRAY

Run No.	Weir Height Inches	Liquid Rate gpm	μ_I, cp	u_s ft/sec	F-Factor	$\frac{x_{avg} - x^*}{x_o - x^*}$	$\ln \frac{x_{avg} - x^*}{x_o - x^*}$	λE_{OG}	$\frac{\frac{x_{avg} - x^*}{x_o - x^*}}{(\lambda E_{OG})0.12}$
47A	2	16.5	~38	2.25	0.733	1.23	0.207	0.473	1.348
47B				2.19	0.714	1.21	0.191	0.368	1.365
35A				2.46	0.780	1.22	0.199	0.376	1.372
35B				2.47	0.779	1.24	0.215	0.411	1.380
36A				2.98	0.941	1.26	0.231	0.426	1.397
36B				2.97	0.940	1.24	0.215	0.410	1.380
30A				4.91	1.497	1.16	0.148	0.572	1.220
30B				4.90	1.506	1.20	0.182	0.576	1.260
50A				4.84	1.539	1.09	0.086	0.460	1.194
50B				4.82	1.522	1.14	0.131	0.570	1.221
43A				5.59	1.710	1.19	0.174	0.760	1.230
43B				5.72	1.756	1.12	0.113	0.806	1.150
33A				6.81	2.004	1.06	0.058	1.452	1.108
33B				6.80	2.004	1.21	0.191	0.966	1.213
44A				6.78	2.060	1.13	0.122	1.094	1.118
44B				6.84	2.064	1.14	0.131	1.091	1.128
48A	2	26.4	~38	2.25	0.719	1.19	0.174	0.287	1.380
48B				2.26	0.719	1.18	0.166	0.277	1.377
28B				3.22	0.979	1.31	0.270	0.444	1.444
31A				4.88	1.480	1.16	0.148	0.785	1.193
31B				4.90	1.482	1.22	0.199	0.642	1.287

BIBLIOGRAPHY

1. American Institute of Chemical Engineers Research Committee, "Third Annual Progress Report" (1955).

2. American Institute of Chemical Engineers Research Committee, "Fourth Annual Progress Report" (1956).

3. American Institute of Chemical Engineers Research Committee, "Final Report on Plate Efficiency" (1958).

4. Anderson, J.E., Sc. D. Thesis, Massachusetts Institute of Technology, 1954.

5. Arnold, J.H., Ind. Eng. Chem., 22, 1091 (1930).

6. Arnold, J.H., Sc. D. Thesis, Massachusetts Institute of Technology, (1932).

7. Ashby, B.B., Ph.D. Thesis, University of Michigan, 1956.

8. Bromley, L.A., and C.R. Wilke, Ind. Eng. Chem., 43, 1641-48 (1951).

9. Brown, J.A., Jr., B.S. Thesis, Massachusetts Institute of Technology, (1954).

10. Calderbank, P.H., Trans. Inst. Chem. Engrs., 34, 79 (1956).

11. Carey, J.S., J. Griswold, W.K. Lewis, and W.H. McAdams, Trans. Am. Inst. Chem. Engrs., 30, 504 (1934).

12. Carlson, Tor, J. Am. Chem. Soc., 33, 1027 (1911).

13. Chang, P. and C.R. Wilke, A.I.Ch.E. Journal, 1, pp. 264-270 (1955).

14. Chilton, T.H. and A.P. Colburn, Ind. Eng. Chem., 26, 1183 (1934).

15. Chilton, T.H. and A.P. Colburn, Ind. Eng. Chem., 26, 1183 (1934).

16. Chrisney, J.B., M.S. Thesis, University of California, 1948.

17. Chu, J.C., Petroleum Processing, 6, 39 (1951).

18. Chu, J.C., Petroleum Processing, 6, 39 and 154 (1951).

19. Chu, J.C., J. Forgrieve, R. Grosso, S.M. Shah, and D.F. Othmer, A.I.Ch.E. Journal, 3, 16 (1957).

20. Colburn, A.P., et al., Chem. Eng. Prog. 45, 716 (1949).

21. Crozier, R.D., Ph.D. Thesis, University of Michigan, 1956.

22. Danckwerts, P.V., Ind. Eng. Chem., 43, 1460 (1951).

23. Danckwerts, P.V., Chem. Eng. Sci., 2, 1 (1953).

24. Dean, P.C., Dow Chemical Company, Personal Communication.

25. Dow Chemical Company, "Products of the Dow Chemical Company - Their Properties and Uses", Copyright 1955.

26. Drickamer, H.G. and J.R. Bradford, Trans. Am. Inst. Chem. Engrs., 39, 319 (1943).

27. Etherington, L.D., Sc. D. Thesis, Massachusetts Institute of Technology, 1949.

28. Fairbrother, F., S.M. Thesis, Massachusetts Institute of Technology, 1941.

29. Farrell, J.K. and J.C. Vyverberg, M.S. Thesis, Massachusetts Institute of Technology, 1940.

30. Foss, A.S., Ph.D. Thesis, University of Delaware, 1956.

31. Gadwa, J.A., Sc.D. Thesis, Massachusetts Institute of Technology, 1936.

32. Gautreaux, M.F. and H.E. O'Connell, Chem. Eng. Prog., 51, 232 (1955).

33. Garner, F.H. and D. Hammerton, Chem. Eng. Sci., 3, 1 (1954).

34. Geddes, R.L., Trans. Am. Inst. Chem. Engrs., 42, 79 (1946).

35. Gerster, J.A., Bonnet, W.E., and I. Hess, Chem. Eng. Prog., 47, 621 (1951).

36. Ibid, 47, 523 (1951).

37. Ibid, 45, 716 (1949).

38. Gerster, J.A., Memorandum to Members of Technical Subcommittee, A.I.Ch.E. Plate Efficiency Research Program, March 21, 1957.

39. Grohse, E.W., et al., Chem. Eng. Prog., 45, 725 (1949).

40. Hadamard, J., Compt. rend., 152, 1735 (1911); 154, 107 (1912).

41. Hatta, S. and M. Katori, J. Soc. Chem. Ind. Japan, 37, 280B (1934).

42. Higbie, R., Trans. Am. Inst. Chem. Engrs., 31, 365 (1935).

43. Hildebrand, F. B., Methods of Applied Mathematics, Prentice-Hall, Inc., Englewood Cliffs, New York, 1952.

44. Horton, G.F., S.M. Thesis, Massachusetts Institute of Technology, 1937.

45. Hughes, R.R. and E.R. Gilliland, Chem. Engl Prog., 48, 497 (1952).

46. Hüfner, G., Ann. Physik. Chem., 60, 134 (1897).

47. International Critical Tables, McGraw Hill Book Co., New York (1931).

48. Johnstone, H.F. and A.D. Singh, Ind. Eng. Chem., 29, 286 (1937).

49. Jordan, J., E. Ackerman, and R.L. Berger, J.A.C.S., 78, pp. 2979-83 (1956).

50. Kirschbaum, E., Forsch, Gebiete Ing., B5, 245 (1935).

51. Kirschbaum, E., "Distillation and Rectification", p. 276, Chemical Pub. Co., New York (1948).

52. Langdon, W.M. and D.B. Keyes, Ind. Eng. Chem., 35, 464 (1943).

53. Lewis, W.K., Jr., Ind. Eng. Chem., 28, 399 (1936).

54. Lynch, E.J. and C.R. Wilke, A.I.Ch.E. Journal, 1, 9 (1955).

55. Maget, H.J.R., A.I.Ch.E. Plate Efficiency Research Assistant, University of Michigan (1956).

56. Mayfield, F.D., et al., Ind. Eng. Chem., 44, 2238 (1952).

57. Mehta, J.J. and R.H. Parekh, M.S. Thesis, Massachusetts Institute of Technology, 1939.

58. Miller, Proc. Roy. Soc. (London), 106, 724 (1924).

59. Murphree, E.V., Ind. Eng. Chem., 17, No. 7, pp. 747-750 (1925).

60. Narsimhan, G. and P.S. Mene, Trans. Indian Inst. Chem. Eng., 5, 59 (1952-53).

61. Nord, M., Trans. Am. Inst. Chem. Engrs., 42, 863 (1946).

62. O'Connell, H.E., Trans. Am. Inst. Chem. Engrs., 42, 741 (1946).

63. Oholm, Medd. Nobelinst, 2, 23 (1913).

64. Oliver, E.D. and C.C. Watson, A.I.Ch.E. Journal, 2, No. 1, 18 (1956).

65. Peaceman, D.W. and J.E. Vivian, A.I.Ch.E. Journal, 2, No. 4, pp. 437-443 (1956).

66. Peavy, C.C. and E.M. Baker, Ind. Eng. Chem., 29, 1056 (1937).

67. Perry, J.H., Ed., Chemical Engineers' Handbook, 1st Edition, McGraw-Hill Book Company, Inc., New York, 1934.

68. Polich, W.F., Ph.D. Thesis, Carnegie Institute of Technology, 1954.

69. Quayle, O.R., Chem. Rev., 53, pp. 439-589 (1953).

70. Quigley, C.J., A.I. Johnson, and B.L. Harris, Chem. Eng. Progress Symposium Series, 51, No. 16, 31

71. Rhodes, F.H. and P.G. Slackman, Ind. Eng. Chem., 29, 51 (1937).

72. Robinson, D., Ph.D. Thesis, in progress, University of Delaware.

73. Rush, F.E., Jr., and C. Stirba, paper presented at A.I.Ch.E. Meeting, Houston (May, 1955).

74. Rybczynski, W., Bull. Acad. Sci., Cracow (A), 40 (1911).

75. Schilling, G.D., G.H. Beyer, and C.C. Watson, Chem. Eng. Prog., 49, 128 (1953).

76. Sherwood, T.K., Absorption and Extraction, 1st Edition, McGraw-Hill Book Company, Inc., New York, 1936.

77. Sherwood, T.K. and F.A.L. Holloway, Trans. Am. Inst. Chem. Engrs., 36, 39 (1940).

78. Sherwood, T.K. and R.L. Pigford, Absorption and Extraction, 2nd Edition, p. 301, McGraw-Hill Book Company, Inc., New York, 1952.

79. Silberman, E., paper presented at Midwest Conference on Fluid and Solid Mechanics, 1956.

80. Simkin, D.J., M.S. Thesis, University of California, 1948.

81. Smolin, W., I. Goldberg, and H. Welsh, Thesis, Polytechnic Institute of Brooklyn, 1956.

82. Smosky, A.E. and B.F. Dodge, Ind. Eng. Chem., 42, 1112 (1950).

83. Spells, K.E. and S. Bakowski, Trans. Inst. Chem. Engrs., 28, 38 (1950).

84. Spells, K.E. and S. Bakowski, Trans. Inst. Chem. Engrs., 30, 189 (1952).

85. Stone, H.L., Sc. D. Thesis, Massachusetts Institute of Technology, 1953.

86. Toor, H.L. and J.M. Marchello, A.I.Ch.E. Journal, 4, 97 (1958).

87. Uchida, S. and K. Matsumoto, J. Soc. Chem. Ind. (Japan), 39, 224 (1936).

88. Van Krevelen, D.W. and J.J. Hoftijzer, Chem. Eng. Prog., 46, 29 (1950).

89. Walter, J.F. and T.K. Sherwood, Ind. Eng. Chem., 33, No. 4, pp. 493-501 (1941).

90. Walter, J.F. and T.K. Sherwood, Ind. Eng. Chem., 33, 493 (1941).

91. Ward, D., Personal Communication, University of Michigan, 1957.

92. Warzel, L.A., Ph.D. Thesis, University of Michigan, 1955.

93. West, F.B., W.D. Gilbert, and T. Shimizu, Ind. Eng. Chem., 44, No. 10, pp. 2470-78 (1952).

94. West, F.B., W.D. Gilbert, and T. Shimizu, Ind. Eng. Chem., 44, 2470 (1952).

95. Wharton, L., B.S. Thesis, Massachusetts Institute of Technology, 1955.

96. Whitman, W.G., Chem. Met. Eng., 29, No. 4, (1923).

97. Wilke, C.R. and C.Y. Lee, Ind. Eng. Chem. 47, 1253 (1955).

98. Winslow, C.E., Jr., Ph.D. Thesis, North Carolina State College, 1955.

99. Sage, B. H., et. al., Ind. Eng. Chem., 48, 275-288, (1956).